



Reaction Kinetics for Hydrothermal Liquefaction of Biomass

Reem Obeid

BE. (Chem) Hons.

Thesis submitted for the degree of Doctor of Philosophy

School of Chemical Engineering and Advanced Materials

Faculty of Engineering, Computer and Mathematical
Sciences

The University of Adelaide, Australia

June 2020

Table of Contents

Abstract	iv
Declaration	vi
Acknowledgements	vii
Preface	ix
Chapter 1 – Introduction	1
1.1 Background	2
1.2 Scope and Structure of Thesis	3
Chapter 2 – Literature Review	5
2.1 Introduction.....	6
2.2 Biomass Selection for HTL.....	6
2.2.1 Algae.....	6
2.2.2 Sewage Sludge.....	7
2.2.3 Pinewood	8
2.3 Variables in HTL Studies.....	12
2.3.1 Reaction Pressure.....	12
2.3.2 Biomass Loading	12
2.3.3 Batch verse Continuous HTL Reactors and Heating Rate.....	13
2.3.4 Solvent for Product Separation	14
2.3.5 Catalysts.....	15
2.4 Kinetic and Additivity Models for HTL Reactions.....	16
2.5 Model Compound Selection for HTL of Biomass	26
2.5.1 Carbohydrates	28

2.5.2 Lignin.....	33
2.5.3 Lipids	35
2.5.4 Proteins	36
2.6 Interactions between the Constituents of Biomass.....	37
2.7 Crude Characterisation.....	39
2.8 Implications of Current Study	41
2.9 Objectives of Thesis	42

Chapter 3 – The elucidation of reaction kinetics for hydrothermal liquefaction of model macromolecules.....43

Chapter 4 – Reaction kinetics and characterisation of species in renewable crude from hydrothermal liquefaction of monomers to represent organic fractions of biomass feedstocks.....62

Chapter 5 – Reaction kinetics and characterisation of species in renewable crude from hydrothermal liquefaction of mixtures of polymer compounds to represent organic fractions of biomass feedstocks.....84

Chapter 6 – A kinetic model for the hydrothermal liquefaction of microalgae, sewage sludge and pinewood with product characterisation of renewable crude114

Chapter 7 – Conclusions172

7.1 Conclusions.....	173
7.1.1 The elucidation of reaction kinetics for hydrothermal liquefaction of model macromolecules	173

7.1.2 Reaction kinetics and characterisation of species in renewable crude from hydrothermal liquefaction of monomers to represent organic fractions of biomass feedstocks	174
7.1.3 Reaction kinetics and characterisation of species in renewable crude from hydrothermal liquefaction of mixtures of polymer compounds to represent organic fractions of biomass feedstocks	175
7.1.4 Reaction kinetics and product characterisation of renewable crude from hydrothermal liquefaction microalgae, sewage sludge and pinewood	176
7.2 Recommendations for Future Work.....	177

Chapter 8 – References179

Abstract

Hydrothermal liquefaction (HTL) involves the conversion of biomass into a renewable crude oil in subcritical water. Co-products of the process include solid, aqueous and gas phase products. In order for the process to be upgraded to industrial scale the products from HTL need to be characterised. Various sources of biomass contain different fractions of carbohydrate, lignin, lipid, protein and inorganic material. At different reaction conditions, including temperature and time, variations in product fractions and their compositions have been observed. The principal objective of this work was to develop a model to predict the trends in HTL product fractions for various biomass compositions at different reaction times and temperatures. This may allow the optimum reaction conditions to produce a maximum amount of crude to be identified for a variety of feedstocks.

In order to develop a kinetic model for the HTL of different biomass feedstocks, model polymer and monomer compounds to represent the organic constituents of biomass were first reacted alone and the trends in product fractions observed. The HTL experiments were conducted at reaction temperatures of 250, 300 and 350°C over reaction times 0 to 60 minutes. The crude produced was analysed via thermogravimetric analysis and gas-chromatography mass-spectrometry to determine the variations in crude from different sources of biomass. Reactions with polymer and monomer model compounds alone allowed the conversion pathways in HTL to be identified. Mixtures of polymer model compounds were also reacted to determine the effects of interactions between the organic fractions of biomass on product distribution and crude composition. The final step in the model development involved building a kinetic model from HTL experiments with microalgae, sewage sludge and pine wood biomass using the reaction pathways developed for model compounds.

Results from experiments with polymer model compounds showed that the lipid produced the highest crude yield, followed by protein, carbohydrate and lignin. Monomer compounds resulted in lower crude yields than polymer compounds, except in the case of lignin. HTL of the intermediate reaction products,

represented by monomers, resulted in the same compounds identified in the crude. It was concluded from experiments with mixtures that the interactions between the organic constituents of biomass result in variations in yields of product fractions compared to those when polymers were reacted alone by 0 to 35%. These variations depend on reactant composition, reaction time and temperature. The compounds identified in the crude produced from a given mixture of polymers were the same as the compounds produced from the individual polymers. In experiments with biomass, product fractions differed compared to what was expected from model compounds by up to 42% due to interactions between the organic constituents of biomass and the presence of inorganic compounds.

From the results of this study, a kinetic model to describe the HTL reactions for microalgae, sewage sludge and pine wood was produced. The model could predict product yields with less than 15% error. The results will allow suitable reaction conditions and biomass feedstocks to be identified for production of crude from HTL at industrial scale.

Declaration

I certify that this work contains no material which has been accepted for the award of any other degree or diploma in my name, in any university or other tertiary institution and, to the best of my knowledge and belief, contains no material previously published or written by another person, except where due reference has been made in the text. In addition, I certify that no part of this work will, in the future, be used in a submission in my name, for any other degree or diploma in any university or other tertiary institution without the prior approval of the University of Adelaide and where applicable, any partner institution responsible for the joint-award of this degree.

I acknowledge that copyright of published works contained within this thesis resides with the copyright holder(s) of those works.

I also give permission for the digital version of my thesis to be made available on the web, via the University's digital research repository, the Library Search and also through web search engines, unless permission has been granted by the University to restrict access for a period of time.

I acknowledge the support I have received for my research through the provision of an Australian Government Research Training Program Scholarship.

Reem Obeid

28/01/2020

Date

Acknowledgements

This thesis would not have been completed without the support and guidance of many people.

I would firstly like to thank my supervisors Dr Philip van Eyk, Professor David Lewis and Dr Neil Smith. I thank Philip for his constant support and always being present to help solve any problem at any time. I thank David for contributing his great knowledge in the area of hydrothermal liquefaction and industrial fuel processing. I thank Neil for constantly helping me improve my work with his insightful ideas and suggestions.

I would like to acknowledge the funding received from the Australian Research Council's Linkage Project grant (LP150101241) and our industry partner Southern Oil Refining Pty Ltd.

I would like to acknowledge the assistance of Dr Tony Hall with the analytical methods used during my PhD which allowed me to gather so many essential results. I would like to thank the members of the Faculty of Engineering Computer and Mathematical Sciences Infrastructure Team, especially Jason Peak, for assisting me with many issues I had during my experimental work in the laboratory. The design of the HTL reactor system was challenging and would not have been successful without his assistance.

I would like to thank my fellow PhD candidates in the HTL research group, Jasim Al-Juboori, Benjamin Keiller, Sylvia Edifor, Md Arafat Hossein, Thomas Scott, Andres Chacon Parra and Robran Cock for always being present to discuss ideas and provide support. I would like to thank the academics who I worked with as a tutor for providing great guidance and teaching me so much, Associate Professor Peter Mullinger and Associate Professor Zeyad Al-Wahabi.

I would like to thank my mum and dad, as well as my siblings, Nadir and Liana, for the complete support and encouragement they have always given me. I would like to thank my grandmother who always advocated strongly for women's

education and encouraged me to pursue my studies. Finally, thank you to Zagros for always being there for me and supporting me.

Preface

This thesis is submitted as a portfolio of publications according to the ‘Specifications for Thesis 2020’ of the University of Adelaide. The journals in which the publications were published are given in the following table:

Journal Title	2020 Impact Factor
The Chemical Engineering Journal	8.355
Energy and Fuels	3.021

The main body of this work is published in the following journal papers:

- 1) **R. Obeid**, D. Lewis, N. Smith, P. van Eyk, The elucidation of reaction kinetics for hydrothermal liquefaction of model macromolecules, *Chemical Engineering Journal* 370 (2019) 637-645. Copyright of this paper belongs to Elsevier.
- 2) **R. Obeid**, D.M. Lewis, N. Smith, T. Hall, P. van Eyk, Reaction kinetics and characterisation of species in renewable crude from hydrothermal liquefaction of monomers to represent organic fractions of biomass feedstocks, *Chemical Engineering Journal* (2020) 1385-8947. Copyright of this paper belongs to Elsevier.
- 3) **R. Obeid**, D. Lewis, N. Smith, T. Hall, P. van Eyk, Reaction kinetics and characterisation of species in renewable crude from hydrothermal liquefaction of mixtures of polymer compounds to represent organic fractions of biomass feedstocks, *Energy & Fuels* 34 (2019) 419-429. Copyright of this paper belongs to the American Chemical Society.
- 4) **R. Obeid**, N. Smith, D. Lewis, T. Hall, P. van Eyk, A kinetic model for the hydrothermal liquefaction of microalgae, sewage sludge and pine wood with product characterisation of renewable crude, Manuscript Ready for Submission.

Chapter 1

Introduction

1.1 Background

A growing energy demand across the globe coupled with the depletion of fossil fuels has led to the requirement for alternate renewable energy sources for fuel security. Hydrothermal liquefaction (HTL) promises to provide a renewable energy source in the form of crude oil as well as a solution for waste management. The process takes organically rich, wet biomass in a solvent, most commonly water, and converts it to a renewable crude oil as well as solid, aqueous and gas phase co-products. This negates the requirement for intensive drying of the biomass which is required for other biomass to fuel processes, including direct combustion, pyrolysis and gasification.

The reactions occur at subcritical conditions. Reaction temperature is up to 350°C and reaction pressure is up to 280 bar (Möller et al. 2011). Water at these subcritical conditions acts as a reactant and catalyst which enables the efficient conversion of biomass with high water content. The high temperature and pressure result in water having a decreased dielectric constant and density so that the hydrocarbons which make up biomass gain higher solubility in water (Peterson, Lachance & Tester 2010). The biomass feed undergoes depolymerisation followed by decomposition of monomers by cleavage, dehydration, decarboxylation and deamination. These decomposition products then undergo recombination reactions (Toor, Rosendahl & Rudolf 2011). The lower oxygen and nitrogen content of the crude produced from HTL results in a fuel with a higher calorific value than the biomass feedstock. Hence, the process allows wet waste to be transformed to more useful products.

Currently several pilot plants are operating internationally, however gaps in current knowledge present limitations to full scale commercialisation of HTL (Castello, Pedersen & Rosendahl 2018). Product distribution and composition from HTL have been found to be highly dependent on the composition of the biomass feedstock, reaction temperature and reaction time (Arturi, Kucheryavskiy & Sjøgaard 2016). In order for the HTL process to be viable at large scale it is

essential to quantify the reaction kinetics, which can be achieved with the development of a reaction model.

The principal objective of this work was to develop a reaction model via multivariate testing based on model compounds representing various biomass feedstocks of interest, including microalgae, waste biomass, such as sludge, and lignocellulosic biomass. Using the yields of solid, aqueous, crude and gas phases, a series of kinetic equations describing the mathematical relationship between these parameters can be developed. By relating feed composition in the modelled HTL process to the fractions of crude oil produced, the process conditions can be investigated to maximise particular target fuel production derived from a characterised waste which, for example, would otherwise create landfill or need to be incinerated.

1.2 Scope and Structure of Thesis

Chapter 2 is composed of a critical review of the available literature on the HTL of model compounds and biomass. The product distributions for the solid, aqueous, crude and gaseous products from various feedstocks at different reaction conditions in HTL are reviewed. Additionally, previous models which have been developed to predict product fractions from HTL are reviewed.

Chapter 3 is the first journal paper which investigates the product distribution from the HTL of model polymer compounds representing carbohydrate, lipid, lignin and protein fractions of biomass feedstock when they are reacted alone. A kinetic model is developed for each polymer model compound reacting in subcritical water at reaction temperatures of 250, 300 and 350°C over reaction times of 0 to 60 minutes. The crude fractions are analysed via thermogravimetric analysis.

Chapter 4 is the second journal paper which investigates the conversion of model monomer compounds in HTL when they are reacted alone. A kinetic model is developed for the conversion of each monomer to solid, aqueous, crude and gas

phase product. The crude fractions are investigated via gas-chromatography mass-spectrometry.

Chapter 5 is the third journal paper. Binary and quaternary mixtures of polymer model compounds are reacted under HTL conditions to investigate the effect of interactions between model compounds on crude yield. A kinetic model is developed for quaternary mixtures of model compounds which can be further developed for biomass by varying kinetic parameters depending on experimental results. The crude composition from mixture experiments is compared to the crude produced from polymers and monomers when they are reacted alone using gas-chromatography mass-spectrometry.

Chapter 6 is the fourth and final journal paper where biomass model compounds, including microalgae, sewage sludge and pinewood, are reacted under HTL conditions. The kinetic model for quaternary mixtures of model compounds is adjusted for each type of biomass by finding new kinetic parameters for the same set of reaction pathways. The composition of the inorganic fraction of biomass and its effect on product distribution is investigated. The crude composition is compared to that from model compounds using gas-chromatography mass-spectrometry.

Chapter 7 summarises the conclusions from this body of work as well as recommendations for future work.

Finally, references are provided for Chapters 1, 2 and 7, while the references for Chapters 3, 4, 5 and 6 are provided in their respective journal papers.

Chapter 2

Literature Review

2.1 Introduction

This chapter provides a critical review on the available literature on HTL of biomass feedstocks. The variables between different HTL studies and their effects on product distributions are reviewed. The models in literature, which have been developed to predict product distribution from hydrothermal liquefaction, are highlighted as well as their limitations. Polymer and monomer compounds to represent biomass and assist in the development of a bulk kinetic model for HTL are explored. The methods used for characterisation of product compositions are also reviewed.

2.2 Biomass Selection for HTL

There is a high variation in the yields reported from the HTL of different biomass sources at given reaction conditions. Previous investigations in literature have indicated that crude yield is strongly dependent on the composition of the feed in HTL (Arturi et al., 2016). Biomass used as a feedstock for the HTL process can have varying composition depending on its source, with different fractions of carbohydrate, lipid, protein, lignin and ash contents.

2.2.1 Algae

Algae is a favourable source for renewable energy production because of its high photosynthetic efficiency which gives it the ability to absorb carbon dioxide from the atmosphere and reduce greenhouse gas emissions. It can be grown in both fresh and salt water, rapidly converting solar to chemical energy without competing with food growth (Guo et al., 2015).

Algae has been extensively studied as a feedstock for HTL (Brown et al., 2010, Valdez et al., 2011, Faeth et al., 2013, Valdez et al., 2012, Tian et al., 2014). The use of algae as a feedstock for crude production in HTL is favourable as it removes the requirement for drying the feedstock. The organic fraction of algae is made up of lipids, carbohydrates and proteins. The organic and ash composition of algae are dependent on its species and growth conditions (Morris et al., 1974, Fábregas et al., 2004). Maximum crude yield and the conditions for optimal crude yield have been found to vary for different species of algae. Optimum crude yields

from the HTL of algae have been reported to be 20 to 78% on a dry ash free basis (Tian et al., 2014). The crude produced from HTL of algae has been found to be composed of many nitrogenous compounds (Vardon et al., 2011, Biller and Ross, 2011). Hence, downstream processing to convert the crude produced from algae HTL to crude which has a more similar composition to the crude from petroleum is required.

2.2.2 Sewage Sludge

Sewage sludge is another feedstock of interest where HTL can act as a waste management process and a renewable fuel is produced. Sewage sludge is a by-product of the waste water industry and composed of lipid, carbohydrate, protein and lignin organic fractions as well as ash (Huang et al., 2013, Li et al., 2001).

HTL experiments with digested sludge were conducted at 300°C and 10-12 MPa for 30 minutes to obtain a crude yield of 9.4% (Vardon et al., 2011). The crude was composed of esters, phenolic and nitrogenous compounds. A higher crude yield of 39.5% was found from the HTL of sludge at reaction conditions of 350°C, 9.4-10.1 MPa and 20 minutes (Huang et al., 2013). A maximum crude yield of 27.5% was obtained in the hydrothermal conversion of sludge at 500°C and 1 minute in another study (Qian et al., 2017). In experiments with primary sludge, secondary sludge and digested solids, Marrone et al. (2018) found crude yields of 25-37%. Experiments with sewage sludge by Xu et al. (2018) yielded 15-23% crude yields where aqueous phase yields were much higher at up to 50%. During continuous HTL of sewage sludge an average crude yield of 25% was found by Anastasakis et al. (2018). Variations in crude yield from different studies are likely due to the varying composition of sludge. Sludge composition is a function of its location and where it has been removed from the waste water treatment process (Sommers et al., 1976). Biomass-assisted filtration of primary sludge to obtain high dry matter content sludge has been utilised where the combined sludge and lignocellulosic feedstocks produced higher crude yields than the feeds reacted alone (Biller et al., 2018). Catalysts including NiMo/Al₂O₃ (KF 851), CoMo/Al₂O₃ (KF 1022) and activated carbon for HTL reactions with a sewage

sludge feedstock have been shown to increase the H/C and reduce O/C ratios by Prestigiacomio et al. (2019). However, the crude yield was not altered with the use of the catalysts.

2.2.3 Pinewood

Lignocellulosic biomass can also be investigated for HTL. Lignocellulosic biomass is rich in carbohydrate (cellulose and hemicellulose) and lignin. Depending on the type of wood used as a feedstock, which contains varying fractions of extractives, lignin, cellulose, hemicellulose and ash, the conversion during HTL has been found to vary (Feng et al., 2014).

Pinewood is another biomass feed which can be used for HTL without competing for food production. A maximum crude yield of 55% was found for HTL of pinewood with a nickel nitrate catalyst (Tungal and Shende, 2014). For HTL of pine without a catalyst at 280°C and 15 minutes a crude yield of 22% was obtained (Singh et al., 2015). At temperatures of 180-260 °C over reaction times of 0-2 hours conversion of saw dust was seen to be 23.1–57.2 wt% by Hardi et al. (2017). HTL of different species of bark in ethanol–water (50:50, v/v) co-solvents resulted in different crude yields for the different species of bark (Feng et al., 2014). These included white pine, white spruce and white birch with crude yields of 36, 58 and 66% respectively. The higher yields corresponded to higher cellulose and lignocellulose contents in the feed.

Table 1: Summary of HTL experiments with biomass feedstock

Feedstock	Ash Content (%)	Reactor	Mass Loading wt%	Solvent	Temperature (°C)	Time (min)	Heat-up Time	Pressure (bar)	Crude Yield (%)	Reference
<i>Nannochloropsis</i> sp.	8	Batch tube, 35mL	-	Dichloromethane	200 250 300 350 400	60	Within 3 minutes	350	27 ± 8 38 ± 2 32 ± 6 43 ± 2 40 ± 3	Brown et al. (2010)
<i>Nannochloropsis</i> sp.	6.25±0.23	Port connector and cap	15	Dichloromethane + hexane	300-400	1-5	None, reaction time began immediately	400	13±7-50±2	Faeth et al. (2013)
<i>Nannochloropsis</i> sp.	-	Batch tube, 31mL	20-25	Hexadecane Decane Hexane Cyclohexane Methoxy cyclopentane Chloroform Dichloromethane	350	60	Within 3 minutes	-	38 39 32 34 33 35 30	Valdez et al. (2011)
<i>Nannochloropsis</i> sp.	-	Mini batch reactor, 4.1mL	5,10,15,20, 35	Dichloromethane + n-hexane	250-400	10-90	Within 3 minutes	-	30-50	Valdez et al. (2012)

Chapter 2 – Literature Review

<i>Chlorella vulgaris</i> <i>Spirulina</i> <i>Nannochloropsis occulta</i> <i>Porphyridium creuntum</i>	7.0 7.6 26.4 24.4	Parr, USA batch reactor, 75 ml	10	Dichloromethane	350	30	10°C/min	200	38 30 35 20	Biller and Ross (2011)
<i>Spirulina algae</i> Swine manure Anaerobic sludge	10 16 31	Parr 4500 2-L batch reactor	20	Dichloromethane	300	30	None, reaction time began immediately	100-120	32.6 30.2 9.4	Vardon et al. (2011)
Sewage sludge	10.3	Mini batch reactor, 4.1mL	10-50	Dichloromethane (DCM), methyl tert-butyl ether (MTBE), methyl isobutyl ketone (MIBK), hexane, xylenes, chloroform, methanol, ethanol, and acetone	400	60	None, reaction time began immediately	200-400	~25	Qian et al. (2017)
Sewage Sludge	35.5	4.4 ml mini-batch reactor	10	Dichloromethane + hexane	260, 280, 300, 320, 340 and 350	10	2-3 minutes (included in total 10 min reaction time)	180	15-23	Xu et al. (2018)

Chapter 2 – Literature Review

Primary Sewage Sludge	-	Continuous reactor with 140m length of the tube	4	No solvent	Up to 350	300	Feed fed in once reactor was heated to reaction temperature	220	~25	Anastasakis et al. (2018)
White pine bark	1.07	Parr 4590 Micro Bench top reactor, 100mL	10 with (ethanol-water co-solvent 50:50-volume)	Acetone (crude defined from solids and acetone soluble organics)	300	15	30 minutes	120	35	Feng et al. (2014)
White spruce bark	3.07								55	
White birch bark	2.68								65	
Loblolly pine	0.4	Parr benchtop Reactor - model 4520, 900mL	13	Cyclohexane Cyclohexane Cyclohexane Acetone Acetone Acetone	250 275 300 250 275 300	30	20-30 minutes	-	1 1 1 9 13 10	Saba et al. (2018)

Table 1 summarises some of the crude yields for different sources of biomass. Even when the same feedstock was used, yields were seen to vary for reaction time and temperature. There are also inconsistencies in reactor set-up, experimental conditions and product separation methodologies. In order to understand variation in product distributions and produce comparable results, these variables need to be identified and eliminated.

2.3 Variables in HTL Studies

Various batch and continuous HTL studies have been published. While the main variations in HTL product distribution have been found to be biomass composition, reaction temperature and reaction time (Arturi et al., 2016), other experimental variables such as reaction pressure, mass loading of the biomass reactant in water, heating rate of the HTL reactor and the solvent used to separate crude from the HTL product mixture also cause variation in HTL products. The presence of catalysts in the HTL reaction mixture also causes variation in product distributions.

2.3.1 Reaction Pressure

Depending on reaction temperature, subcritical water can have pressures of 100 to 280 bar. Increased pressure increases solvent density and this has been seen to result in enhanced decomposition of biomass in subcritical water. Increasing pressure from 250 to 350 bar was found to increase biomass decomposition by Chan et al. (2015). However, once the water is at sub-critical conditions, the effect of pressure on product distribution of solid, aqueous, crude and gas phases has been found to be minimal (Yu et al., 2011).

2.3.2 Biomass Loading

For higher concentrations of biomass, more side reactions are likely to occur which will produce products that are different to those produced at lower mass loadings (Möller et al., 2011). Increasing biomass loading from 5 to 35% increased renewable crude yield from 36% to 46% in a study by Valdez et al. (2012) where yield was defined by the mass of crude as a percentage of the mass of dry biomass reactant for HTL. Ratios of water to biomass from 2 to 6 were

seen to cause an increase in crude yield by 9% in the HTL of sawdust. A further increase in the ratio of water to sawdust from 6 to 10 saw a decrease in crude yield of 3.1% (Jindal and Jha, 2016). For product yields to be comparable from different feedstocks, biomass loading must be kept constant.

2.3.3 Batch versus Continuous HTL Reactors and Heating Rate

Most of the research in HTL reactions has been conducted with batch reactors. To be a viable waste management solution, HTL of biomass must be a continuous large scale process. Work on continuous reactors has been done by Jazrawi et al. (2013) and Biller et al. (2015). The products from batch reactor HTL have been compared with products from continuous reactor HTL by Jazrawi et al. (2013). In the continuous reactor, higher mass loading, higher temperature and longer residence time were shown to result in higher crude yields. Reactions were conducted at mass loading of 1-10%, 250-350°C and 3-5 minutes. These results were consistent with those from batch reactors and the more severe conditions produced lower molecular weight crude.

An important consideration when modelling the HTL reactor is the difference in heating and cooling rate for batch and continuous processes. Jazrawi et al. (2013) found that the residence time for maximum yield in batch reactors was longer than for the continuous reactor. This is most likely due to variation in heating rate. A heating rate of 300°C/minute was seen to produce higher yields of energy dense crude than reactions with a slower heating rate of 150°C/minute for a reaction time of 1 minute by Faeth et al. (2013).

Experiments performed by Anthony (2015) indicated that regardless of the heating rate to achieve a constant reaction temperature of 325 °C, the crude composition was approximately the same for the HTL of sewage sludge. Zhang et al. (2008) found that increasing the heating rate in a batch HTL reactor did not vary the crude composition though it increased the liquid yield from HTL of corn stover and aspen pulping wood chips. They also observed that the cooling rate did not cause variation in the final HTL products and this is likely because equilibrium conditions have already been reached. Decreasing the heating rate

was shown to increase decomposition of cellulose by Kamio et al. (2008). From their results, heating rate only affected the reaction products when the heating rate was less than 1 °C/s. Depending on how reaction time is defined, heating rate can cause the reaction time to be extended and this will have an effect on product distribution.

Equation 1 for predicting liquid yield with varied heating rate was developed by Zhang et al. (2009) for high diversity grass land perennials. They investigated heating rates of 5 to 140 °C/min as well as cooling rates of 5 to 66 °C/min. They agreed that yields were independent of cooling rate. For this range of heating rates the crude yield increased from 63% to 76% with increasing heating rate. Increased heating rate was seen to decrease char formation and increase liquid yield. The correlation in Equation 1 was developed from regression analysis.

$$\text{liquid yield (\%)} = [0.0042 \times \ln(\text{heating rate}) + 0.5514] \times 100$$

Equation 1

2.3.4 Solvent for Product Separation

Solvents are used in product separation for HTL mixtures at small-scale because they can extract the organic compounds and then be evaporated from the crude at low boiling points with minimal loss of crude product. This allows efficient quantification of the crude product. Investigations have demonstrated that renewable crude yield is dependent on the solvent selected for renewable crude extraction from the product mixture and that different solvents extract different compounds (Valdez et al., 2011, Yang et al., 2018a). While chloroform was found to recover 88 to 93% of the organics in the different crude oils tested, and dichloromethane recovered 85 to 95%, hexane recovered 85 to 89% of the organics (Valdez et al., 2011). Solvent choice needs to be considered further as Teri et al. (2014) found that some proteins and polysaccharides were insoluble in DCM and so not all of the compounds which make up crude were extracted. This gives inaccurate crude yield results. Other solvents have been investigated by

Abdel Kader (2015) where the greatest crude yield was obtained with tetrahydrofuran (THF) followed by DCM, acetone, chloroform, methanol, ethyl-acetate, hexane and toluene. THF gave a crude yield of 26.55%, DCM gave a crude yield of 23.95% and the rest gave between 0.18 to 15.52% crude yields. Valdez et al. (2011) found that more polar solvents, like DCM, THF and acetone, extracted more fatty acids in the crude. This led to a higher carbon content in the crude and hence a higher heating values.

Dote et al. (1992) proposed another method to remove the liquid product from the solid products of HTL of sewage sludge. Steam distillation, where the products of HTL were pressurised to the saturated vapour pressure of water at 100 °C, so that low molecular weight compounds and water evaporated then condensed again, was used in the first stage of separation. DCM extraction was then used to extract the oil which was separated into strongly acidic, weakly acidic, neutral and basic fractions with further extractions using different solvents.

For comparable yields from different biomass sources and reaction conditions, quantification of the crude needs to be consistent. The method used to extract crude at industrial scale may not involve the use of solvents for economic reasons, however the use of solvent has proven to be an effective method for product quantification for small-scale batch reactions to achieve maximum product recovery.

2.3.5 Catalysts

Some HTL studies involve the use of homogenous or heterogeneous catalysts. Commonly used catalysts for hydrothermal liquefaction include potassium hydroxide, potassium carbonate, sodium carbonate, sodium hydroxide and nickel (Toor et al., 2011). Heterogeneous catalysts were found to increase crude yield from microalgae by up to 20% by Duan and Savage (2011). Alkali metals can also inhibit conversion to crude and result in higher aqueous phase as was found in the case for potassium hydroxide by Anastasakis and Ross (2011). The inorganic content of the biomass feedstocks could contain some catalysing or inhibiting components and these could also result in varied product yield from HTL.

The high variability in experimental methods used for HTL by different groups in literature results in many product yields which are not comparable. In order to compare the products from HTL for biomass with various composition, as well as the effects of time and temperature on product distribution, reactions need to be completed under the same conditions. The development of a kinetic model requires constant reaction pressure, mass loading of the biomass reactant in water, heating rate of the HTL reactor and product separation methodologies.

2.4 Kinetic and Additivity Models for HTL Reactions

Many different types of biomass have been considered as feedstocks for HTL reactions and different kinetic models have been developed for different feedstocks. Hydrothermal processing is favoured as a method for producing crude from algae and aquatic biomass due to its high water content, hence several models have been developed for HTL of algae. Different types of algae have different compositions made up primarily of carbohydrates, lipids and proteins. The proportions of these have been varied by Biller and Ross (2011), Valdez et al. (2014) and Li et al. (2017) to observe changes in crude composition. These authors agree that an increase in lipid proportion in the algae feed will allow a higher yield of crude. They agreed that following the lipid proportion, most of the crude resulted from the reactions of protein and then carbohydrates.

Simplified first order kinetic models have been developed for three types of microalgae, *Chlorella protothecoides*, *Scenedesmus* sp. and *Nannochloropsis* sp., fitted from experimental data by Valdez et al. (2014) to model the decomposition rate of proteins, lipids and carbohydrates. The formation of aqueous, gaseous and crude phases are predicted. Rate constants were found at 250, 300, 350 and 400 °C. The model assumes that protein, lipid and carbohydrate fractions react independently. The reaction model is given in Equations 2 to 7 and the reaction network is visible in Figure 1. x is the mass fraction for carbohydrate (1, c), lipid (1, l), or protein (1, p) feed components, aqueous phase (2), crude (3), or gas (4) product components and k is the reaction rate constant.

$$\text{Proteins: } \frac{dx_{1,p}}{dt} = -(k_{1,p} + k_{2,p})x_{1,p}$$

Equation 2

$$\text{Lipids: } \frac{dx_{1,l}}{dt} = -(k_{1,l} + k_{2,l})x_{1,l}$$

Equation 3

$$\text{Carbohydrates: } \frac{dx_{1,c}}{dt} = -(k_{1,c} + k_{2,c})x_{1,c}$$

Equation 4

$$\text{Aqueous-phase products: } \frac{dx_2}{dt} = -(k_4 + k_5)x_2 + k_{1,p}x_{1,p} + k_{1,l}x_{1,l} + k_{1,c}x_{1,c} + k_3x_3$$

Equation 5

$$\text{Bio-crude: } \frac{dx_3}{dt} = -(k_3 + k_6)x_3 + k_{2,p}x_{1,p} + k_{2,l}x_{1,l} + k_{2,c}x_{1,c} + k_4x_2$$

Equation 6

$$\text{Gas: } \frac{dx_4}{dt} = k_5x_2 + k_6x_3$$

Equation 7

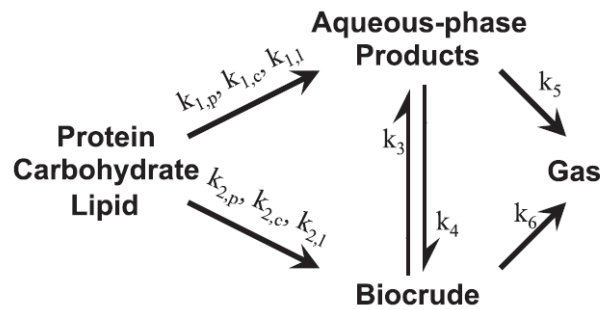


Figure 1: Reaction network for HTL of algae biomass (Valdez et al., 2014)

This kinetic model was compared with experimental data by Luo et al. (2016) for soy protein concentrate. The rate constants for the protein content of microalgae in HTL did not give suitable results for soy protein HTL. This may be due to the Valdez et al. (2014) work using a biomass feed containing a mixture of different compounds or the different characteristics of soy protein and microalgae protein in HTL. The reaction network in Figure 2 was adapted from the model by Valdez et al. (2014) for microalgae to be suitable for soy protein. Increasing reaction time and temperature were both found to increase crude yield in the range of 0 to 60 minutes and 200 to 350 °C respectively.

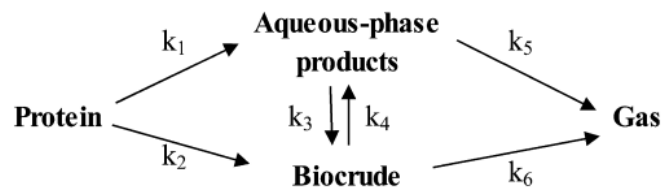


Figure 2: Reaction network for HTL of soy protein (Luo et al., 2016)

Following the development of the kinetic model shown in Figure 1, a model for fast and isothermal HTL of microalgae was developed which included a pathway from aqueous phase products to volatiles, shown in Figure 3 (Hietala et al., 2016). *S* represents solids, *B* for biocrude, *G* for gas, *A* for aqueous and *V* for volatiles. Reaction times for this model varied from 10 seconds to 60 minutes. The model in Figure 1 was then further correlated to HTL of microalgae with varying biochemical content and yields from fast HTL (Sheehan and Savage, 2017a). This model was developed from 112 HTL experiments from literature.

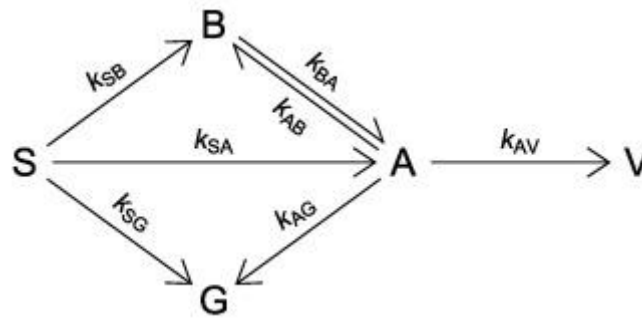


Figure 3: Reaction network for fast and isothermal HTL of algae biomass
(Hietala et al., 2016)

The method for developing kinetic equations to describe HTL by Valdez et al. (2014), Luo et al. (2016), and Sheehan and Savage (2017a) involved first defining the reaction pathways. For these reaction pathways, ordinary differential equations (ODEs) could be applied which were solved using an ODE solver paired with a minimisation function on software including MATLAB. An objective function was then used to find the least error between experimental and calculated results for different reaction coefficients. The reaction coefficient with the smallest error was then selected for the kinetic equation. The experimental data required for these models included yields of products from HTL experiments conducted at different temperatures and residence times.

Li et al. (2017) developed model equations to predict yields of HTL product phases and the HHV of products from the feedstock composition. The models were developed from unmixed batch experiments by using 24 different types of algae in batch experiments. When sufficient reaction time of around 60 minutes was allowed, the model could accurately predict the HTL products of anaerobic sludge, sewage sludge and swine manure. The yield of the product (crude, aqueous, gas or biochar phase), i , is given by the sum of the yields from individual components of the feed (lipid (L), protein (P), carbohydrate (C) and ash (A)), ij . The reaction rate constants are dependent on temperature and residence time. This model assumes no interactions between the reactants or products. The conversion coefficients for the multiphase component additivity (MCA) model

were fitted from the experimental data using Solver and Regression programs in Microsoft Excel Analysis Toolpak. Different reactor and experimental set-ups have led to deviations from this model. This indicates that the model needs to be refined for continuous processes. The MCA model used to predict phase yields is given in Equation 8.

$$Y_i = \sum Y_{ij} = \sum k_{ij} \times j = k_{iL} \times L + k_{iP} \times P + k_{iC} \times C + k_{iA} \times A$$

Equation 8

Biller and Ross (2011) proposed a model with the same form to predict crude yield only and neglected the presence of ash. They used model compounds which were sunflower oil, soy protein and starch. Li et al. (2017) predicted HHV of the crude from the average oxidation state of feedstock carbon (AOS_C) given in Equation 9. HHV of crude is calculated using Equation 10. The carbon, hydrogen and nitrogen composition of the feed are required as well as protein content. This resulted in 87.5% of the HHV predictions being within $\pm 10\%$ of the experimental values even though it was developed empirically from observed trends.

$$AOS_C = \frac{3 \times N \text{ mol}\% + 2 \times O \text{ mol}\% - H \text{ mol}\%}{C \text{ mol}\%}$$

Equation 9

$$HHV_{crude}(\text{MJ/kg}) = 30.74 - 8.52 \times AOS_C + 0.024 \times Prot\%$$

Equation 10

Yin et al. (2015) developed a more detailed kinetic model for the hydrothermal decomposition of sewage sludge. The first process in the model is dissolution of biomass to macromolecular products, which is followed by hydrolysis and oxidation of soluble organic matter in the liquid phase. The model is shown in Figure 4. They performed batch experiments at temperatures between 180 °C and 300 °C with sludge at a mass loading of 7.47wt%. Residence times for the batch reactions ranged between 5 and 90 minutes. From this data a modified first-order

kinetic equation was developed for the decomposition and formation of the model compounds. The biomass decomposition was characterised by a first order equation for total carbon content. Total organic carbon (TOC) in the liquid phase was used to measure biomass dissolution. The activation energy for the modelled compounds was found using the Arrhenius equation. Since formation of acetic acid was dependent on temperature and its degradation was not, oxidation in the liquid was well defined by monitoring acetic acid. Acetic acid was found to be the major organic intermediate by-product in hydrothermal oxidation by Shanableh and Jones (2001) as well as Yin et al. (2015). Experiments with more than one source of sewage sludge need to be performed to see how adequately this model represents the biomass. Many of the product compounds are not represented by this model.

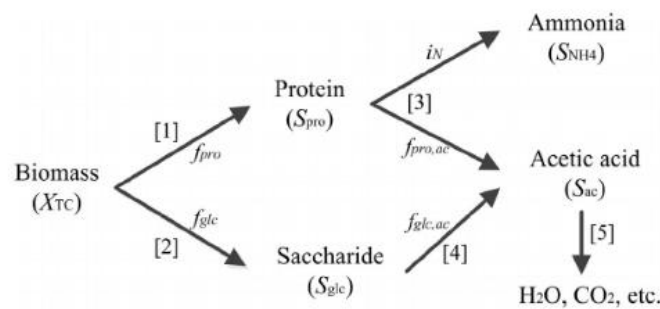


Figure 4: Kinetic model for hydrothermal degradation of sludge (Yin et al., 2015)

A reaction mechanism for hydrothermal degradation of sewage sludge has been described in a review by He et al. (2014) in Figure 5. The pathways were developed based on a sludge composition of approximately 40% proteins, 10 to 25% lipids, 14% carbohydrates and the remaining 30 to 50% is made up of lignin and ash.

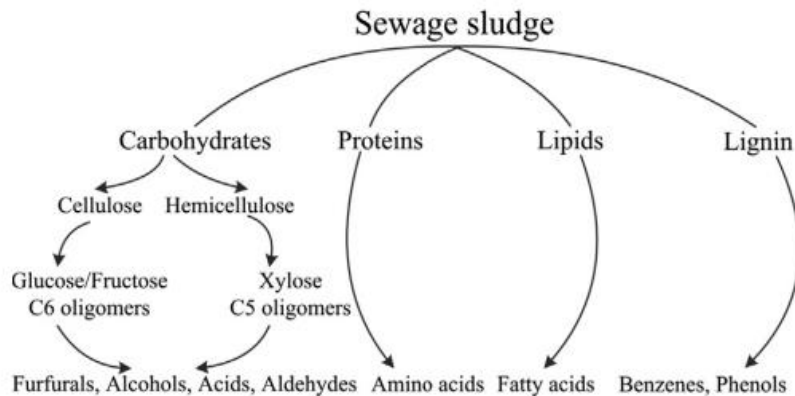


Figure 5: Reaction mechanism for hydrothermal degradation of sewage sludge (He et al., 2014)

A more recent kinetic model for sewage sludge has been developed by Qian et al. (2020). They conducted experiments with sludge at temperatures of 300-600°C and 1-60 minutes to obtain crude yields of up to 30.9%. To develop the model, they used the set of pathways shown in Figure 3, removing the pathway from aqueous to crude phases. Further data from HTL of sludge with varying composition as the feedstock is required to improve the model as feedstock composition affects product yields.

A set of reaction pathways in HTL has also been developed for Maillard reactions. Interactions between the products of carbohydrate and protein HTL were observed by Croce et al. (2017) where Maillard reactions produced substituted pyridines and pyrroles. Kruse et al. (2007) also found that the addition of protein or the amino acid, alanine, to glucose in HTL reactions lead to Maillard reactions. The products of these were nitrogen containing cyclic organic compounds. They developed the reaction pathway in Figure 6.

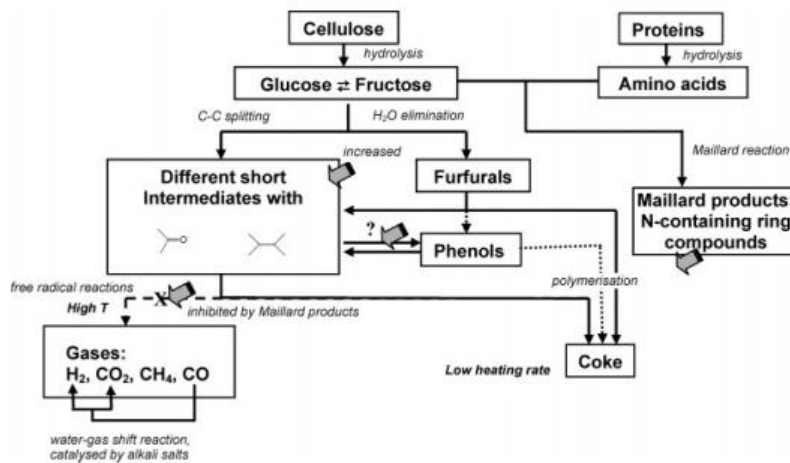


Figure 6: Reaction pathways for hydrothermal degradation of biomass (Kruse et al., 2007)

The interactions between model compounds were also characterised by Teri et al. (2014) with an equation that used mass fractions of lipid (L), carbohydrate (C) and protein (P) to predict crude yield. The model compounds were albumin and soy protein for protein. Sunflower oil and castor oil were chosen to represent lipids. The carbohydrate model compounds were cornstarch and cellulose. They performed experiments with single model compounds as well as binary mixtures of model compounds to observe the differences in yield. From their results on composition of the HTL products they obtained coefficients at 300 and 350 °C for the crude yield predicted by Equation 11.

$$\text{yield (wt\%)} = aX_L + bX_C + cX_P + dX_LX_C + eX_LX_P + fX_CX_P$$

Equation 11

The model predicted crude yield less accurately than one which neglected the interactions of products. However, evidence was found that interactions between products of HTL did affect the yields. Further work is required to model the effect of these interactions. An attempt to include interactions between the carbohydrate, protein and lipid constituents of microalgae biomass by Sheehan and Savage (2017a) also resulted in a kinetic model which predicted product yields less accurately.

Another additive model developed by Yang et al. (2019) included temperature, time and the mass ratio of water/feedstock shown in Equations 12-13. X_1 is soya protein, X_2 is saccharide, X_3 is alkaline lignin, X_4 is soya bean oil, X_5 is temperature, X_6 is time and X_7 is mass ratio. They also found that interactions between model feed compounds affected crude yields.

Biocrude yield (wt. %)

$$\begin{aligned}
 &= 19.99 * X_1 + 9.75 * X_2 + 1.75 * X_3 + 97.37 * X_4 \\
 &- 33.1 * X_1X_4 + 26.4 * X_2X_3 + 59.8 * X_2X_4 - 65.6 \\
 &* X_3X_4 - 25.46 * X_3X_4X_5 - 18.93 * X_1X_4X_6 - 38.63 \\
 &* X_1X_4X_7
 \end{aligned}$$

Equation 12

Solid Residue yield^{0.5} (wt. %)

$$\begin{aligned}
 &= 2.184 * X_1 + 5.396 * X_2 + 5.514 * X_3 + 0.870 * X_4 \\
 &+ 6.025 * X_1X_3 - 2.051 * X_2X_3 + 4.349 * X_3X_4 + 0.455 \\
 &* X_3X_5 - 2.957 * X_1X_2X_5 - 3.396 * X_2X_3X_5 - 1.838 \\
 &* X_1X_2X_6 - 0.339 * X_2X_7 - 0.359 * X_3X_7
 \end{aligned}$$

Equation 13

Many attempts have been made to model the reaction products from hydrothermal liquefaction. However, these models are limited by specific feedstocks, reaction temperatures or reaction times. These models are summarised in Table 2. Some models only predict crude yield and most of the existing kinetic models in literature do not include lignin which is a major constituent of lignocellulosic feedstock. As well as this, reaction pressure, mass loading of the biomass reactant in water and heating rate of the HTL reactor vary for each reaction model. Further work is required to develop a model which can predict the product composition of HTL product from reactions with varying biomass feed at different reaction times and temperature. As the reactions influence fluid dynamics and heat transfer in the reactor, they need to be well defined for the overall design of the HTL process to be optimised at industrial scale.

In order to model biomass feed, the organic components can be represented by carbohydrates, lignin, lipids and proteins, as can be seen from the examples above. Croce et al. (2017) modelled organic waste biomass with binary and ternary mixtures of carbohydrate, protein and lipid representative compounds. Their analysis involved identifying the compounds in the product streams of the HTL reactions. Results were compared for crude composition from HTL of organic wastes and crude produced from the model compounds. They were found to have similar compositions. The reference compounds chosen were cellulose, to represent carbohydrates, bovine serum albumin (BSA), to represent proteins, and tripalmitin, to represent lipids. Even simplifying the biomass composition in this way still resulted in sixty-four compounds being identified via GC-MS in the water soluble organics and crude product samples. Investigation into other model compounds for different types of biomass HTL feedstocks is required. The effect of different proportions of these model compounds on the products should also be investigated. Croce et al. (2017) agree that understanding of model compounds will be vital in implementing the models of HTL reactors to enable scale-up of the process.

To build a suitable kinetic model, representative polymer and monomer compounds can be used to represent the biomass feedstocks. The polymer and monomer compounds represent the different organic constituents of biomass. Model compounds are simpler in structure compared to biomass and hence undergo fewer reactions. This will allow identification of each of the reaction pathways for the carbohydrate, lipid, lignin and protein constituents of biomass. Once these are understood they can be used to build a model for more complex sources of biomass.

Table 2: Summary of Existing HTL Models

Model	Feedstock	Temperature (°C)	Reaction Time	Reaction Pressure (bar)	Mass Loading	Heat-up Time
Valdez et al. (2014)	Microalgae: <i>Chlorella protothecoides</i> , <i>Scenedesmus</i> sp., and <i>Nannochloropsis</i> sp.	250, 300, 350, and 400	0-60 min	-	15wt%	-
Luo et al. (2016)	Soy protein	200, 250, 300, and 350	0-60 min	-	15wt%	3 min
Hietala et al. (2016)	<i>Nannochloropsis</i> sp.	200, 300 and 400	0-60 min	-	15wt%	110–350 °C min ⁻¹
Sheehan and Savage (2017a)	Microalgae (70 published biocrude yields)	200, 250, 300, 350 and 400	0-60 min	Varying	Varying	Varying
Li et al. (2017)	24 different batches of microalgae feedstocks	300	30 min	-	-	-
Yin et al. (2015)	Sewage sludge	180, 220, 260 and 300	0-90 min	-	-	-
Qian et al. (2020)	Sewage Sludge	300, 350, 400, 500 and 600	0-60 min	400	2.2wt%	-
Teri et al. (2014)	Carbohydrate, protein and lipid model compounds	300, 350	20 and 60 min	86 and 165	15 wt%	-
Yang et al. (2019)	Lipid, cellulose, hemicellulose, lignin and protein model compounds	290	10 min	-	10 wt%	35-38 min

2.5 Model Compound Selection for HTL of Biomass

In order to create a reaction model which will be suitable for the many different types of biomass with varying compositions, model compounds can be used to represent the biomass. Model compounds which represent carbohydrate, lipid, lignin and protein content of the biomass feed are required. The literature available on the decomposition of these model compounds under hydrothermal conditions will assist in further developing reaction models. While yields as a function of a range of reaction conditions are reported in literature, as far as can be seen from the available literature, a set of kinetic equations which describes the crude, aqueous, gas and solid yields for the HTL of model compounds has only

been developed for glucose and soy protein. Previous HTL studies which have used model compounds as a feedstock and can be used to develop a kinetic model are discussed here.

Polymers are more similar to biomass feedstocks because of the additional cross links in their structures. Even though the chemical structures of monomer model compounds differ more from real biomass than do polymer model compounds, the use of monomer compounds in HTL experiments will give further insight into the decomposition products from HTL since the monomer compounds make up a large fraction of the intermediate products formed during reactions of biomass (Gao et al., 2012, Biller et al., 2011, Kruse et al., 2007, Ye et al., 2012). The interconversion pathways between solid, aqueous, crude and gas phases can be further understood from reactions with monomers.

Crude yields from HTL of polymers and monomers were 1% and 7% higher than real biomass respectively in an investigation of the variation in HTL products from mixtures of monomer and polymer model compounds (Dénier et al., 2017b). Yields were determined from the mass of the product fraction obtained divided by the mass of dry model compound or biomass feedstock. Model compounds were used to simulate the composition of black currant pomace. These model compounds were glucose, glutamic acid, guaiacol and linoleic acid for monomers. The model compounds for polymers were cellulose and alkali lignin. The better predictions from polymers are suspected to be due to the existence of crosslinked fibres in model polymers, which require more energy to decompose than do model monomers. During HTL of biomass, decomposition and hydrolysis break down these fibres. Lower gas yields by 3% for polymers and by 5% for monomers were also identified compared to biomass by Dénier et al. (2017b). For polymers solid yield was 8% lower and for monomers solid yield 23% lower than biomass. Further data is required to validate the differences between polymers and monomers in HTL reactions as these experiments were limited to one mixture to represent one type of biomass at one reaction time and temperature.

Model compounds can be used to identify the reaction pathways for HTL as well as the contributions of carbohydrate, lipid, lignin and protein components of biomass to the solid, aqueous, crude and gas product fractions. The reaction pathways identified for model compounds can then be further developed to model biomass including algae, lignocellulosic and sludge feedstocks.

2.5.1 Carbohydrates

2.5.1.1 Cellulose

Cellulose has been selected as a model compound for HTL in the current work as it is the most abundant organic compound on Earth. It is present in plants, algae and municipal solid wastes. Cellulose is made up of $\beta(1\rightarrow4)$ linked D-glucose monomers. Sasaki et al. (2004) investigated the reaction mechanism of microcrystalline cellulose decomposition in sub- and supercritical water. The experiments were carried out in a continuous-flow-type micro-reactor at temperatures between 320 to 400°C for residence times of 0.02 to 13.1 seconds and 25 MPa of pressure. Cellulose degradation was shown to follow Arrhenius behaviour, though different relationships were seen below and above 370°C. Above 370°C cellulose degradation became much faster. At higher temperatures swelling and dissolution of cellulose as well as pyrolytic depolymerisation increase. The reaction mechanism has been estimated by Sasaki et al. (2004) in Figure 7. A reaction rate model for cellulose conversion as a function of the radius of a cylindrical grain of cellulose was developed.

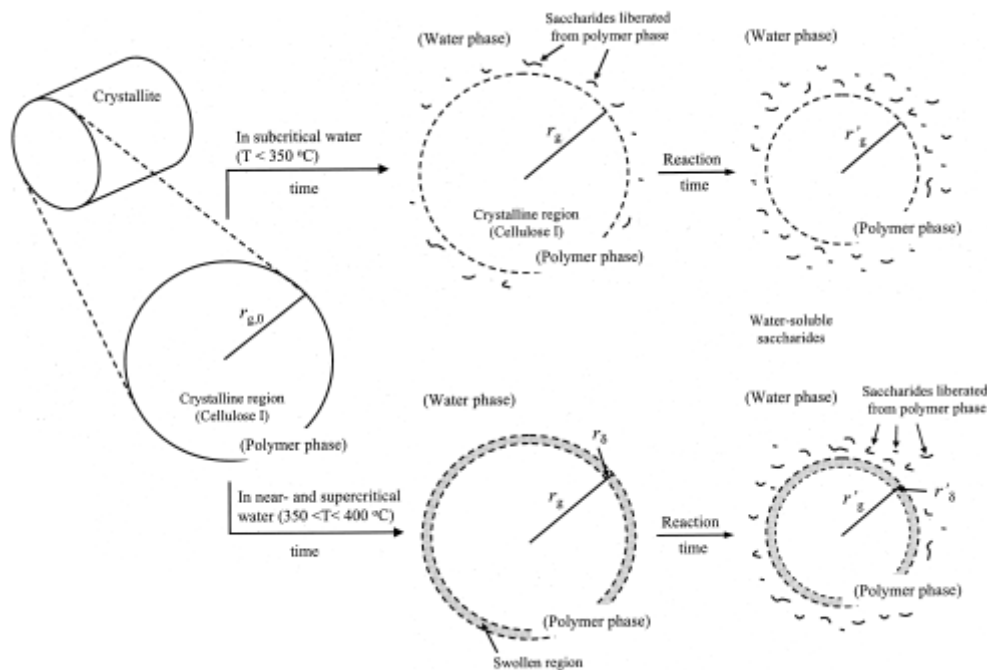


Figure 7: Cellulose reaction mechanism in sub- and supercritical water (Sasaki et al., 2004)

Yin and Tan (2012) analysed the compounds from the hydrothermal degradation of cellulose under acidic, neutral and basic conditions. pH was adjusted by using hydrochloric acid to prepare acidic solutions and sodium hydroxide to prepare alkaline solutions. Regardless of pH, crude yield increased from 275 to 320°C. Experiments were conducted at a pressure of 25 MPa. Crude yields decreased with increasing residence time from 0 to 30 minutes. Residence time began once the desired reaction temperature had been reached in the batch reactor and did not include heat-up time. Crude yield was highest under acidic conditions followed by neutral then basic conditions. Different mechanisms at different pH led to the formation of different compounds as show in Figure 8.

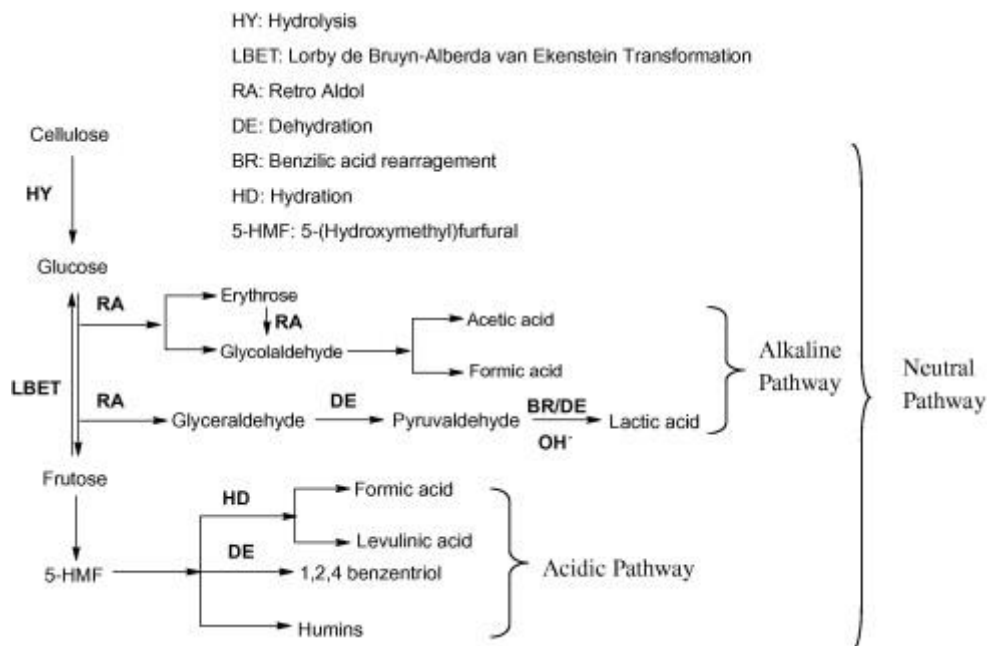


Figure 8: Products from cellulose decomposition at different pH (Yin and Tan, 2012)

Hemicelluloses are another group of carbohydrates which constitute a significant portion of lignocellulosic biomass. They have been found to hydrolyse at a lower temperature of 180°C in comparison to cellulose which hydrolyses at 230°C (Ando et al., 2000). However, the product distribution from HTL of hemicellulose has been found to be similar to the product distribution from HTL of cellulose. Xylan has been utilised as a model compound for hemicellulose in HTL. At a HTL reaction temperature of 300°C and reaction time of 30 minutes, crude yield from HTL of cellulose was found to be 15.00% and crude yield from the HTL of xylan was found to be 11.61% (Gao et al., 2011). In experiments with model compounds including xylan and cellulose at 290°C and 10 minutes, cellulose produced a crude yield of 14.23% and a solid yield of 32.43%, while xylan produced a crude yield of 5.27% and solid yield of 20.98% (Yang et al., 2018b). The more rapid decomposition of hemicellulose can result in higher aqueous and gas phase products compared to cellulose. Cellulose has been selected to model carbohydrates in this work as it is more abundant than hemicellulose and the product distributions from cellulose and hemicellulose are comparable.

2.5.1.2 Glucose

Glucose has been used as a model feed for HTL as the polysaccharides cellulose, hemicellulose and starch, which make up the majority of carbohydrates in biomass feeds, undergo rapid hydrolysis to form glucose among other saccharides (Toor et al., 2011). The mechanisms of glucose decomposition in sub-critical water have been studied and kinetic models have been suggested by Knežević et al. (2009) and Promdej and Matsumura (2011). At residence times of up to 60 minutes, glucose decomposition was confirmed to be a first order reaction.

Promdej and Matsumura (2011) performed experiments in a continuous tubular reactor where glucose was mixed with water and preheated to temperatures between 300 to 450°C at 25 MPa. The residence time was up to 60 seconds and glucose was almost completely decomposed at this range of temperatures. Not all of the many compounds from the hydrothermal reactions were identified. Promdej and Matsumura (2011) proposed the simplified reaction pathways shown in Figure 9. The kinetic equations and kinetic parameters were then derived.

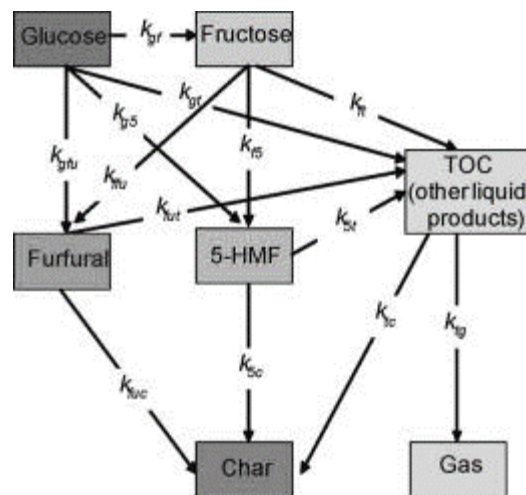


Figure 9: Reaction network for HTL of glucose (Promdej and Matsumura, 2011)

For the Arrhenius equation the pre-exponential factor was found to be $6.9 \times 10^7 \text{ s}^{-1}$ and activation energy 95.54 kJ/mol. These results agreed with previous work. However, not all of the reactions were found to follow Arrhenius behaviour in the

super-critical region even though overall glucose decomposition did follow Arrhenius behaviour. In the sub-critical region Arrhenius behaviour was observed.

Knežević et al. (2009) agreed that a first order kinetic model would provide sufficient accuracy for glucose decomposition in HTL with an activation energy of 114 kJ/mol. They performed experiments for up to 10 days and found that the reaction rate became much slower for residence times greater than 10 minutes. The reaction pathway was predicted and a lumped kinetic model developed as seen in Figure 10. The reaction products were divided into water soluble (WS), water solvent soluble (WSS), solvent soluble (SS) and water solvent insoluble (WSIS) fractions. Stoichiometric and kinetic parameters were found at 300 and 350°C.

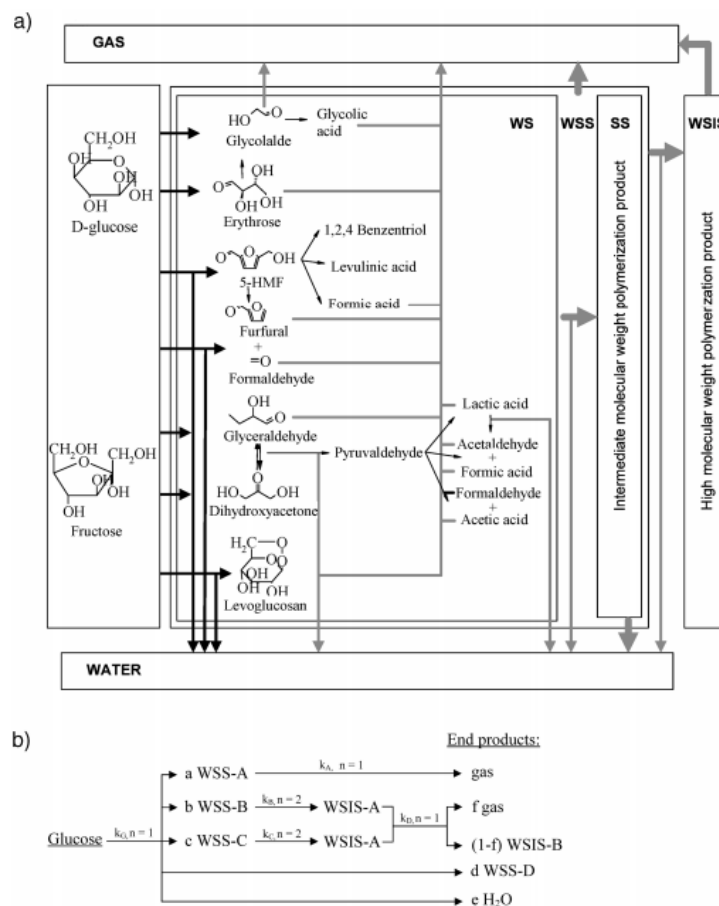


Figure 10: (a) Proposed reaction pathway and (b) kinetic reaction model for HTL of glucose (Knežević et al., 2009)

Surprisingly, another study by Knežević et al. (2010) found that the products from the HTL of glucose and the products from the HTL of wood gave similar yields and molecular weight distributions. This finding enabled the authors to build on their original kinetic model of glucose. A wood dissolution step at subcritical conditions was added to the start of the model as can be seen in Figure 11. They used a lumped model to describe the formation of WSS, WSIS and gas products.

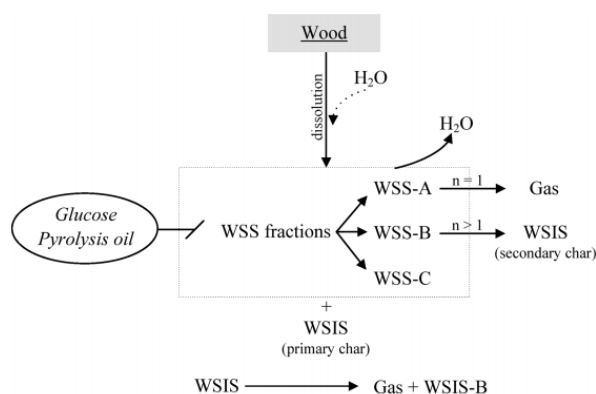


Figure 11: Lumped reaction network for HTL of wood (Knežević et al., 2010)

2.5.2 Lignin

2.5.2.1 Alkaline Lignin

Lignin is a class of complex organic polymers which are present in plant tissue and organic wastes. Kraft or alkaline lignin, which is extracted from plants using sodium hydroxide, sodium sulphide and water, has also been used as a model compound in HTL. Its decomposition products have been identified in sub- and supercritical water as catechol, phenol, m,p-cresol and o-cresol (Wahyudiono et al., 2008).

In experiments by Yong and Matsumura (2013) the decomposition of alkaline lignin at sub- and supercritical conditions was found to follow Arrhenius behaviour for the residence time of 0.5 to 10 seconds. A simplified reaction network was found in Figure 12. Unlike with the decomposition of carbohydrates, lignin decomposition at higher temperatures led to greater char formation.

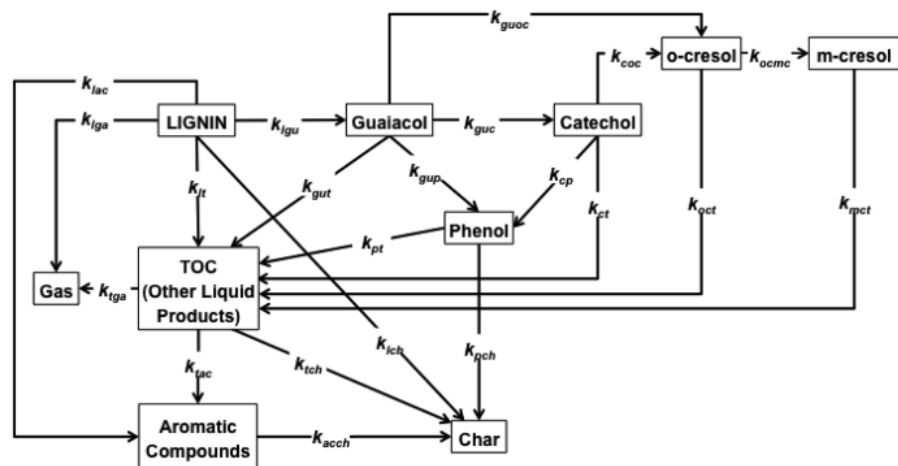


Figure 12: Proposed lignin conversion pathway in sub-critical water (Yong and Matsumura, 2013)

Zhou (2014) used Kraft lignin extracted from bamboo in HTL experiments. The yields of crude, gas and residual lignin were measured at temperatures of 130, 180 and 230°C and residence times of 15 and 60 minutes. The range of crude yields was between 5.4-10.6%. Longer residence times resulted in increased crude yields and higher temperatures resulted in decreased crude yields. Guaiacol was the main compound found in the crude making up 19 to 78%. Increasing reaction temperature and residence time increased lignin decomposition.

2.5.2.2 Guaiacol

Guaiacol has been used as a model compound for lignin degradation in supercritical water by Kanetake et al. (2007). Catechol, phenol and o-cresol were the main products identified and a set of first order kinetic equations was developed to describe this. Figure 13 shows the simplified reaction pathway for guaiacol. The decomposition of guaiacol was seen to follow Arrhenius behaviour.

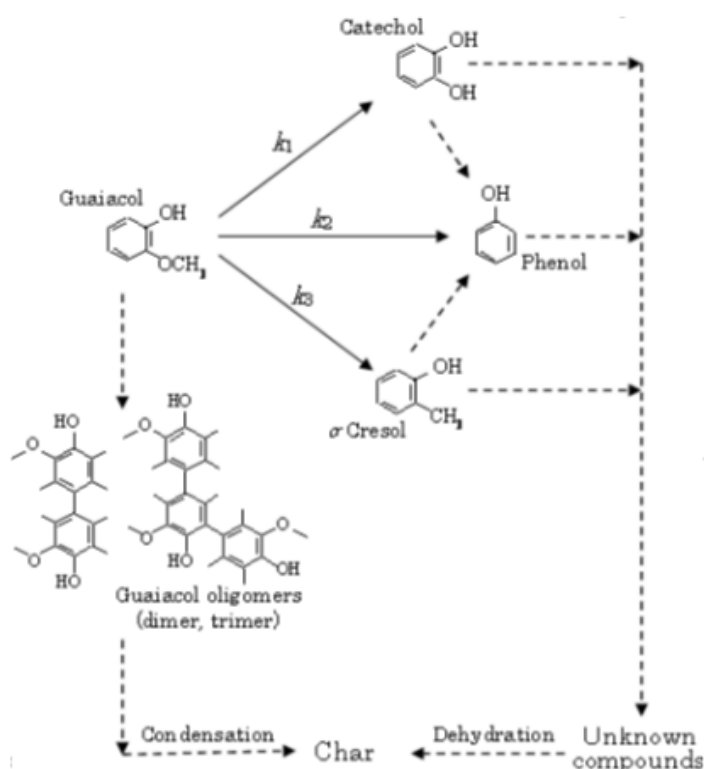


Figure 13: Simple reaction pathway for guaiacol in near- and supercritical water
(Kanetake et al., 2007)

2.5.3 Lipids

2.5.3.1 Sunflower Oil

Sunflower oil has been chosen to represent lipids by Biller and Ross (2011). They found that the decomposition of sunflower oil in HTL mostly resulted in the triglyceride being decomposed to fatty acids. Teri et al. (2014) also used sunflower oil as a model compound for HTL with reactions at 300°C for 20 minutes and 350°C for 60 minutes. They found the crude yield as a percentage of the sunflower oil added to the reaction mixture to be greater than 90%. Glycerol was found to be an intermediate product from HTL as well as fatty acids.

2.5.3.2 Oleic Acid

The fatty acid, oleic acid, has been identified as a product from the depolymerisation of sunflower oil in HTL (Biller and Ross, 2011). A study on the

decomposition of fatty acids in HTL has found them to be relatively stable, however decarboxylation to form long chained hydrocarbons has been observed (Gai et al., 2015). Understanding how lipids react in HTL after depolymerisation is necessary to be able to predict HTL product distribution.

2.5.4 Proteins

2.5.4.1 Bovine serum albumin (BSA)

Bovine serum albumin (BSA) is a protein model compound derived from cows. It was used by Croce et al. (2017) and Teri et al. (2014) in mixtures with other model compounds in HTL experiments. These experiments were conducted at one temperature and residence time combination by Teri et al. (2014) so the individual effect of temperature and residence time on crude production was not clear. Croce et al. (2017) conducted experiments with BSA in mixtures only, so the product yields from reactions of BSA alone are not identified. HTL of BSA by Sheehan and Savage (2017b) resulted in the findings that the yield of polypeptides, which make up the solid phase product in HTL, decreased with increased reaction temperature from 200 to 400°C.

2.5.4.2 Alanine

Proteins are composed of amino acid monomers, hence HTL of amino acids has been studied to understand HTL decomposition products. Alanine decomposition under hydrothermal conditions has been investigated by Klingler et al. (2007). The reaction network for temperatures between 300 to 450 °C and residence times of 2.5 to 35 seconds is shown in Figure 14.

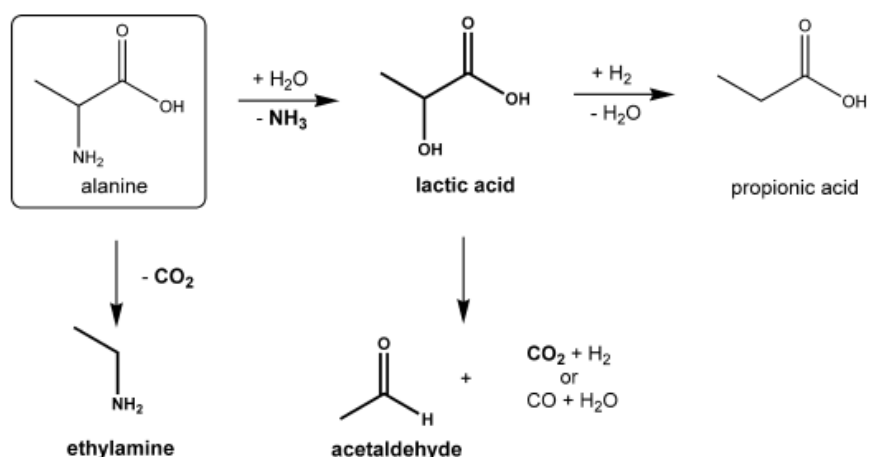


Figure 14: Alanine decomposition under hydrothermal conditions (Klingler et al., 2007)

Polymers and monomers to represent each of the organic constituents of biomass should be used in HTL experiments in order to develop a set of reaction pathways which represents all of the available biomass feedstocks for HTL. These include lipid, carbohydrate, and protein and lignin model compounds. Polymers can be used to more closely represent biomass and monomers simplify the HTL reactions further, allowing the reactions of intermediate compounds formed during HTL to be identified. Once these compounds are reacted alone, the model compounds can be reacted together to understand the reactions that occur between the include lipid, carbohydrate, and protein and lignin constituents of biomass.

2.6 Interactions between the Constituents of Biomass

Investigations on mixtures of model compounds in HTL have been reported in literature (Teri et al., 2014, Sheng et al., 2018, Lu et al., 2018, Déniel et al., 2017b) but are limited by reaction times, temperatures, mass loading of the biomass, heating rate of the reactor and the use of a particular solvent to extract the crude phase from the product mixture. Teri et al. (2014) found that the reactants in binary mixtures reacted independently from each other except for carbohydrate and protein binary mixtures where crude yield increased by around 10% at reaction conditions of 350°C and 60 minutes compared to single component reactions at the same conditions. At the less severe reaction conditions

of 300°C and 20 minutes, no increase in crude yields was observed for the mixture experiments compared to single component experiments. Hence, the mass averaged yield from independent model compounds could predict the products from the binary mixtures adequately. The study was limited to a total of six experiments with binary mixtures. Sheng et al. (2018) found that experiments with binary mixtures of castor oil, soya protein and glucose produced higher crude yields by up to 6% for the reaction temperature of 280°C and time of 60 minutes compared to single component experiments. Lu et al. (2018) identified that a lower crude yield by around 8% was produced from the mixture of lignin and lipid but the rest of the mixtures (protein and cellulose; protein and xylose; cellulose and lignin; xylose and lignin) produced greater yields than individual experiments by up to 35% at the reaction conditions of 350°C and 30 minutes investigated. Déniel et al. (2017b) conducted experiments on monomer and polymer model compounds in binary, ternary and quaternary mixtures at 300°C and 60 minutes and found that some combinations of model compounds increased crude yield, including carbohydrate and protein by 10%, whereas including lignin in binary mixtures with lipid, carbohydrate and protein resulted in decreased crude yields by up to 15%.

Several studies have focused on the Maillard reactions between the model carbohydrate and protein fractions of biomass (Minowa et al., 2004, Peterson et al., 2010, Zhang et al., 2016, Fan et al., 2018) which can cause an increase in crude yield at given reaction times and temperatures as opposed to the carbohydrates or proteins alone. Maillard reactions were studied with lactose and maltose as carbohydrate model compounds and lysine as the protein model compound by Fan et al. (2018). For the reactions at 250 and 350°C with a reaction time of 20 minutes, crude yield was higher by 10 to 39% for the mixtures compared to individual model compounds for carbohydrate and protein.

In summary, the literature reveals wide variation in crude yield from HTL of mixtures, and yields that also vary from the mass averaged yields from reactions with individual model compounds. However, there is no overall agreement on the

synergistic effect (increase in crude yield from mixtures compared to reactions with individual model compounds) or antagonistic effect (decrease in crude yield from mixtures compared to reactions with individual model compounds) of different mixtures on crude yield so this requires further investigation. In order to further understand the influence of different compositions of feedstocks on HTL products, the crude can be characterised using varied analytical techniques.

2.7 Crude Characterisation

Simulated distillation by thermogravimetric analysis (TGA) uses boiling point distribution to analyse crude and has been used by Vardon et al. (2011), Jazrawi et al. (2013) and Biller et al. (2015). The different boiling point ranges of proportions of crude allow the type of oil to be identified. For three different biomass feeds of *Spirulina* algae, swine manure and anaerobic sludge, Vardon et al. (2011) identified different proportions of heavy naphtha, kerosene, gas oil, vacuum gas oil and vacuum residue in the crude. Jazrawi et al. (2013) identified different fractions of heavy naphtha, kerosene, gas oil, vacuum gas oil and vacuum residue in the crude produced for the same species of algae feed at different temperatures and residence times. The relationship between crude composition, feed composition and reaction conditions is a vital part of understanding the HTL process.

Another method that can be used to characterise crude is Simulated Distillation using gas-chromatography flame ionisation detection (GC-FID) where the organics undergo combustion and the ion products from combustion are detected. Unlike TGA, GC-FID allows the identification of the organic compounds in the product to characterise the crude more accurately. Ramirez et al. (2017) utilised Fourier transform infrared (FTIR) analysis alongside gas-chromatography mass-spectrometry (GC-MS) to identify compounds. FTIR uses the different emission or absorption properties of compounds to identify the compounds existing in crude.

Gas-chromatography mass-spectrometry (GC-MS) has previously been utilised to identify the composition of crude. Characterisation of the crude produced from

HTL of biomass has proven to be difficult because of the many compounds formed during HTL as well as the large fraction of high molecular weight products which cannot be identified due to temperature limitations in GC-MS (Vardon et al., 2011). Crude characterisation via GC-MS has been undertaken for the HTL products of algae, manure and sludge feeds by Vardon et al. (2011) where they identified up to 13 different compounds for the crude produced from each feedstock. Each type of biomass, which was reacted at 300°C, 10-12 MPa and 30 minutes reaction time, produced crude which was primarily made up of different compounds. Hence crude composition is dependent on feedstock composition. Déniel et al. (2017a) conducted GC-MS on the crude produced from HTL of monomer model compounds. These monomer model compounds included glucose, xylose, glutamic acid, guaiacol and linoleic acid. The reaction conditions for HTL were 300°C for 60 minutes with a 30-35 minute heat up time with 15wt% dry matter. Monomer model compounds produced fewer reaction products which allowed the crude to be better characterised than the crude produced from real biomass. Hundreds of compounds were identified by GC-MS in the crude produced from microalgae by Shuping et al. (2010). The effect of reaction time and temperature on crude composition as well as identification of the compounds in the crude produced from carbohydrate, lipid, protein and lignin fractions of biomass should be identified.

Source rock analysis is a pyrolysis technique used to find petroleum-generative potential of rocks. The method finds the free crude content of a solid (S1), the free hydrocarbons that can be thermally distilled. As well as finding the source potential for crude generation (S2), hydrocarbons generated by pyrolytic degradation (Peters, 1986). This method can be used to determine the crude present in the solids generated from HTL. Since solvents have limited ability in extracting crude from HTL product mixtures, an alternative pyrolysis method to extract crude from the solids can also be employed. This analysis technique has not yet been used for identification of crude in HTL products to the best of our knowledge.

A combination of these analytical techniques can assist in the development of a kinetic model for the HTL of biomass. Further, the effect of reaction time and temperature on crude composition requires investigation.

2.8 Implications of Current Study

The evaluation of the literature above has indicated that many studies on the HTL of biomass and model compounds have been conducted and some advances in modelling the products from HTL have been made. Prediction of HTL products from varying types of biomass and the optimum reaction conditions for HTL is necessary to make the process viable for energy generation and waste management.

The focus of previous investigations on the products from HTL are on microalgae as a feedstock. Many feedstocks are being considered for HTL, including sewage sludge, food waste and lignocellulosic biomass. These sources are composed of different organic and inorganic fractions which will react differently under HTL conditions to produce variable products. In order to understand how these biomass feedstocks react, their organic constituents can be reacted alone and in mixtures to find optimum reaction conditions for maximum crude production.

Further limitations of previous work include inconsistent reaction conditions, including reaction pressure, mass loading of the biomass reactant in water, heating rate of the HTL reactor and the solvent used to separate crude from the HTL product mixture. Reactions should be conducted with consistent methods used so the effect of reaction temperature, time and feedstock composition can be clearly identified.

Using model compounds, the kinetic pathways to predict the products from HTL of various biomass sources can be developed. Experiment with biomass can then be conducted to validate the use of this model.

2.9 Objectives of Thesis

The objective of this study is to develop a kinetic model for hydrothermal liquefaction of various types of biomass and characterise the renewable crude product by completing the following detailed objectives:

1. Develop a kinetic model for the HTL of individual carbohydrate, lipid, lignin and protein polymer model compounds which predict solid, aqueous, crude and gas phase yields.
2. Investigate the relationship between the products from polymer model compounds in HTL and monomer model compounds. A kinetic model for the reactions of monomers in HTL will be developed to assist in understanding the conversion pathways of intermediate products produced during HTL.
3. By conducting experiments with mixtures of carbohydrate, lipid, lignin and protein model compounds in HTL, interactions between the reactants and products can be observed and a kinetic model which accounts for these interactions can be developed.
4. Modify the reaction model to account for real biomass including algae, lignocellulosic biomass and sludge. The variations in the product distribution and crude composition between model compounds and different types of biomass can be identified.

Chapter 3

The elucidation of reaction kinetics for
hydrothermal liquefaction of model
macromolecules

R. Obeid ^a, D.M. Lewis ^a, N. Smith ^a, P. van Eyk ^a

^aThe School of Chemical Engineering and Advanced
Materials

The University of Adelaide, SA 5000, Australia

The Chemical Engineering Journal, Published.

Statement of Authorship

Title of Paper	The elucidation of reaction kinetics for hydrothermal liquefaction of model macromolecules
Publication Status	<input checked="" type="checkbox"/> Published <input type="checkbox"/> Accepted for Publication <input type="checkbox"/> Submitted for Publication <input type="checkbox"/> Unpublished and Unsubmitted work written in manuscript style
Publication Details	Published in The Chemical Engineering Journal R. Obeid, D. Lewis, N. Smith, P. van Eyk, The elucidation of reaction kinetics for hydrothermal liquefaction of model macromolecules, Chemical Engineering Journal 370 (2019) 637-645.

Principal Author

Name of Principal Author (Candidate)	Reem Obeid
Contribution to the Paper	HTL reactor design and methods HTL batch experiments completed Methods developed for product separation and product separation completed Thermogravimetric analysis completed Construction of model Writing and editing
Overall percentage (%)	80
Certification:	This paper reports on original research I conducted during the period of my Higher Degree by Research candidature and is not subject to any obligations or contractual agreements with a third party that would constrain its inclusion in this thesis. I am the primary author of this paper.
Signature	Date 28/01/2020

Co-Author Contributions

By signing the Statement of Authorship, each author certifies that:

- the candidate's stated contribution to the publication is accurate (as detailed above);
- permission is granted for the candidate to include the publication in the thesis; and
- the sum of all co-author contributions is equal to 100% less the candidate's stated contribution.

Name of Co-Author	David Lewis
Contribution to the Paper	Concept development Assistance with analysis and interpretation of data Drafting of paper
Signature	Date 21-Feb-2020

Chapter 3 – The elucidation of reaction kinetics for hydrothermal liquefaction of model macromolecules

Name of Co-Author	Neil Smith		
Contribution to the Paper	Concept development Assistance with analysis and interpretation of data Drafting of paper		
Signature		Date	28/1/2020

Name of Co-Author	Philip van Eyk		
Contribution to the Paper	HTL reactor design and methods Concept development Assistance with analysis and interpretation of data Drafting of paper		
Signature		Date	28/1/2020



Contents lists available at ScienceDirect

Chemical Engineering Journal

journal homepage: www.elsevier.com/locate/cej



The elucidation of reaction kinetics for hydrothermal liquefaction of model macromolecules



Reem Obeid, David Lewis, Neil Smith, Philip van Eyk*

School of Chemical Engineering, The University of Adelaide, Adelaide, South Australia 5005, Australia

HIGHLIGHTS

- Reaction time and temperature varied for optimum crude yield for each compound.
- Simulated distillate fractions of crude vary with reaction time and temperature.
- Bulk kinetic model to predict product yields from HTL of model compounds developed.

ARTICLE INFO

Keywords:

Hydrothermal liquefaction
Kinetics
Model
Lipid
Carbohydrate
Protein
Lignin

ABSTRACT

Conversion of waste to energy via the hydrothermal liquefaction (HTL) of biomass in hot compressed water is an emerging technology. In order to efficiently design and optimise industrial scale HTL processes, it is necessary to be able to predict the quantity and composition of the products. Various biomass feedstocks are being considered as feedstock for the HTL process and they are composed of different combinations of carbohydrate, lignin, lipid, protein and inorganic compounds, which react very differently under HTL to form distinctive products. The yields of the products from HTL, including renewable crude oil, gaseous, solid and aqueous phases, have been quantified via multivariate experiments in this work for four model compounds: cellulose, alkaline lignin, sunflower oil and bovine serum albumin (BSA). Simulated distillation via thermogravimetric analysis (TGA) has been used to find the hydrocarbon fractions of the renewable crude products. A bulk kinetic reaction model has been established for each of the four model compounds in order to develop a general model which can predict the HTL products of various feedstocks. For temperatures of 250, 300 and 350 °C and residence times from 0 to 60 min in a HTL batch reactor, higher reaction temperatures and longer reaction times generally resulted in lower renewable crude yields containing higher proportions of the more preferable diesel-like petroleum fractions.

1. Introduction

Hydrothermal liquefaction (HTL) involves the conversion of biomass in sub-critical water conditions to a renewable crude oil that has an increased calorific value along with other by-products. Biomass feedstocks with up to 90% water content are favourable for conversion via HTL. Hence, HTL has the potential to provide an effective waste management solution for various biomass sources including sewage sludge, agricultural waste and food waste. Currently there is a lack of kinetic data which will allow the products from HTL to be predicted and quantified. The products from HTL include renewable crude oil, aqueous, solid and gas phases. Biomass is made up of different fractions of carbohydrate, lignin, lipid and protein as well as an unreactive ash fraction. However, this can vary significantly depending on the source

and time period from which it is obtained. Previous studies have confirmed variation in the chemical properties of HTL product from different biomass sources including diverse strains of algae, agricultural waste and products from waste water treatment [1,2]. The use of different reactants for HTL also produced variation in renewable crude molecular weight distribution, boiling point range of compounds in the renewable crude, individual compounds produced from HTL and differences in renewable crude functional group chemistry. It is therefore uncertain what effect variations in the properties of biomass will have on the yield of HTL products.

To enable the products from HTL to be quantitatively modelled, the chemical composition of the feedstock needs to be related to the product phases. This requires finding the yield of each product phase via multivariate HTL experiments on model compounds representing the

* Corresponding author.

E-mail address: philip.vaneyk@adelaide.edu.au (P. van Eyk).

<https://doi.org/10.1016/j.cej.2019.03.240>

Received 12 December 2018; Received in revised form 22 February 2019; Accepted 26 March 2019

Available online 27 March 2019

1385-8947/ © 2019 Elsevier B.V. All rights reserved.

carbohydrate, lignin, lipid and protein fractions of biomass. During HTL the model compounds are hydrolysed and degraded at different rates, in conjunction with recombination of intermediate products. This results in the production of different compounds with varying time, temperature and pressure. Previous work using model compounds has been done by Teri, Luo and Savage [3] where sunflower oil, soy protein and corn starch were individually subjected to HTL at 350 °C, 165 bar and varying residence times from 10 to 90 min. The authors also reported results for sunflower oil, soy protein and corn starch at another set of reaction conditions, 300 °C, 86 bar and 20 min, however more experiments are required to further elucidate how reaction conditions affect phase yields. Biller and Ross [4] performed HTL on the model compounds albumin, soya protein, asparagine, glutamine, glucose, starch and sunflower oil at 350 °C and 1 h to give an indication of the different yields from specific feed fractions. Teri, Luo and Savage [3] and Biller and Ross [4] agree that the HTL of lipids results in the highest yield of crude oil product followed by proteins, then carbohydrates. Many studies on HTL of individual model compounds have also been undertaken [5–9], however inconsistent reaction conditions and separation methods for product quantification were reported which can give inconsistent product yields. It is then necessary to determine kinetics of the model compounds under consistent and well controlled conditions. A greater number of experiments at different temperatures and residence times are also required in order to develop a predictive model.

Quantitative reaction kinetics that enable the yields of each product phase to be predicted in HTL are currently limited in literature. Kinetic models for the HTL of different strains of algae have been presented [10–14] as well as a kinetic model for soy protein [6]. The work from these papers involved fitting a set of first order differential equations to experimental data obtained from laboratory scale batch HTL reactions. A multicomponent additivity model has been developed by Li, Leow, Fedders, Sharma, Guest and Strathmann [15] for microalgae from experiments at 300 °C and 30 min. The model was then used to predict yields for HTL products from wastewater sludge and manure with some accuracy. However, further research is needed due to the limited data available on reactants, reaction conditions and products from these biomass sources. All of these models use the lipid, protein and carbohydrate contents of the reactant to predict the product phase yields. Further development of a model is required to predict the HTL product phase yields given a range of feedstocks which undergo HTL under varying reaction conditions.

The effect of reaction conditions on the composition of biocrude should also be quantified to enable the yield of a specific target fuel to be optimised. Previously, different solvents have been used to distinguish between heavy and light renewable crude fractions. Valdez, Dickinson and Savage [16] found varying yields of light and heavy renewable crude with different HTL processing time and temperature for the same algae. As the solvents extract compounds based on their solubility, different solvents will result in different yields for various fractions dependent on the polarity of the extractable compounds [17]. Another possible method to characterise the crude fractions is distillation by thermogravimetric analysis (TGA), where the biocrude can be separated by boiling point [18].

The aim of this work was to quantify the product yields from biomass HTL with water as the solvent so that a general kinetic model could be generated. The development of a kinetic model will assist with scale-up of the HTL process as further information on reaction products are required for the design of large-scale reactors. Other limitations for scale-up, including wall thickness of the reactors required at high pressures are currently being tackled in several pilot scale plants being developed globally [19]. To generate the kinetic model, product yields were found during experiments with different model compounds under the same reaction conditions to give comparable yields. Plausible reaction paths for the formation of the renewable crude, gas, solid and aqueous product phases from the four different model compounds have been postulated and first order differential equations for reaction

kinetics have been fit to the data. This allows the product yields from the HTL of carbohydrate, lignin, lipid and protein compounds to be sufficiently predicted. Yields of renewable crude in the boiling point range of petroleum crude fractions obtained from TGA allow the identification of favourable feed stocks and conditions to produce a particular target fuel.

2. Materials and methods

2.1. Materials and feedstock analysis

The lipid used as a model compound was Crisco 100% Pure Premium Sunflower Oil from the supermarket. The carbohydrate model compound was extra pure microcrystalline cellulose from Acros Organics with an average particle size of 90 µm and a maximum impurity level of 10 ppm heavy metals. Alkaline lignin from Tokyo Chemical Industries was the model compound for lignin which contained a maximum of 10% moisture. Bovine serum albumin purchased from Serana Europe specified at over 98% purity and composed of over 96% amino acids was the protein model compound used. Chloroform was the organic solvent used to extract the renewable crude from the HTL product.

Thermogravimetric analysis was performed on a Netzsch simultaneous thermal analyser (STA) 449 F5 Jupiter for each of the model feedstocks. This allowed the simulated distillate fractions for the untreated feed to be compared to the simulated distillate fractions of the HTL renewable crude product, giving insight into the variations in renewable crude product from different reaction time and temperature.

2.2. Hydrothermal liquefaction in a batch reactor

2.2.1. Reactor

The batch HTL reactor, presented in Fig. 1, was made up of a 20 cm long 316 stainless steel tube, which has a 12.5 mm outer diameter and 2 mm wall thickness. On each end it had a 12.5 mm Swagelok® port connector and fittings made from 316 stainless steel. The tube section of the reactor has a volume of 11 mL. One end was capped and the other was connected to a tube where a Type K mineral insulated thermocouple had been inserted. The top of the reactor was connected to a tube with a diameter of 3.2 mm to prevent the reactor contents entering the top half of the reactor. A cross section from this tube connected a pressure transducer and pressure relief valve to the reactor system. Ball valves were connected to each side of the top section of the reactor. These allowed the reactor to be purged of oxygen and pressurised with nitrogen prior to HTL reactions. The gas was released from the reactor via a ball valve after reaction.

2.2.2. Batch HTL experimental procedure

The starting pressure for each experiment was determined by trial and error in preliminary experiments for each model compound at each temperature by measuring pressure for the duration of each experiment. At each of the three different temperatures for the four different model compounds a different starting pressure was required to achieve 200 bar of pressure at the reaction temperature. Starting pressures were between 80 and 120 bar.

For each of the single model compounds, the reactor was filled to 50% of the reactor tube volume at room temperature. The model compound made up 30% of the mass of the reactant mixture with 70% water. The reactor was then weighed.

The reactor was charged with nitrogen from a high pressure nitrogen gas cylinder. It was charged to 200 bar with nitrogen and left for 3 min to ensure that the reactor would not leak at the starting pressure. The reactor was then vented and charged to the starting pressure required to achieve a pressure of 200 bar at the given reaction temperature. This ensured that reaction pressure was consistent for each experiment. The reactor was then weighed to find the mass of nitrogen

Chapter 3 – The elucidation of reaction kinetics for hydrothermal liquefaction of model macromolecules

R. Obeid, et al.

Chemical Engineering Journal 370 (2019) 637–645

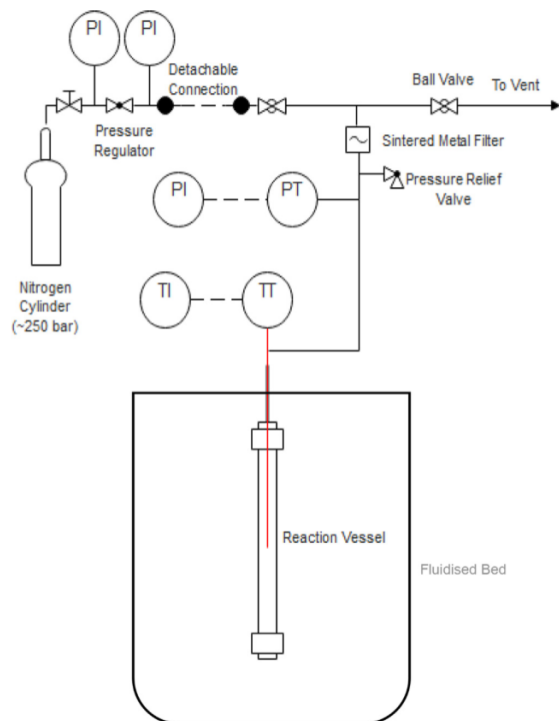


Fig. 1. HTL reactor configuration.

added.

The reactor was heated in a Techne SBL-2D fluidised bed with a Techne-9D temperature controller to vary temperature set-point and air flow rate through the bed. This allowed uniform heating of the reactor at the range of reaction temperatures required. Once the reactor was placed in the pre-heated fluidised bed the reactor contents were heated at a rate of approximately 125 °C per minute. When the reactor contents reached 98% of the reaction temperature, the timer was set for the desired residence time. After the residence time elapsed, the reactor was removed from the bed and cooled with a fan to 70 °C within 4 min before being quenched in water at ambient temperature.

2.3. Recovery and separation of products from HTL

2.3.1. Product recovery

Immediately after cooling, the reactor was wiped with a cloth to remove any sand or water from the outside. It was then weighed before gas release and then after gas release to find the mass of gas present after HTL. The mass of nitrogen added to the reactor prior to reactions was subtracted from the total mass of gas released after HTL to obtain the mass of gas produced from reactions.

The reactor top was then removed to empty the reactor of its liquid and solid contents. Following this the reactor was rinsed three times with a total of 10 g of chloroform solvent to remove any soluble oil or solids stuck to the reactor walls. The solvent-product mixture was then centrifuged for 15 min at 2000 rpm to form three distinct layers. These include an organic, aqueous and solid phase. The organic phase was pipetted from the centrifuge tube and placed in a separate tube for analysis. The organic renewable crude-solvent mixture was then dried at ambient temperature by applying a stream of nitrogen to a Büchner flask containing the mixture and venting the evaporated solvent for four and a half hours or until there was no mass change observed for the renewable crude. Renewable crude has been defined as the solvent-

soluble product.

The mass of solid produced from HTL was found by filtering the solids from the liquid phases and then drying the solids in an oven at 80 °C overnight. The yield of gas, renewable crude and solid phases was calculated by dividing the mass of each by the mass of the biomass model compound initially fed to the reactor. Aqueous phase product yield was calculated by difference from the initial mass of the biomass model compound added to the reactor. The aqueous phase has been defined as the liquid HTL product that is not soluble in solvent.

The HTL experiments and extractions were repeated three times for each model compound for experimental conditions of 350 °C and 20 min to check variation in yields and product fractions. The variation in yields for all four product phases and model compounds was $\pm 5\%$.

2.3.2. Product separation variations

The four model compounds produced very different products. While the lipid and protein produced no to minimal solids, carbohydrate and lignin produced a significant amount of solid. This meant that product separation after HTL had to be varied to optimise renewable crude recovery.

To recover the maximum quantity of HTL product in this work, extractions with and without solvent were performed. While solvent is not likely to be used at commercial scale, in order to provide accurate product yields from small scale batch reactions, maximum product recovery was essential in the extraction process. For the carbohydrate model compound, solvent was not required for maximum recovery of product. For lipid, protein and lignin model compounds, solvent was required for maximum product recovery due to the crude being attached to the reactor walls. The average recovery of product from the reactor was 90% of the feed placed into the reactor for all four model compounds.

The formation of carbon microspheres have been observed on chars from the hydrothermal treatment of cellulose [20,21]. The porous and readily transformed structure of the char from HTL of cellulose made it difficult to extract the renewable crude with solvent so that the majority of it stayed bound up in the solids. This was observed as the solids analysed via TGA after solvent extraction contained a large majority of product in the boiling point range of biocrude. Hence, for the cellulose product instead of adding solvent to the HTL product from the reactor, the product was removed, then filtered and the solids were put into a TGA to determine the renewable crude yield. A similar method has been used by Chen, Zhang, Zhang, Yu, Schideman, Zhang and Minarick [22] for product separation from algae HTL where oil was absorbed by the porous char.

TGA of the solid product from HTL of lignin indicated that much less product in the distillate range of renewable crude was present and the majority of it could be extracted with the use of solvent. This could be due to the stable phenolic structure of lignin preventing significant conversion during hydrothermal treatment [21]. Comparing crude yields from solvent extraction to crude yields found via TGA resulted in negligible variations in yield for lignin, so solvent extraction was used to quantify yields for lignin.

2.4. Analysis of products from HTL

Approximate fuel fractions are predicted via simulated distillation using TGA of the renewable crude using the ranges given by the ASTM [23]. This gives further insight into conversions of the product with time and temperature so that the reaction paths can be understood and reaction conditions can be controlled depending on the target fuel. The fuel fractions from TGA are the percentage of biocrude with boiling point in the range of gasoline and naphthas (80–205 °C), kerosene (205–255 °C), diesel (205–290 °C), gas oil (255–425 °C) and wax, lubricating oil and vacuum gas oil (425–600 °C). The renewable crude fractions with higher boiling points are the heavier fractions.

Industrial scale refining of renewable crude would result in the

Chapter 3 – The elucidation of reaction kinetics for hydrothermal liquefaction of model macromolecules

R. Obeid, et al.

Chemical Engineering Journal 370 (2019) 637–645

removal hetero-atoms including sulphur, oxygen and nitrogen. This would cause the fuel fractions to deviate from what is predicted by TGA of the renewable crude extracted in these experiments.

2.5. Kinetic parameters

Rate constants have been fitted to multiple reaction pathways for each model compound using the *lsqcurvefit* optimisation function in MATLAB to solve for the different sets of first order ordinary differential equations (ODEs). Initially rate constants were found for the all of the pathways shown in Fig. 1a. The addition of some of these pathways which gave chemically meaningful results but similar fits to the data were ignored to make the model suitable for use in separate computer fluid dynamics (CFD) modelling of the HTL process. Hence, the simplified pathways shown in Fig. 1b-e were chosen for the model.

To find the initial conditions for the mathematical model, the untreated biomass model compounds were added to 5.5 mL of water followed by 10 mL of chloroform solvent. This allowed the organic phase (renewable crude), solid phase and aqueous phase products to be quantified by using the same separation procedure for the untreated feed mixture as the HTL product.

Experiments were also performed with individual model compounds at each temperature where the products were extracted immediately after heat up time to give a zero minute reaction time. Conversions after this time are presented in the [Supplementary Material in Table S1](#) and were significant. Hence, the untreated feed mixture composition was used to give the initial conditions in the model to give a clearer representation of conversion due to hydrothermal treatment.

3. Results and discussion

3.1. Lipid

The renewable crude yields shown in Fig. 3(a), were higher for sunflower oil than they were for any other compound used in this investigation, as is anticipated for the lipid model compound. The yield results for HTL reactions at 250 °C and 300 °C for all four model compounds as well as the TGA results for the renewable crude formed at these reaction temperatures can be found in the [Supplementary Materials in Figs. S1–S8](#). The symbols on the graphs depicting TGA results represent experimental results and they are connected in a line graph. TGA of the raw model compound showed that the untreated sunflower oil product was completely in the distillate range of renewable crude between 80 and 600 °C. Extractions using chloroform on the unreacted feed and water mixture demonstrated that all of the sunflower oil was soluble in chloroform. HTL treatment caused an increase in aqueous phase soluble compounds. Before HTL treatment ~80% of raw sunflower oil reported in the heavier gas oil distillate range (255–425 °C). After hydrothermal treatment the two heaviest oil fractions decreased by a total of around 20% as can be seen in Fig. 3(b) for experiments at 350 °C. TGA results also indicated that longer residence times generally result in higher diesel-like yields (205–290 °C) for the renewable crude product from the HTL of sunflower oil. This is likely the result of degradation of high molecular weight long chained fatty acids to lighter compounds. Unprocessed soya oil was also found to have a higher molecular weight distribution than the HTL product by Biller, Riley and Ross [24]. In the work by Teri, Luo and Savage [3] where dichloromethane soluble and hexane insoluble products were classified as heavy biocrude, the lipid biocrude product was made up primarily of lighter product, however in this work where TGA has been used, the opposite result was found. A solvent which removes lower molecular weight products from the HTL product mixture, like hexane, was not used in this work to extract the renewable crude that was analysed via TGA. Hence, these low molecular weight products could have remained in the aqueous phase.

The highest percentage of renewable crude was produced at the

mildest reaction conditions, 0 and 10 min residence time at a reaction temperature of 250 °C in Fig. S1(a). This is because the product from the hydrothermal treatment of sunflower oil was similar to the raw feed composition at low reaction time and temperature. After this, yield decreased with increasing residence times at each temperature. Optimum renewable crude yield with more favourable light oil fractions occurred at 300 °C and at lower residence times at 350 °C. More severe reaction conditions, with higher reaction temperature and time, appeared to lead to degradation of heavier compounds which created more aqueous phase soluble compounds. However, the most severe reaction conditions produce the highest amount of renewable crude in the distillate range of diesel.

Hydrothermal treatment of sunflower oil has been reported to produce renewable crude yields of over 90% [3]. Biller and Ross [4] achieved a yield of 80% for sunflower oil HTL at 350 °C and 200 bar for 1 h. The biocrude yield reported in this work at these conditions is 60%, with a higher gas yield of 14% being produced. The heating rate of the reactor is suspected to affect product yields because of the many chemical reactions that occur during heat up time of the reactor [25,26]. This could be the cause of these discrepancies. Another possibility for the variation is the smaller compounds not being included in the renewable crude yield because the chloroform solvent did not extract them in this work as hexane has in previous studies [3].

Gas yield was highest at the 20 and 30 min residence times for sunflower oil and very low at a residence time of 0 min at all three reaction temperatures, which suggests that the sunflower oil required longer reaction times to be converted to gaseous products. It remained between 0 and 19% for all tests. No solids were visible in any test with sunflower oil.

Low energy recovery from HTL of cooking oils to produce biocrude was also reported by Midgett, Stevens, Dassey, Spivey and Theegala [27]. However, feedstocks that contain a higher amount of lipids will produce more biocrude because the lipids still produce the greatest amount of biocrude after hydrothermal treatment.

3.2. Carbohydrate

For the carbohydrate model compound renewable crude yield reached a maximum of 30% up to 30 min reaction time at 250 and 300 °C in Figs. S3(a) and S4(a). At 350 °C the maximum renewable crude yields was 20%. The results shown in Fig. 4(b) for 350 °C where the heavy renewable crude fraction decreases by over 30% between 10 and 20 min correspond with a decreasing total renewable crude yield of 5% between 10 and 20 min in Fig. 4(a). As the heavier compounds are reduced so is the renewable crude yield here. According to the work by Rogalinski, Liu, Albrecht and Brunner [28] carbohydrate decomposition increased rapidly with temperature for residence times of 0 to 3 min. Yin and Tan [29] also observed that higher temperatures from 300 to 320 °C and residence times from 0 to 30 min had a negative effect on renewable crude yield because the main biocrude compound formed, hydroxymethylfurfural (HMF), was converted to solid and gas phase products at these conditions.

Solid yield decreased most substantially from 0 to 10 min residence time then did not vary as significantly after that at all three temperatures. Gas yield was highest for experiments at 350 °C followed by 250 °C then 300 °C. At the two higher temperatures, a higher aqueous phase yield also resulted. Reaction time caused very little variation on the renewable crude fractions from cellulose HTL after 30 min residence time as can be seen in Fig. 4(b), S3(b) and S4(b). This could be due to the high molecular weight compounds formed from cellulose decomposition and the high molecular weight compounds formed from recombination of the decomposition products from cellulose HTL having a high thermal stability. Hence, increased residence time resulted in fewer heavy compounds being decomposed to lighter compounds.

Chapter 3 – The elucidation of reaction kinetics for hydrothermal liquefaction of model macromolecules

R. Obeid, et al.

Chemical Engineering Journal 370 (2019) 637–645

3.3. Protein

The protein model compound produced minimal solids except at the two lowest residence times at 250 °C. This is consistent with the work by Sheehan and Savage [26] where maximum solid yield was obtained at 1 min residence time and 200 and 250 °C. The untreated BSA was not fully soluble in water at room temperature and 30% mass loading. For all three temperatures at a residence time of 10 min, HTL of BSA resulted in a renewable crude yield of around 10% and the aqueous phase yield was at a maximum, which can be seen in Fig. 5(a), S5(a) and S6(a). From reaction times of 10 to 20 min the renewable crude yields increased by 20 to 70% at the three reaction temperatures. Lower temperature resulted in higher renewable crude yield and for the two lower temperatures, increasing residence time over 30 min had a negative effect on renewable crude yield as the products moved into the aqueous phase. Sheehan and Savage [26] also found that a residence time of 30 min and higher resulted in lower crude yields than the crude yields obtained at shorter residence times for 300 and 350 °C. They identified that during HTL polypeptides were broken down to smaller molecules, including amino acids, which would be soluble in the aqueous phase.

For the HTL product of algae protein, gas yields were found to be 30 to 45% by Yang and Jones [30] for a temperature range of 220 to 300 °C. For soy protein Luo, Sheehan, Dai and Savage [6] found gas yields of 0 to 20% for a temperature range of 200 to 350 °C. The gas yields from this work were calculated to be 0 to 30% at 250, 300 and 350 °C. Different sources of protein compounds appear to produce different gas yields.

For the two higher temperatures there was little variation with residence times in the yields of each of the different renewable crude-like product fractions from HTL of BSA. This is visible for reactions at 300 °C in Fig. S6(b) and 350 °C in Fig. 5(b). Lower temperatures and residence times in HTL resulted in greater proportions of the heavy product fraction, which is consistent with the heavier fraction present in the untreated BSA. After 10 min residence time at the two higher temperatures renewable crude fractions did not vary significantly. For optimum renewable crude yield and a greater proportion of the more favourable lighter petroleum-like fractions, a residence times of 30 min was favourable at each of the three temperatures.

3.4. Lignin

Renewable crude yield was under 7% for all experimental conditions for the alkaline lignin which can be seen for the highest temperature as shown in Figs. 6, S7 and S8. At a reaction temperature of 280 °C and 15 min residence time Karagöz, Bhaskar, Muto and Sakata [31] found an oil yield of ~ 4% from the HTL of alkaline lignin. Alkali lignin was also used in HTL experiments at 350 °C and 30 min by Lu, Liu, Zhang and Savage [32] where a biocrude yield of 1.4% was obtained. This low yield was likely due to the increase in cross-linked materials that occurs with the extraction of lignin, which makes it even more resistant to hydrothermal degradation than the lignin in plant form [33]. While native lignin mostly contains -O-4 linkages depending on the biomass type, for example in rye straw [34], the treated alkaline lignin contain more C-C linkages due to cleavage of ester linkages [35].

At 250 °C in Fig. S7 the highest gas yield resulted as well as the highest set of renewable crude yields. The majority of the lignin HTL product was distributed into the aqueous phase. High lignin content in biomass was also found to produce a higher proportion of water soluble organics by Arturi, Kucheryavskiy and Søgaaard [36]. Minimum solid residue was achieved just after heat up time for the three temperatures with less solid product at the higher temperature. The raw lignin was partially soluble in water at room temperature with a 30% mass loading. High solids yields are expected with increasing reaction temperature and time as polymerisation and carbonisation of mono-phenols has been predicted by Nonaka and Funaoka [37] for a lignin model

compound and this was also seen in this work.

The yields of renewable crude from lignin after drying the solvent were too small to obtain samples for TGA. TGA of the solids after HTL showed a yield of heavy oil bound to the solids which is under 4% of the original biomass feed.

3.5. Postulating kinetic pathways

From the data for yields of the different HTL products, probable reaction pathways were postulated for each of the model compounds. The yields obtained are indicative of the product phases obtained once the HTL product has been cooled to room temperature and the pressure of the reactor has been returned to atmospheric pressure. Hence, the reaction paths postulated are related to the product phases produced at room temperature and atmospheric pressure. The zero minute reaction time was determined by the solubility of the feedstock for the mass loading in reactions at room temperature.

For the sunflower oil product from HTL, aqueous phase product was formed in the early residence times at the two higher temperatures which indicates there was direct conversion from sunflower oil to aqueous phase products. There appeared to be some transfer of compounds between the aqueous and renewable crude phase as they increased and decreased in opposite directions at all three temperatures. No solid product was found in any of the HTL experiments with sunflower oil so there was no kinetic path from sunflower oil to solid product. A gas yield was present so there was conversion of products from liquid phases to the gas phase.

For cellulose the gas phase increased with increasing residence time so it appeared not to be converted to any other phase. There was also an increase in the amount of aqueous phase present with increasing temperature for the heat up time to reach reaction temperature. Different aqueous phase compounds were likely formed directly from the cellulose in HTL. Renewable crude could also be the result of a direct reaction from the raw feed as the crude was present after the heat up time with a different distillate fraction composition to the raw feed. As the solid phase generally decreased with increasing residence time, the solid phase was clearly being converted to liquid and gas phase products.

The protein model compound produced minimal gas phase product at the lower two temperatures so it is not likely that the protein was converted directly to a gas phase product in HTL. The aqueous phase was initially high as the BSA was partially soluble in water at atmospheric conditions. The aqueous phase rose significantly in the first 10 min while renewable crude yield decreased and there was a clear transfer of compounds between the aqueous and renewable crude phases. At the lowest temperature the solid yield was seen to decrease to almost nothing with increasing residence time. Hence there may be no reaction path for any of the protein model compound or its HTL products to form solids.

The aqueous phase decreased with increasing residence time at all three temperatures for the alkaline lignin product from HTL, while the solid yield increased. Immediately after heating up time the solid yield was lowest because the untreated lignin was partially soluble in water. The increase in solids was under 30% at all three temperatures. This indicates that the original solid lignin feed could be converted to a solid with different structure. Some of the aqueous phase was converted to gas phase and this is evident by the increase in the gas phase as the aqueous phase decreased. The renewable crude yield remained to be minimal regardless of temperature and residence time.

Numerical models were then fitted to these kinetic pathways using the method presented in Section 2.5. Solid yield is given by x_1 , aqueous yield by x_2 , renewable crude yield by x_3 and gas yield by x_4 . These resulted in the bulk reaction kinetics shown in Fig. 2 with the following corresponding ODEs:

Sunflower Oil

Chapter 3 – The elucidation of reaction kinetics for hydrothermal liquefaction of model macromolecules

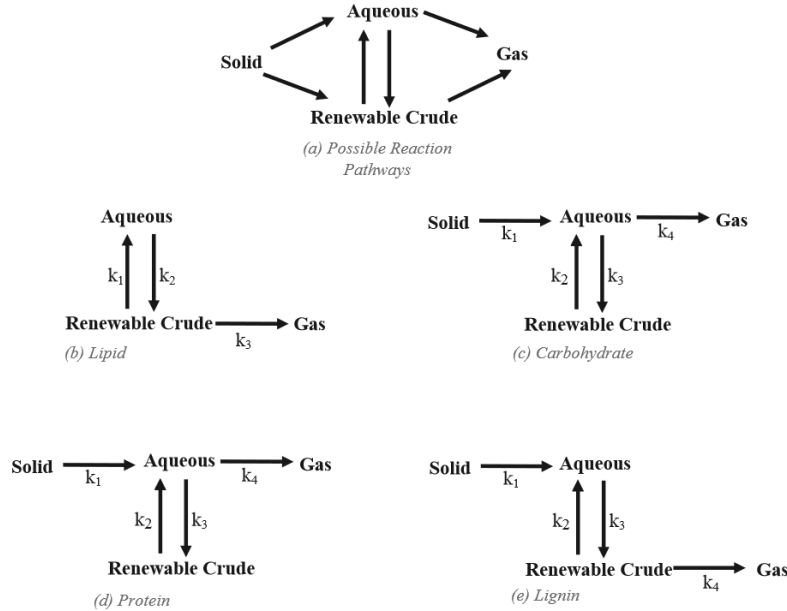


Fig. 2. Possible reaction pathways for the four different model compounds.

$$\frac{dx_2}{dt} = -k_2x_2 + k_1x_3 \quad (1)$$

$$\frac{dx_3}{dt} = -(k_1 + k_3)x_3 + k_2x_2 \quad (2)$$

$$\frac{dx_4}{dt} = k_3x_3 \quad (3)$$

Cellulose and BSA

$$\frac{dx_1}{dt} = -k_1x_1 \quad (4)$$

$$\frac{dx_2}{dt} = -(k_3 + k_4)x_2 + k_1x_1 + k_2x_3 \quad (5)$$

$$\frac{dx_3}{dt} = -k_2x_3 + k_3x_2 \quad (6)$$

$$\frac{dx_4}{dt} = k_4x_2 \quad (7)$$

Alkaline Lignin

$$\frac{dx_1}{dt} = -k_1x_1 \quad (8)$$

$$\frac{dx_2}{dt} = -k_3x_2 + k_1x_1 + k_2x_3 \quad (9)$$

$$\frac{dx_3}{dt} = -(k_2 + k_4)x_3 + k_3x_2 \quad (10)$$

$$\frac{dx_4}{dt} = k_4x_3 \quad (11)$$

Each rate constant quantifies the transition to or from one phase to another. The rate constants for these ODEs are listed in Table 1. The ODEs are plotted against the experimental data in Figs. 3–6.

3.6. Fit of the model

The magnitude of the error bars for product yields in Figs. 3–6 as

well as those for Figs. S1(a)–S7(a) were determined by the experimental repeats discussed in Section 2.3.1. The goodness of fit of the reaction models developed in this work to the data that was collected in the experimental section has been quantified by calculating the 95% confidence interval for the kinetic parameters using the *nlparci* function in MATLAB. This function calculates the nonlinear regression parameter confidence interval. The errors in Arrhenius parameters presented in Table 1 were calculated from the standard deviation of the 95% confidence interval using the MATLAB function *polyconf* for the Arrhenius parameters calculated by *polyfit*. For some pathways for individual model compounds, the errors are a large fraction of the value of the Arrhenius parameter which indicates that the reactions could be over simplified by first order kinetics.

The yields calculated by the model are closest to experimental yields at the highest temperature. While there is significant variation between the model and experimental yields at some reaction conditions, a quantitative understanding of the trends of HTL product yields with time and temperature is provided. Gas yields in particular prove difficult to model due to their irregular trends. This could be due to the possibility of very minor gas leaks that occur during heat up and cool down times and would cause significant variation in gas yields. Many chemical reactions occur simultaneously during HTL and this model simplifies the kinetics significantly, but sufficiently to further elucidate research focus and commercial relevance respectively.

The rate constants for solid to aqueous phase conversion were highest for the protein and increased most steeply with temperature. Hence, BSA was the most readily converted from solid to liquid phases and this occurred with shorter residence times at higher temperatures. The conversion of aqueous phase and renewable crude to gas was expected for all four model compounds as the high content of hydrocarbons in the feed combined with the removal of oxygen during HTL reactions will generate carbon dioxide. Analysis of HTL products has confirmed that carbon dioxide is the dominant gas product formed [38,39].

The existence of the reaction pathways from aqueous phase to renewable crude is expected because recombination of products after the removal of oxygen is one of the key reaction steps in HTL [40]. The

Chapter 3 – The elucidation of reaction kinetics for hydrothermal liquefaction of model macromolecules

R. Obeid, et al.

Chemical Engineering Journal 370 (2019) 637–645

Table 1
Kinetic parameters fit to reaction pathways in Fig. 1.

Compound	Path	Reaction	k["C(sec ⁻¹) Temperature (°C)			lnA	E _a (kJ/mol)
			250	300	350		
Lipid	1	Renewable crude to Aqueous	0.74	0.74	2.44	6.7 ± 7.4	31.1 ± 6.0
	2	Aqueous to Renewable crude	0.06	9.58	9.60	6.7 ± 35.4	141.1 ± 21.4
	3	Renewable crude to Gas	0.08	0.18	0.30	5.9 ± 1.6	36.7 ± 1.3
Carbohydrate	1	Solid to Aqueous	1.69	2.73	3.33	4.8 ± 1.3	18.6 ± 1.0
	2	Renewable crude to Aqueous	3.19	3.97	8.35	7.0 ± 3.4	25.6 ± 2.8
	3	Aqueous to Renewable crude	4.80	4.88	5.73	2.6 ± 0.9	4.7 ± 0.9
	4	Aqueous to Gas	1.20	1.29	1.40	1.1 ± 0.1	4.2 ± 0.1
Protein	1	Solid to Aqueous	4.18	9.22	15.12	9.5 ± 1.1	35.0 ± 0.9
	2	Renewable crude to Aqueous	1.22	3.01	4.63	8.6 ± 2.0	36.3 ± 1.6
	3	Aqueous to Renewable crude	2.70	2.86	3.00	1.7 ± 0.0	2.9 ± 0.0
	4	Aqueous to Gas	0.60	0.76	0.78	14.7 ± 4.9	67.7 ± 21.4
Lignin	1	Solid to Aqueous	1.10	1.14	1.32	1.2 ± 0.7	4.9 ± 0.6
	2	Renewable crude to Aqueous	0.86	0.90	3.82	8.6 ± 8.6	39.0 ± 7.1
	3	Aqueous to Renewable crude	0.23	0.35	0.65	4.8 ± 1.8	27.6 ± 1.5
	4	Renewable crude to Gas	0.36	0.38	0.48	0.7 ± 1.2	7.6 ± 1.0

activation energies from renewable crude to aqueous phase were higher than those from aqueous phase to renewable crude for the carbohydrate, protein and lignin. This indicates additional compounds were being broken down and converted to water-soluble products. For the lipid, the activation energy for aqueous phase to renewable crude was significantly higher than the renewable crude to aqueous as well as being the highest activation energy calculated in the model. This was due to the unreacted sunflower oil product all being in the solvent-soluble renewable crude phase. As there was no aqueous phase present initially, there were fewer compounds which could be converted from aqueous phase to renewable crude phase during the reaction.

Reaction parameters from the algae HTL model by Valdez, Tocco and Savage [11] have been compared to the experimental data collected in this work. For the protein model compound in previous work, the rate constants were found to give accurate yield predictions for the solid and aqueous phases but lower predictions for the gas and higher predictions for the renewable crude in this work. The model for soy protein by Luo, Sheehan, Dai and Savage [6] calculated biocrude yield in current work accurately, however the results deviated for the yields of the other product phases. This has been demonstrated in Fig. S9 where their model is fit to the HTL reactions of BSA at 250 °C from this work. By optimising the model in the current work, the same reaction pathways were selected in their work for protein as presented in

Fig. 2(c), despite the difference in reaction parameters. For the lipid HTL product the trends for decreasing biocrude yield, increasing aqueous phase yield and increasing gas yield in the Valdez, Tocco and Savage [11] model for algae are the same as the trends observed in this work, while the quantitative values for yields are different.

The model produced is predicated on one reaction pressure and a single set of heating and cooling times. The solvent used in extractions and overall extraction process also bounds the model. There are many other model compounds of carbohydrate, lipid, protein and lignin that could be explored as feed for HTL. However, it is evident that the elucidation and modelling of the intermediate compounds formed in HTL would provide the insight required for the development of a multi-variate feedstock model. For example, for protein these could be amino acids, for carbohydrates monosaccharides, for lipids fatty acids and for lignin phenolic compounds could be used. Using intermediate or model monomer compounds will allow more accurate reaction pathways to be developed in future work that can be integrated into the reported model. The model can also be built upon in the opposite direction where complex biomass sources are broken down to simpler carbohydrate, lipid, lignin and protein compounds.

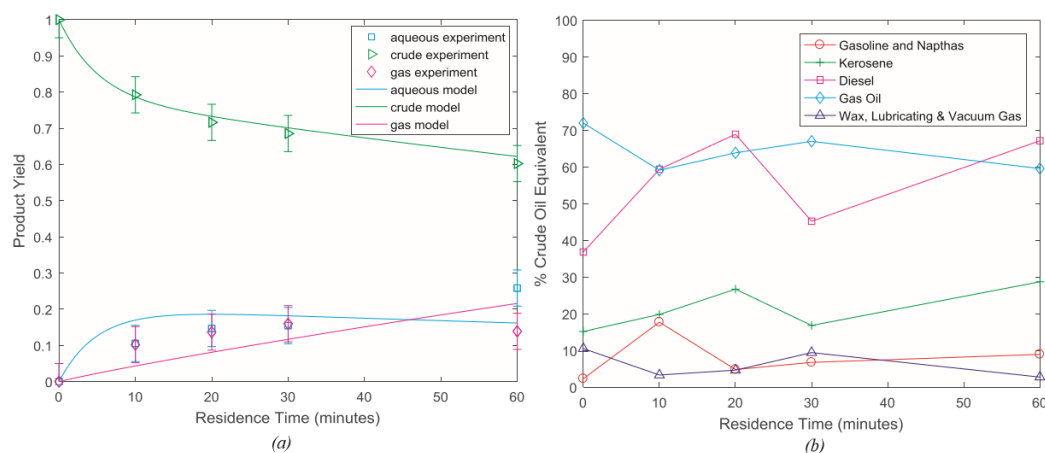


Fig. 3. (a) Product yields from HTL of lipid at 350 °C (b) Percentage of renewable crude in the boiling point ranges of petroleum fractions for the lipid HTL product at 350 °C.

Chapter 3 – The elucidation of reaction kinetics for hydrothermal liquefaction of model macromolecules

R. Obeid, et al.

Chemical Engineering Journal 370 (2019) 637–645

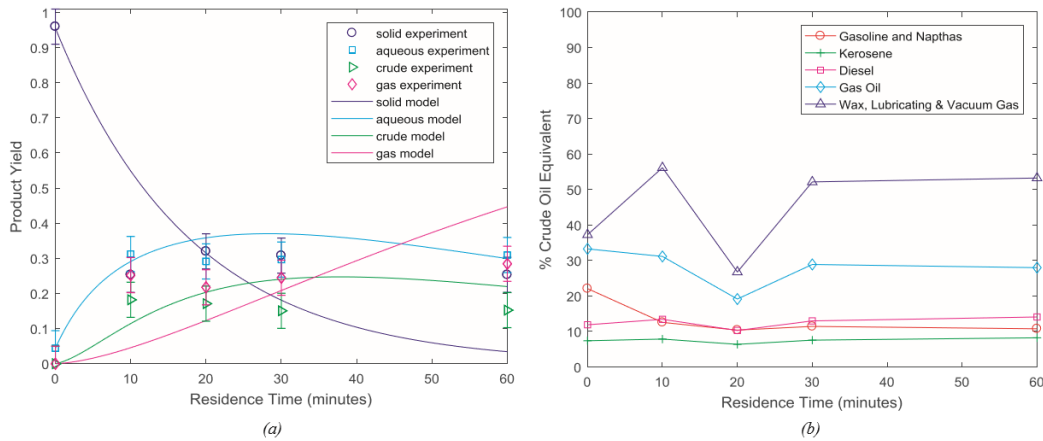


Fig. 4. (a) Product yields from HTL of carbohydrate at 350 °C (b) Percentage of renewable crude in the boiling point ranges of petroleum fractions for the carbohydrate HTL product at 350 °C.

4. Conclusions

A kinetic model which identifies the trends with time and temperature for the yields of HTL products from carbohydrate, lipid, lignin and protein model compounds has been formulated. Experimental results quantified the amounts of aqueous, gas, crude and solid phases produced by HTL of the model compounds. HTL treatment of lipids will result in more aqueous and gas phase products being produced, which decreases the amount of renewable crude obtained by solvent extraction than what was present in the original feedstock. However, HTL treatment does result in less renewable crude being formed in the unfavourable heavier gas oil distillate range. Short residence times and higher temperatures are favourable for maximum renewable crude yields for the HTL of cellulose. Most of the crude products from HTL of the carbohydrate are the less favourable heavy compounds. For HTL treatment of the protein, temperatures of 300 and 350 °C and a residence time of around 30 min will result in optimum renewable crude yield which is made up of a greater proportion of the more favourable lighter distillate fraction than the initial feed. In agreement with other work using lignin as a feed for HTL without a catalyst, little renewable crude has been extracted from the HTL product. The crude that is formed is mostly heavy oil and HTL treatment of lignin results in mostly

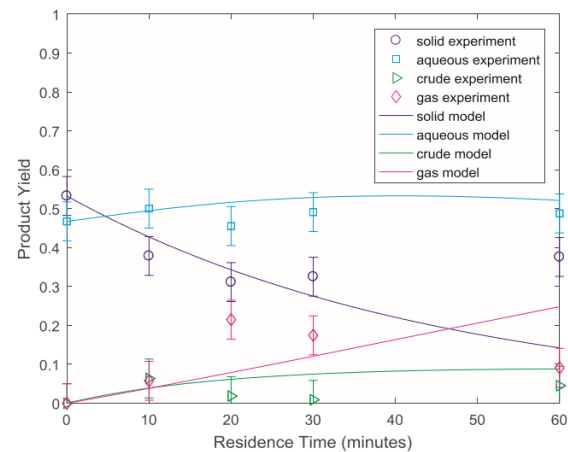


Fig. 6. Product yields from HTL of lignin at 350 °C.

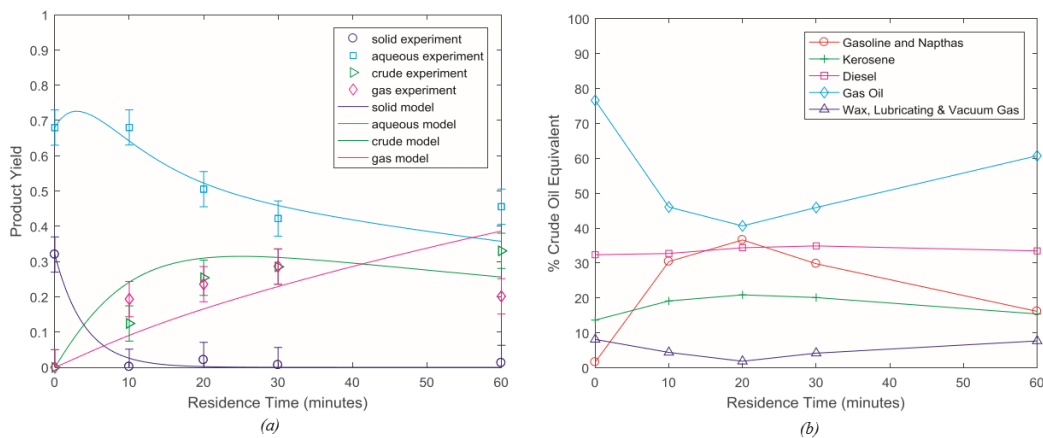


Fig. 5. (a). Product yields from HTL of protein at 350 °C (b) Percentage of renewable crude in the boiling point ranges of petroleum fractions for the protein HTL product at 350 °C.

Chapter 3 – The elucidation of reaction kinetics for hydrothermal liquefaction of model macromolecules

R. Obeid, et al.

Chemical Engineering Journal 370 (2019) 637–645

aqueous phase products. The initial feeds are converted to liquid fuels which can be refined to more useful fuels, like diesel, after further treatment and cracking of the biocrude. This work has resulted in comparable yields and petroleum-like fractions for the four primary components of biomass at three different temperatures and residence times from 0 to 60 min. The dominant reaction pathways for each of the model compounds have been identified, however more detailed reaction pathways are necessary for better predictions of HTL products.

Acknowledgements

- Assistance from The University of Adelaide Chemical Engineering Workshop in the development of the HTL batch reactor is acknowledged.
- Funding for this work was provided by Australian Research Council Linkage Project LP150101241.

Appendix A. Supplementary data

Supplementary data to this article can be found online at <https://doi.org/10.1016/j.cej.2019.03.240>.

References

- [1] D.R. Vardon, B.K. Sharma, J. Scott, G. Yu, Z. Wang, L. Schideman, Y. Zhang, T.J. Strathmann, Chemical properties of biocrude oil from the hydrothermal liquefaction of *Spirulina* algae, swine manure, and digested anaerobic sludge, *Bioresour. Technol.* 102 (2011) 8295–8303.
- [2] D.R. Vardon, B.K. Sharma, G.V. Blazina, K. Rajagopalan, T.J. Strathmann, Thermochemical conversion of raw and defatted algal biomass via hydrothermal liquefaction and slow pyrolysis, *Bioresour. Technol.* 109 (2012) 178–187.
- [3] G. Teri, L. Luo, P.E. Savage, Hydrothermal Treatment of Protein, Polysaccharide, and Lipids Alone and in Mixtures, *Energy Fuels* 28 (2014) 7501–7509.
- [4] P. Biller, A.B. Ross, Potential yields and properties of oil from the hydrothermal liquefaction of microalgae with different biochemical content, *Bioresour. Technol.* 102 (2011) 215–225.
- [5] Y. Gao, H.-P. Chen, J. Wang, T. Shi, H.-P. Yang, X.-H. Wang, Characterization of products from hydrothermal liquefaction and carbonation of biomass model compounds and real biomass, *J. Fuel Chem. Technol.* 39 (2011) 893–900.
- [6] L. Luo, J.D. Sheehan, L. Dai, P.E. Savage, Products and Kinetics for Isothermal Hydrothermal Liquefaction of Soy Protein Concentrate, *ACS Sustain. Chem. Eng.* 4 (2016) 2725–2733.
- [7] M. Sasaki, B. Kabyemela, R. Malaluan, S. Hirose, N. Takeda, T. Adschiri, K. Arai, Cellulose hydrolysis in subcritical and supercritical water, *J. Supercritical Fluids* 13 (1998) 261–268.
- [8] M. Sasaki, T. Adschiri, K. Arai, Kinetics of cellulose conversion at 25 MPa in sub- and supercritical water, *AIChE J.* 50 (2004) 192–202.
- [9] Z. Wang, Reaction mechanisms of hydrothermal liquefaction of model compounds and biowaste feedstocks, University of Illinois at Urbana-Champaign, 2011.
- [10] P.J. Valdez, P.E. Savage, A reaction network for the hydrothermal liquefaction of *Nannochloropsis* sp., *Algal Res.* 2 (2013) 416–425.
- [11] P.J. Valdez, V.J. Tocco, P.E. Savage, A general kinetic model for the hydrothermal liquefaction of microalgae, *Bioresour. Technol.* 163 (2014) 123–127.
- [12] T.K. Vo, S.-S. Kim, H.V. Ly, E.Y. Lee, C.-G. Lee, J. Kim, A general reaction network and kinetic model of the hydrothermal liquefaction of microalgae *Tetraselmis* sp., *Bioresour. Technol.* 241 (2017) 610–619.
- [13] D.C. Hietala, J.L. Faeth, P.E. Savage, A quantitative kinetic model for the fast and isothermal hydrothermal liquefaction of *Nannochloropsis* sp., *Bioresour. Technol.* 214 (2016) 102–111.
- [14] J.D. Sheehan, P.E. Savage, Modeling the effects of microalga biochemical content on the kinetics and biocrude yields from hydrothermal liquefaction, *Bioresour. Technol.* 239 (2017) 144–150.
- [15] Y. Li, S. Leow, A.C. Fedders, B.K. Sharma, J.S. Guest, T.J. Strathmann, Quantitative multiphase model for hydrothermal liquefaction of algal biomass, *Green Chem.* 19 (2017) 1163–1174.
- [16] P.J. Valdez, J.G. Dickinson, P.E. Savage, Characterization of Product Fractions from Hydrothermal Liquefaction of *Nannochloropsis* sp. and the Influence of Solvents, *Energy Fuels* 25 (2011) 3235–3243.
- [17] W.-H. Yan, P.-G. Duan, F. Wang, Y.-P. Xu, Composition of the bio-oil from the hydrothermal liquefaction of duckweed and the influence of the extraction solvents, *Fuel* 185 (2016) 229–235.
- [18] M. Garcia-Perez, A. Chaala, H. Pakdel, D. Kretschmer, C. Roy, Characterization of bio-oils in chemical families, *Biomass Bioenergy* 31 (2007) 222–242.
- [19] K. Anastakis, P. Biller, R. Madsen, M. Glasius, I. Johannsen, Continuous Hydrothermal Liquefaction of Biomass in a Novel Pilot Plant with Heat Recovery and Hydraulic Oscillation, *Energies* 11 (2018) 2695.
- [20] Y. Gao, X.-H. Wang, H.-P. Yang, H.-P. Chen, Characterization of products from hydrothermal treatments of cellulose, *Energy* 42 (2012) 457–465.
- [21] S. Kang, X. Li, J. Fan, J. Chang, Characterization of Hydrochars Produced by Hydrothermal Carbonization of Lignin, Cellulose, d-Xylose, and Wood Meal, *Ind. Eng. Chem. Res.* 51 (2012) 9023–9031.
- [22] W.-T. Chen, Y. Zhang, J. Zhang, G. Yu, L.C. Schideman, P. Zhang, M. Minarick, Hydrothermal liquefaction of mixed-culture algal biomass from wastewater treatment system into bio-crude oil, *Bioresour. Technol.* 152 (2014) 130–139.
- [23] ASTM, *Characterization and Properties of Petroleum Fractions, 1.1.3 Petroleum Fractions and Products West Conshohocken, PA, 2005.*
- [24] P. Biller, R. Riley, A.B. Ross, Catalytic hydrothermal processing of microalgae: decomposition and upgrading of lipids, *Bioresour. Technol.* 102 (2011) 4841–4848.
- [25] J.L. Faeth, P.J. Valdez, P.E. Savage, Fast Hydrothermal Liquefaction of *Nannochloropsis* sp. To Produce Biocrude, *Energy Fuels* 27 (2013) 1391–1398.
- [26] J.D. Sheehan, P.E. Savage, Molecular and Lumped Products from Hydrothermal Liquefaction of Bovine Serum Albumin, *ACS Sustain. Chem. Eng.* 5 (2017) 10967–10975.
- [27] J.S. Midgett, B.E. Stevens, A.J. Dassey, J.J. Spivey, C.S. Theegala, Assessing Feedstocks and Catalysts for Production of Bio-Oils from Hydrothermal Liquefaction, *Waste Biomass Valorization* 3 (2012) 259–268.
- [28] T. Rogalinski, K. Liu, T. Albrecht, G. Brunner, Hydrolysis kinetics of biopolymers in subcritical water, *J. Supercritical Fluids* 46 (2008) 335–341.
- [29] S. Yin, Z. Tan, Hydrothermal liquefaction of cellulose to bio-oil under acidic, neutral and alkaline conditions, *Appl. Energy* 92 (2012) 234–239.
- [30] D. Yang, K.S. Jones, Effect of alginate on innate immune activation of macrophages, *J. Biomed. Mater. Res. A* 90 (2009) 411–418.
- [31] S. Karagöz, T. Bhaskar, A. Muto, Y. Sakata, Comparative studies of oil compositions produced from sawdust, rice husk, lignin and cellulose by hydrothermal treatment, *Fuel* 84 (2005) 875–884.
- [32] J. Lu, Z. Liu, Y. Zhang, P.E. Savage, Synergistic and Antagonistic Interactions during Hydrothermal Liquefaction of Soybean Oil, Soy Protein, Cellulose, Xylose, and Lignin, *ACS Sustain. Chem. Eng.* 6 (2018) 14501–14509.
- [33] O. Bobleter, Hydrothermal degradation of polymers derived from plants, *Prog. Polym. Sci.* 19 (1994) 797–841.
- [34] R.C. Sun, J. Fang, J. Tomkinson, Delignification of rye straw using hydrogen peroxide, *Ind. Crops Prod.* 12 (2000) 71–83.
- [35] B. Xiao, X.F. Sun, R. Sun, Chemical, structural, and thermal characterizations of alkali-soluble lignins and hemicelluloses, and cellulose from maize stems, rye straw, and rice straw, *Polym. Degrad. Stab.* 74 (2001) 307–319.
- [36] K.R. Arturi, S. Kucheryavskiy, E.G. Søgaard, Performance of hydrothermal liquefaction (HTL) of biomass by multivariate data analysis, *Fuel Process. Technol.* 150 (2016) 94–103.
- [37] H. Nonaka, M. Funaoka, Decomposition characteristics of softwood ligninphenol under hydrothermal conditions, *Biomass Bioenergy* 35 (2011) 1607–1611.
- [38] G. Yu, Y. Zhang, L. Schideman, T. Funk, Z. Wang, Distributions of carbon and nitrogen in the products from hydrothermal liquefaction of low-lipid microalgae, *Energy Environ. Sci.* 4 (2011) 4587–4595.
- [39] D.C. Elliott, T.R. Hart, A.J. Schmidt, G.G. Neuenschwander, L.J. Rotness, M.V. Olarte, A.H. Zacher, K.O. Albrecht, R.T. Hallen, J.E. Holladay, Process development for hydrothermal liquefaction of algae feedstocks in a continuous-flow reactor, *Algal Res.* 2 (2013) 445–454.
- [40] C. Gai, Y. Zhang, W.-T. Chen, P. Zhang, Y. Dong, An investigation of reaction pathways of hydrothermal liquefaction using *Chlorella pyrenoidosa* and *Spirulina platensis*, *Energy Convers. Manage.* 96 (2015) 330–339.

Supporting Information

The elucidation of reaction kinetics for hydrothermal liquefaction of model macromolecules

Reem Obeid[†], David Lewis[†], Neil Smith[†] and Philip van Eyk^{†*}

[†]School of Chemical Engineering, The University of Adelaide, Adelaide, South Australia
5005, Australia

*E-mail: philip.vaneyk@adelaide.edu.au.

Chapter 3 – The elucidation of reaction kinetics for hydrothermal liquefaction of model macromolecules

Experimental yields and the model fit at the two lower temperatures for HTL are provided here in the supplementary material.

The crude fractions from TGA are also presented. The zero minute crude fractions presented in the supplementary material are for the crude product which has been removed from the reactor immediately after being heated to 98% of the reaction temperature.

The yields for the four product phases after heat-up time are shown in Table S1.

An example of the fit of a previous model for soy protein to our experimental data on the model protein BSA is provided in Figure S9.

Chapter 3 – The elucidation of reaction kinetics for hydrothermal liquefaction of model macromolecules

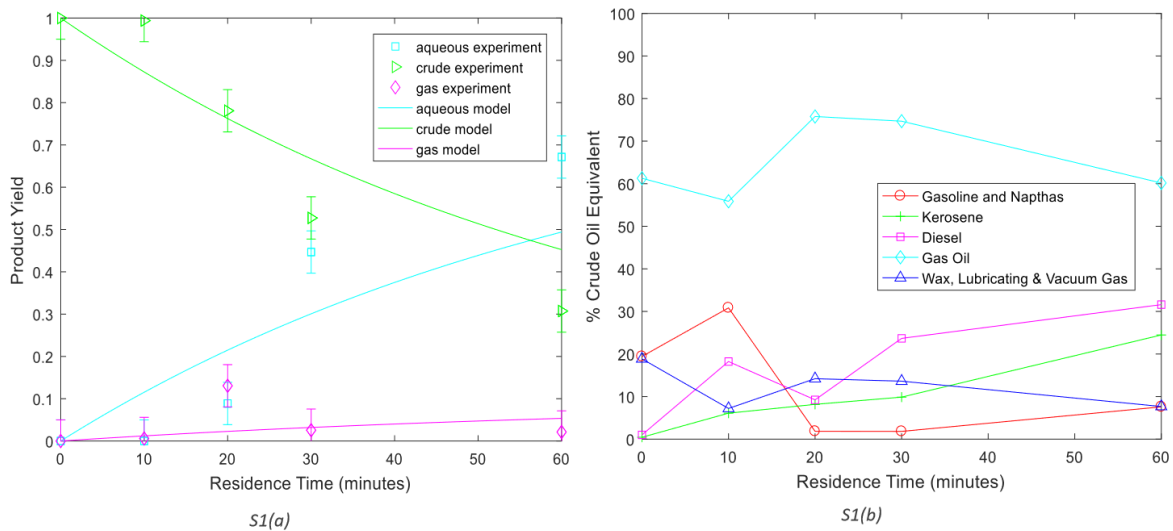


Figure S1 (a) Product yields from HTL of lipid at 250°C
 (b) Percentage of renewable crude in the boiling point ranges of petroleum fractions for the lipid HTL product at 250°C

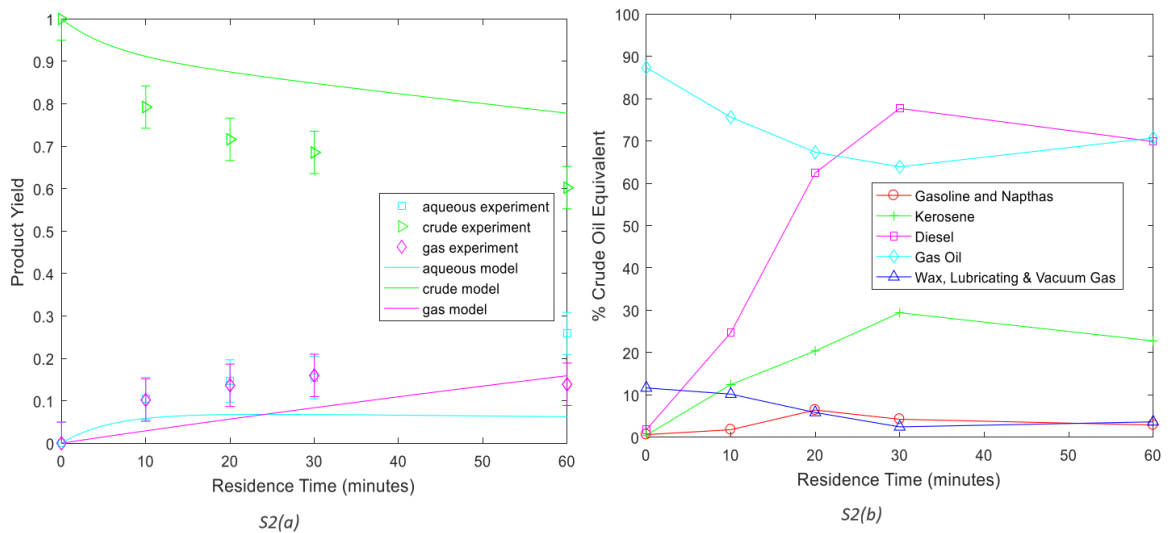


Figure S2 (a) Product yields from HTL of lipid at 300°C
 (b) Percentage of renewable crude in the boiling point ranges of petroleum fractions for the lipid HTL product at 300°C

Chapter 3 – The elucidation of reaction kinetics for hydrothermal liquefaction of model macromolecules

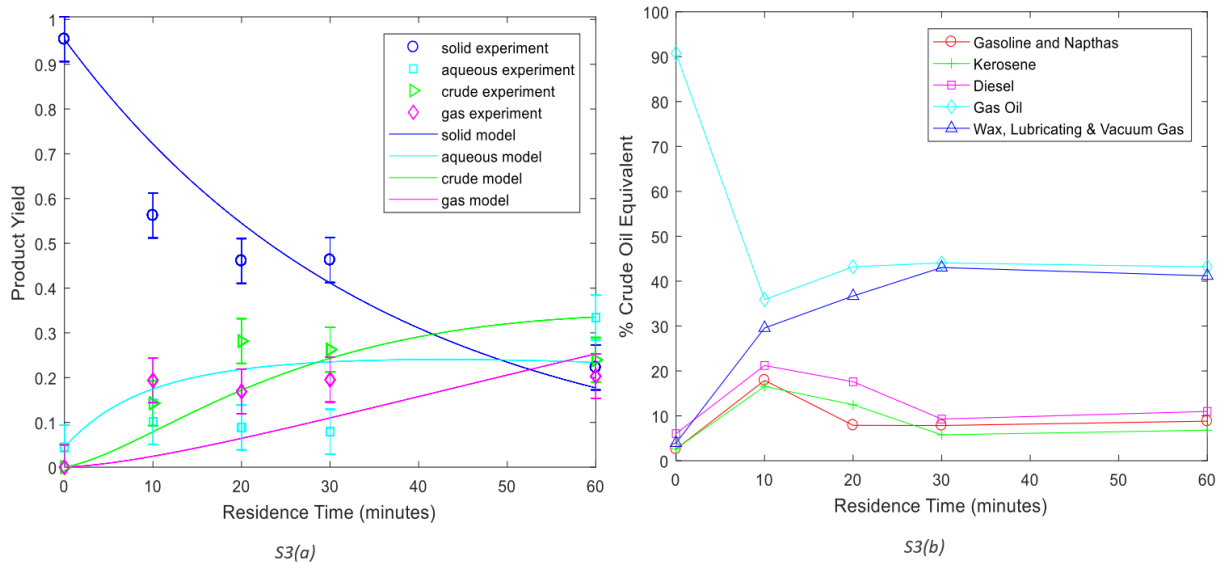


Figure S3 (a) Product yields from HTL of carbohydrate at 250°C
(b) Percentage of renewable crude in the boiling point ranges of petroleum fractions for the carbohydrate HTL product at 250°C

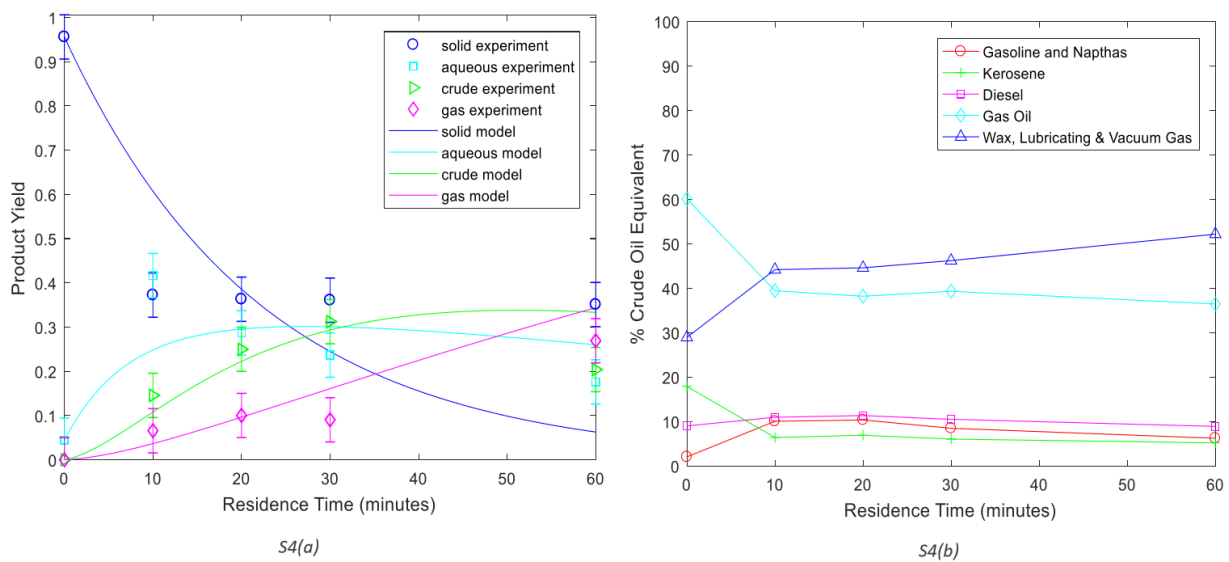


Figure S4 (a) Product yields from HTL of carbohydrate at 300°C
(b) Percentage of renewable crude in the boiling point ranges of petroleum fractions for the carbohydrate HTL product at 300°C

Chapter 3 – The elucidation of reaction kinetics for hydrothermal liquefaction of model macromolecules

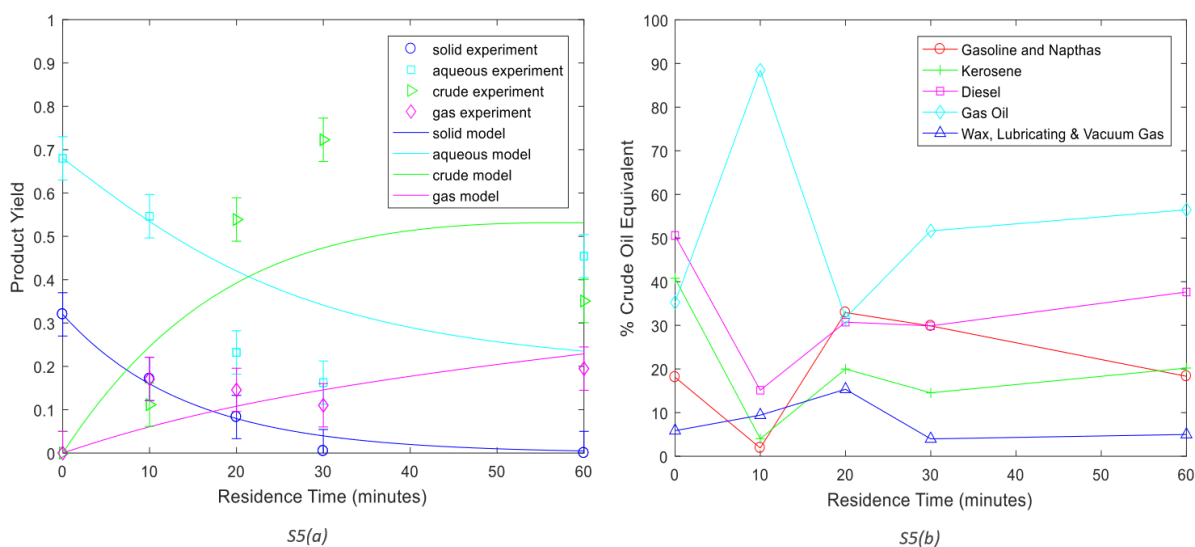


Figure S5 (a) Product yields from HTL of protein at 250°C
 (b) Percentage of renewable crude in the boiling point ranges of petroleum fractions for the protein HTL product at 250°C

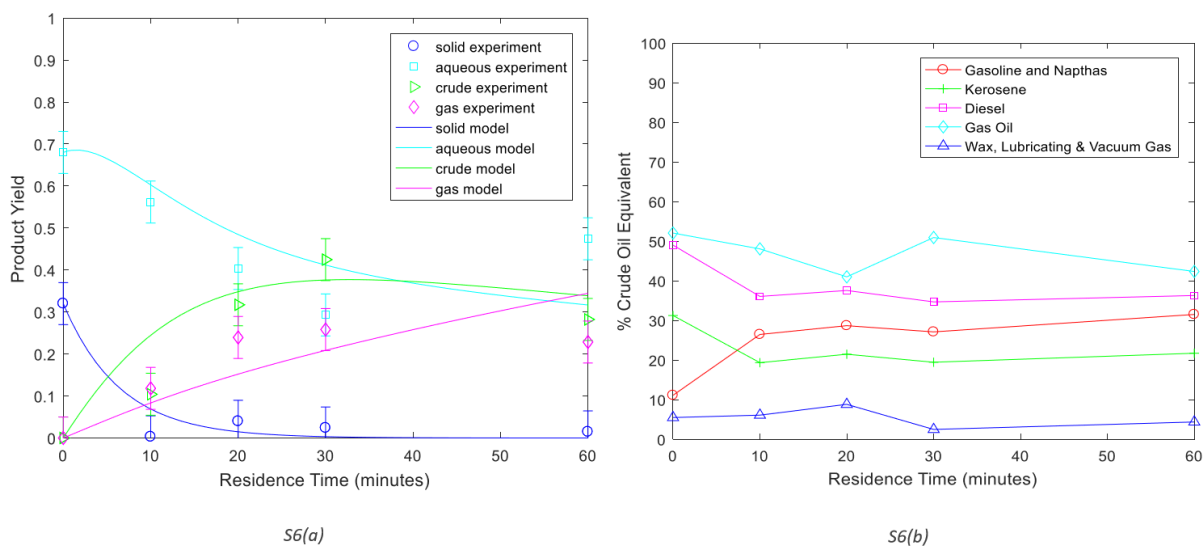


Figure S6 (a) Product yields from HTL of protein at 300°C
 (b) Percentage of renewable crude in the boiling point ranges of petroleum fractions for the protein HTL product at 300°C

Chapter 3 – The elucidation of reaction kinetics for hydrothermal liquefaction of model macromolecules

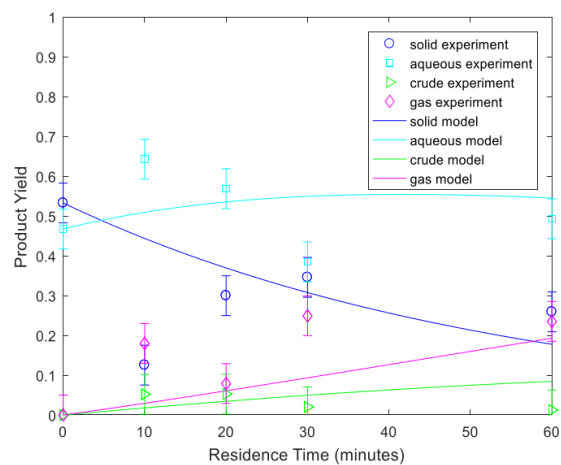


Figure S7. Product yields from HTL of lignin at 250°C

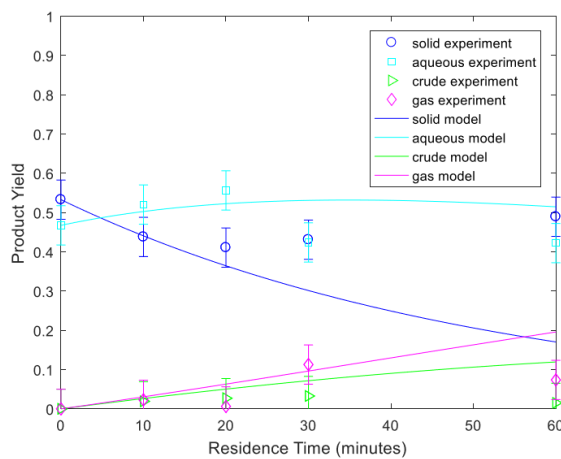


Figure S8. Product yields from HTL of lignin at 300°C

Chapter 3 – The elucidation of reaction kinetics for hydrothermal liquefaction of model macromolecules

Table S1: Yields from reactions where the residence time was the time for the reactants to reach 98% of the reaction temperature

Model Compound	Temperature (°C)	Solid Yield (%)	Aqueous Yield (%)	Renewable Crude Yield (%)	Gas Yield (%)
Sunflower oil	250	0	0	100	0
Sunflower oil	300	0	68.51	28.82	2.67
Sunflower oil	350	0	23.9	76.1	0
Cellulose	250	22.26	10.97	41.72	25.05
Cellulose	300	43.85	21.38	27.47	7.3
Cellulose	350	36.87	18.49	42.83	1.81
Bovine serum albumin	250	18.75	49.31	27.21	4.73
Bovine serum albumin	300	7.61	55.12	37.27	0
Bovine serum albumin	350	4.62	48.76	29.99	16.63
Lignin	250	7.13	68.51	4.4	19.96
Lignin	300	5.55	89.38	1.58	3.49
Lignin	350	19.26	69.92	1.68	9.14

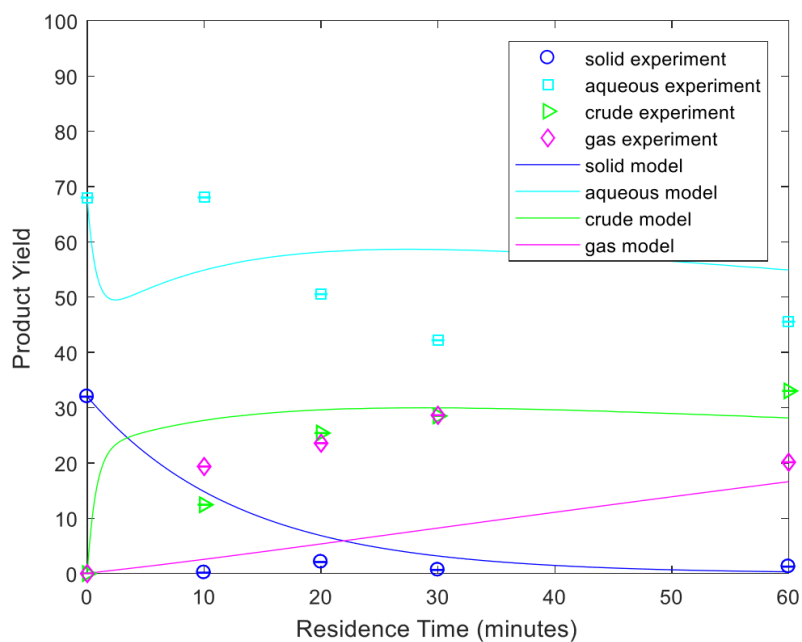


Figure S9. Product yields from HTL experiments for BSA at 250°C fit to the model for soy protein by Luo, Sheehan, Dai and Savage [6]

Chapter 4

Reaction kinetics and characterisation of species in renewable crude from hydrothermal liquefaction of monomers to represent organic fractions of biomass feedstocks

R. Obeid ^a, D.M. Lewis ^a, N. Smith ^a, T. Hall ^b, P. van Eyk ^a

^aThe School of Chemical Engineering and Advanced Materials

^b Faculty of Sciences

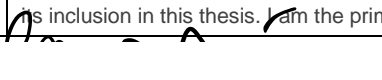
The University of Adelaide, SA 5000, Australia

The Chemical Engineering Journal, Published.

Statement of Authorship

Title of Paper	Reaction kinetics and characterisation of species in renewable crude from hydrothermal liquefaction of monomers to represent organic fractions of biomass feedstocks
Publication Status	<input checked="" type="checkbox"/> Published <input type="checkbox"/> Accepted for Publication <input type="checkbox"/> Submitted for Publication <input type="checkbox"/> Unpublished and Unsubmitted work written in manuscript style
Publication Details	Published in The Chemical Engineering Journal R. Obeid, D.M. Lewis, N. Smith, T. Hall, P. van Eyk, Reaction kinetics and characterisation of species in renewable crude from hydrothermal liquefaction of monomers to represent organic fractions of biomass feedstocks, Chemical Engineering Journal (2020) 1385-8947.

Principal Author


Name of Principal Author (Candidate)	Reem Obeid
Contribution to the Paper	HTL reactor design and methods HTL batch experiments completed Methods developed for product separation and product separation completed Interpretation of GC-MS results Construction of model Writing and editing
Overall percentage (%)	80
Certification:	This paper reports on original research I conducted during the period of my Higher Degree by Research candidature and is not subject to any obligations or contractual agreements with a third party that would constrain its inclusion in this thesis. I am the primary author of this paper.
Signature	
Date	17/01/20


Co-Author Contributions


By signing the Statement of Authorship, each author certifies that:


- i. the candidate's stated contribution to the publication is accurate (as detailed above);
- ii. permission is granted for the candidate to include the publication in the thesis; and
- iii. the sum of all co-author contributions is equal to 100% less the candidate's stated contribution.

Chapter 4 – Reaction kinetics and characterisation of species in renewable crude from hydrothermal liquefaction of monomers to represent organic fractions of biomass feedstocks

Name of Co-Author	David Lewis		
Contribution to the Paper	Concept development Assistance with analysis and interpretation of data Drafting of paper		
Signature		Date	22-Feb-2020

Name of Co-Author	Neil Smith		
Contribution to the Paper	Concept development Assistance with analysis and interpretation of data Drafting of paper		
Signature		Date	28/1/2020

Name of Co-Author	Tony Hall		
Contribution to the Paper	Method design and analysis using Source Rock Analyser and GC-MS Drafting of paper		
Signature		Date	23/1/20

Name of Co-Author	Philip van Eyk		
Contribution to the Paper	HTL reactor design and methods Concept development Assistance with analysis and interpretation of data Drafting of paper		
Signature		Date	28/1/2020



Contents lists available at ScienceDirect

Chemical Engineering Journal

journal homepage: www.elsevier.com/locate/cej



Reaction kinetics and characterisation of species in renewable crude from hydrothermal liquefaction of monomers to represent organic fractions of biomass feedstocks



Reem Obeid^a, David M. Lewis^a, Neil Smith^a, Tony Hall^b, Philip van Eyk^{a,*}

^a School of Chemical Engineering and Advanced Materials, The University of Adelaide, Adelaide, South Australia 5005, Australia

^b Faculty of Sciences, The University of Adelaide, Adelaide, South Australia 5005, Australia

HIGHLIGHTS

- HTL of monomers produced lower crude yields than HTL of polymers.
- Crude produced at different conditions contained the same compounds from GC-MS.
- Bulk kinetic model for product yields from HTL of monomer compounds developed.

ARTICLE INFO

Keywords:

Hydrothermal liquefaction
Kinetics
Lipid
Carbohydrate
Protein
Lignin

ABSTRACT

Hydrothermal liquefaction (HTL) can be used to convert a range of biomass feedstocks to a renewable crude with solid, aqueous and gas co-products. In order to characterise the HTL process so that the products can be predicted for a range of reaction conditions from varying feedstock, bulk kinetic models that predict the yield of each phase from the organic composition of the feed biomass, including carbohydrate, lipid, protein and lignin components are required. Due to the complexity of the reactions and variation in the organically rich wet feedstocks being considered for HTL, investigations using model compounds have been performed by numerous researchers. In the current work monomer model compounds including glucose, oleic acid, alanine and guaiacol have been used in multivariate HTL experiments in a batch reactor at reaction temperatures of 250, 300 and 350 °C for reaction times of 5 to 60 min. The resulting yields of renewable crude, solid, aqueous and gas products allowed a model to be developed for HTL of these monomer model compounds that could be compared to a second model previously developed for products from HTL of polymer compounds from the same families. Gas chromatography-mass spectrometry analysis of renewable crude products identified that lipid produced fatty acids. Carbohydrates produced crude consisting of phenol, furans, aldehydes, aromatics and ketones. HTL of the protein monomer resulted in a renewable crude composed of amides, aromatics, amines, carboxylic acids and short hydrocarbon chains and phenolic compounds made up the majority of the renewable crude from the lignin model compound.

1. Introduction

Hydrothermal liquefaction (HTL) involves chemical reactions in sub-critical water that can convert biomass to a renewable crude oil, which can be further refined to a petroleum-like fuel, as well as other co-products. HTL has been used on a wide range of feedstocks to produce renewable crude, aqueous soluble, solid and gas phase products. The composition of biomass feedstock has been shown to have a significant influence on the yields of these phases [1,2]. Due to the high

variability in biomass composition, a model which can accommodate different feedstocks and predict the yields of these phases is essential to enable the HTL technology to be upgraded to industrial scale and utilised as a renewable energy source.

Biomass can be classified by four organic fractions - lipid, carbohydrate, protein and lignin. A bulk kinetic model which predicts the yields of product phases from HTL reactions given the lipid, carbohydrate, protein and lignin content of the biomass feedstock can be used to encompass the many chemical reactions occurring during HTL of

* Corresponding author.

E-mail address: philip.vaneyk@adelaide.edu.au (P. van Eyk).

<https://doi.org/10.1016/j.cej.2020.124397>

Received 21 August 2019; Received in revised form 14 December 2019; Accepted 7 February 2020

Available online 08 February 2020

1385-8947/ © 2020 Elsevier B.V. All rights reserved.

Chapter 4 – Reaction kinetics and characterisation of species in renewable crude from hydrothermal liquefaction of monomers to represent organic fractions of biomass feedstocks

R. Obeid, et al.

Chemical Engineering Journal 389 (2020) 124397

biomass. Previous models developed on this basis have mainly focused on algae as a feedstock [3-7], while others have modelled HTL of single compounds such as soy protein or lignin which constitute significant proportions of other biomass feedstocks [8,9]. A preliminary investigation of the fit of an algae based model to other biomass feedstock, including manure and waste water sludge was conducted by Li, et al. [10]. They used data from HTL experiments conducted at 300 °C for 30 min to predict crude, aqueous, gas, and biochar products from manure and sludge feedstocks. Further data are required to validate the algae model for different feedstocks. This example illustrates that models currently available in literature are limited with respect to reaction times and temperatures and to specific feedstock compositions, and that further experimental results from HTL of different biomass feedstocks at varying reaction conditions are required to provide validation data for models.

The influence on HTL yield of experimental variables such as reaction pressure, mass loading of the biomass reactant in water, heating rate of the HTL reactor and the solvent used to separate crude from the HTL product mixture have been studied. Increasing pressure from 25 MPa to 35 MPa was found to increase biomass decomposition by Chan, et al. [11]. Increasing pressure in HTL reactions has also been seen to result in lower crude yields [12]. Increasing biomass loading from 5 to 35% increased renewable crude yield from 36% to 46% in a study by Valdez, et al. [13]. A study by Anastasakis and Ross [14] using macroalgae as a HTL feedstock indicated that crude yield did not always increase when increasing biomass loading. Different heating rates during HTL reactions are also suspected to cause variation in renewable crude yields. A heating rate of 300 °C/minute was seen to produce higher yields of energy dense crude than reactions with a slower heating rate of 150 °C/minute for a reaction time of 1 min by Faeth, et al. [15]. Another investigation on heating rate found that solid residue was increased by around 10% with a decrease in heating rate from 140 °C/minute to 14 °C/minute. This variation in product distribution with different heating rates is due to the reactions which result in some degree of conversion during heat up periods. Hence, faster heating times are preferable to define reaction kinetics. Investigations have demonstrated that renewable crude yield is dependent on the solvent selected for renewable crude extraction from the product mixture and that different solvents extract different compounds [16,17]. While chloroform was found to recover 88–93% of the organics in the different crudes tested and dichloromethane recovered 85–95%, hexane recovered 85–89% of the organics [16]. At present there is a lack of experimental results from consistent experimental conditions in published literature, which may enable the generation of a general reaction model for HTL.

During HTL the first step in biomass conversion involves depolymerisation of the polymers to monomers. These monomers are further decomposed via decarboxylation, deamination, dehydration and cleavage. Following this, recombination of the reactive intermediate products occurs [18]. In order to understand the interconversion pathways between different product fractions in HTL, model monomer compounds should be investigated as HTL feedstocks.

An investigation of the variation in HTL products from mixtures of monomer and polymer model compounds has shown that experiments with model polymers result in product yields which are closer to those from real biomass than model monomers [19]. Crude yields from HTL of polymers and monomers were 1% and 7% higher than real biomass respectively. The improvement is suspected to be due to the existence of crosslinked fibres in model polymers which require more energy to decompose than do model monomers. These fibres are broken down and hydrolysed during HTL of real biomass. Lower gas yields by 3% for polymers and for 5% monomers were also identified compared to real biomass by Déniel, et al. [19]. Solid yield was 8% lower for polymers and 23% lower for monomers than real biomass. While monomer model compounds have chemical structures that differ more from real biomass than do polymer model compounds, and produce the noted differences

in HTL yields, the use of monomer compounds in HTL experiments will give further insight into the decomposition products since the monomer compounds make up a large fraction of the intermediate products formed during HTL [20-23]. We have recently developed a first order bulk kinetic reaction model for the polymers cellulose, sunflower oil, alkaline lignin and bovine serum albumin to represent carbohydrate, lipid, lignin and protein fractions of biomass respectively [24]. The reaction model results contain some significant deviations from experimental results due to the complexity of reactions occurring during the HTL of the polymer model compounds. The reaction model needs to be further improved so that the products from different carbohydrate, lipid, lignin and protein compounds can be predicted. Experiments with monomer model compounds under the same reaction conditions should be carried out to allow comparison of product yields and add to the limited literature on the different reaction products from different sources of carbohydrate, lipid, lignin and protein fractions with varying reaction times and temperatures.

Previous gas chromatography-mass spectrometry (GC-MS) and high performance liquid chromatography (HPLC) analysis of the crude from HTL of biomass has proven to be difficult to interpret because of the many compounds formed during HTL as well as the large fraction of high molecular weight products which cannot be identified due to temperature limitations in GC-MS [1]. GC-MS analysis has been completed on products from HTL of monomer model compounds by Déniel, et al. [25]. The monomer model compounds they tested include glucose, xylose, glutamic acid, guaiacol and linoleic acid. HTL of the monomer model compounds was conducted at 300 °C for 60 min with a 30–35 min heat up time with 15 wt% dry matter in each reaction. While identification of compounds from real biomass can be difficult because of the many compounds formed, monomer model compounds produce fewer reaction products which allows the crude to be better characterised. Hence, GC-MS can be conducted on the crude produced from monomer model compounds

Further investigation on the yields from HTL products of monomer lipid, carbohydrate, protein and lignin compounds is required. The effect of reaction time and temperature can also be investigated. These investigations will allow the products from HTL of different classes of biomass to be further understood and a predictive reaction model to be developed.

Monomer compounds were selected for the current work to represent the lipid, carbohydrate, protein and lignin fractions of biomass. Triglycerides are a group of lipids which are composed of a glycerol backbone linked to three fatty acid molecules. A model which predicts renewable crude yield from fatty acid content of microalgae has been developed by Leow, et al. [26]. They determined that HTL acts as a water-based extraction process for fatty acids. Hence, the hydrothermal treatment of a fatty acid model compound should be studied. Monosaccharides are the simplest carbohydrates. Glucose has been selected as the model monosaccharide in this work because it is the most abundant monosaccharide in nature. During hydrothermal treatment, protein components of biomass are hydrolysed to produce amino acids [27]. The amino acid decomposition then needs to be characterised for HTL pathways to be understood. Different amino acids are expected to undergo similar decarboxylation and deamination reactions [28]. Rogalinski, et al. [29] showed that the complex amino acids from HTL of the protein compound, bovine serum albumin (BSA), degraded to alanine and glycine. Alanine was selected as the amino acid model compound in this work. Guaiacol was selected as the model monomer for lignin HTL as it is one of the most abundant phenolic compounds in nature [30]. A phenolic monomer was selected to model lignin as lignin is a polyphenolic material.

The aim of the current work is to further develop a model for biomass HTL products which can predict yields from lipid, carbohydrate, protein and lignin monomers. The investigation requires experiments with varying time and temperature of HTL of monomer model compounds. Developing a model for monomer compounds for lipid,

Chapter 4 – Reaction kinetics and characterisation of species in renewable crude from hydrothermal liquefaction of monomers to represent organic fractions of biomass feedstocks

R. Obeid, et al.

Chemical Engineering Journal 389 (2020) 124397

carbohydrate, protein and lignin fractions of biomass will allow comparisons to be made to the trends of HTL reaction products from alternate model compounds, including polymers from the same families of compounds. Interconversion pathways between the intermediate compounds formed from decarboxylation, deamination, dehydration and cleavage, followed by the recombination of the reactive intermediates in HTL can be identified with the use of monomers. Identification of these interconversion pathways are essential to be able to properly model biomass reactions in HTL. The use of monomer model compounds will also allow the main compounds being formed from HTL to be identified via GC-MS.

2. Materials and methods

2.1. Materials and feedstock analysis

The carbohydrate monomer selected was D-Glucose Anhydrous $\geq 99\%$ from Chem-Supply. The lipid was modelled by oleic acid $\geq 99\%$ from Chem-Supply. Lignin was modelled by Guaiacol $\geq 98\%$ from Sigma-Aldrich. The protein was modelled by L-Alanine $\geq 98\%$ from Sigma-Aldrich. The solvent selected in this work was dichloromethane (DCM) from Sigma-Aldrich. Previously, chloroform was used as a solvent to extract crude from the HTL product mixture [24]. Less than 5% difference in crude yields were found when using chloroform and DCM to extract crude from the same HTL product mixtures by Valdez, et al. [16].

2.2. Hydrothermal liquefaction in a batch reactor

The reactor and HTL procedure has been described in detail in previous work [24]. All HTL reactions used 30% biomass model compound, by weight, in distilled water and a reaction pressure of 200 bar. Reaction temperatures of 250, 300 and 350 °C were selected. For each reaction temperature, experiments with reaction times of 5, 10, 20, 30 and 60 min were performed.

Prior to experiments, nitrogen was used to pressure test the reactor to ensure gas would not leak from the reactor during reactions. At the start of each experiment the reactor was filled to approximately 50% by volume with the biomass / distilled water mixture and it was then closed and pre-charged with nitrogen to a specific calculated pressure that would result a final pressure of 200 bar (with an error of plus or minus 10 bar) once the reactor was heated.

To heat the reactor to the desired reaction temperature, a Techne SBL-2D fluidised bed with a Techne-9D temperature controller was employed. The heating rate of the reactor was approximately 125 °C per minute. The experimental reaction time began once the reactor reached 98% of the reaction temperature. After the reaction time was complete, the reactor was cooled by a fan to 70 °C within 4 min before being quenched in water at ambient temperature.

Each experiment was conducted twice. If the difference between the two product yield results was greater than $\pm 5\%$, the experiment was repeated and all three results used. The standard deviation is presented in Figs. 2, 4, 6 and 8 by the error bars.

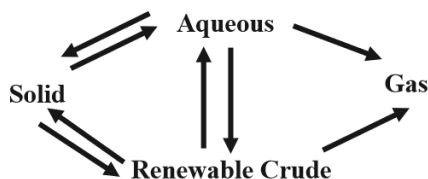


Fig. 1. Possible reaction pathways for bulk kinetic model for monomer model compounds.

2.3. Recovery and separation of products from HTL

Once the HTL reactions were complete and the reactor was cooled to ambient temperature, the gas yield was found by weighing the reactor before and after gas release and subtracting the mass of nitrogen added to the reactor prior to reactions. The liquid and solid product was poured into a centrifuge tube. For reactions with lipid, lignin and protein model compounds the reactor was rinsed with 10 g of DCM to remove any soluble oil or solids stuck to the reactor walls and the rinsing liquid and any solids removed from walls were added to the centrifuge tube.

The product mixture was then centrifuged for 20 min at 2000 rpm so that it formed three separate layers - a solvent-soluble organic layer (renewable crude), a solid and an aqueous phase. The organic layer was pipetted from the centrifuge tube so that the solid and aqueous phases remained. Filtration was used to separate solid and aqueous products. The solid residue was dried in an oven at 40 °C for 24 h to remove any moisture before being weighed to determine solids mass for the lipid, lignin and protein model compounds.

The organic layer was dried in a Techne Sample Concentrator at 40 °C for 6 h with a stream of nitrogen. The yield of gas, renewable crude and solid phases were calculated by dividing the mass of each phase by the mass of the biomass model compound initially fed to the reactor. The yield of each phase was defined at ambient conditions. The aqueous phase was determined by difference. The methods have been found to achieve an average recovery of 90% of the reactor product. This is because some product is lost via condensation to the top half of the reactor tubing while cooling the reactor to ambient conditions. The mass of product lost is most likely the lower boiling point aqueous phase as opposed to the crude which has higher boiling point range.

The solid yield from glucose was inflated by bound crude as seen previously [24]. To account for increased solid content, an alternative method using a Weatherfords Source Rock Analyser™, which employs pyrolysis, was utilised to separate the crude bound to the solids to determine the yields for carbohydrate reactants, as described in Section 2.4.1. No solvent was added to the HTL product mixture for carbohydrate, instead the reactor contents was emptied into a centrifuge tube and then filtered. The solid product was dried in an oven at 40 °C for 24 h before being analysed via the Weatherfords Source Rock Analyser™.

2.4. Analysis of products from HTL

2.4.1. Pyrolysis measurements for carbohydrate yields

Pyrolysis measurements were undertaken using a Weatherfords Source Rock Analyser™. Crucibles were loaded into the carousel and heated under inert Helium in both the pyrolysis (to obtain S1, S2, Tmax and S3 peaks) and oxidation modes (to obtain the S4 peak). S1 represents the free hydrocarbons in the sample. S2 is the organic matter that can be converted to hydrocarbons. S3 is the carbon dioxide released from the organic matter. S4 is the organic matter which will not be converted to hydrocarbons. The pyrolysis oven was first held at 300 °C for 5 min and ramped at 25 °C per minute from 300 °C to 650 °C. Subsequently the oven temperature was reduced to 220 °C and held for 5 min with the carrier gas changed to inert air (CO & CO₂ free). It was then purged, ramped at maximum heating rate to 580 °C and held for 20 min. The flame ionisation detector (FID) was calibrated by running Weatherford Laboratories Instruments Division Standard 533. The IR Analysers were calibrated against standard gas with known concentration of CO₂ and CO. An analysis blank was run as 'blank' mode with the sample batch and the blank data was automatically subtracted from all analyses. An external check standard was also run prior to each batch to ensure the instrument status with additional check standards run every 10 samples. The results were processed where peak areas and geochemical indices including Total organic carbon (TOC), Oxygen Index (OI), Hydrogen Index (HI) and Production Index (PI) are

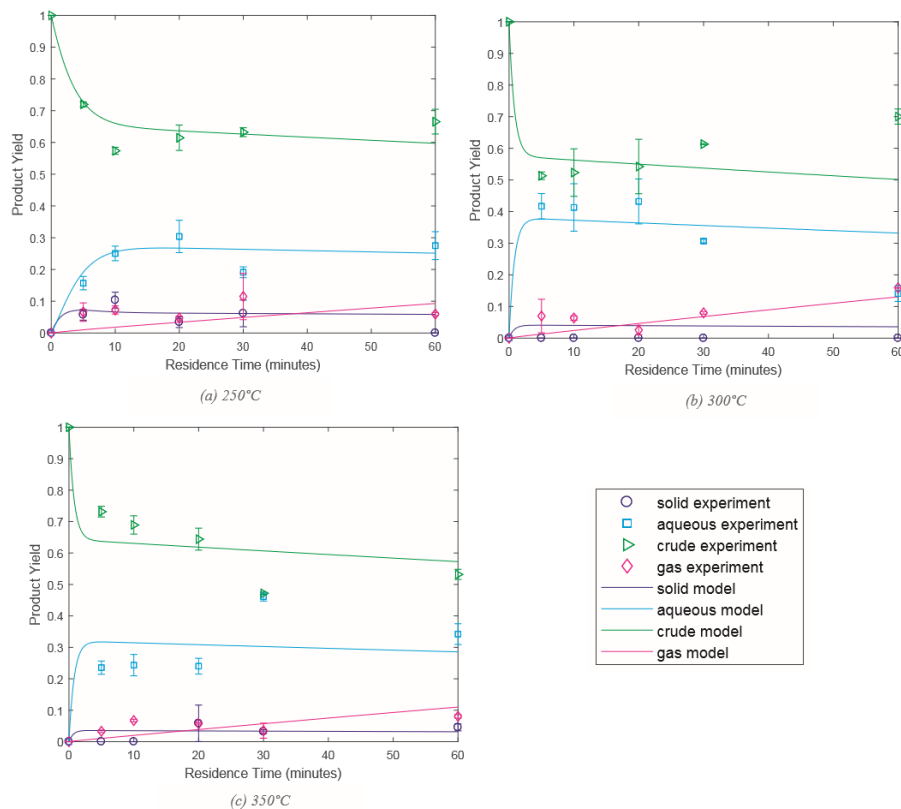


Fig. 2. HTL product from oleic acid, the lipid monomer model compound.

automatically calculated. S1 was used to determine the crude yield while the remaining fractions of analysis product in pyrolysis were used to calculate solid yield.

Previously, use of distillation by thermogravimetric analysis to separate crude from solid for carbohydrate HTL products was utilised [24]. This method uses the principle of heating the solid to release crude fractions which were measured to calculate product yields. The difference in crude yields from the two methods was found by performing each method on the same samples. Analysis on the same samples indicated that TGA resulted in a higher crude yield by, on average, less than 5% than the pyrolysis method on the Weatherfords Source Rock Analyser™. Use of the Source Rock Analyser™ was more time efficient than TGA, so was used in preference in order to perform the over 100 experiments conducted for this work. These methods were employed in order to gain maximum crude recovery so product distribution could be more accurately defined than when using solvent alone. The use of solvent alone was not able to recover all the crude from the carbohydrate product mixture due to the porous nature of the solids [20,31].

2.4.2. GC-MS of renewable crude products

Hydrocarbon characterisation for the liquid crude products was undertaken using a Perkin Elmer SQ8 Gas Chromatograph-Mass Spectrometer (GC-MS). Compound separation was undertaken using a Perkin Elmer Elite-5MS capillary column (30 m × 0.25 mm ID × 0.25 μm phase thickness) with helium carrier gas at a flow of 1 ml/min. 1 μL of sample was injected in split mode (200:1) with an injection temperature of 300 °C. The oven temperature program was 50 °C, held for one minute, prior to a 10 °C/minute ramp to 300 °C and

a final hold of 19 min. The mass spectrometer scanned from m/z 50–600. Data interpretation was undertaken using Perkin Elmer TurboMass 6.0 software with comparison of compound spectra to the NIST14 Spectral Library Database.

Hydrocarbon characterisation for the solid products from HTL of glucose was undertaken using a Fisons MD800 Mass Spectrometer coupled to an Agilent 7980 Gas Chromatograph fitted with a Quantum MSSV Pyrolysis Injector. Compound separation was undertaken using J & W Scientific DB-5MS capillary column (30 m × 0.25 mm ID × 0.25 μm phase thickness) with helium carrier gas at a flow of 1 ml/min. Approximately 2 mg of sample was loaded into pre-cleaned MSSV glass tubes (100ul capacity), sealed and placed into the Quantum MSSV injector at 300 °C. The tube was taken through a fast ramped GC heating cycle to remove any exterior organic components. The tube was cracked open within the MSSV injector and evolved components were cryo-focused in liquid nitrogen on the head of the capillary for 1 min prior to analysis. The oven temperature program was 35 °C, held for one minute, prior to a 10 °C/minute ramp to 300 °C and a final hold of 14 min. The mass spectrometer scanned from m/z 40–500. Data interpretation was undertaken using Perkin Elmer TurboMass 6.0 software with comparison of compound spectra to the NIST14 Spectral Library Database. Example chromatograms are given in the Supporting Information in Figures S1–S4.

2.5. Kinetic parameters

The method for modelling the reaction products by fitting a set of ODEs to the experimental values found in this work using the least square errors optimisation function in MATLAB has been described

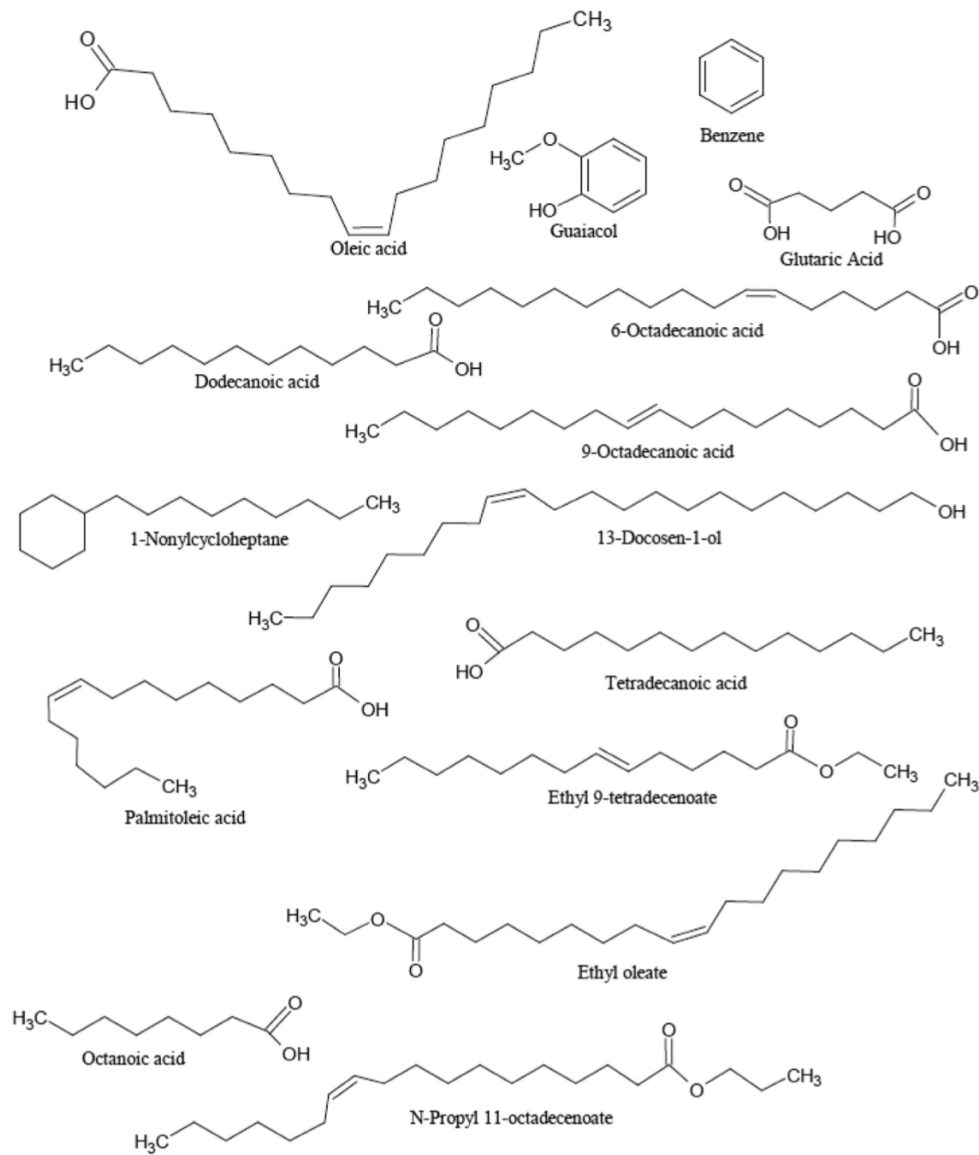


Fig. 3. Compounds identified in renewable crude from the lipid monomer model compound.

previously in Obeid, et al. [24]. The initial pathways considered are shown in Fig. 1. Kinetic parameters were fitted to these pathways, however depending on the model compound, some pathways resulted in kinetic parameters of zero. Hence, some of the pathways in Fig. 1 were removed as part of the modelling method. Additionally, some of these pathways could be omitted to get the same fit of the model, hence the pathways selected in the final model are shown in Fig. 10(a)-(d). The 95% confidence interval to calculate error in Arrhenius parameters has also been utilised as described in previous work [24].

The model required initial conditions to be input so that kinetic parameters could be found. The initial conditions for the model were found by adding 30 wt% model compound to 70 wt% distilled water. Solvent was used to separate the organic phase to obtain the renewable crude yield at zero minutes residence time for the untreated mixtures of lipid, protein and lignin model compounds. Filtration and then drying

the solids in the oven at 40 °C for 24 h was used to measure solid yield for initial conditions. For the carbohydrate model compound, initial conditions for crude yield and solid yield were found by performing the pyrolysis measurements on the untreated solid after filtering and drying the untreated mixture. For all four model compounds the initial gas yield was zero and the aqueous yield was calculated by difference.

3. Results and discussion

3.1. Lipid

3.1.1. Product yields and the bulk kinetic model from HTL of lipid

Fig. 2 depicts the product yields from HTL of the lipid model compound, oleic acid, and the results of the kinetic model. Oleic acid is a long-chain fatty acid and was the monomer model compound for lipid

Chapter 4 – Reaction kinetics and characterisation of species in renewable crude from hydrothermal liquefaction of monomers to represent organic fractions of biomass feedstocks

R. Obeid, et al.

Chemical Engineering Journal 389 (2020) 124397

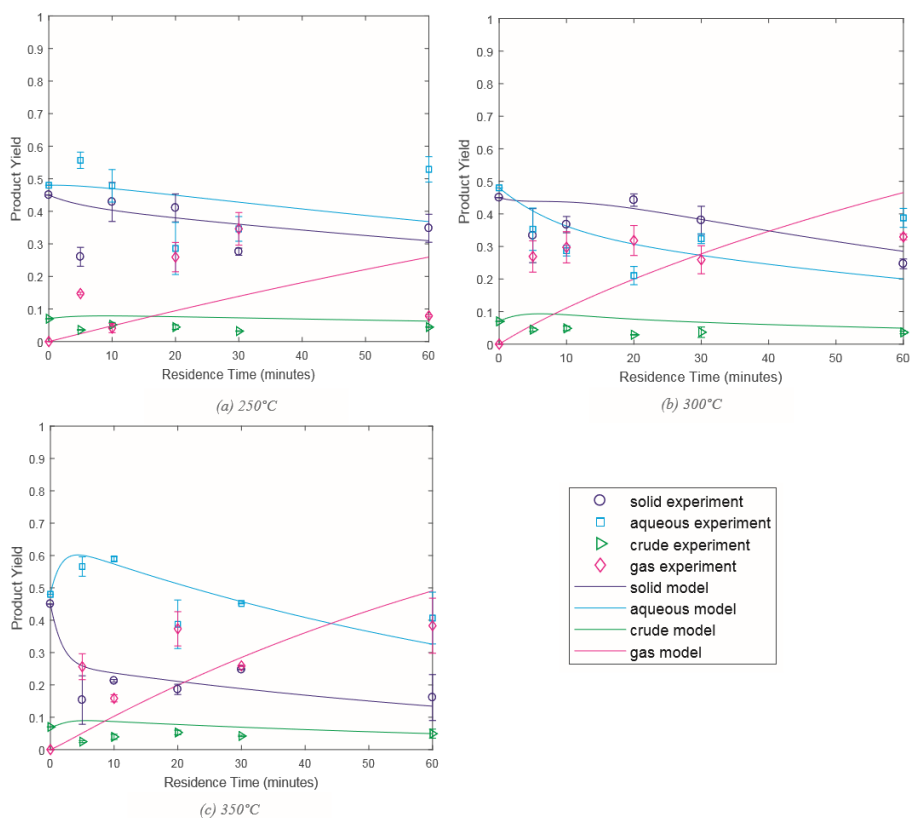


Fig. 4. HTL product from glucose, the carbohydrate monomer model compound.

used in experiments for this work. Some intermediate products of HTL of oleic acid recombine to form solid and renewable crude compounds with a higher number of carbons than the original feed identified by GC-MS (Fig. 3). The presence of solids in the product mixture from HTL of oleic acid (a solid-free feed) is further evidence of recombination of intermediate products during HTL. Hence, a reaction path from crude to solid was required in the HTL model for oleic acid in Fig. 10(a). The first order ODE model fit to the products from HTL of oleic acid depicts the general trends of decreasing crude yield and increasing aqueous and gas phase yield with reaction time. Some experimental yields deviate from the model which indicates that the bulk kinetic paths of the simpler model monomer compounds do not follow first order kinetics with great accuracy. This is emphasised by the error in Arrhenius parameters presented in Table 1.

In experiments with the fatty acid, linoleic acid, renewable crude yields between 38% and 77% were found for reaction temperatures between 250 and 350 °C. The highest yield was for a reaction temperature of 300 °C and reaction time of 20 min [32]. For oleic acid in this work, crude yields were between 47% and 73%. Apart from crude yield being highest for the untreated oleic acid at a reaction time of zero minutes, the highest crude yield obtained after HTL treatment was at 350 °C and 5 min. While the range of yields for linoleic at similar reaction conditions is similar to the present work for oleic acid, the differences in yields at specific reaction conditions for the fatty acids could be due to the different chemical structure, the different heat-up times and the higher mass loading in this work. The same solvent, DCM, was used to extract the renewable crude from the liquid phases.

For the majority of experimental conditions, the HTL product of

oleic acid consisted of a lower crude yield than the products that were observed at the same reaction conditions for sunflower oil, a polymer model compound for lipid [24]. The range of crude yields from the HTL of sunflower oil at different reaction times varied by around 90% [24] while the range of crude yields for oleic acid varied by under 30% in Fig. 2. Residence time and reaction temperature did not cause as much variation in yields for all four product phases from HTL of oleic acid compared to sunflower oil. The conversion of the monomer model compound resulted in the compounds from the organic phase moving to the aqueous phase and the production of under 10% solid products. In contrast, HTL of the polymer model compound did not result in any solid products forming [24]. The trend of decreasing crude yield with increased residence time for all three reaction temperatures, due to product being converted to the aqueous phase, is consistent for both the monomer and polymer model compounds. However, the activation energy for the pathway from renewable crude to aqueous phase is 37.4 kJ/mol higher than that from aqueous to renewable crude for monomers, while the opposite is true for polymers where the pathway from aqueous phase to renewable crude has an activation energy which is 110 kJ/mol higher than the pathway from renewable crude to aqueous phase. The models indicate that the crude produced from the polymer is more easily converted to aqueous phase than the crude produced from the monomer. This is because the model for the monomer compound includes the additional reaction pathway from crude to solid and the crude is converted to an additional product phase.

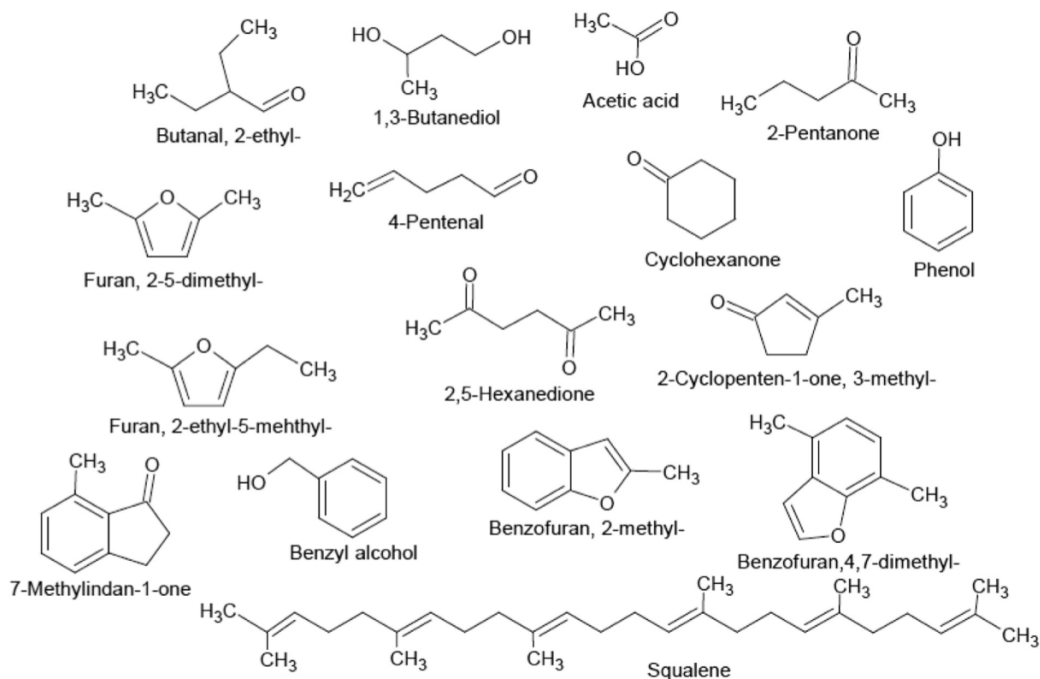


Fig. 5. Compounds identified in renewable crude-solid mixture from the glucose monomer model compound.

3.1.2. GC-MS results for renewable crude produced from HTL of lipid

GC-MS was performed for renewable crudes produced from experiments conducted at 250, 300 and 350 °C and residence times of 5 and 30 min. While the chromatograms produced from GC-MS analysis varied for each different renewable crude produced from the same model compound due to different product formation from HTL, the compounds interpreted from the mass spectra for each peak on the chromatogram were consistent. This resulted in identification of the same compounds for each set of reaction conditions as shown in Fig. 3, which shows 15 of the commonly identified product compounds produced from oleic acid.

Partial decarboxylation of fatty acids was predicted to be one of the main reactions by Watanabe, et al. [33] in their HTL reactions with stearic acid, so fatty acids and long chain hydrocarbons should be the main products from HTL of lipids. This has been confirmed by the GC-MS results from this work (Fig. 3) with compounds including 13-docosen-1-ol and 1-nonylcycloheptane. The decomposition of oleic acid is shown by the presence of the lower molecular weight compounds in the renewable crude including guaiacol, dodecanoic acid, glutaric acid, octanoic acid and benzene. However, oleic acid was still present in all six renewable crude samples, so the compound displays some stability during hydrothermal treatment. Minor changes to the oleic acid molecule can be seen in the presence of 6-octadecanoic acid and 9-octadecanoic acid where cis-trans isomerisation is seen on the fatty acid chain. Evidence of the recombination of HTL decomposition products from HTL of oleic acid is provided by the higher molecular weight molecules produced, including N-propyl 11-octadecenoate and 13-docosen-1-ol.

The fatty acid, tetradecanoic acid, was identified as a HTL product from sunflower oil and algae by Biller and Ross [34]. Phenols were also identified in the renewable crude of algae with lipid content of 5 to 32% [34]. The GC-MS results collected in our work indicate that the presence of fatty acids and phenolic compounds from the renewable crude produced from the HTL of real biomass could evolve from the lipid fraction of the real biomass.

3.2. Carbohydrate

3.2.1. Product yields and the bulk kinetic model from HTL of carbohydrate

The yields from HTL of the carbohydrate model compound, glucose, as well as the results of the kinetic model for glucose are shown in Fig. 4. HTL of glucose resulted in a general trend of decreasing solid phase with increased residence time. Crude yield was under 6% with minimal variation at different residence times and temperatures. Gas yield was high at 10–40% after 5 min residence time.

The results for renewable crude yield from the HTL of glucose shown in Fig. 4 were much lower than those found for cellulose in our previous work at the same reaction conditions [24]. This is likely due to the higher solubility of glucose and its HTL products in the aqueous phase than those from cellulose. At the same HTL reaction conditions, renewable crude yields ranged from 14–43% for cellulose and 3–6% for glucose. This difference resulted in a much higher aqueous phase for glucose HTL product. Previous investigations on the products from cellulose HTL have identified organic acids and hydroxymethylfurfural (HMF) among the main liquid phase compounds formed [20]. These can be soluble in either water or an organic phase and this will greatly affect the yield of aqueous and renewable crude obtained. From the GC-MS results, some of which are displayed in Fig. 5, no HMF was identified in the crude-solid fraction so HMF appears to exist in the aqueous phase.

Previous models which predict the degradation of cellulose during HTL suggest that the cellulose polymer is broken down to the glucose monomer [35,36]. In subcritical conditions, Sasaki, et al. [37] showed that glucose decomposition was faster than cellulose decomposition. Hence, the HTL product from cellulose likely contains cellulose which has not degraded and would not enter the aqueous phase while the glucose degrades to lower molecular weight compounds much more quickly. The solid product formed from the HTL of carbohydrates is likely a result of the reactions between glucose and HMF which result in the formation of humins [35]. Humins are organic compounds which are insoluble in water at all pHs but can decompose to form crude

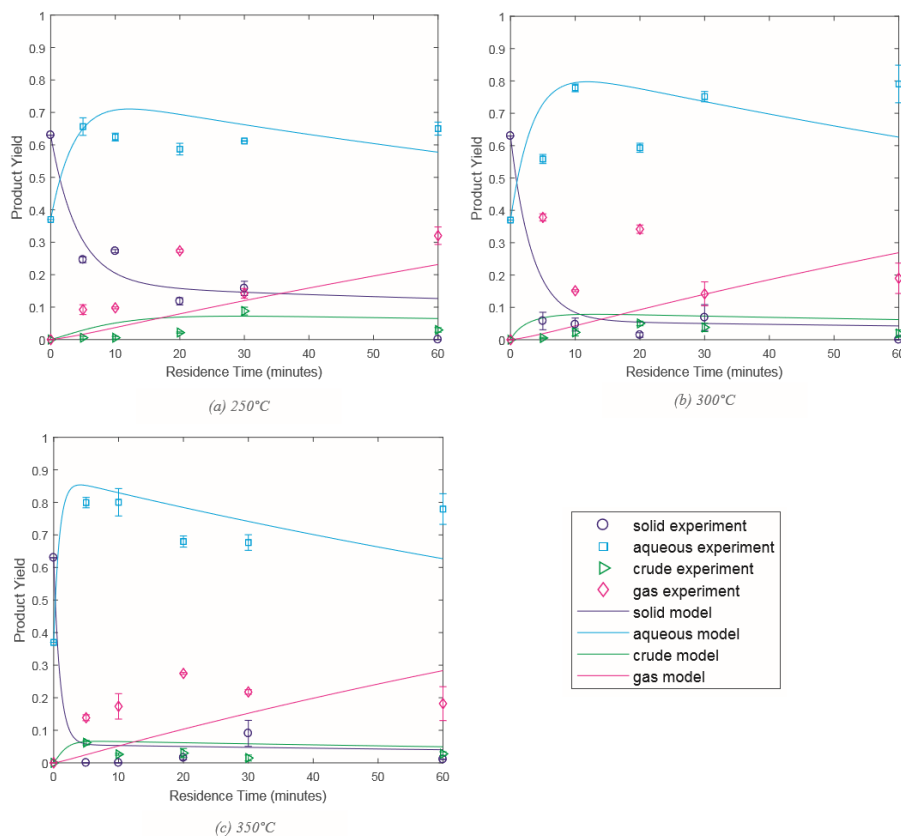


Fig. 6. HTL product from alanine, the protein monomer model compound.

product.

The predictive bulk kinetic model for glucose derived from experimental data in this work presented in Fig. 4 was found at all three temperatures. Unlike the previously developed cellulose model [24], a reaction path from renewable crude to solid phase products was required to give the best fitting model. This path could be representative of humin formation. The reaction pathway with the highest activation energy for the polymer carbohydrate was for renewable crude to aqueous phase at 25.6 kJ/mol and for the monomer model compound it was for the pathway from solid to aqueous phase at 46.5 kJ/mol. This agrees with the higher crude yields seen from polymers compared to monomers, as the crude is less easily converted to aqueous phase. The aqueous to gas phase pathway has the lowest activation energy for both the polymer and monomer which is indicative of the high gas yields from HTL of carbohydrates.

3.2.2. GC-MS results for renewable crude produced from HTL of carbohydrate

Fig. 5 depicts some of the products identified in the crude produced from the HTL of glucose. The glucose product contained the highest number of different products which could be identified by GC-MS of the four monomer model compounds analysed in this work. Squalene was identified at 300 and 350 °C and acetic acid was identified at 250 and 300 °C. Hence, higher temperatures for HTL could result in some higher molecular weight product and lower temperatures could result in some lower molecular weight product. The yield of humins has also been found to increase with increasing temperature by van Zandvoort, et al. [38]. Glucose and its isomer, fructose, were not identified in the

crude-solid mixture and if any of the model compound was present in the product it would likely be in the aqueous phase. However, previous investigations of glucose and fructose as HTL feedstocks have identified that they rapidly decompose to form other products [39].

Srokol, et al. [40] studied the products from HTL of glucose and other monosaccharides and also identified low molecular weight aldehydes and organic acids. Phenols, furans, acids and aldehydes have also been identified from the products of glucose HTL [40]. In Fig. 5 phenol, furans, aldehydes, aromatics and ketones were likewise identified in the crude-solid product from the HTL of glucose in this work. The main reactions of glucose appear to be recombination to form heavy molecular weight products including squalene (see Fig. 5), followed by solids conversion to aqueous phase products and low molecular weight organic compounds.

3.3. Protein

3.3.1. Product yields and the bulk kinetic model from HTL of protein

The yields for products from the HTL of the model protein monomer, alanine, and the results of the kinetic model are shown in Fig. 6. The experimental product yields for alanine deviated most significantly from those predicted by the model out of the four model compounds in this work and this is likely due to the non-uniform trends of the aqueous and gas phase which do not clearly increase or decrease with increasing residence time. The recombination products seen in Fig. 7 as well as the presence of solids at most of the reaction conditions for HTL of alanine resulted in the reaction path back to solid in Fig. 10(c). Crude yield from the HTL of alanine was also under 10%

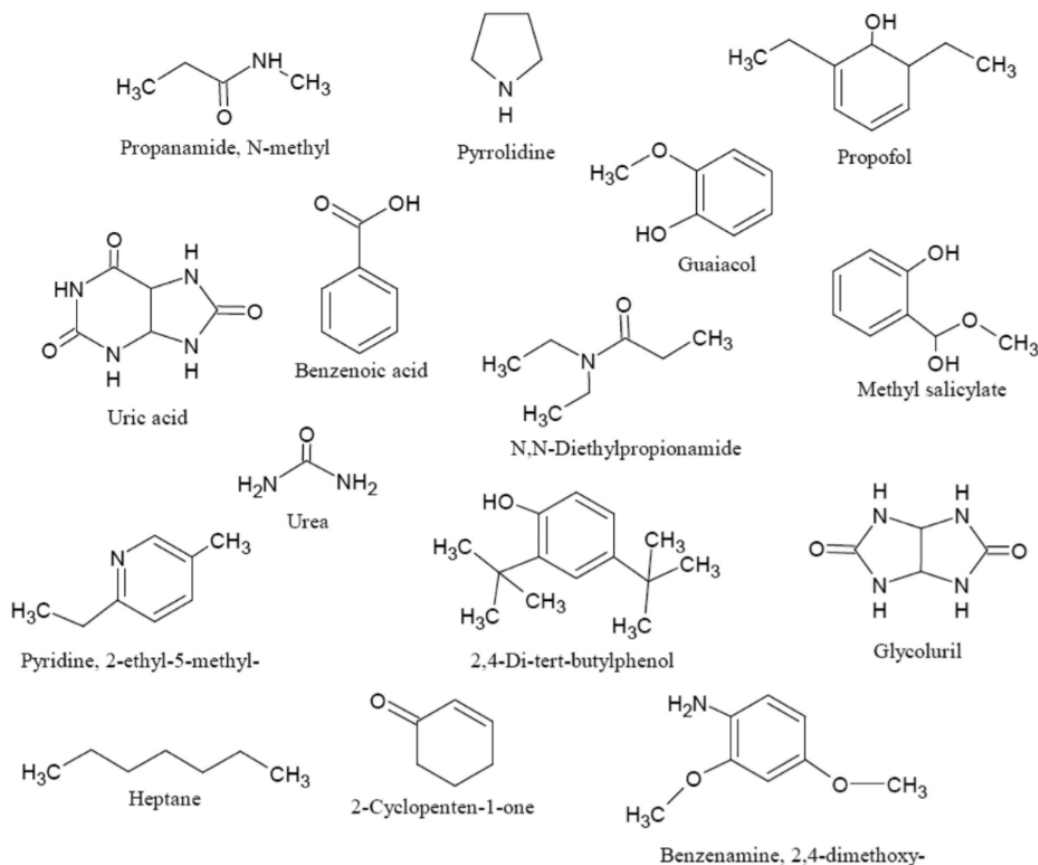


Fig. 7. Compounds identified in renewable crude from the protein monomer model compound.

with little variation with different reaction times and temperatures.

The model amino acids phenylalanine and leucine were used for HTL by Matayeva, et al. [41]. Using water as a solvent at reaction conditions of 300 °C and 60 min resulted in renewable crude yields of 7.9% for phenylalanine and 6.0% for leucine. At 300 °C and 60 min for alanine in this work a renewable crude yield of 2% was found. The amino acids from the previous work have higher molecular weights which are likely to result in fewer aqueous phase compounds being produced. This is demonstrated where phenylalanine, $C_9H_{11}NO_2$, has a greater crude yield than leucine, $C_5H_{13}NO_2$.

The amino acid monomer used to represent protein in this work produced far less organic soluble renewable crude products in Fig. 6 than the protein polymer, BSA, used previously which resulted in an average crude yield of 30% [24]. More aqueous phase products are formed from the monomer as opposed to conversion to organics. This is likely due to the low molecular weight of alanine, having the chemical formula $C_3H_7NO_2$, while the protein, BSA, is made up of many amino acids linked together. While the activation energy for the pathway from aqueous to gas phase was highest for the protein polymer model [24], this pathway had the lowest activation energy for the monomer model compound, even though the gas yields were in the same range. This is due to the different pathways used to describe the HTL reactions of polymers and monomers. The yield of aqueous phase is higher for the monomer model compound at most reaction conditions and this is reflected in the higher activation energy of 43.8 kJ/mol for the pathway from aqueous to renewable crude to phase for the monomer compound compared to the polymer at 2.9 kJ/mol. The aqueous phase from the

polymer is more easily converted to crude.

In HTL experiments where the polymers albumin and soya protein, as well as the amino acids asparagine and glutamine, were reacted at 350 °C and 60 min, the amino acids were found to produce the lowest renewable crude yields by Biller and Ross [34]. The aqueous yield was highest for the asparagine and the solid yield was highest for glutamine. Déniel, et al. [25] also identified that HTL of the amino acid, glutamic acid, resulted in over 90% aqueous phase products.

3.3.2. GC-MS results for renewable crude produced from HTL of protein

Compounds identified in the crude produced from the protein model compound are presented in Fig. 7. The second largest number of compounds was identified in the crude from the protein model compound as many variations of amides, amines and aldehydes were identified in the crude. Many nitrogen containing compounds have been identified in the renewable crude from the amino acid, however, decomposition during HTL has resulted in some organic low molecular weight compounds including heptane, benzoic acid, guaiacol, propofol and 2-Cyclopenten-1-one, which do not contain nitrogen. Most compounds identified via GC-MS contain more than the three carbons present in alanine, signifying recombination of HTL decomposition products.

The renewable crude from HTL of the protein monomer is expected to produce mainly organic acids [25]. Amides, aromatics, saturated and unsaturated hydrocarbons have been identified in the crude as was found for soy protein HTL product by Luo, et al. [8]. The HTL experiments with alanine as a feedstock by Klingler, et al. [42] identified ethylamine, acetaldehyde, lactic acid and carbon dioxide as the main

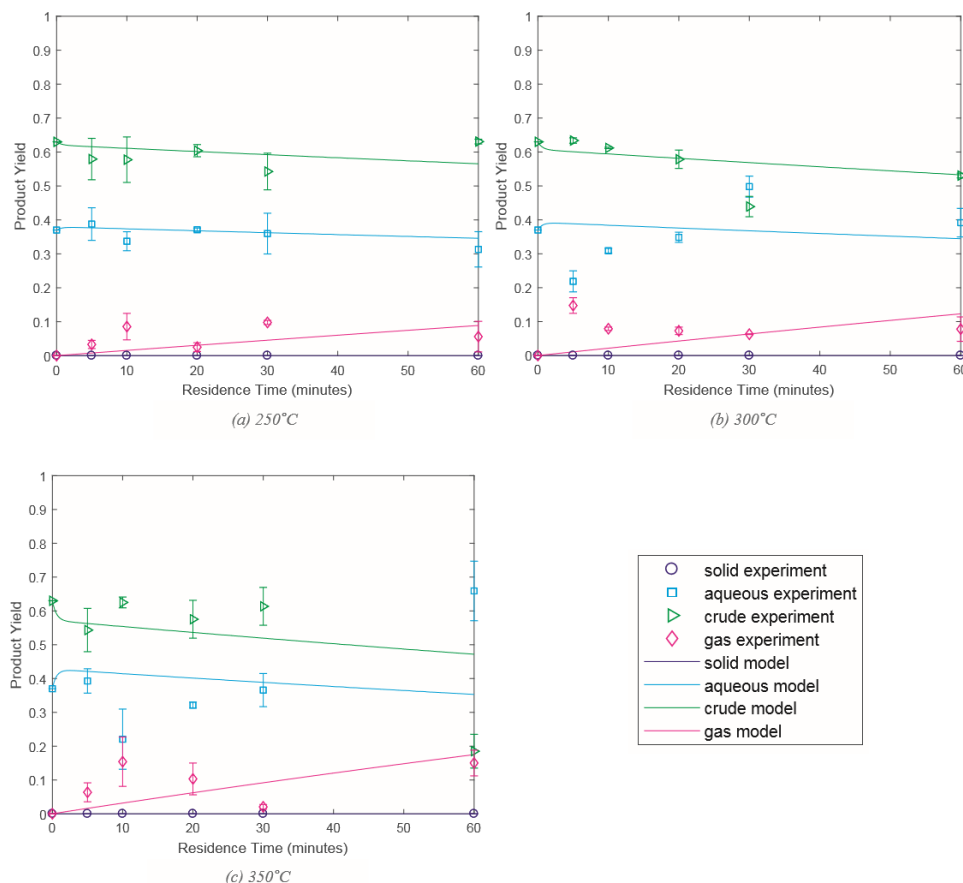


Fig. 8. HTL product from guaiacol, the lignin monomer model compound.

HTL products. The varying reaction conditions for HTL of alanine in this work, including 250, 300 and 350 °C at residence times of 5 and 30 min, also resulted in identification of amides, aromatics, amines, carboxylic acids, saturated and unsaturated hydrocarbon chains. Alanine is soluble in the aqueous phase, hence no alanine was identified in the renewable crude from GC-MS.

3.4. Lignin

3.4.1. Product yields and the bulk kinetic model from HTL of lignin

Fig. 8 shows the yields produced from HTL of the lignin model compound, guaiacol. For the unreacted guaiacol, 63% was soluble in the DCM solvent and after HTL reactions the organic phase product was reduced. The lowest crude yield of 18% was obtained at the harshest reaction conditions of 350 °C and 60 min. No solids were produced from HTL reactions of guaiacol and the initial reactant was in liquid form. Hence, there are no reaction paths for solids in Fig. 10(d).

Due to the lesser variation in product yields with reaction time for guaiacol, as opposed to the other three model compounds used in this work, the first order bulk kinetic model can predict product yields with the most accuracy for guaiacol. The model captures the trends of increasing gas yield as well as the decreasing crude and aqueous phase yields with increased residence time. While previous work has found alkaline lignin to be an unfavourable HTL feedstock for producing crude oil, the intermediate phenolic compounds from the degradation of the lignin from real biomass during HTL can produce high crude

yields. Guaiacol has been identified as an intermediate product from the HTL of lignocellulosic biomass in multiple studies [23,43,44]. Déniel, et al. [19] conducted HTL on guaiacol at reactions conditions of 300 °C and 60 min to find a crude yield of 71.1% which is about 20% higher than the yield found in this work. Their heating time was around 30 min longer than the heating time in this work.

The model lignin monomer produced much higher organic phase yield from HTL treatment than the alkaline lignin polymer used in previous work [24]. While crude yields for guaiacol remained between 18 and 64% in Fig. 8, the maximum crude yield for alkaline lignin was 7% at the same set of reaction conditions [24]. Mostly lower gas yields were seen for the monomer lignin compound compared to the polymer and this is reflected in the higher activation energy of 21.7 kJ/mol for the pathway from renewable crude to gas for the monomer compared to 7.6 kJ/mol for the polymer.

3.4.2. GC-MS results for renewable crude produced from HTL of lignin

The compounds identified from the crude produced from HTL of guaiacol are presented in Fig. 9. As is consistent with the other model compounds used in this work, the same renewable crude products were identified via GC-MS for all six samples produced at experimental conditions of 250, 300 and 350 °C and residence times of 5 and 30 min for HTL of guaiacol. Phenolic compounds were the main compounds identified in the renewable crude in agreement with previous analysis of lignin and guaiacol HTL products [25,45]. Previously catechol has been identified in the aqueous phase HTL product of guaiacol by Déniel,

Chapter 4 – Reaction kinetics and characterisation of species in renewable crude from hydrothermal liquefaction of monomers to represent organic fractions of biomass feedstocks

R. Obeid, et al.

Chemical Engineering Journal 389 (2020) 124397

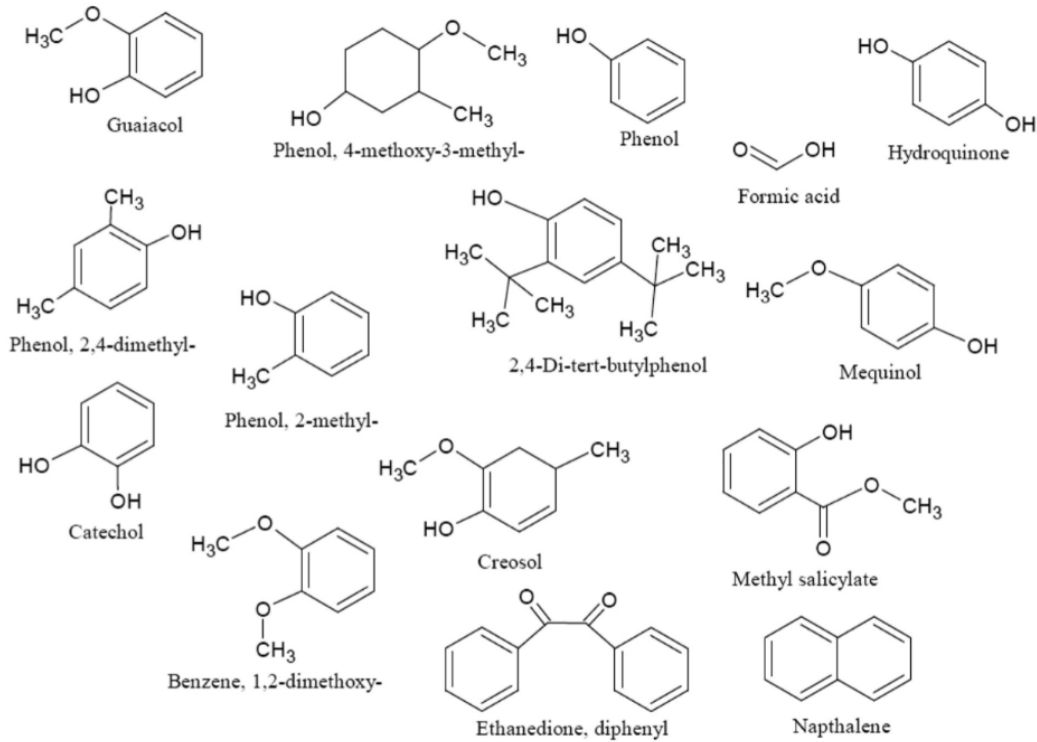


Fig. 9. Compounds identified in renewable crude from the lignin monomer model compound.

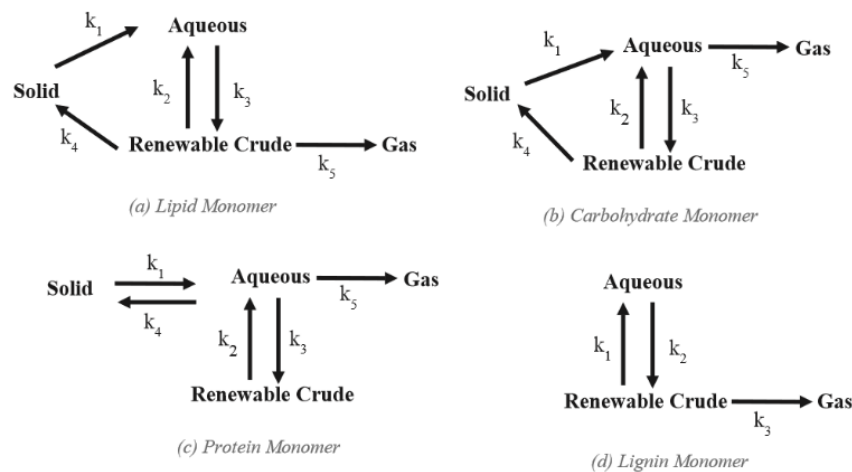


Fig. 10. Bulk kinetic model reaction pathways for monomer model compounds.

et al. [25]. This is due to the use of an alternative solvent, ethyl acetate. DCM in this work extracted the catechol as part of the renewable crude. A reaction mechanism for the HTL of guaiacol has been derived by Kanetake, et al. [30]. Catechol, phenol and o-cresol were identified as the main products from HTL of guaiacol which is in agreement with this work.

Organic acids were also identified from the decomposition of guaiacol as shown in Fig. 9, including formic acid. Guaiacol was also identified in all six renewable crude samples so had some stability

during HTL treatment. The majority of products in the renewable crude from HTL of guaiacol are aromatics as is visible in Fig. 9.

3.5. Kinetic model

The bulk kinetic models for the monomer compounds in Fig. 10 are described by the ODEs shown in Equations 1–15. Solid yield is given by x_1 , aqueous yield by x_2 , renewable crude yield by x_3 and gas yield by x_4 . The yields, x_1 , x_2 , x_3 and x_4 , are based on the mass of each product phase

Chapter 4 – Reaction kinetics and characterisation of species in renewable crude from hydrothermal liquefaction of monomers to represent organic fractions of biomass feedstocks

R. Obeid, et al.

Chemical Engineering Journal 389 (2020) 124397

Table 1
Kinetic parameters for monomer model compounds.

Compound	Path	Reaction	k[°C](sec ⁻¹)	Temperature (°C)	lnA	E _A (kJ/mol)	
Lipid	1	Solid to Aqueous	250		300	350	
	2	Renewable crude to Aqueous	33.00		45.13	60.00	7.2 ± 0.1
	3	Aqueous to Renewable crude	2.14		28.58	28.8	16.7 ± 14.6
	4	Renewable crude to Solid	12.89		48.19	60.00	11.9 ± 6.0
	5	Renewable Crude to Gas	3.23		3.23	3.30	0.6 ± 18.5
Carbohydrate	1	Solid to Aqueous	0.14		0.24	0.17	-0.3 ± 4.4
	2	Renewable crude to Aqueous	3.81		3.00	22.73	11.7 ± 13.8
	3	Aqueous to Renewable crude	0.60		0.90	1.20	3.8 ± 0.3
	4	Renewable crude to Solid	3.00		3.49	9.16	7.8 ± 5.2
	5	Aqueous to Gas	17.34		13.96	60.00	10.0 ± 10.2
Protein	1	Solid to Aqueous	0.61		1.61	1.06	1.9 ± 18.6
	2	Renewable crude to Aqueous	12.24		16.99	59.79	12.0 ± 6.1
	3	Aqueous to Renewable crude	7.87		59.24	51.48	12.8 ± 11.4
	4	Renewable crude to Solid	0.85		5.84	4.03	10.2 ± 12.3
	5	Aqueous to Gas	2.62		1.13	3.82	2.6 ± 11.9
Lignin	1	Renewable crude to Aqueous	0.36		0.38	0.38	-0.8 ± 0.2
	2	Aqueous to Renewable crude	33.01		38.32	44.64	5.2 ± 0.3
	3	Renewable crude to Gas	54.06		59.40	59.84	4.6 ± 0.45
			0.15		0.22	0.34	3.1 ± 0.8
							21.7 ± 0.7

as a percentage of the dry biomass feedstock.

Lipid

$$\frac{dx_1}{dt} = -k_1x_1 + k_4x_3 \quad (1)$$

$$\frac{dx_2}{dt} = -k_3x_2 + k_1x_1 + k_2x_3 \quad (2)$$

$$\frac{dx_3}{dt} = -(k_2 + k_4 + k_5)x_3 + k_3x_2 \quad (3)$$

$$\frac{dx_4}{dt} = k_5x_3 \quad (4)$$

Carbohydrate

$$\frac{dx_1}{dt} = -k_1x_1 + k_4x_3 \quad (5)$$

$$\frac{dx_2}{dt} = -(k_3 + k_5)x_2 + k_1x_1 + k_2x_3 \quad (6)$$

$$\frac{dx_3}{dt} = -(k_2 + k_4)x_3 + k_3x_2 \quad (7)$$

$$\frac{dx_4}{dt} = k_5x_2 \quad (8)$$

Protein

$$\frac{dx_1}{dt} = -k_1x_1 + k_4x_2 \quad (9)$$

$$\frac{dx_2}{dt} = -(k_3 + k_4 + k_5)x_2 + k_1x_1 + k_2x_3 \quad (10)$$

$$\frac{dx_3}{dt} = -k_2x_3 + k_3x_2 \quad (11)$$

$$\frac{dx_4}{dt} = k_5x_2 \quad (12)$$

Lignin

$$\frac{dx_2}{dt} = -k_2x_2 + k_1x_3 \quad (13)$$

$$\frac{dx_3}{dt} = -(k_1 + k_3)x_3 + k_2x_2 \quad (14)$$

$$\frac{dx_4}{dt} = k_3x_3 \quad (15)$$

Each rate constant quantifies the transition to or from one phase to another. The rate constants for these ODEs are listed in Table 1. Rate constants were determined in MATLAB using the ODE solver, *ODE45* alongside the *lsqnonlinear* function. This function minimises the difference between the experimental data points and the model results using a least squares algorithm. The bounds for k[°C](min⁻¹) were set to [0 1]. The ODEs are plotted against the experimental data in Figs. 2, 4, 6 and 8.

The deviations of some experimental yields from the model discussed for lipid, carbohydrate, protein and lignin monomer model compounds, as well as the errors in Arrhenius parameters can be seen in Table 1. The many chemical reactions involving depolymerisation of the polymers to monomers, further decomposition via decarboxylation, deamination, dehydration and cleavage, and then recombination of the intermediate products during HTL are oversimplified by the bulk kinetic model. Another limitation of the model is that the kinetics are defined by the separation methods used in this work. The methods were employed to obtain maximum recovery of the HTL product mixture, though different separation methods could be used at an industrial scale and these can cause variations in product distribution. However, the product yields can be approximated by these models and the trends for the product yields with different reaction time and reaction temperature for each class of monomer model compounds are evident from this work.

This model also neglects the interactions that can occur when the different constituents of biomass, including carbohydrate, lipid, lignin and protein, are reacted together. Previous investigations have indicated that a higher crude yield can be obtained at some reaction conditions when carbohydrates and proteins are reacted together due to Maillard reactions [46]. The presence of lignin in mixtures of model compounds in HTL has also been seen to result in a lower crude yield [47]. Further investigation on the product distribution when mixtures of model compounds are reacted together in HTL will allow the model to be developed to be more suitable for real biomass. Despite these limitations, this work provides a basis for identifying the reaction pathways for real biomass as a feed in HTL as well as an indication of how lipid, carbohydrate, protein and lignin fractions of biomass will contribute to the product phase yields in HTL.

4. Conclusions

Hydrothermal liquefaction of individual model monomer compounds for carbohydrate, lipid, protein and lignin fractions of biomass at varying reaction time and temperature generally resulted in higher

Chapter 4 – Reaction kinetics and characterisation of species in renewable crude from hydrothermal liquefaction of monomers to represent organic fractions of biomass feedstocks

R. Obeid, et al.

Chemical Engineering Journal 389 (2020) 124397

aqueous phase product yields and lower renewable crude yields than the polymer compounds from the same families, except in the case of guaiacol where much higher crude yields were produced for the lignin monomer model compound. Longer residence times resulted in a decreasing trend in crude yield for all four monomer model compounds. The use of monomer model compounds in HTL experiments allowed identification of the different compounds in biocrude from different biomass model compounds. For all four classes of model monomer compounds, the same 15 compounds could be identified for renewable crude produced via HTL for each model compound at temperatures of 250, 300 and 350 °C at 5 and 30 min. Hence, reaction time and temperature did not significantly affect the composition of compounds in the crude produced from monomers as identified by GC–MS. The main compounds produced from lipid HTL are fatty acids. HTL of carbohydrates produced crude consisting mainly of phenol, furans, aldehydes, aromatics and ketones. HTL of the protein monomer resulted in a renewable crude composed of amides, aromatics, amines, carboxylic acids and short hydrocarbon chains. Phenolic compounds made up the majority of the renewable crude from the lignin model compound. This work allowed the identification of the interconversion reaction pathways in HTL for lipid, carbohydrate, protein and lignin components of biomass to be identified as well as providing an indication of how lipid, carbohydrate, protein and lignin fractions of biomass will contribute to the composition of product phases in HTL.

Declaration of Competing Interest

The authors declare that they have no known competing financial interests or personal relationships that could have appeared to influence the work reported in this paper.

Acknowledgements

The authors acknowledge the financial support of the Australian Research Council's Linkage Project grant (LP150101241) and our industry partner Southern Oil Refining Pty Ltd.

Appendix A. Supplementary data

Supplementary data to this article can be found online at <https://doi.org/10.1016/j.cej.2020.124397>.

References

- [1] D.R. Vardon, B.K. Sharma, J. Scott, G. Yu, Z. Wang, L. Schideman, Y. Zhang, T.J. Strathmann, Chemical properties of biocrude oil from the hydrothermal liquefaction of *Spirulina* algae, swine manure, and digested anaerobic sludge, *Bioresource Technology* 102 (2011) 8295–8303.
- [2] D.R. Vardon, B.K. Sharma, G.V. Blazina, K. Rajagopalan, T.J. Strathmann, Thermochemical conversion of raw and defatted algal biomass via hydrothermal liquefaction and slow pyrolysis, *Bioresource Technology* 109 (2012) 178–187.
- [3] P.J. Valdez, P.E. Savage, A reaction network for the hydrothermal liquefaction of *Nannochloropsis* sp., *Algal Research* 2 (2013) 416–425.
- [4] P.J. Valdez, V.J. Tocco, P.E. Savage, A general kinetic model for the hydrothermal liquefaction of microalgae, *Bioresource Technology* 163 (2014) 123–127.
- [5] D.C. Hietala, J.L. Faeth, P.E. Savage, A quantitative kinetic model for the fast and isothermal hydrothermal liquefaction of *Nannochloropsis* sp., *Bioresource Technology* 214 (2016) 102–111.
- [6] T.K. Vo, S.-S. Kim, H.V. Ly, E.Y. Lee, C.-G. Lee, J. Kim, A general reaction network and kinetic model of the hydrothermal liquefaction of microalgae *Tetraselmis* sp., *Bioresource Technology* 241 (2017) 610–619.
- [7] J.D. Sheehan, P.E. Savage, Modeling the effects of microalga biochemical content on the kinetics and biocrude yields from hydrothermal liquefaction, *Bioresource Technology* 239 (2017) 144–150.
- [8] L. Luo, J.D. Sheehan, L. Dai, P.E. Savage, Products and Kinetics for Isothermal Hydrothermal Liquefaction of Soy Protein Concentrate, *ACS Sustainable Chemistry & Engineering* 4 (2016) 2725–2733.
- [9] B. Zhang, H.-J. Huang, S. Ramaswamy, Reaction Kinetics of the Hydrothermal Treatment of Lignin, *Applied Biochemistry and Biotechnology* 147 (2008) 119–131.
- [10] Y. Li, S. Leow, A.C. Fedders, B.K. Sharma, J.S. Guest, T.J. Strathmann, Quantitative multiphase model for hydrothermal liquefaction of algal biomass, *Green Chemistry* 19 (2017) 1163–1174.
- [11] Y.H. Chan, S. Yusup, A.T. Quitain, R.R. Tan, M. Sasaki, H.L. Lam, Y. Uemura, Effect of process parameters on hydrothermal liquefaction of oil palm biomass for bio-oil production and its life cycle assessment, *Energy Conversion and Management* 104 (2015) 180–188.
- [12] S. Xiu, A. Shahbazi, V. Shirley, D. Cheng, Hydrothermal pyrolysis of swine manure to bio-oil: Effects of operating parameters on products yield and characterization of bio-oil, *Journal of Analytical and Applied Pyrolysis* 88 (2010) 73–79.
- [13] P.J. Valdez, M.C. Nelson, H.Y. Wang, X.N. Lin, P.E. Savage, Hydrothermal liquefaction of *Nannochloropsis* sp.: Systematic study of process variables and analysis of the product fractions, *Biomass and Bioenergy* 46 (2012) 317–331.
- [14] K. Anastasakis, A.B. Ross, Hydrothermal liquefaction of the brown macro-alga *Laminaria Saccharina*: Effect of reaction conditions on product distribution and composition, *Bioresource Technology* 102 (2011) 4876–4883.
- [15] J.L. Faeth, P.J. Valdez, P.E. Savage, Fast Hydrothermal Liquefaction of *Nannochloropsis* sp. To Produce Biocrude, *Energy & Fuels* 27 (2013) 1391–1398.
- [16] P.J. Valdez, J.G. Dickinson, P.E. Savage, Characterization of Product Fractions from Hydrothermal Liquefaction of *Nannochloropsis* sp. and the Influence of Solvents, *Energy & Fuels* 25 (2011) 3235–3243.
- [17] J. Yang, Q. He, K. Corscadden, H. Niu, The impact of downstream processing methods on the yield and physicochemical properties of hydrothermal liquefaction bio-oil, *Fuel Processing Technology* 178 (2018) 353–361.
- [18] S.S. Toor, L. Rosendahl, A. Rudolf, Hydrothermal liquefaction of biomass: A review of subcritical water technologies, *Energy* 36 (2011) 2328–2342.
- [19] M. Déniel, G. Haarlemmer, A. Roubaud, E. Weiss-Hortala, J. Pages, Modelling and Predictive Study of Hydrothermal Liquefaction: Application to Food Processing Residues, Waste and Biomass Valorization 8 (2017) 2087–2107.
- [20] Y. Gao, X.-H. Wang, H.-P. Yang, H.-P. Chen, Characterization of products from hydrothermal treatments of cellulose, *Energy* 42 (2012) 457–465.
- [21] P. Biller, R. Riley, A.B. Ross, Catalytic hydrothermal processing of microalgae: Decomposition and upgrading of lipids, *Bioresource Technology* 102 (2011) 4841–4848.
- [22] A. Kruse, P. Maniam, F. Spieler, Influence of Proteins on the Hydrothermal Gasification and Liquefaction of Biomass. 2. Model Compounds, *Industrial & Engineering Chemistry Research* 46 (2007) 87–96.
- [23] Y. Ye, J. Fan, J. Chang, Effect of reaction conditions on hydrothermal degradation of cornstarch lignin, *Journal of Analytical and Applied Pyrolysis* 94 (2012) 190–195.
- [24] R. Obeid, D. Lewis, N. Smith, P. van Eyk, The elucidation of reaction kinetics for hydrothermal liquefaction of model macromolecules, *Chemical Engineering Journal* 370 (2019) 637–645.
- [25] M. Déniel, G. Haarlemmer, A. Roubaud, E. Weiss-Hortala, J. Pages, Hydrothermal liquefaction of blackcurrant pomace and model molecules: understanding of reaction mechanisms, *Sustainable Energy & Fuels* 1 (2017) 555–582.
- [26] S. Leow, J.R. Witter, D.R. Vardon, B.K. Sharma, J.S. Guest, T.J. Strathmann, Prediction of microalgae hydrothermal liquefaction products from feedstock biochemical composition, *Green Chemistry* 17 (2015) 3584–3599.
- [27] C. Gai, Y. Zhang, W.-T. Chen, P. Zhang, Y. Dong, An investigation of reaction pathways of hydrothermal liquefaction using *Chlorella pyrenoidosa* and *Spirulina platensis*, *Energy Conversion and Management* 96 (2015) 330–339.
- [28] N. Sato, A.T. Quitain, K. Kang, H. Daimon, K. Fujie, Reaction kinetics of amino acid decomposition in high-temperature and high-pressure water, *Industrial & Engineering Chemistry Research* 43 (2004) 3217–3222.
- [29] T. Rogalinski, S. Herrmann, G. Brunner, Production of amino acids from bovine serum albumin by continuous sub-critical water hydrolysis, *The Journal of Supercritical Fluids* 36 (2005) 49–58.
- [30] T. Kanetake, M. Sasaki, M. Goto, Decomposition of a lignin model compound under hydrothermal conditions, *Chemical Engineering & Technology: Industrial Chemistry-Plant Equipment-Process Engineering-Biotechnology* 30 (2007) 1113–1122.
- [31] S. Kang, X. Li, J. Fan, J.J.I. Chang, e.c. research, Characterization of hydrocarbons produced by hydrothermal carbonization of lignin, cellulose, D-xylose, and wood, *meal* 51 (2012) 9023–9031.
- [32] R. Posmanik, D.A. Cantero, A. Malkani, D.L. Sills, J.W. Tester, Biomass conversion to bio-oil using sub-critical water. Study of model compounds for food processing waste, *The Journal of Supercritical Fluids* 119 (2017) 26–35.
- [33] M. Watanabe, T. Iida, H. Inomata, Decomposition of a long chain saturated fatty acid with some additives in hot compressed water, *Energy Conversion and Management* 47 (2006) 3344–3350.
- [34] P. Biller, A.B. Ross, Potential yields and properties of oil from the hydrothermal liquefaction of microalgae with different biochemical content, *Bioresource Technology* 102 (2011) 215–225.
- [35] H. Rasmussen, H.R. Sørensen, A.S. Meyer, Formation of degradation compounds from lignocellulosic biomass in the biorefinery: sugar reaction mechanisms, *Carbohydrate Research* 385 (2014) 45–57.
- [36] M. Sasaki, B. Kabyemela, R. Malaluan, S. Hirose, N. Takeda, T. Adschiri, K. Arai, Cellulose hydrolysis in subcritical and supercritical water, *The Journal of Supercritical Fluids* 13 (1998) 261–268.
- [37] M. Sasaki, Z. Fang, Y. Fukushima, T. Adschiri, K. Arai, Dissolution and Hydrolysis of Cellulose in Subcritical and Supercritical Water, *Industrial & Engineering Chemistry Research* 39 (2000) 2883–2890.
- [38] I. van Zandvoort, Y. Wang, C.B. Rasrendra, E.R. van Eck, P.C. Bruijninx, H.J. Heeres, B.M. Weckhuysen, Formation, molecular structure, and morphology of humins in biomass conversion: influence of feedstock and processing conditions, *ChemSusChem* 6 (2013) 1745–1758.
- [39] B.M. Kabyemela, T. Adschiri, R.M. Malaluan, K. Arai, Kinetics of Glucose Epimerization and Decomposition in Subcritical and Supercritical Water, *Industrial & Engineering Chemistry Research* 36 (1997) 1552–1558.

Chapter 4 – Reaction kinetics and characterisation of species in renewable crude from hydrothermal liquefaction of monomers to represent organic fractions of biomass feedstocks

R. Obeid, et al.

Chemical Engineering Journal 389 (2020) 124397

- [40] Z. Srokol, A.-G. Bouche, A. van Estrik, R.C.J. Strik, T. Maschmeyer, J.A. Peters, Hydrothermal upgrading of biomass to biofuel; studies on some monosaccharide model compounds, *Carbohydrate Research* 339 (2004) 1717–1726.
- [41] A. Matayeva, D. Bianchi, S. Chiaberge, F. Cavani, F. Basile, Elucidation of reaction pathways of nitrogenous species by hydrothermal liquefaction process of model compounds, *Fuel* 240 (2019) 169–178.
- [42] D. Klingler, J. Berg, H. Vogel, Hydrothermal reactions of alanine and glycine in sub- and supercritical water, *The Journal of Supercritical Fluids* 43 (2007) 112–119.
- [43] R. Singh, K. Chaudhary, B. Biswas, B. Balagurumurthy, T. Bhaskar, Hydrothermal liquefaction of rice straw: Effect of reaction environment, *The Journal of Supercritical Fluids* 104 (2015) 70–75.
- [44] B. Zhang, M. von Keitz, K. Valentas, Thermochemical liquefaction of high-diversity grassland perennials, *Journal of Analytical and Applied Pyrolysis* 84 (2009) 18–24.
- [45] J. Schuler, U. Hornung, N. Dahmen, J. Sauer, Lignin from bark as a resource for aromatics production by hydrothermal liquefaction, *Gcb Bioenergy* (2019).
- [46] L. Sheng, X. Wang, X. Yang, Prediction model of biocrude yield and nitrogen heterocyclic compounds analysis by hydrothermal liquefaction of microalgae with model compounds, *Bioresource Technology* 247 (2018) 14–20.
- [47] M. Déniel, G. Haarlemmer, A. Roubaud, E. Weiss-Hortala, J.J.W. Fages, b. valorization., Modelling and predictive study of hydrothermal liquefaction: application to food processing, residues 8 (2017) 2087–2107.

Supporting Information

Reaction kinetics and characterisation of species in renewable crude from hydrothermal liquefaction of monomers to represent organic fractions of biomass feedstocks

Reem Obeid^a, David Lewis^a, Neil Smith^a, Tony Hall^b and Philip van Eyk^{a*}

^aSchool of Chemical Engineering, The University of Adelaide, Adelaide, South Australia 5005, Australia

^bFaculty of Sciences, The University of Adelaide, Adelaide, South Australia 5005, Australia

*E-mail: philip.vaneyk@adelaide.edu.au

Chromatograms from Gas Chromatography-Mass Spectrometry

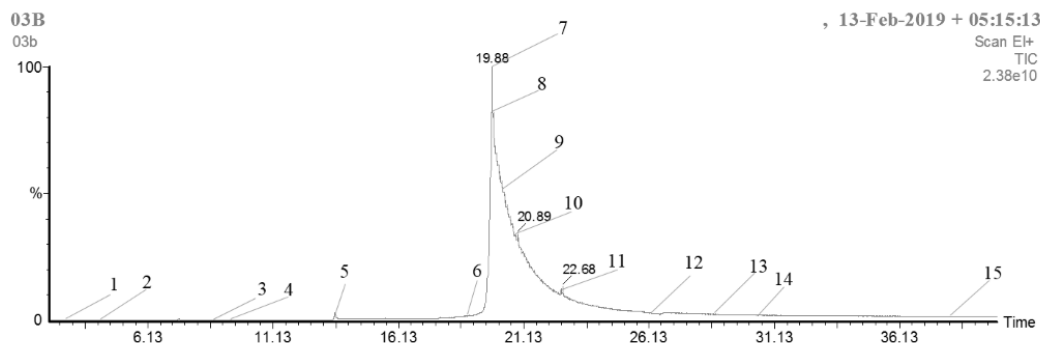


Figure S1. Chromatogram for renewable crude from HTL of oleic acid at 350°C and 30 minutes

Table S1. Corresponding compound identified in chromatogram for renewable crude from HTL of oleic acid at 350°C and 30

Number	Compound
1	Glutaric acid
2	Octanoic acid
3	Guaiacol
4	Benzene
5	Dodecanoic acid
6	Tetradecanoic acid
7	Oleic acid
8	9-Octadecanoic acid
9	Ethyl oleate
10	Palmitoleic acid
11	13-Docosen-1-ol
12	N-Propyl 11-octadecenoate
13	1-Nonylcycloheptane
14	6-Octadecanoic acid
15	Ethyl 9-tetradecenoate

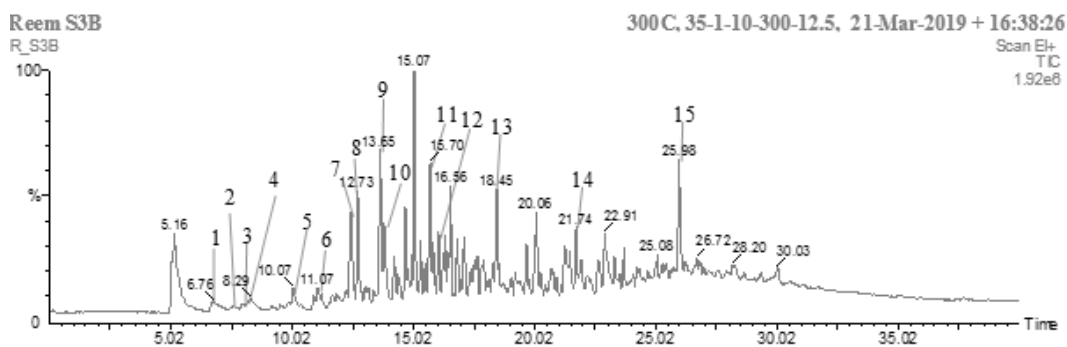


Figure S2. Chromatogram for renewable crude from HTL of glucose at 350°C and 30 minutes

Table S2. Corresponding compound identified in chromatogram for renewable crude from HTL of glucose at 350°C and 30 minutes

Number	Compound
1	Butanal, 2-ethyl-
2	1,3-Butanediol
3	2-Pentanone
4	Furan, 2,5-dimethyl-
5	4-Pentenal
6	Cyclohexanone
7	Furan, 2-ethyl-5-methyl-
8	2,5-Hexanedione
9	2-Cyclopenten-1-one, 3-methyl-
10	Phenol
11	Benzyl alcohol
12	Benzofuran, 2-methyl-
13	Benzofuran, 4,7-dimethyl-
14	7-Methylindan-1-one
15	Squalene

Chapter 4 – Reaction kinetics and characterisation of species in renewable crude from hydrothermal liquefaction of monomers to represent organic fractions of biomass feedstocks

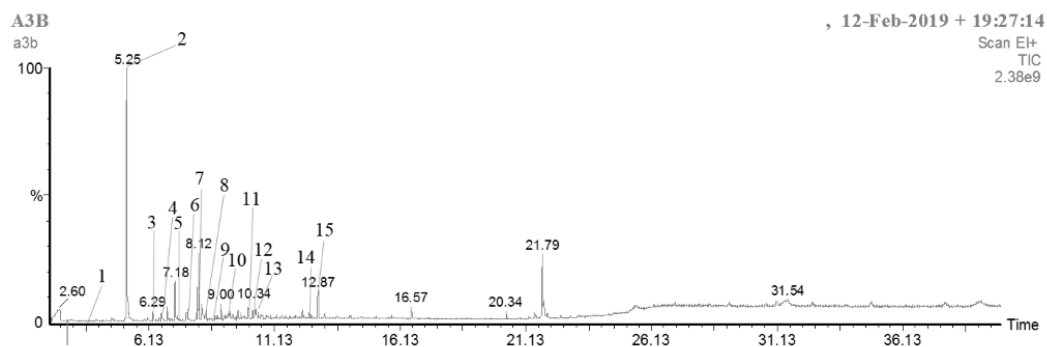


Figure S3. Chromatogram for renewable crude from HTL of alanine at 350°C and 30 minutes

Table S3. Corresponding compound identified in chromatogram for renewable crude from HTL of alanine at 350°C and 30 minutes

Number	Compound
1	2-Cyclopenten-1-one
2	Propanamide, N-methyl
3	Pyridine, 2-ethyl-5-methyl-
4	N,N-Diethylpropionamide
5	Guaiacol
6	Pyrrolidine
7	Heptane
8	Methyl salicylate
9	Benzoic acid
10	Urea
11	Benzenamine, 2-4-dimethoxy-
12	2-Cyclopenten-1-one
13	Glycoluril
14	Propofol
15	2,4-Di-tert-butylphenol

Chapter 4 – Reaction kinetics and characterisation of species in renewable crude from hydrothermal liquefaction of monomers to represent organic fractions of biomass feedstocks

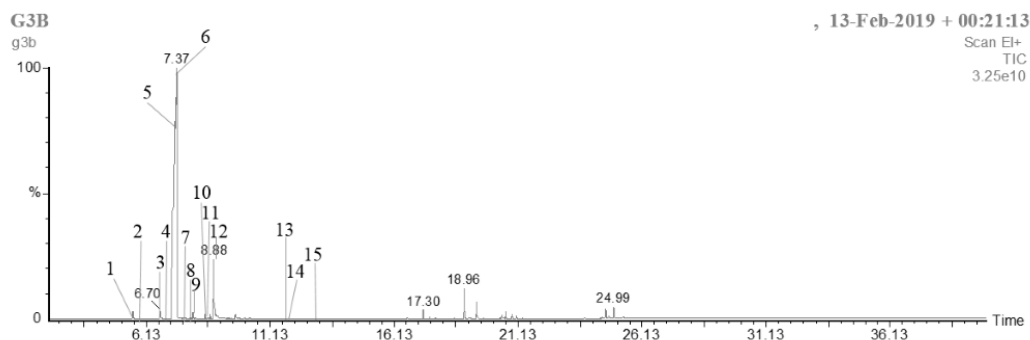


Figure S4. Chromatogram for renewable crude from HTL of guaiacol at 350°C and 30 minutes

Table S4. Corresponding compound identified in chromatogram for renewable crude from HTL of guaiacol at 350°C and 30

Number	Compound
1	Phenol
2	Methyl salicylate
3	Phenol, 2-methyl-
4	Ethanedione, diphenyl-
5	Mequinol
6	Guaiacol
7	Phenol, 2,4-dimethyl
8	Benzene, 1,2-dimethoxy
9	Hydroquinone
10	Phenol, 4-methoxy-3-methyl
11	Creosol
12	Catechol
13	Formic acid
14	Naphthalene
15	2,4-Di-tert-butylphenol

Chapter 5

Reaction kinetics and characterisation of species in renewable crude from hydrothermal liquefaction of mixtures of polymer compounds to represent organic fractions of biomass feedstocks

R. Obeid ^a, D.M. Lewis ^a, N. Smith ^a, T. Hall ^b, P. van Eyk ^a

^aThe School of Chemical Engineering and Advanced Materials

^b Faculty of Sciences

The University of Adelaide, SA 5000, Australia

Energy & Fuels, Published.

Statement of Authorship

Title of Paper	Reaction kinetics and characterization of species in renewable crude from hydrothermal liquefaction of mixtures of polymer compounds to represent organic fractions of biomass feedstocks
Publication Status	<input checked="" type="checkbox"/> Published <input type="checkbox"/> Accepted for Publication <input type="checkbox"/> Submitted for Publication <input type="checkbox"/> Unpublished and Unsubmitted work written in manuscript style
Publication Details	Published in Energy & Fuels R. Obeid, D.M. Lewis, N. Smith, T. Hall, P. van Eyk, Reaction Kinetics and Characterization of Species in Renewable Crude from Hydrothermal Liquefaction of Mixtures of Polymer Compounds To Represent Organic Fractions of Biomass Feedstocks, Energy & Fuels 34 (2020) 419-429.

Principal Author


Name of Principal Author (Candidate)	Reem Obeid		
Contribution to the Paper	HTL reactor design and methods HTL batch experiments completed Methods developed for product separation and product separation completed Interpretation of GC-MS results Construction of model Writing and editing		
Overall percentage (%)	80		
Certification:	This paper reports on original research I conducted during the period of my Higher Degree by Research candidature and is not subject to any obligations or contractual agreements with a third party that would constrain its inclusion in this thesis. I am the primary author of this paper.		
Signature	<table border="1" style="display: inline-table; vertical-align: middle;"> <tr> <td style="width: 50px;">Date</td> <td>17/01/2020</td> </tr> </table>	Date	17/01/2020
Date	17/01/2020		


Co-Author Contributions


By signing the Statement of Authorship, each author certifies that:


- i. the candidate's stated contribution to the publication is accurate (as detailed above);
- ii. permission is granted for the candidate to include the publication in the thesis; and
- iii. the sum of all co-author contributions is equal to 100% less the candidate's stated contribution.

Chapter 5 – Reaction kinetics and characterisation of species in renewable crude from hydrothermal liquefaction of mixtures of polymer compounds to represent organic fractions of biomass feedstocks

Name of Co-Author	David Lewis		
Contribution to the Paper	Concept development Assistance with analysis and interpretation of data Drafting of paper		
Signature		Date	22-Feb-2020

Name of Co-Author	Neil Smith		
Contribution to the Paper	Concept development Assistance with analysis and interpretation of data Drafting of paper		
Signature		Date	22/1/2020

Name of Co-Author	Tony Hall		
Contribution to the Paper	Method design and analysis using Source Rock Analyser and GC-MS Drafting of paper		
Signature		Date	23/1/20

Name of Co-Author	Philip van Eyk		
Contribution to the Paper	HTL reactor design and methods Concept development Assistance with analysis and interpretation of data Drafting of paper		
Signature		Date	28/1/2020

Reaction Kinetics and Characterization of Species in Renewable Crude from Hydrothermal Liquefaction of Mixtures of Polymer Compounds To Represent Organic Fractions of Biomass Feedstocks

Reem Obeid,[†] David M. Lewis,[†] Neil Smith,[†] Tony Hall,[‡] and Philip van Eyk^{*,†}

[†]School of Chemical Engineering and Advanced Materials and [‡]Faculty of Sciences, The University of Adelaide, Adelaide, South Australia 5005, Australia

Supporting Information

ABSTRACT: Hydrothermal liquefaction (HTL) is being investigated as a potential process to provide a renewable energy source from waste biomass. Organically rich wet waste can be partially converted to a renewable crude in subcritical water. Byproducts from HTL include solid, gaseous, and aqueous phases. As a result of the variations in the types of biomass that can be used as a feedstock for HTL, reaction products can vary significantly. To quantify the product distribution from HTL of biomass, the development of a process-based model is necessary. The organic fraction of biomass is typically made up of carbohydrates, lignin, lipids, and proteins. To quantify reaction kinetics, multivariate HTL experiments were performed with variable temperatures (250–350 °C) and times (0–60 min) on mixtures of model compounds representing the carbohydrate, lignin, lipid, and protein components of biomass. Previously, we have investigated the reaction kinetics of different monomer and polymer model compounds by reacting them alone. In this work, we report the investigation of mixtures of the model compounds as HTL reactants to determine the yields of crude, aqueous, gas, and solid phases. Interactions between different model compounds in experiments with mixtures resulted in variable yields compared to the mass-averaged yields from reactions with individual model compounds. From the relation of feed composition in the modeled HTL process to the observed fractions of products, the process conditions can be optimized to maximize the production of oil and a feedstock can be selected on the basis of its composition. Crude fractions from model biomass sources have been characterized via gas chromatography–mass spectrometry analysis.

1. INTRODUCTION

Hydrothermal liquefaction (HTL) is being investigated as a method for converting organically rich wet waste to a renewable crude energy source. Subcritical water is employed to convert the organic matter to renewable crude as well as solid, aqueous, and gas co-products. A wide variety of biomass, including sewage sludge, algae, lignocellulosic waste, and food waste, are being considered as feedstocks for the process. Hence, there can be great variation in products from the HTL. The products from biomass HTL have been found to be dependent upon the lipid, carbohydrate, protein, and lignin contents of the biomass. Different sources of each of these classes of compounds have been shown to result in different product distributions in solid, aqueous, crude, and gas phases.^{1–5} Even different model compounds from the same class used to represent the biomass in HTL have resulted in varied chemical compositions.⁶ Variations of the reaction time and temperature have also been found to result in variable product distribution for the same feedstock in HTL.⁷ To further understand the products from the HTL process, investigations on mixtures of model compounds at varying reaction conditions are also required to identify the interactions between different reactants and how they affect product yields.

Investigations on mixtures of model compounds in HTL have been reported in the literature^{3,8–10} but are limited by reaction times, temperatures, mass loading of the biomass, heating rate of the reactor, and use of a particular solvent to

extract the crude phase from the product mixture. More data are required to validate trends and the effects of interactions between feedstock organic fractions on the product distribution. Teri et al.³ found that the reactants in binary mixtures reacted independently from each other, except for carbohydrate and protein binary mixtures, where the crude yield increased by around 10% at reaction conditions of 350 °C and 60 min compared to single-component reactions at the same conditions. At the less severe reaction conditions of 300 °C and 20 min, no increase in crude yields was observed for the mixture experiments compared to single-component experiments. Hence, the mass-averaged yield from independent model compounds could predict the products from the binary mixtures adequately. The study was limited to a total of six experiments with binary mixtures. Sheng et al.⁸ found that experiments with binary mixtures of castor oil, soy protein, and glucose produced higher crude yields by up to 6% for the reaction temperature of 280 °C and time of 60 min compared to single-component experiments. Lu et al.⁹ identified that a lower crude yield by around 8% was produced from the mixture of lignin and lipid, but the rest of the mixtures (protein and cellulose, protein and xylose, cellulose and lignin, and xylose and lignin) produced greater yields than individual experiments by up to 35% at the reaction conditions of 350 °C

Received: August 30, 2019

Revised: November 12, 2019

Published: December 12, 2019

and 30 min investigated. Déniel et al.¹⁰ conducted experiments on monomer and polymer model compounds in binary, ternary, and quaternary mixtures at 300 °C and 60 min and found that some combinations of model compounds increased the crude yield, including carbohydrate and protein by 10%, whereas including lignin in binary mixtures with lipid, carbohydrate, and protein resulted in decreased crude yields by up to 15%. Several studies have focused on the Maillard reactions between the model carbohydrate and protein fractions of biomass,^{11–14} which can cause an increase in the crude yield at given reaction times and temperatures, as opposed to the carbohydrates or proteins alone. Maillard reactions were studied with lactose and maltose as carbohydrate model compounds and lysine as the protein model compound by Fan et al.¹⁴ For the reactions at 250 and 350 °C with a reaction time of 20 min, the crude yield was higher by 10–39% for the mixtures compared to individual model compounds for carbohydrate and protein. In summary, the literature reveals a wide variation in the crude yield from HTL of mixtures and yields that also vary from the mass averaged yields from reactions with individual model compounds. However, there is no overall agreement on the synergistic or antagonistic effect of different mixtures on the crude yield; therefore, this requires further investigation.

Identification of compounds in the crude produced via HTL provides further insight into the different reaction products from mixtures of model feed compounds compared to reactions of individual model compounds. Different compounds were identified in the crude produced from algae, manure, and sludge biomass by Vardon et al.⁵ A total of 12–13 different product compounds were identified for each type of biomass, including fatty acids, phenolic and aromatic compounds, and esters. Previously, in HTL of model monomer feed compounds, we have identified distinctly different product compounds for each class of model compounds.⁶ The main compounds produced from HTL of the lipid were fatty acids. HTL of carbohydrates produced crude consisting mainly of phenol, furans, aldehydes, aromatics, and ketones. HTL of the protein monomer resulted in a renewable crude composed of amides, aromatics, amines, carboxylic acids, and short hydrocarbon chains. From HTL of the lignin model compound, phenolic compounds made up the majority of the crude. Gas chromatography–mass spectrometry (GC–MS) of the crude produced from mixtures of model feed compounds would give further insight into the reactions occurring during HTL and how they differ for reactions with single model compounds.

Various kinetic models have been developed to describe the reactions in HTL.^{1,15–18} These models predict solid, aqueous, crude, and gas phase yields for feedstocks, including algae and the model compound soy protein. The product phases are predicted at a range of times and temperatures for HTL based on the feedstock organic content, including lipid, carbohydrate, and protein fractions. A model that can be used to predict the HTL products for various biomass feedstocks, including sewage sludge, food waste, and lignocellulosic materials, as well as algae, would assist in identifying the optimum reaction conditions to maximize the crude yield for various feedstocks. In previous work, we have developed kinetic models for individual monomer and polymer model compounds representing lipid, carbohydrate, protein, and lignin contents.^{4,6} A model that includes all four organic components of the biomass feedstock is required to account for the interactions

that occur when the organic components are combined, as present in real biomass.

The aim of this work is to identify how the interactions between model compound reactants in HTL may result in different products. These results can be compared to reactions with individual model compounds at varying reaction conditions. Quaternary mixtures of lipid, carbohydrate, protein, and lignin model compounds can be used to represent a wide range of biomass feedstocks, including sewage sludge and food waste, which consist of each of these organic fractions. The differences in products are identified by quantifying the solid, aqueous, renewable crude, and gas product phases as well as analysis of the crude produced from HTL via GC–MS. A kinetic model is developed for mixtures of biomass model compounds, which can predict solid, aqueous, crude, and gas phase products from the lipid, carbohydrate, protein, and lignin contents of biomass at reaction temperatures of 250, 300, and 350 °C over reaction times of 0–60 min.

2. EXPERIMENTAL SECTION

2.1. Materials. For the lipid model polymer, Crisco 100% pure premium sunflower oil was used. The carbohydrate model compound was extra pure microcrystalline cellulose from Acros Organics, with an average particle size of 90 μm. The protein model compound was bovine serum albumin (BSA) from Serana Europe specified at over 98%. The lignin model compound was alkaline lignin from Tokyo Chemical Industries. Dichloromethane (DCM) of ≥98% from Sigma-Aldrich was the solvent selected to extract the crude from the HTL product mixture. Dichloromethane was selected as the solvent because it has been shown to recover the highest amount of crude with a high carbon content from HTL product mixtures, and this was necessary to define HTL kinetics.¹⁹ As a result of its low boiling point of 40 °C, the solvent can be separated from the crude with minimal loss of product. Alternative separation methods may be used for downstream processing of the HTL product at industrial scale as a result of the environmental and economic concerns of using DCM.²⁰

2.2. Hydrothermal Liquefaction in a Batch Reactor. The reactor setup and HTL procedure were consistent with previous work.⁴ A reactor with 11 mL volume, filled with 5.5 g of product was employed. The total biomass loading was 30 wt % with 70 wt % water. For binary and quaternary mixtures of model compounds, an equal mass of each model compound was added to the reactor to give a total mass loading of 30 wt %. Reaction temperatures of 250, 300, and 350 °C were selected. Reaction times of 5 and 30 min were selected for each temperature for the binary mixtures. For quaternary mixtures, reaction times of 5, 10, 20, 30, and 60 min were selected.

A reaction pressure of 200 bar was maintained for all HTL reactions by pre-charging the reactor with nitrogen at the start of each experiment. A Techne SBL-2D fluidized bed with the Techne-9D temperature controller was used to heat the reactor to the reaction temperature. The heating rate in the fluidized bed was approximately 125 °C/min, and the timer was set for reactions once the reactor reached 98% of the reaction temperature. Once the reaction time was complete, the reactor was removed from the fluidized bed. The reactor was cooled to ambient conditions within 4 min, first by a fan to 70 °C and then quenched in water at ambient temperature.

To minimize error, each experiment was repeated twice, and if the standard deviation was greater than 5% for any product yield, the experiment was repeated again to get two sets of yields with less than 5% standard deviation.

2.3. Recovery and Separation of Products from HTL. After the reactor was cooled to ambient temperature, the reactor was weighed. The gas was released, and the reactor weighed again, to find the total mass of gas released. The mass of gas produced from HTL was calculated by subtracting the mass of nitrogen added to the reactor prior to reactions from the total mass of gas released. The

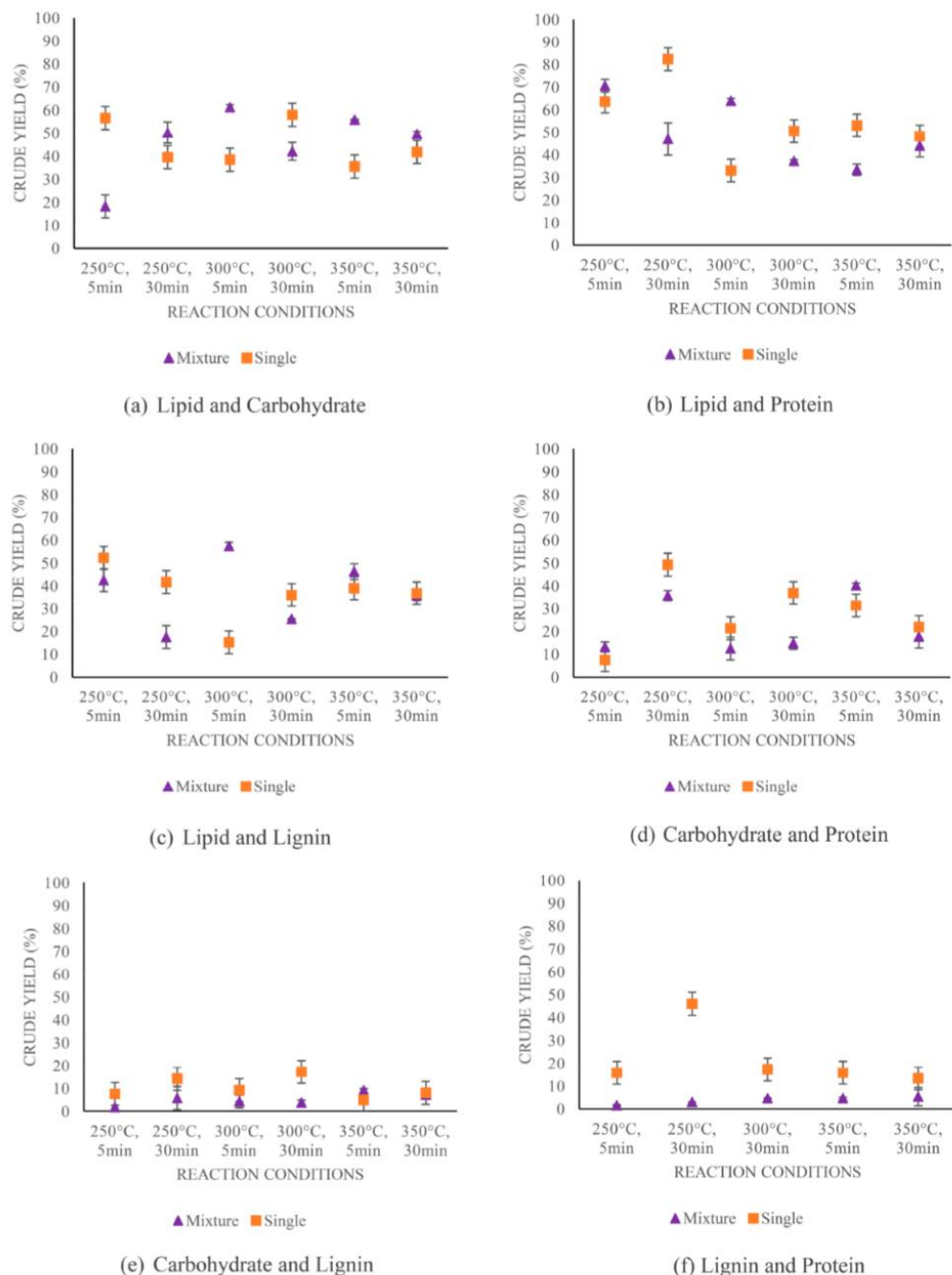


Figure 1. Crude yields for binary mixtures of model compounds (triangles) plotted beside crude yields for mass-averaged crude yields for individual model compounds (squares), with error bars representing standard deviation.

reactor contents were poured into a centrifuge tube for each product mixture. The reactor was rinsed with 10 g of DCM to remove any

soluble oil or solids stuck to the reactor walls and poured into the centrifuge tube.

Following this, the product mixture was centrifuged for 20 min at 2000 rpm, so that it formed three separate layers, including an organic (renewable crude), solid, and aqueous phase. The renewable crude has been defined as the solvent-soluble portion of the product mixture. The organic layer was pipetted from the centrifuge tube, so that the solid and aqueous phases remained. Vacuum filtration was used to separate solid and aqueous products. The solid residue was dried in an oven at 40 °C over 24 h to remove any moisture before being weighed.

Mixtures that contained the carbohydrate model compound, cellulose, in the feed mixture produced excess solids, which were analyzed via a pyrolysis method using a Weatherfords source rock analyzer, as consistent with previous work.⁶ This allowed for the total mass of crude to be calculated because some fraction of the crude was bound to the porous solids. The crude was calculated from the sum of organics dissolved in the DCM solvent and the crude quantified from the pyrolysis measurements.

To obtain the mass of crude dissolved in the solvent, the organic layer was dried in a Techne sample concentrator at 40 °C over 6 h with a stream of nitrogen. Because the boiling point of DCM is 40 °C, this allowed for efficient removal of DCM from the crude. The mass of solid produced was found from the remaining mass of product after the renewable crude was removed for products analyzed in the Weatherfords source rock analyzer. Where minimum solids were produced and pyrolysis measurements were not required, the solid yield was calculated from the mass of solids removed from the oven.

The aqueous phase was determined by subtracting the mass of gas, solid, and crude phases from the mass of the biomass model compound initially loaded into the reactor. On average, it is estimated that 90% of the reactor product has been recovered in our work from experiments where the aqueous phase was measured. Some of the aqueous phase is likely evaporated and condenses in the top section of the reactor and, therefore, cannot be recovered. The yield of each phase was calculated by dividing the mass of each phase by the mass of the biomass model compound initially fed to the reactor. Yields have been defined at ambient conditions.

2.4. Analysis of Products from HTL. **2.4.1. Pyrolysis Measurements for Carbohydrate Yields.** A Weatherfords source rock analyzer was used for pyrolysis measurements. Crucibles were loaded into the carousel and heated under inert helium in both the pyrolysis (to obtain S1, S2, T_{max} , and S3 peaks) and oxidation modes (to obtain the S4 peak). S1 represents the free hydrocarbons in the sample. S2 is the organic matter that has the potential to be converted to hydrocarbons. S3 is carbon dioxide released from the organic matter. S4 is the organic matter that cannot be converted to hydrocarbons. The pyrolysis oven was first held at 300 °C for 5 min and ramped at 25 °C/min from 300 to 650 °C. Subsequently, the oven was reduced to 220 °C and held for 5 min with the carrier gas changed to inert air (CO and CO₂ free). It was then purged, ramped at a maximum heating to 580 °C, and held for 20 min. The flame ionization detector (FID) was calibrated by running Weatherford Laboratories Instruments Division Standard 533. The infrared (IR) analysers were calibrated against standard gas with a known concentration of CO₂ and CO. An analysis blank was run as “blank” mode with the sample batch, and the blank data were automatically subtracted from all analyses. An external check standard was also run prior to each batch to ensure the instrument status, with additional check standards run every 10 samples. The results were processed where peak areas and geochemical indices, including total organic carbon (TOC), oxygen index (OI), hydrogen index (HI), and production index (PI), are automatically calculated. S1 was used to determine the crude yield, while the remaining fractions of the analysis product in pyrolysis were used to calculate the solid yield.

2.4.2. GC–MS of Renewable Crude Products. GC–MS analysis of the liquid crude products was completed using a PerkinElmer SQ8 gas chromatograph–mass spectrometer as in previous work.⁶ While the crude yield was defined from the product separation methods described in section 2.3, GC–MS allowed the compounds with a boiling point under 300 °C to be identified and compared from different HTL products. Between approximately 5 and 70 wt % of the

crude produced from each different feedstock could be identified via GC–MS depending upon the boiling point distribution of the crude. A PerkinElmer Elite-5MS (30 m × 0.25 mm inner diameter × 0.25 μm phase thickness) capillary column with helium carrier gas at a flow of 1 mL/min was used for compound separation. A total of 1 μL of sample was injected in split mode (200:1) with an injection temperature of 300 °C. The oven temperature program was 50 °C, held for 1 min, prior to a 10 °C/min ramp to 300 °C, and a final hold of 19 min. The scanning range of the mass spectrometer was m/z 50–600. Data interpretation was undertaken using PerkinElmer TurboMass 6.0 software with comparison of compound spectra to the NIST14 spectral library database.

Hydrocarbon characterization for the crude bound to the solid products from HTL of cellulose was completed using a Fisons MD800 mass spectrometer coupled to an Agilent 7980 gas chromatograph fitted with a Quantum MSSV pyrolysis injector. A J&W Scientific DB-5MS (30 m × 0.25 mm inner diameter × 0.25 μm phase thickness) capillary column with helium carrier gas at a flow of 1 mL/min was used for compound separation. Approximately 2 mg of sample was loaded into pre-cleaned MSSV glass tubes (100 μL capacity), sealed, and placed into the Quantum MSSV injector at 300 °C. To remove any exterior organic components, the tube was taken through a fast ramped GC heating cycle. The tube was cracked open within the MSSV injector, and evolved components were cryo-focused in liquid nitrogen on the head of the capillary for 1 min prior to analysis. The oven temperature program was 35 °C, held for 1 min, prior to a 10 °C/min ramp to 300 °C, and a final hold of 14 min. The mass spectrometer scanned from m/z 40 to 500. To interpret the data, a PerkinElmer TurboMass 6.0 software with comparison of compound spectra to the NIST14 spectral library database was used.

2.5. Kinetic Model. A kinetic model was developed from the results of the quaternary mixture experiments. The reaction products were modeled by fitting a set of ordinary differential equations (ODEs) to the experimental values found in this work using the least squares errors optimization function in MATLAB with the ODE45 solver. The 95% confidence interval to calculate error in Arrhenius parameters has also been used as described in previous work.⁴

The initial conditions for the model used to define the kinetic parameters were 25% each for lipid, carbohydrate, protein, and lignin. This was because the experiments were all completed with an equal mass of each of the four model compounds. The reaction pathways for the quaternary mixture were determined from the kinetics from single model compounds.⁴ The lipid model compound was initially composed of organic soluble crude, which was quickly converted to some aqueous phase product; hence, the lipid has direct conversion pathways to lipid and aqueous phases. The carbohydrate, protein, and lignin compounds were all initially solids with some solubility in water at the mass loading of 30 wt %; hence, they all have direct pathways to solid and aqueous phases. The interconversions between solid, aqueous, renewable crude, and gas phases as witnessed from the model monomers and polymers^{4,6} are also present as reaction paths in the model.

3. RESULTS AND DISCUSSION

3.1. Binary Mixtures. The variations between the crude yield for binary mixtures of model compounds and the mass-averaged crude yields of experiments with single model compounds are seen in Figure 1. Synergistic effects occur when the binary or quaternary mixture of model compounds results in higher yields compared to the mass averaged yields from reactions with individual model compounds. Antagonistic effects occur when the binary or quaternary mixture of model compounds results in lower yields compared to the mass averaged yields from reactions with individual model compounds. For the six mixtures of binary model compounds, both synergistic and antagonistic effects were seen on the crude yield compared to reactions with individual model compounds, depending upon the reaction time and temper-

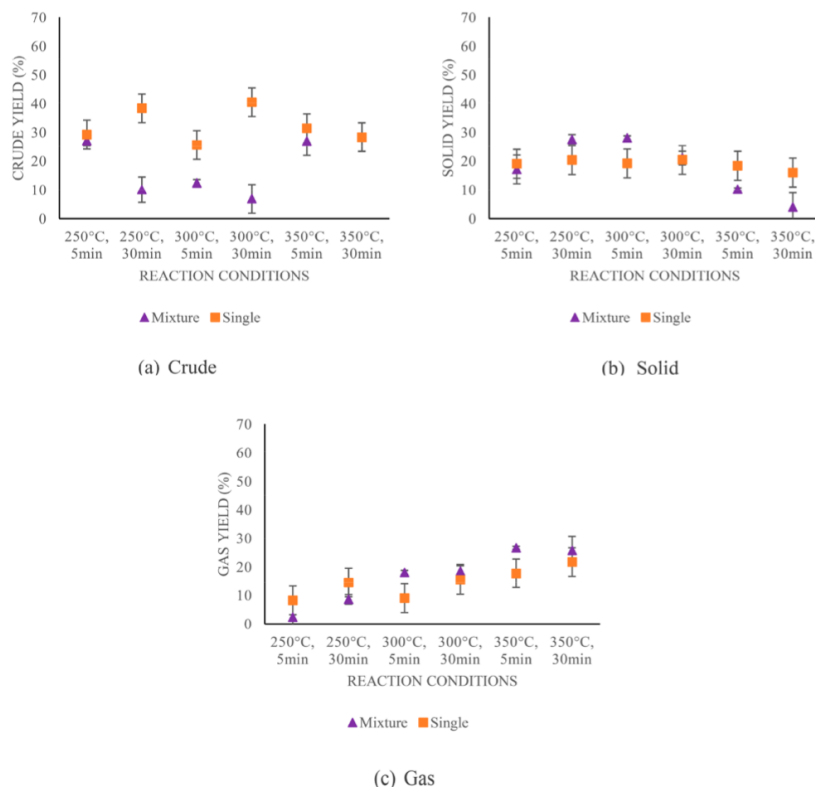


Figure 2. Yields from lipid, carbohydrate, protein, and lignin quaternary mixtures of model compounds (triangles) plotted beside crude yields for mass-averaged yields for individual model compounds (squares), with error bars representing standard deviation.

ature. Binary experiments with lignin mostly resulted in lower crude yields for mixture experiments than single compound experiments by up to 43% in panels c, e, and f of Figure 1. The addition of the lignin model compound, guaiacol, as a feedstock to binary experiments for HTL was also seen to result in lower crude yields compared to the mass-averaged yields of individual experiments by Déniel et al.¹⁰ The crude yield was up to 15% lower for the protein–lignin, lipid–lignin, and carbohydrate–lignin mixtures than individual reactions at 300 °C and 60 min. A study on the influence of phenol on glucose degradation during hydrothermal gasification found that phenolic compounds inhibited the oxidation of cellulose because of the stability of phenolic compounds under oxidation conditions.²¹ The addition of alkaline lignin to binary mixtures appears to be promoting the formation of aqueous phase products in this work while inhibiting the formation of crude.

Figure 1 shows that the reaction temperature can cause up to 35% deviation in crude yields for the same binary mixture and the reaction time can cause up to 30% deviation in crude yields for the same binary mixture. For lipid and lignin mixture experiments, the crude yield was higher at the lower residence time of 5 min compared to 30 min in Figure 1c. This is also the case for most mass-averaged single experiments because the sunflower oil is initially all solvent-soluble and hydrothermal

treatment causes the sunflower oil to be converted to aqueous phase products.

Solid yields are shown in Figure S1 of the Supporting Information. Across the six different binary mixtures, the solid yield was generally higher for mass-averaged experiments with individual model compounds than with mixtures of model compounds. The variation in the solid yield was 1–30%, with only six of the experimental conditions resulting in yield variations of more than 10%.

Reaction conditions of 270 °C and 5 min and 295 °C and 12.5 min resulted in higher solids formation in reactions with carbohydrate and protein in the work by Yang et al.²² They determined that the Maillard reactions, which cause an increase in the crude yield for carbohydrate and protein mixtures occur at the more severe reaction conditions, 320 °C and 20 min. Carbohydrate and protein mixtures were reported to produce higher crude yields and lower solid yields than the individual reactant experiments by Teri et al.³ at the experimental conditions reported of 350 °C and 60 min. The solid yield was also highest for the lowest reaction time and temperature in this work of 5 min and 250 °C. Some sets of reaction conditions did result in higher crude yields for the carbohydrate–protein mixture in this work, but this was not true for all conditions.

A higher temperature of 320 °C and reaction time of 20 min were seen to reduce solid formation by Yang et al.²² in the

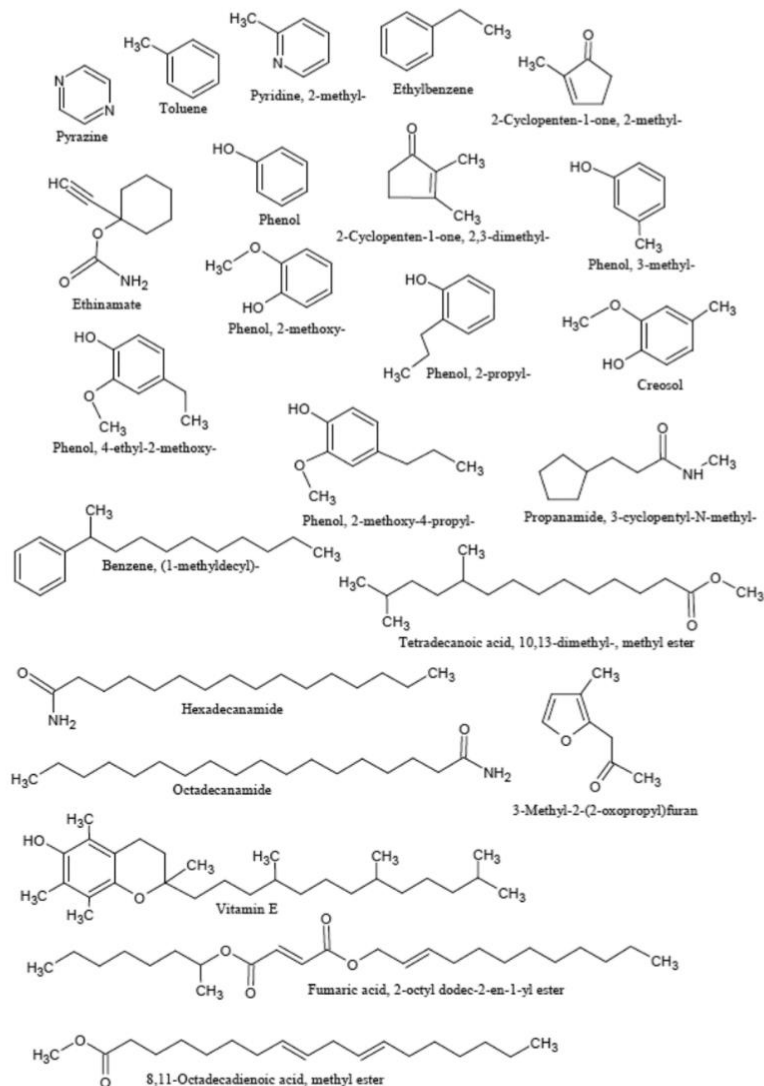


Figure 3. Compounds identified in renewable crude from GC–MS of products from HTL of quaternary mixtures of model compounds.

binary mixture of carbohydrate and lignin. In this work, the solid yield also decreased for the mixtures of carbohydrate and lignin, as opposed to individual reactants, except at 350 °C and 5 min in Figure S1e of the Supporting Information. Cellulose and lignin mixtures were found to have a synergistic effect on the crude yield and an antagonistic effect on the solid yield in experiments by Yang et al.²³ at 290 °C and 10 min.

Gas yields are shown in Figure S2 of the Supporting Information. A low variation in the gas yield of less than 10% was also seen for most cases between mixtures of model compounds and the mass-averaged yields from single experiments. The greatest difference is seen in the experiments with carbohydrate and lignin, where the gas yields are up to 30% higher for mixtures in Figure S2e of the Supporting Information. In most cases, gas yields were higher for both

mass-averaged yields from single experiments and yields from mixture experiments at 30 min compared to the lower residence time of 5 min.

By comparison of the yields of the HTL product obtained from experiments with mixtures of binary model compounds to the mass-averaged yields from experiments with single model compounds in this work, it can be concluded that interactions between different feedstocks will result in varied product fractions from HTL. The synergistic or antagonistic effect of mixtures on the crude yield depends upon the reaction time and temperature. However, the crude yield was mostly negatively affected by the addition of lignin in the binary experiments in this work.

3.2. Quaternary Mixtures. The crude, solid, and gas yields found for quaternary mixtures are depicted in Figure 2.

For mixtures with all four of the model compounds used in this work, the crude yield was mostly lower for mixtures by up to 35% compared to the reactions with individual model compounds, as seen in Figure 2a. The solid yield was also mostly lower for mixtures in Figure 2b, resulting in a higher aqueous phase yield for quaternary mixture experiments. The gas yield was higher for mixtures at 300 and 350 °C but lower for mixtures at 250 °C compared to reactions with individual model compounds in Figure 2c. The interactions between reactant model compounds appear to modify the product fractions from HTL when all four model compounds are included in experiments, varying with the reaction time and temperature.

In experiments by Teri et al.,³ different compositions of ternary mixtures of carbohydrate (cornstarch or cellulose), protein (soy protein or albumin), and lipid (sunflower oil or castor oil) resulted in less than 4% variation in the crude yield compared to individual reactions. However, lignin was not included in their experiments. As with the binary mixture experiments, the addition of lignin could be the cause of the lower crude yields. The crude yield was found to be 2% higher for the quaternary mixture in the current work compared to mass-averaged calculated yields by Déniel et al.¹⁰ at reaction conditions of 300 °C and 60 min. However, they used monomer model compounds rather than the polymer compounds used here. Model monomer compounds have been shown to result in lower crude yields than model polymer compounds because they decompose to produce more aqueous phase products during HTL.⁶

3.3. Identification of Compounds via GC–MS. GC–MS of the crude produced from each individual model polymer and each mixture of model polymers at 350 °C reaction temperature and 5 min reaction time was conducted. Chromatograms and the lists of compounds identified with different elution times are presented in the Supporting Information. The GC–MS results indicated that the lipid contributes some phenolic compounds, cyclic hydrocarbons, long-chain hydrocarbons (including vitamin E), and fatty acid chains. HTL of the carbohydrate resulted in a crude consisting of cyclic hydrocarbons, ketones, aldehydes, esters, fatty acid chains, and furans. The protein contributes many amides as well as phenolics and low-molecular-weight compounds, including toluene and pyridine. The addition of lignin resulted in phenolic compounds as well as other organic cyclic compounds. Some of the compounds identified in the crude from quaternary mixtures of model compounds are presented in Figure 3. The higher molecular weight compounds are mostly provided from the lipid followed by the protein. Thermogravimetric analysis previously identified that the lipid produced the crude with the highest boiling point range of the four classes of model compounds, followed by the protein.⁴

The crude produced from the model polymers could be compared to the crude produced from the model monomers in previous work.⁶ The crude produced from both the lipid polymer and monomer consisted of mostly fatty acids. For the crude produced from the monomer carbohydrate feed, furans, aldehydes, cyclic compounds, and ketones were identified. The same compounds were identified from the polymer feed. HTL of both the protein monomer and polymer also resulted in a renewable crude composed of amides, phenolic compounds, and short hydrocarbon chains. From the lignin model compounds, both monomer and polymer reactants resulted in a crude rich in phenolic compounds. While the product

fractions varied for monomer and polymer compounds, the crude compositions were very similar.

Lipid and carbohydrate mixtures resulted in crude containing fatty acids, monocyclic compounds, esters, and furans. For lipid and protein, GC–MS identified fatty acids, phenolic compounds, esters, and amides from the crude. For lipid and lignin mixtures, the crude consisted of fatty acids, aromatic compounds, cyclic ketones, phenolics, aldehydes, and esters. Carbohydrate and protein mixtures resulted in pyrazines, cyclic compounds, phenolics, and aldehydes in the crude. Carbohydrate and lignin mixtures resulted in crude composed of phenolics, cyclic ketones, and cycloalkenes identifiable via GC–MS. The crude from protein and lignin mixtures consisted of phenolic compounds, cyclic ketones, and amides.

Interestingly, no amides were identified in the mixtures with carbohydrate and protein compounds; however, many amides were identified in mixtures with protein and lipid and protein and lignin reactants. This difference is likely due to the Maillard reactions occurring between amino acids and reducing sugars. Fan et al.¹⁴ also investigated the crude from mixtures of protein and carbohydrate and did not identify any amides via GC–MS. They proposed that pyrazines were the main reaction products from Maillard reactions in agreement with this work. Zhang et al.¹³ also observed enhanced production of pyrazines from Maillard reactions. Overall, the crude produced from mixtures of model compounds contained many of the same classes of compounds identified in the HTL product from the individual model compounds.

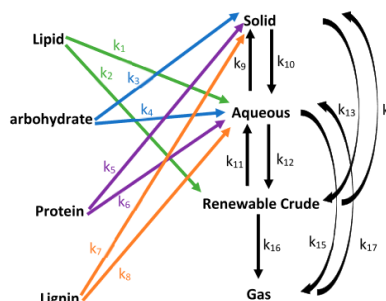


Figure 4. Kinetic pathways for the quaternary mixture of model compounds.

3.4. Kinetic Model for Mixtures. Kinetic pathways for the model developed from quaternary mixtures of model biomass compounds are shown in Figure 4. Equations 1–8 are the ODEs for the model, where x_1 represents lipid, x_2 represents carbohydrate, x_3 represents protein, x_4 represents lignin, x_5 represents solid phase product, x_6 represents aqueous phase product, x_7 represents crude phase product, and x_8 represents gas phase product. The kinetic parameters and Arrhenius parameters calculated from the experimental results using MATLAB are presented in Table 1. For the kinetic pathways shown in Figure 4, the ODEs in eqs 1–8 were solved in MATLAB using ODE45 coupled with the lsqcurvefit function. The bounds for the k [°C] (min^{-1}) values were set between 0 and 1. The kinetic equations were fit to the data using a least-squares algorithm, which minimizes the difference between the model and experimental data points.

Table 1. Kinetic Parameters for the First-Order Bulk Kinetic Model in Figure 4 and Equations 1–8

compound	path	reaction	k [$^{\circ}\text{C}$] (s^{-1})			$\ln A$	E_a (kJ/mol)
			250 $^{\circ}\text{C}$	300 $^{\circ}\text{C}$	350 $^{\circ}\text{C}$		
quaternary mixture	1	lipid to aqueous	0.3	51.1	53.0	32.6 ± 26.5	143.8 ± 21.5
	2	lipid to renewable crude	21.0	22.8	51.5	8.4 ± 4.6	23.7 ± 3.8
	3	carbohydrate to solid	4.8	18.6	20.4	11.0 ± 6.4	40.0 ± 5.2
	4	carbohydrate to aqueous	18.0	19.7	54.8	9.5 ± 5.9	29.3 ± 4.8
	5	protein to solid	4.2	17.7	18.4	11.1 ± 7.3	41.2 ± 5.9
	6	protein to aqueous	19.8	20.6	57.3	9.3 ± 6.1	28.0 ± 5.0
	7	lignin to solid	12.7	26.7	27.4	7.5 ± 3.7	21.3 ± 3.0
	8	lignin to aqueous	9.0	9.2	51.7	12.5 ± 10.6	45.9 ± 8.6
	9	aqueous to solid	0.3	4.3	13.4	22.8 ± 6.9	103.8 ± 5.6
	10	solid to aqueous	2.3	19.0	56.9	21.1 ± 4.3	87.9 ± 3.5
	11	renewable crude to aqueous	0.3	8.3	57.0	31.7 ± 5.3	142.3 ± 4.3
	12	aqueous to renewable crude	1.1	6.6	57.9	24.8 ± 3.8	108.1 ± 3.1
	13	solid to renewable crude	0.3	0.6	55.1	29.8 ± 24.3	137.8 ± 19.8
	14	renewable crude to solid	1.7	3.0	3.2	4.8 ± 2.7	18.1 ± 2.2
	15	aqueous to gas	0.5	15.6	22.8	23.5 ± 15.0	103.2 ± 12.2
	16	renewable crude to gas	0.9	1.4	13.3	15.9 ± 12.0	71.2 ± 9.8
	17	gas to aqueous	5.6	44.4	44.4	15.3 ± 10.8	57.6 ± 8.7

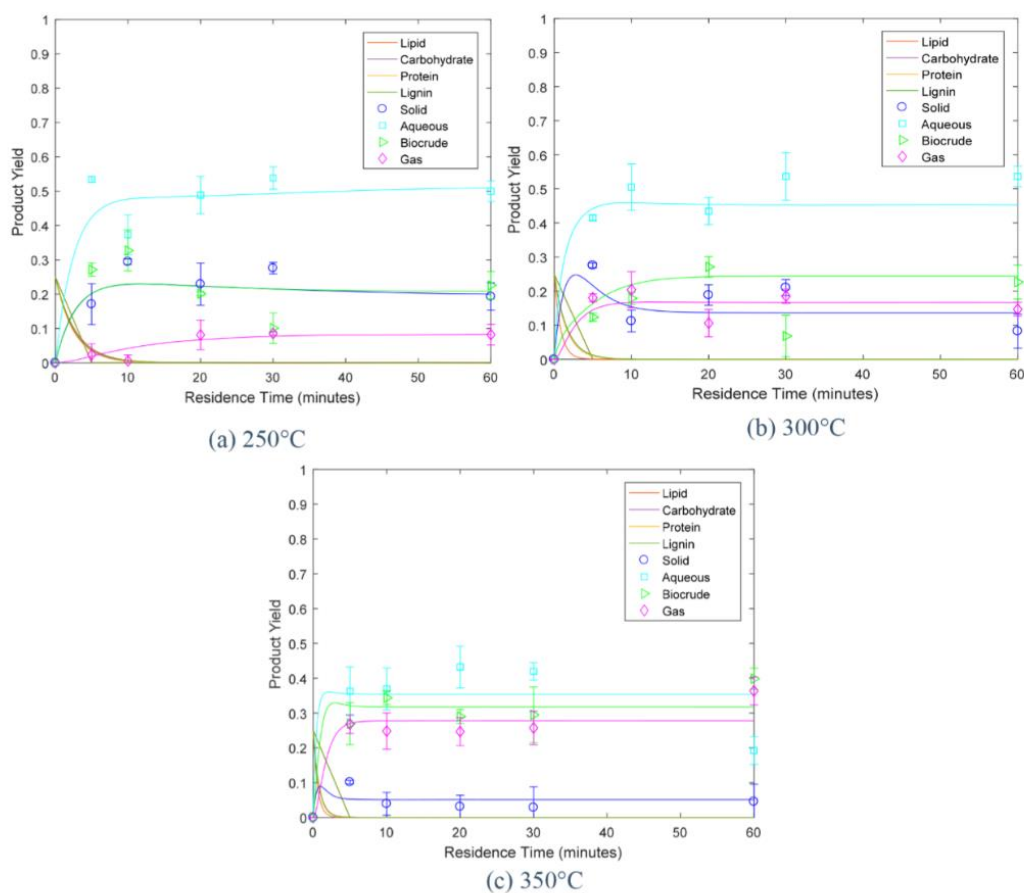


Figure 5. Experimental results shown with symbols and kinetic model shown with lines for quaternary mixtures of model compounds. The standard deviation in experimental yields is represented by error bars.

$$\frac{dx_1}{dt} = -(k_1 + k_2)x_1 \quad (1)$$

$$\frac{dx_2}{dt} = -(k_3 + k_4)x_2 \quad (2)$$

$$\frac{dx_3}{dt} = -(k_5 + k_6)x_3 \quad (3)$$

$$\frac{dx_4}{dt} = -(k_7 + k_8)x_4 \quad (4)$$

$$\frac{dx_5}{dt} = -(k_{10} + k_{13})x_5 + k_3x_2 + k_5x_3 + k_7x_4 + k_9x_6 + k_{14}x_7 \quad (5)$$

$$\frac{dx_6}{dt} = -(k_9 + k_{12} + k_{15})x_6 + k_{11}x_1 + k_4x_2 + k_6x_3 + k_8x_4 + k_{10}x_5 + k_{11}x_7 + k_{17}x_8 \quad (6)$$

$$\frac{dx_7}{dt} = -(k_{11} + k_{14} + k_{16})x_7 + k_2x_1 + k_{12}x_6 + k_{13}x_5 \quad (7)$$

$$\frac{dx_8}{dt} = -k_{17}x_8 + k_{15}x_6 + k_{16}x_7 \quad (8)$$

The results of the kinetic model shown in Figure 5 demonstrate the low variation in solid, aqueous, crude, and gas phase products after 5 min of residence time. The activation energy for the path from lipid to aqueous phase products is highest, and this is likely due to the lipid contributing the highest proportion to the crude product. The lowest activation energy is for the conversion of lignin to the solid phase because most of the lignin product is converted to the aqueous phase when reacted alone.⁴ The pathway from gas to aqueous phase was added to the model in this work because the gas yield is not seen to be increasing significantly after 5 min of residence time; hence, an equilibrium exists between the gas and liquid products. The gas phase products are more likely to return to the aqueous phase because they are composed of lower molecular weight products. The poorer fit of the model without the gas to aqueous pathway is shown in the Supporting Information, where gas yields are overpredicted by up to 30%. The high error in Arrhenius parameters for some pathways indicates that the mixture reactions do not follow first-order reaction kinetics with great accuracy. However, at 250, 300, and 350 °C, all experimental yields match the model with a maximum error of 10%.

Previous models have used lipid, carbohydrate, and protein contents of microalgae to generate kinetic models; however, they do not include lignin.^{15,17,24} Another variation between the model in this work and those from previous work is the addition of pathways to form solids. From our experiments with intermediate compounds where initially liquid phase model compounds were reacted and solids were formed as HTL co-products, it was made clear that recombination of intermediate products to form solids during HTL occurs.⁶

The activation energies calculated for reaction pathways shown in Table 1 can be compared to those found in previous kinetic models that have been developed for algae. In the model presented in the current work, the pathway from lipid to aqueous phase is highest at 143.8 kJ/mol, followed by lignin to aqueous phase at 45.9 kJ/mol, carbohydrate to aqueous phase

at 29.3 kJ/mol, and then protein to aqueous phase at 28.0 kJ/mol. In the model for algae by Sheehan and Savage,¹⁷ the activation energy for carbohydrate to aqueous phase is highest at 57.9 kJ/mol, followed by lipid to aqueous phase at 57.6 kJ/mol and then protein to aqueous phase at 53.3 kJ/mol. There is less variation in the activation energies for the pathways for the organic constituents in biomass to aqueous phase products in the algae model; however, the variation between models is expected as the absence of lignin in algae results in different interactions between organic fractions. The previous model also contains only 6 reaction pathways, while the model developed here contains 17 reaction pathways. The low activation energy for the crude to solid pathway for the model for quaternary mixtures of 18.1 kJ/mol compared to the activation energy of 103.8 kJ/mol for aqueous to solid is expected because recombination of the heavier molecular weight products in crude results in high-boiling-point products.²⁵

By adjustment of the initial values of the model for a particular biomass feedstock, the model can be used to predict the yields for HTL of biomass in the literature. Experimental crude yields for algae from Vo et al.¹⁸ were mostly higher than those predicted by the model by 4–17%. From the experiments by Vardon et al.,⁵ the crude yield was under-predicted for algae by 11%, underpredicted by 8% for swine manure, and overpredicted by 13% for anaerobic sludge.

The yields from binary experiments are not modeled accurately by the model for quaternary mixtures developed in this work. This is because the interactions between each two model compounds affect the crude yield, and experiments with all four model compounds will have interactions that will also cause variation in the crude yield. Because the lipid, carbohydrate, protein, and lignin fractions do not react independently from each other, each type of biomass with a given composition could be modeled with more accuracy using a different set of parameters.

The reactions have been oversimplified by the first-order kinetic model; however, it can be used as a basis to approximate the product yields from various sources of biomass. The model has some dependence upon the solvent used in the experiments reported here, because different solvents extract different compounds, resulting in different crude yields.^{19,26} Other limitations include not accounting for different reactor heating and cooling times and applicability to varying ratios of model compounds because our experiments were conducted with equal ratios of model compounds. Experiments with real biomass can be performed to improve the model.

4. CONCLUSION

Solid, aqueous, crude, and gas phase yields from binary and quaternary mixtures of model compounds resulted in different yields compared to the mass averaged yields from experiments with individual model compounds. Yields from mixtures were neither consistently higher nor lower than yields from individual compounds. Variation was dependent upon the reaction time and temperature. This variation in yields between mixtures and individual compounds was 0–35%. The addition of lignin to binary mixtures mostly resulted in lower crude yields for experiments with mixtures compared to individual model compounds. GC–MS results from crude produced via HTL identified that the lipid contributes phenolic compounds and fatty acid chains. Carbohydrate

contributes cyclic hydrocarbons, ketones, aldehydes, esters, fatty acid chains, and furans. Protein contributes amides and phenolic and low-molecular-weight compounds. The addition of lignin as a reactant in HTL resulted in phenolic compounds as well as other organic cyclic compounds. The GC–MS results indicated that the compounds in the crude from individual model compounds mostly exist in the crude from mixtures with those model compounds. Like the product phase yields, the amounts of the compounds identified would also vary. A first-order kinetic model was developed using experimental data from quaternary mixtures of model compounds. These reaction pathways can be used to model biomass with varying organic content; however, this will require further experiments with biomass to develop suitable kinetic parameters to account for the effects of the inorganic fractions of biomass.

■ ASSOCIATED CONTENT

📄 Supporting Information

The Supporting Information is available free of charge at <https://pubs.acs.org/doi/10.1021/acs.energyfuels.9b02936>.

Solid yields (Figure S1) and gas yields (Figure S2) for binary mixtures of model compounds (triangles) plotted beside crude yields for mass-averaged solid yields for individual model compounds (squares), with error bars representing standard deviation, chromatogram of crude produced from sunflower oil (Figure S3), cellulose (Figure S4), BSA (Figure S5), alkaline lignin (Figure S6), sunflower oil and cellulose (Figure S7), sunflower oil and BSA (Figure S8), sunflower oil and alkaline lignin (Figure S9), cellulose and BSA (Figure S10), cellulose and alkaline lignin (Figure S11), BSA and alkaline lignin (Figure S12), and quaternary mixture (Figure S13) at reaction temperature of 350 °C and reaction time of 5 min, kinetic pathways without the addition of the gas to aqueous pathway (Figure S14), and kinetic model without the addition of the gas to aqueous pathway (Figure S15) (PDF)

■ AUTHOR INFORMATION

Corresponding Author

*E-mail: philip.vaneyk@adelaide.edu.au.

ORCID

Philip van Eyk: 0000-0003-3768-2044

Notes

The authors declare no competing financial interest.

■ ACKNOWLEDGMENTS

The authors acknowledge the financial support of the Australian Research Council's Linkage Project Grant (LP150101241) and our industry partner Southern Oil Refining Pty Ltd.

■ REFERENCES

- (1) Luo, L.; Sheehan, J. D.; Dai, L.; Savage, P. E. Products and Kinetics for Isothermal Hydrothermal Liquefaction of Soy Protein Concentrate. *ACS Sustainable Chem. Eng.* **2016**, *4* (5), 2725–2733.
- (2) Biller, P.; Ross, A. B. Potential yields and properties of oil from the hydrothermal liquefaction of microalgae with different biochemical content. *Bioresour. Technol.* **2011**, *102* (1), 215–225.
- (3) Teri, G.; Luo, L.; Savage, P. E. Hydrothermal Treatment of Protein, Polysaccharide, and Lipids Alone and in Mixtures. *Energy Fuels* **2014**, *28* (12), 7501–7509.
- (4) Obeid, R.; Lewis, D.; Smith, N.; van Eyk, P. The elucidation of reaction kinetics for hydrothermal liquefaction of model macromolecules. *Chem. Eng. J.* **2019**, *370*, 637–645.
- (5) Vardon, D. R.; Sharma, B. K.; Scott, J.; Yu, G.; Wang, Z.; Schideman, L.; Zhang, Y.; Strathmann, T. J. Chemical properties of biocrude oil from the hydrothermal liquefaction of Spirulina algae, swine manure, and digested anaerobic sludge. *Bioresour. Technol.* **2011**, *102* (17), 8295–8303.
- (6) Obeid, R.; Lewis, D.; Smith, N.; Hall, T.; van Eyk, P. Reaction kinetics and characterisation of species in renewable crude from hydrothermal liquefaction of monomers to represent organic fractions of biomass feedstocks. Manuscript submitted for publication, **2019**.
- (7) Valdez, P. J.; Nelson, M. C.; Wang, H. Y.; Lin, X. N.; Savage, P. E. Hydrothermal liquefaction of *Nannochloropsis* sp.: Systematic study of process variables and analysis of the product fractions. *Biomass Bioenergy* **2012**, *46*, 317–331.
- (8) Sheng, L.; Wang, X.; Yang, X. Prediction model of biocrude yield and nitrogen heterocyclic compounds analysis by hydrothermal liquefaction of microalgae with model compounds. *Bioresour. Technol.* **2018**, *247*, 14–20.
- (9) Lu, J.; Liu, Z.; Zhang, Y.; Savage, P. E. Synergistic and Antagonistic Interactions during Hydrothermal Liquefaction of Soybean Oil, Soy Protein, Cellulose, Xylose, and Lignin. *ACS Sustainable Chem. Eng.* **2018**, *6* (11), 14501–14509.
- (10) Déniel, M.; Haarlemmer, G.; Roubaud, A.; Weiss-Hortala, E.; Fages, J. Modelling and Predictive Study of Hydrothermal Liquefaction: Application to Food Processing Residues. *Waste Biomass Valorization* **2017**, *8* (6), 2087–2107.
- (11) Minowa, T.; Inoue, S.; Hanaoka, T.; Matsumura, Y. Hydrothermal reaction of glucose and glycine as model compounds of biomass. *Nippon Enerugi Gakkaishi* **2004**, *83* (10), 794–798.
- (12) Peterson, A. A.; Lachance, R. P.; Tester, J. W. Kinetic Evidence of the Maillard Reaction in Hydrothermal Biomass Processing: Glucose-Glycine Interactions in High-Temperature, High-Pressure Water. *Ind. Eng. Chem. Res.* **2010**, *49* (5), 2107–2117.
- (13) Zhang, C.; Tang, X.; Sheng, L.; Yang, X. Enhancing the performance of Co-hydrothermal liquefaction for mixed algae strains by the Maillard reaction. *Green Chem.* **2016**, *18* (8), 2542–2553.
- (14) Fan, Y.; Hornung, U.; Dahmen, N.; Kruse, A. Hydrothermal liquefaction of protein-containing biomass: Study of model compounds for Maillard reactions. *Biomass Convers. Biorefin.* **2018**, *8* (4), 909–923.
- (15) Valdez, P. J.; Tocco, V. J.; Savage, P. E. A general kinetic model for the hydrothermal liquefaction of microalgae. *Bioresour. Technol.* **2014**, *163*, 123–127.
- (16) Hietala, D. C.; Faeth, J. L.; Savage, P. E. A quantitative kinetic model for the fast and isothermal hydrothermal liquefaction of *Nannochloropsis* sp. *Bioresour. Technol.* **2016**, *214*, 102–111.
- (17) Sheehan, J. D.; Savage, P. E. Modeling the effects of microalga biochemical content on the kinetics and biocrude yields from hydrothermal liquefaction. *Bioresour. Technol.* **2017**, *239*, 144–150.
- (18) Vo, T. K.; Kim, S.-S.; Ly, H. V.; Lee, E. Y.; Lee, C.-G.; Kim, J. A general reaction network and kinetic model of the hydrothermal liquefaction of microalgae *Tetraselmis* sp. *Bioresour. Technol.* **2017**, *241*, 610–619.
- (19) Valdez, P. J.; Dickinson, J. G.; Savage, P. E. Characterization of Product Fractions from Hydrothermal Liquefaction of *Nannochloropsis* sp. and the Influence of Solvents. *Energy Fuels* **2011**, *25* (7), 3235–3243.
- (20) Xu, D.; Savage, P. E. Characterization of biocrudes recovered with and without solvent after hydrothermal liquefaction of algae. *Algal Res.* **2014**, *6* (PartA), 1–7.
- (21) Jin, F.; Cao, J.; Kishida, H.; Moriya, T.; Enomoto, H. Impact of phenolic compounds on hydrothermal oxidation of cellulose. *Carbohydr. Res.* **2007**, *342* (8), 1129–1132.

(22) Yang, J.; He, Q.; Corscadden, K.; Niu, H.; Lin, J.; Astatkie, T. Advanced models for the prediction of product yield in hydrothermal liquefaction via a mixture design of biomass model components coupled with process variables. *Appl. Energy* **2019**, *233–234*, 906–915.

(23) Yang, J.; He, Q.; Niu, H.; Corscadden, K.; Astatkie, T. Hydrothermal liquefaction of biomass model components for product yield prediction and reaction pathways exploration. *Appl. Energy* **2018**, *228*, 1618–1628.

(24) Vo, T. K.; Lee, O. K.; Lee, E. Y.; Kim, C. H.; Seo, J.-W.; Kim, J.; Kim, S.-S. Kinetics study of the hydrothermal liquefaction of the microalga *Aurantiochytrium* sp. KRS101. *Chem. Eng. J.* **2016**, *306*, 763–771.

(25) Toor, S. S.; Rosendahl, L.; Rudolf, A. Hydrothermal liquefaction of biomass: A review of subcritical water technologies. *Energy* **2011**, *36* (5), 2328–2342.

(26) López Barreiro, D.; Riede, S.; Hornung, U.; Kruse, A.; Prins, W. Hydrothermal liquefaction of microalgae: Effect on the product yields of the addition of an organic solvent to separate the aqueous phase and the biocrude oil. *Algal Res.* **2015**, *12*, 206–212.

Supporting Information

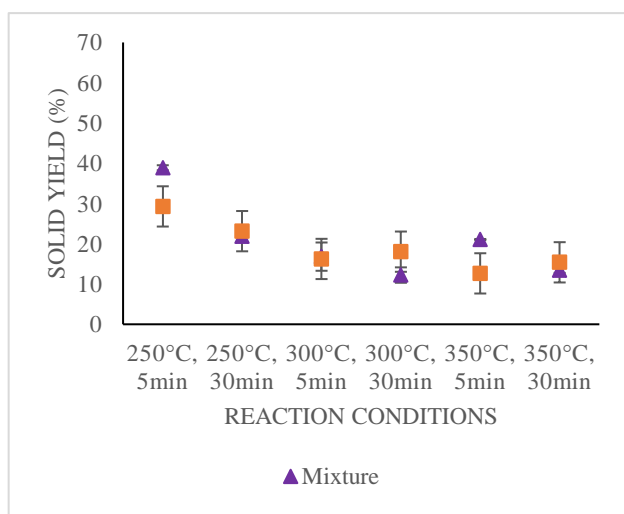
Reaction kinetics and characterisation of species in renewable crude from hydrothermal liquefaction of mixtures of polymer compounds to represent organic fractions of biomass feedstocks

Reem Obeid^a, David M. Lewis^a, Neil Smith^a, Tony Hall^b and Philip van Eyk^{a}*

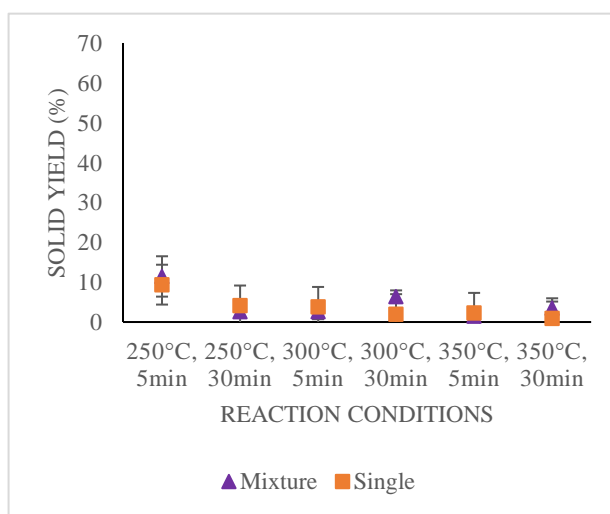
^a School of Chemical Engineering and Advanced Materials, The University of
Adelaide, Adelaide, South Australia 5005, Australia

^b Faculty of Sciences, The University of Adelaide, Adelaide, South Australia
5005, Australia

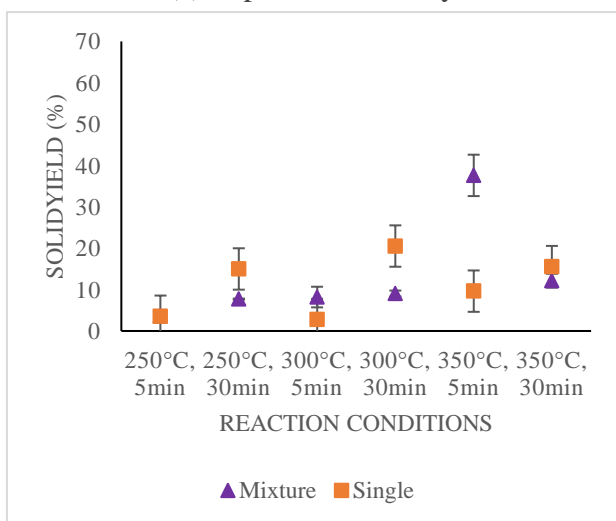
*E-mail: philip.vaneyk@adelaide.edu.au.



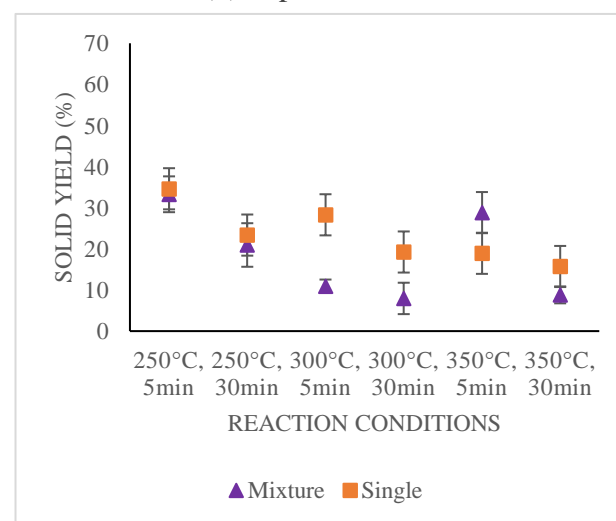
(a) Lipid and Carbohydrate



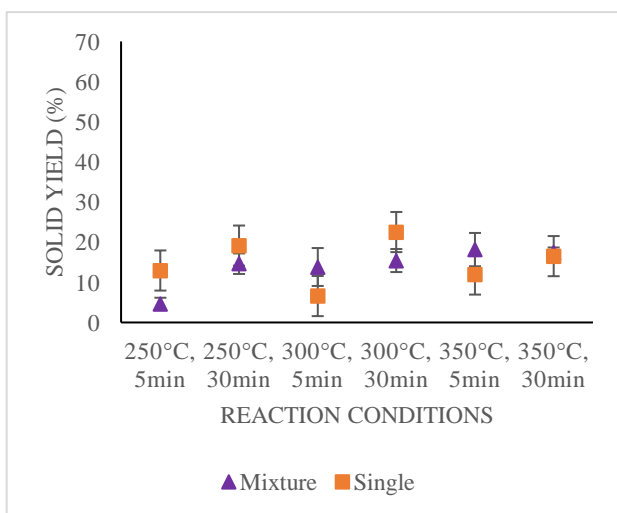
(b) Lipid and Protein



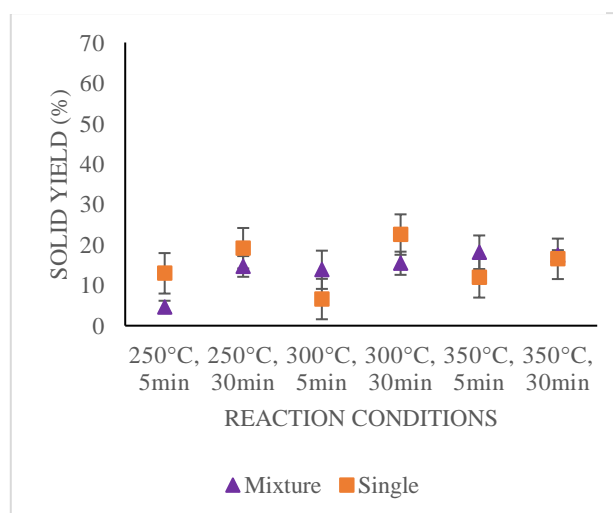
(c) Lipid and Lignin



(d) Carbohydrate and Protein



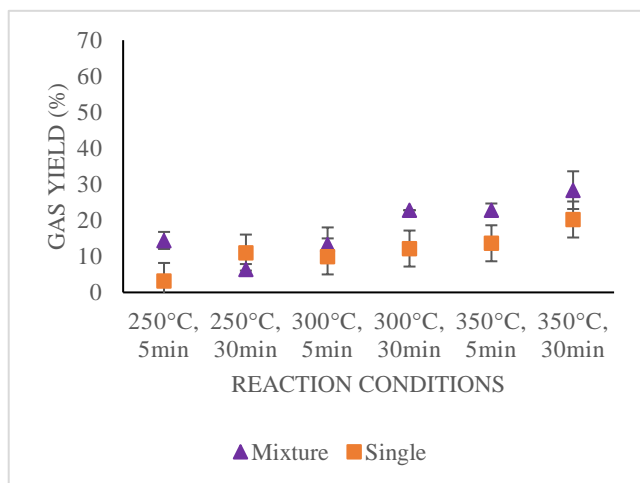
(e) Carbohydrate and Lignin



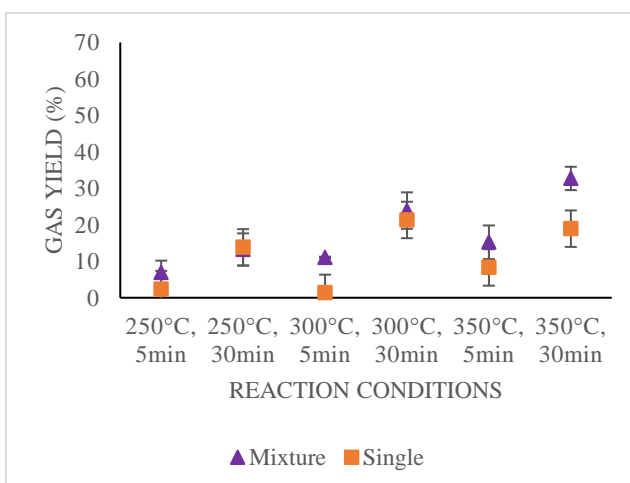
(f) Lignin and Protein

Figure S1: Solid yields for binary mixtures of model compounds (triangles) plotted beside crude yields for mass-averaged solid yields for individual model compounds (squares) with error bars representing standard deviation

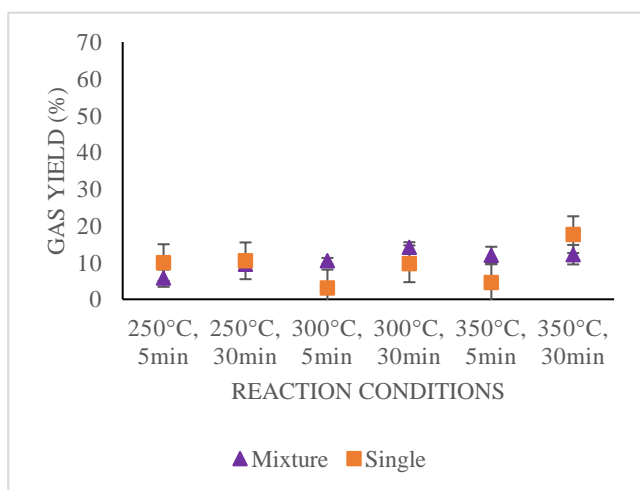
Chapter 5 – Reaction kinetics and characterisation of species in renewable crude from hydrothermal liquefaction of mixtures of polymer compounds to represent organic fractions of biomass feedstocks



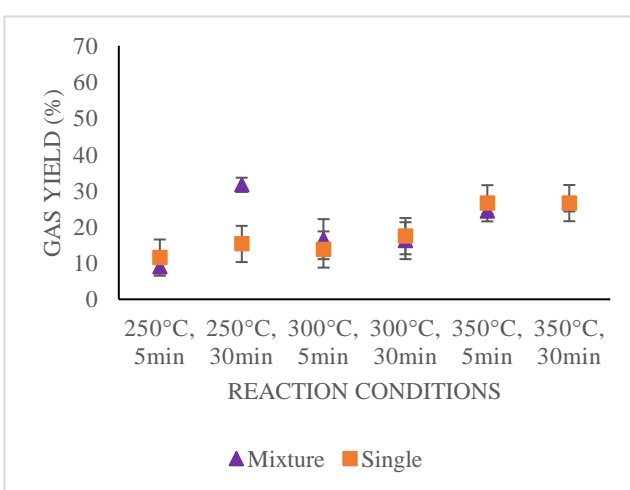
(a) Lipid and Carbohydrate



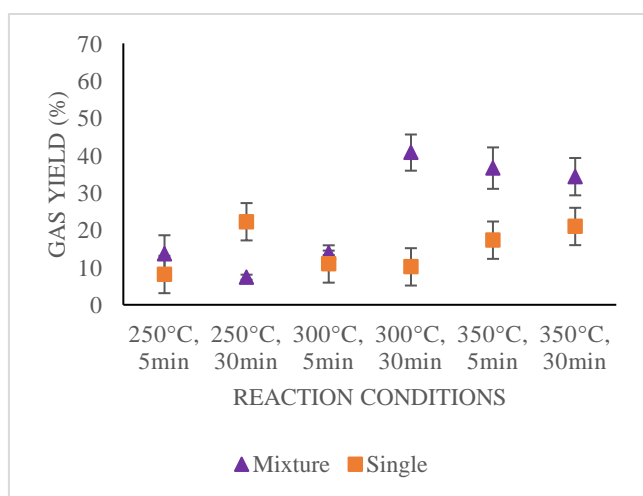
(b) Lipid and Protein



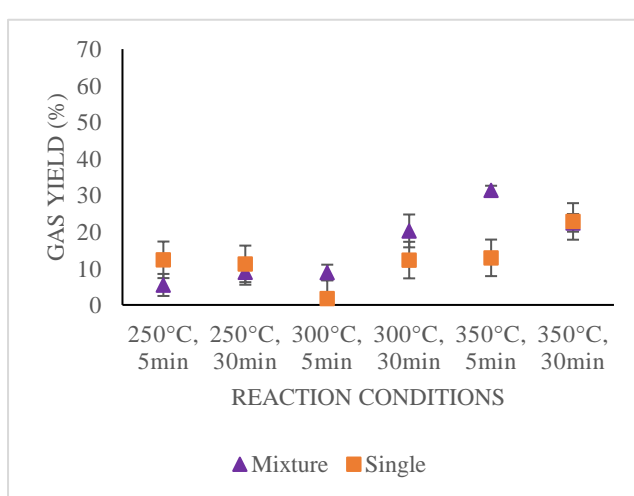
(c) Lipid and Lignin



(d) Carbohydrate and Protein



(e) Carbohydrate and Lignin



(f) Lignin and Protein

Figure S2: Gas yields for binary mixtures of model compounds (triangles) plotted beside crude yields for mass-averaged solid yields for individual model compounds (squares) with error bars representing standard deviation

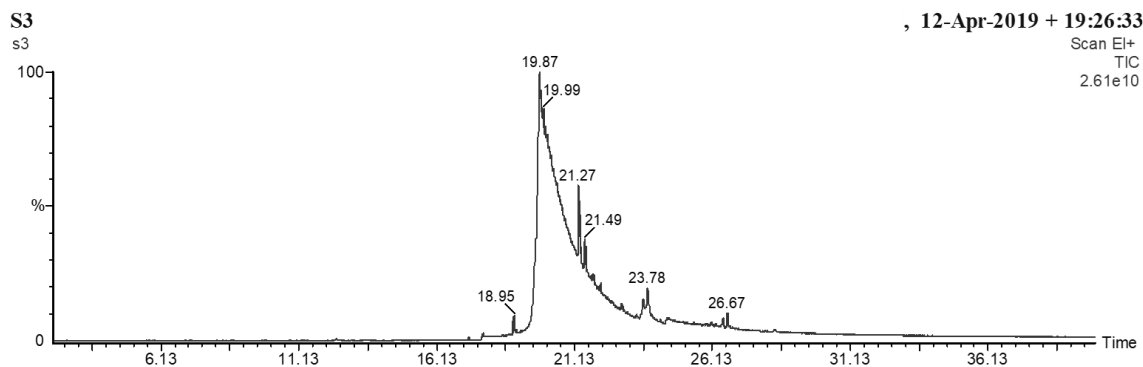


Figure S3: Chromatogram of crude produced from sunflower oil at reaction temperature of 350°C and reaction time of 5 minutes

Crude produced from sunflower oil at reaction temperature of 350°C and reaction time of 5 minutes	
Elution Time	Compound
2.71	Toluene
3.07	2-Ethyl-5-propylcyclopentanone
3.80	Ethylbenzene
7.02	Phenol, 3-methyl-
7.17	Phenol, 2-methoxy-
8.68	Creosol
15.70	Tetradecanoic acid
15.90	Benzene, (1-methyldecyl)-
17.82	N-Hexadecanoic acid
18.95	13-Octadecenoic acid, methyl ester
19.01	1-Nonylcycloheptane
19.91	Isopropyl linoleate
19.23	13-Docosen-1-ol
20.03	9,12-Octadecadienoic acid
21.49	Eicosen-1-ol, cis-9-
26.68	Vitamin E

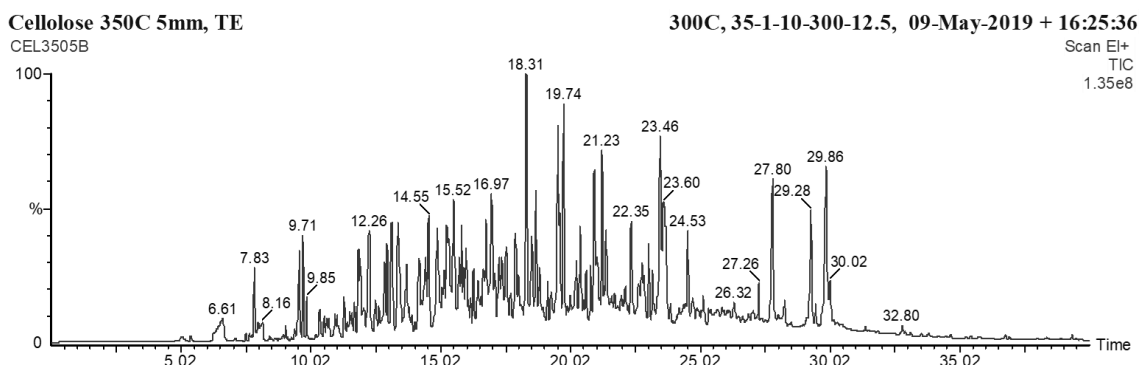


Figure S4: Chromatogram of crude produced from cellulose at reaction temperature of 350°C and reaction time of 5 minutes

Crude produced from cellulose at reaction temperature of 350°C and reaction time of 5 minutes	
Elution Time	Compound
5.39	Butane
6.61	Acetic acid
7.10	Propane, 2-(ethenyloxy)-
7.52	2-Pentanone
7.83	Furan, 2,5-dimethyl-
9.04	Toluene
9.39	1-Hexyne, 5-methyl-
9.55	Furan, 2-ethyl-5-methyl-
9.85	Furan, 2,3,5-trimethyl-
10.34	2-Cyclopenten-1-one
10.53	Cyclohexanone
11.29	5-Ethyl-2-furaldehyde
11.69	2-Cyclopenten-1-one, 2-hydroxy
11.85	2-Cyclopenten-1-one, 3-methyl-
13.70	Cyclohexene, 1,2-dimethyl-
14.19	4-Oxoanal
17.88	1-Naphthalenol, 5,8-dihydro-
19.74	Benzaldehyde, 3-[4-(1,1-dimethylethyl)phenoxy]-
23.03	3-Benzofurancarboxaldehyde, 2-methoxy-
27.26	Tetradecanoic acid, 10,13-dimethyl-, methyl ester
27.81	N-Hexadecanoic acid
29.28	7-Octadecenoic acid, methyl ester
29.86	Octadec-9-enoic acid

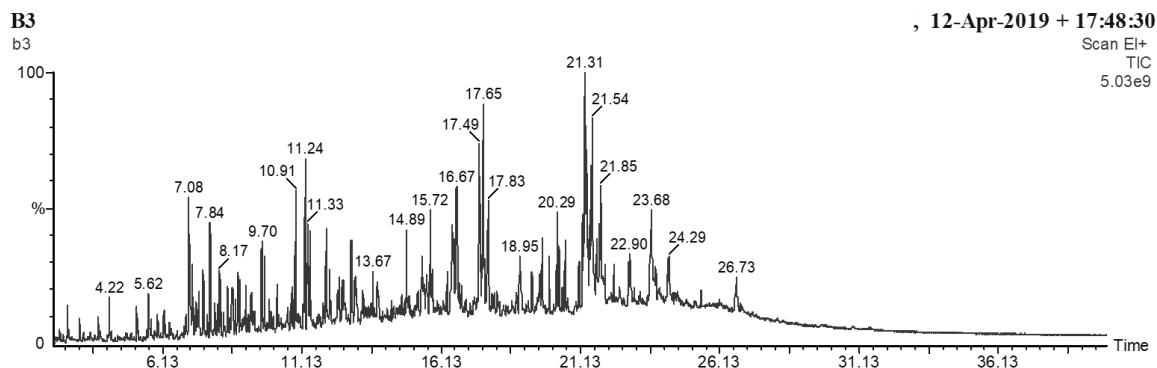


Figure S5: Chromatogram of crude produced from BSA at reaction temperature of 350°C and reaction time of 5 minutes

Crude produced from BSA at reaction temperature of 350°C and reaction time of 5 minutes	
Elution Time	Compound
2.35	Urea, N-tert-butyl-N'-ethyl-N'-methyl-
2.43	5-Noanone
2.55	Pyridine
2.57	1-Cyclopentylacetonitrile
2.70	Toluene
2.38	Pyridine, 2-methyl-
3.36	Pyrimidine, 5-methyl-
3.54	2-Propenoic acid, cyclohexyl ester
3.60	Piperazine, 2,5-dimethyl-
3.80	Ethylbenzene
3.84	Pyridine, 3-methyl-
3.88	Pyridine, 4-methyl-
4.18	Cyclohexylamine, N-ethyl-
4.22	Styrene
4.83	Pyridine, 3,4-dimethyl-
5.00	Pyridine, 2,4-dimethyl-
5.19	Pyridine, 3-ethyl-
5.25	Dihydrotomatidine
5.62	Phenol
5.94	Pyrrolidine, 2-butyl-1-methyl-
6.06	Pyrrolidine, 2-decyl-1-methyl-
6.91	Pyridine, 5-ethyl-2-methyl-
7.08	P-cresol
7.20	2,5-Pyrrolidinedione, 1-methyl-
7.34	Benzeneethanamine

8.17	N-methyldodecanamide
8.47	Phenol, 4-ethyl-
8.91	Morpholine, 4-propionyl-
9.70	Caprolactam
10.24	Indole
10.91	Dodecanamide
11.24	Octanoic acid
11.41	N-methyldodecanamide
12.46	2,5-Pyrrolidinedione, 1-propyl-
12.57	Hexanoic acid, pyrrolidide
12.90	Acetamide, N-(2-phenylethyl)-
13.03	Phenylpropanamide
13.32	Propanamide, 3-phenyl-N- methyl-
13.67	Dodecanamide, N-isobutyl-
14.89	Octanoic acid, morpholide
15.72	Fumaric acid, ethyl 2- phenylethyl ester
16.67	Pyrrolidine, 1-(1-oxobutyl)-
19.75	Hexadecanamide
20.01	Myristamide, N-methyl-
21.31	9-Octadecenamide, (Z)-
21.50	Propanamide, 3-cyclopentyl-N- methyl-
22.32	Oleic diethanolamide
22.90	9-Octadecenamide, N-butyl-
25.46	Nonanoic acid, 2-phenylethyl ester
26.72	Succinic acid, cyclohexylmethyl phenethyl ester

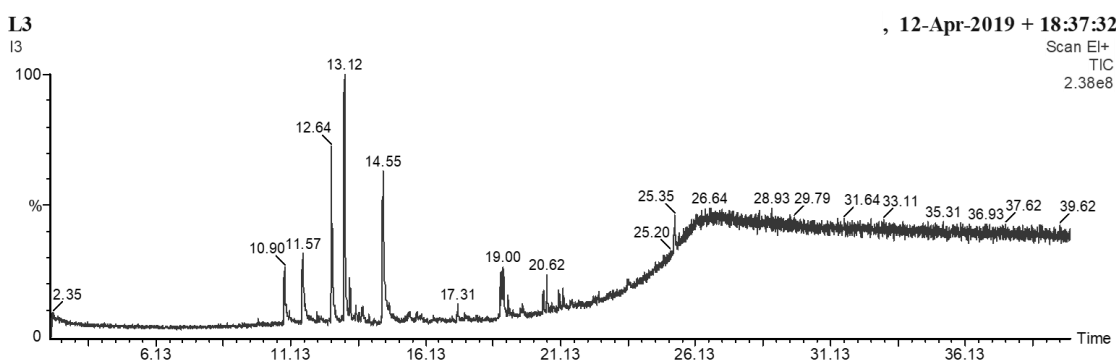


Figure S6: Chromatogram of crude produced from alkaline lignin at reaction temperature of 350°C and reaction time of 5 minutes

Crude produced from alkaline lignin at reaction temperature of 350°C and reaction time of 5 minutes	
Elution Time	Compound
10.90	Phenol, 2,6-dimethoxy-
11.08	Phenol, 2-methoxy-4-propyl-
11.57	Vanillin
12.64	Apocynin
13.12	2-Propanone, 1-(4-hydroxy-3-methoxyphenyl)-
13.31	Benzene, 4-butyl-1,2-dimethoxy-
13.54	3',5'-Dimethoxyacetophenone
14.02	2,5-Dimethoxyethylbenzene
14.55	Benzenepropanol, 4-hydroxy-3-methoxy-
19.01	6-Octadecenoic acid
19.18	Heptacosanoic acid, 25-methyl-, methyl ester
21.06	Carinol

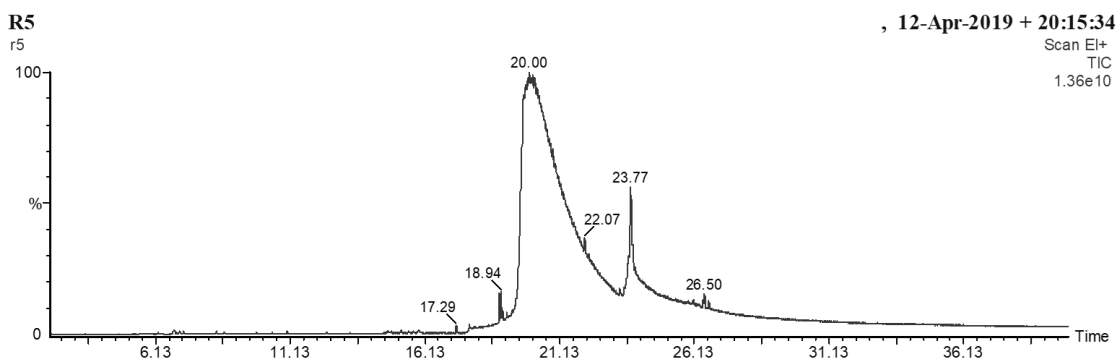


Figure S7: Chromatogram of crude produced from sunflower oil and cellulose at reaction temperature of 350°C and reaction time of 5 minutes

Crude produced from sunflower oil and cellulose at reaction temperature of 350°C and reaction time of 5 minutes	
Elution Time	Compound
6.24	2-Ethyl-5-propylcyclopentanone
6.39	2-Cyclopenten-1-one, 2,3-dimethyl-

6.83	Butyl caprate
7.02	Heptanoic acid
7.17	2-Cyclopenten-1-one, 3,4,5-trimethyl-
8.40	Octanoic acid
8.69	Creosol
9.02	Benzofuran, 4,7-dimethyl-
10.00	1H-Inden-1-one, 2,3-dihydro-
13.35	1-Phenylcyclohexanol
14.77	3-Methyl-2-(2-oxopropyl)furan
15.68	Hexadecanoic acid, cyclohexyl ester
15.91	Benzene, (1-methyldecyl)-
18.95	13-Octadecenoic acid, methyl ester
20.17	13-Docosen-1-ol
23.77	Isopropyl linoleate
26.50	Methyl 2-octylcyclopropene-1-octanoate
26.67	Methyl 8,9-octadecadienoate

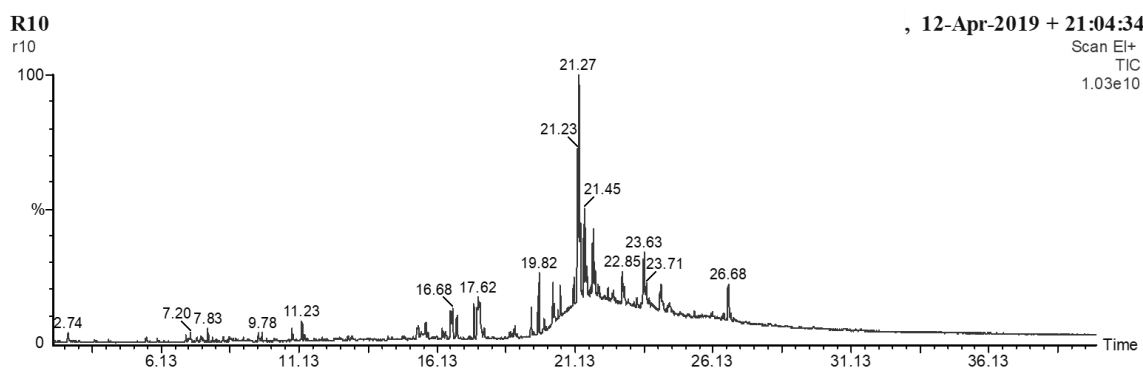


Figure S8: Chromatogram of crude produced from sunflower oil and BSA at reaction temperature of 350°C and reaction time of 5 minutes

Crude produced from sunflower oil and BSA at reaction temperature of 350°C and reaction time of 5 minutes	
Elution Time	Compound
3.71	Piperidine, 1-ethyl-
4.22	Styrene
5.00	Phenol
5.98	Pyrrolidine, 2-butyl-1-methyl-
6.24	Pyridine, 2-ethyl-5-methyl
7.02	Phenol, 3-methyl-

7.56	Octanamide
7.83	2,5-Pyrrolidinedione, 1-ethyl-
8.38	Benzeneethanol, 4-hydroxy-
9.65	Caprolactam
11.23	Octanoic acid, pyrrolidide
13.02	Phenylpropanamide
14.87	2-Pyrrolidinethione, 5,5-dimethyl-
17.62	Diethyl glutaconate
18.95	Ricinoleic acid
19.82	Hexadecanamide
20.33	2,5-Piperazinedione, 3-benzyl-6-isopropyl-
21.23	Ethyl 9,12-hexadecadienoate
21.27	9-Octadecenamide
21.81	Fumaric acid, 4-octyl dodec-2-en-1-yl ester
23.63	Ethyl 9-tetradecenoate
23.81	Eicosen-1-ol, cis-9-

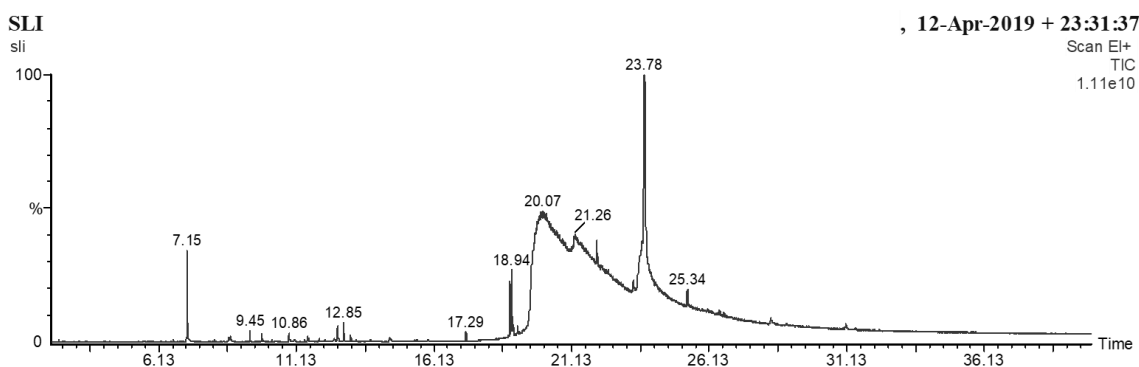


Figure S9: Chromatogram of crude produced from sunflower oil and alkaline lignin at reaction temperature of 350°C and reaction time of 5 minutes

Crude produced from sunflower oil and alkaline lignin at reaction temperature of 350°C and reaction time of 5 minutes	
Elution Time	Compound
2.99	2-Pentoxy-tetrahydropyran
6.40	2-Cyclopenten-1-one, 2,3-dimethyl-
6.66	Benzene, N-butyl-
7.98	Benzene, 1,2-dimethoxy-
8.16	Benzene, pentyl-
8.49	Creosol

8.75	Methyl salicylate
9.87	Phenol, 4-ethyl-2-methoxy-
10.86	Phenol, 2,6-dimethoxy-
11.06	Phenol, 2-methoxy-4-propyl-
11.54	Vanillin
12.50	Propofol
12.61	Apocynin
12.85	2,4-Di-tert-butylphenol
13.31	Benzene, 4-butyl-1,2-dimethoxy-
17.29	Tetradecanoic acid, 10,13-dimethyl-, methyl ester
18.94	13-Octadecenoic acid, methyl ester
19.00	N-Propyl 11-octadecenoate
21.27	Eicosen-1-ol, cis-9-
23.78	Isopropyl linoleate
28.40	Decane, 2-cyclohexyl-

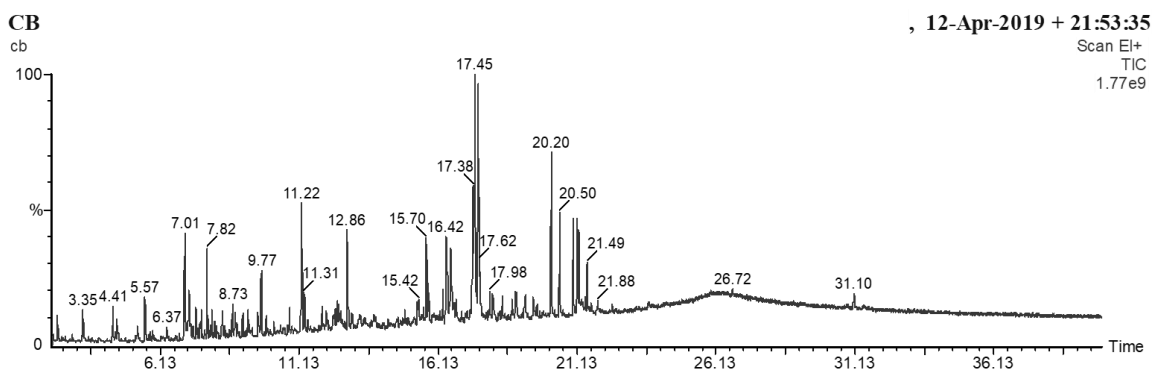


Figure S10: Chromatogram of crude produced from cellulose and BSA at reaction temperature of 350°C and reaction time of 5 minutes

Crude produced from cellulose and BSA at reaction temperature of 350°C and reaction time of 5 minutes	
Elution Time	Compound
2.43	Pyrazine
2.97	2-Butenal, 2-methyl-
3.66	Pyrazine, methyl-
4.41	2-Cyclopenten-1-one, 2-methyl-
4.57	Pyrazine, ethyl-
5.31	2-Cyclopenten-1-one, 3-methyl-
5.58	Phenol
7.01	Phenol, 3-methyl-
7.16	Phenol, 2-methoxy-

7.82	2,5-Pyrrolidinedione, 1-ethyl-
8.73	3,4-Methylpropylsuccinimide
9.10	2,5-Pyrrolidinedione, 1-propyl-
11.22	Octanoic acid, pyrrolidide
12.86	2,4-Di-tert-butylphenol
15.70	Benzenebutanal
17.37	2,5-Piperazinedione,3,6-bis(2-methylpropyl)-

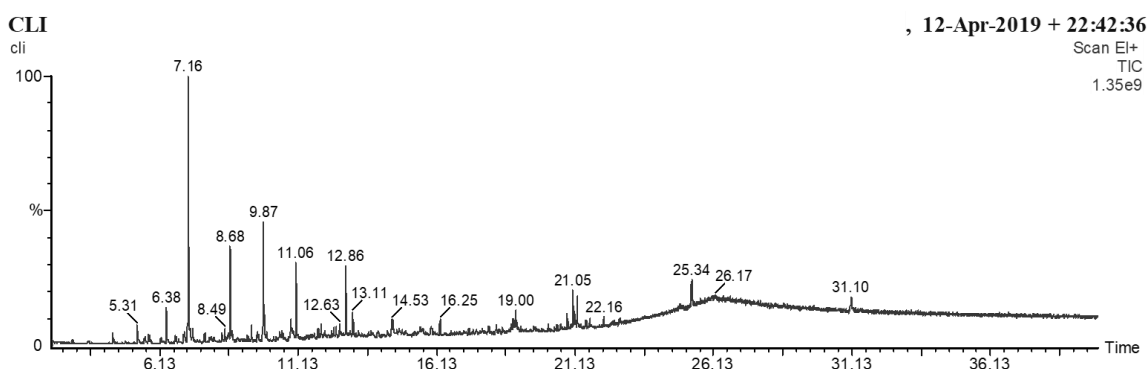


Figure S11: Chromatogram of crude produced from cellulose and alkaline lignin at reaction temperature of 350°C and reaction time of 5 minutes

Crude produced from cellulose and alkaline lignin at reaction temperature of 350°C and reaction time of 5 minutes	
Elution Time	Compound
4.44	2-Cyclopenten-1-one, 2-methyl-
4.53	Cyclopentene, 1,2,3-trimethyl-
5.00	5,5-Dimethyl-1,3-hexadiene
5.17	Decane, 4-methylene-
5.22	2,3-Dihydro-2-methyl-5-ethylfuran
5.31	2-Cyclopenten-1-one, 3-methyl-
5.60	Phenol
6.38	2-Cyclopenten-1-one, 2,3-methyl-
6.69	Phenol, 2-methyl-
7.03	Phenol, 3-methyl-
7.16	Mequinol
7.76	Cyclohexene, 3,3,5-trimethyl-
8.68	Creosol
9.46	Benzene, 1,3-bis(1,1-dimethylethyl)-
9.87	Phenol, 4-ethyl-2-methoxy-
10.55	2,5-Dimethoxyethylbenzene

10.87	Phenol, 2,6-dimethoxy-
11.06	Phenol, 2-methoxy-4-propyl-
12.50	Propofol
12.86	Phenol, 3,5-bis(1,1-dimethylethyl)-
14.53	Benzenepropanol, 4-hydroxy-3-methoxy-
17.29	Tetradecanoic acid, 10,13-dimethyl-, methyl ester
19.00	Methyl 11-docosenoate
20.15	Retene
20.85	Hexacosyl acetate

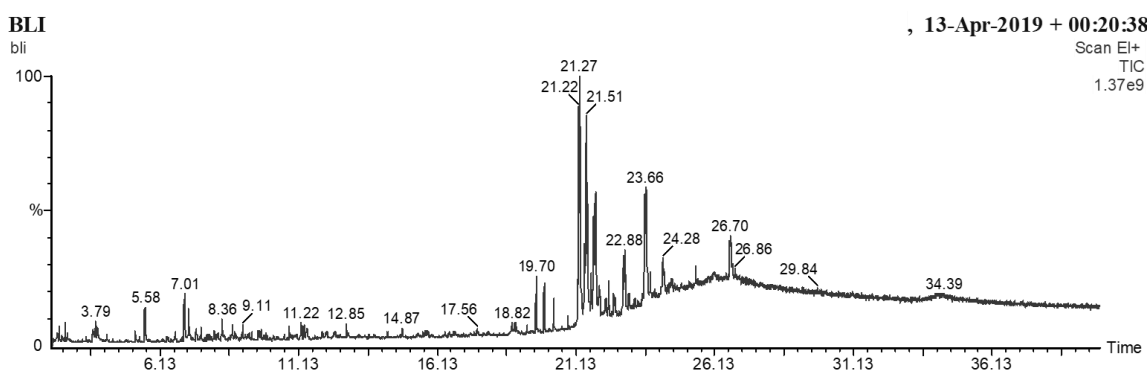


Figure S12: Chromatogram of crude produced from BSA and alkaline lignin at reaction temperature of 350°C and reaction time of 5 minutes

Crude produced from BSA and alkaline lignin at reaction temperature of 350°C and reaction time of 5 minutes	
Elution Time	Compound
2.27	Cyclopentanone, 2-(1-methylpropyl)-
2.70	Toluene
3.34	Pyridine, 2-methyl-
3.79	Ethylbenzene
3.86	Pyridine, 2-methyl-
4.22	Styrene
5.22	Pyridine, 3-ethyl-
5.58	Phenol
7.01	P-Cresol
7.16	Phenol, 2-methoxy-
8.36	Phenol, 4-ethyl-
8.74	Cyclohexylidencyanoacetic acid
9.69	Caprolactam

11.22	Octanoic acid, pyrrolidide
12.85	2,4-Di-tert-butylphenol
13.66	Octanoic acid-tert butyl ester
14.32	Pyridine, 4-(2-phenylethyl)-
18.82	1-Undecene, 11-nitro-
19.70	Hexadecanamide
19.99	Myristamide, N-methyl-
21.27	9-Octadecanamide
21.47	Propanamide, 3-cyclopentyl-N-methyl-
21.82	Myristamide, N-ethyl-
22.88	9-Octadecenamide, N-butyl-
23.66	Oleic diethanolamide
23.81	Glycidyl oleate
26.70	Succinic acid, cyclohexymethyl phenethyl ester

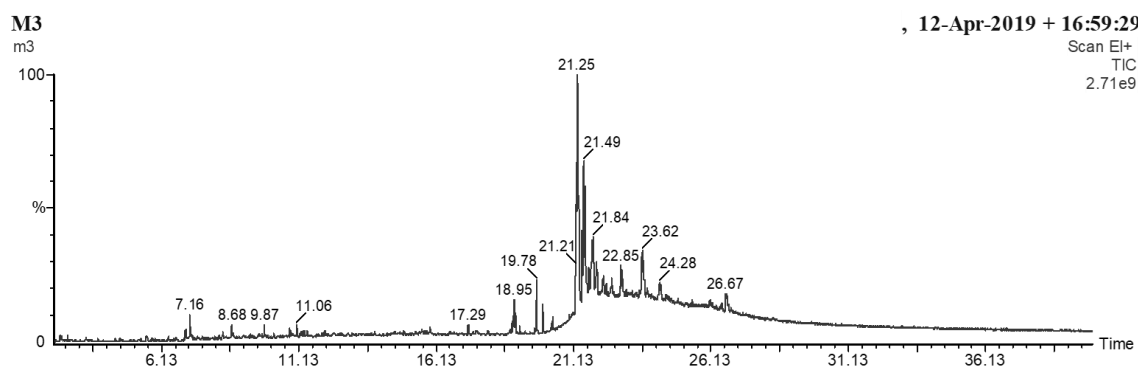


Figure S13: Chromatogram of crude produced from quaternary mixture at reaction temperature of 350°C and reaction time of 5 minutes

Crude produced from quaternary mixture at reaction temperature of 350°C and reaction time of 5 minutes	
Elution Time	Compound
2.44	Pyrazine
2.70	Toluene
3.38	Pyrimidine, 5-methyl-
3.80	Ethylbenzene
3.85	1H-Pyrrole, 2,4-dimethyl-
4.45	2-Cyclopenten-1-one, 2-methyl-
6.50	Pyridinium, 1-ethyl-, hydroxide
5.12	Ethinamate
5.58	Phenol

Chapter 5 – Reaction kinetics and characterisation of species in renewable crude from hydrothermal liquefaction of mixtures of polymer compounds to represent organic fractions of biomass feedstocks

5.78	2-Cyclopenten-1-one, 2,3-dimethyl-
7.01	Phenol, 3-methyl-
7.16	Phenol, 2-methoxy-
8.36	Phenol, 2-propyl-
8.68	Creosol
9.87	Phenol, 4-ethyl-2-methoxy-
11.06	Phenol, 2-methoxy-4-propyl-
11.22	N-[2-hydroxyethyl]succinimide
12.07	4-(2-Pyrrol-1-yl-ethyl)pyridine
15.91	Benzene, (1-methyldecyl)-
17.29	Tetradecanoic acid, 10,13-dimethyl-, methyl ester
19.78	Hexadecanamide
20.01	Myristamide, N-methyl-
21.25	9-Octadecanamide
21.49	Propanamide, 3-cyclopentyl-N-methyl-
21.69	3-Methyl-2-(2-oxopropyl)furan
21.84	Fumaric acid, 2-octyl dodec-2-en-1-yl ester
21.96	11,14-Octadecadienoic acid, methyl ester
22.21	9,12-Octadecadienoic acid, methyl ester
23.62	Glycidyl Oleate
26.67	Vitamin E

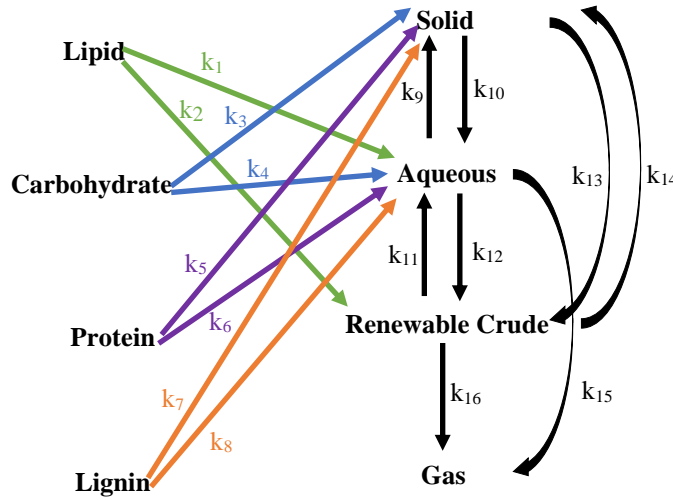


Figure S14: Kinetic pathways without the addition of the gas to aqueous pathway

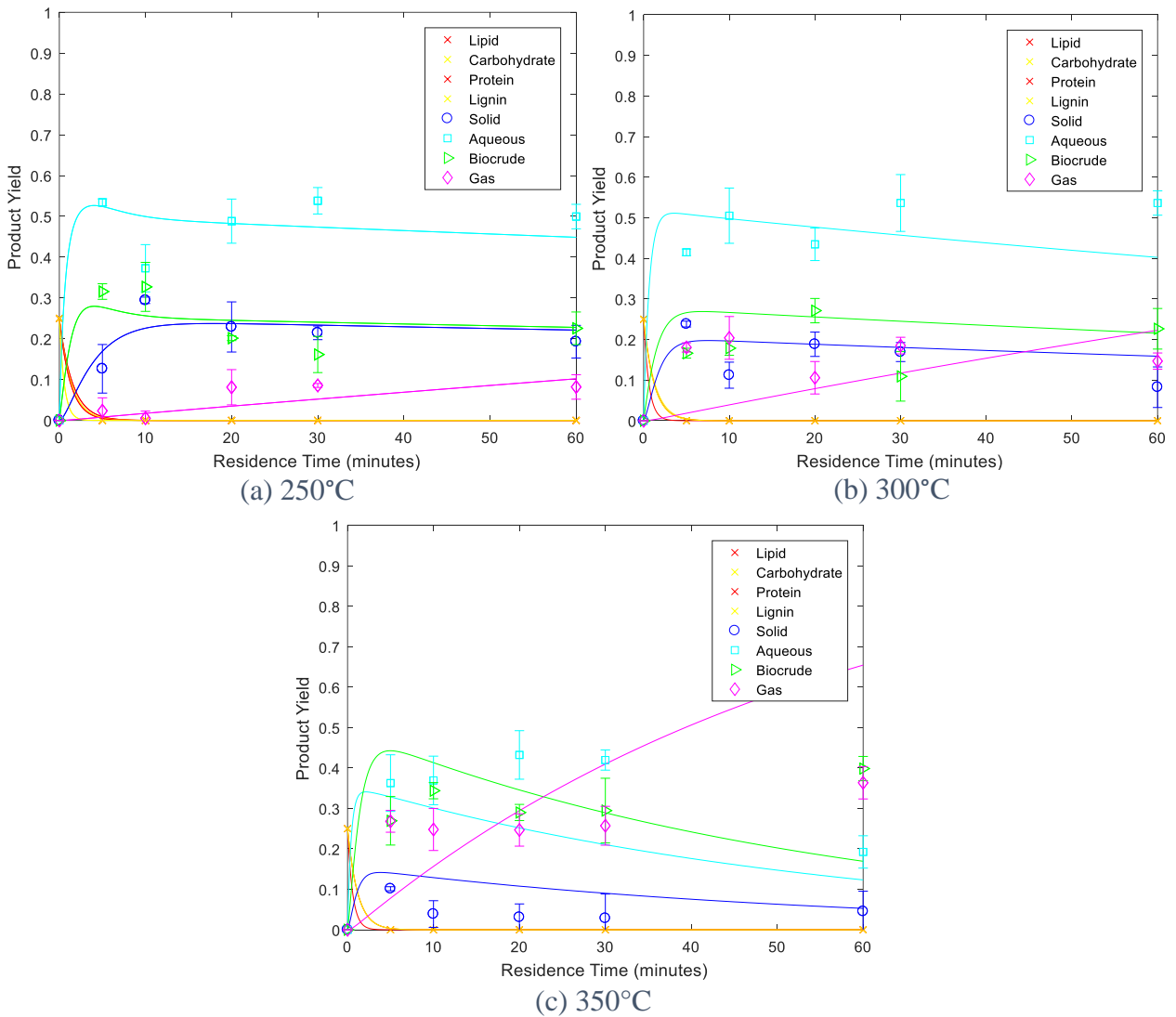


Figure S15: Kinetic model without the addition of the gas to aqueous pathway

Chapter 6

A kinetic model for the hydrothermal
liquefaction of microalgae, sewage
sludge and pinewood with product
characterisation of renewable crude

R. Obeid ^a, N. Smith ^a, D.M. Lewis ^a, T. Hall ^b, P. van
Eyck ^a

^aThe School of Chemical Engineering and Advanced
Materials

^b Faculty of Sciences

The University of Adelaide, SA 5000, Australia

**Unpublished and Unsubmitted work written in
manuscript style.**

Statement of Authorship

Title of Paper	A kinetic model for the hydrothermal liquefaction of microalgae, sewage sludge and pinewood with product characterisation of renewable crude
Publication Status	<input type="checkbox"/> Published <input type="checkbox"/> Accepted for Publication <input type="checkbox"/> Submitted for Publication <input checked="" type="checkbox"/> Unpublished and Unsubmitted work written in manuscript style
Publication Details	Unpublished and Unsubmitted work written in manuscript style.

Principal Author

Name of Principal Author (Candidate)	Reem Obeid				
Contribution to the Paper	Carbohydrate, protein, lipid and lignin analysis for biomass HTL reactor design and methods and HTL batch experiments completed Methods developed for product separation and product separation completed Interpretation of GC-MS results Construction of model Writing and editing				
Overall percentage (%)	80				
Certification:	This paper reports on original research I conducted during the period of my Higher Degree by Research candidature and is not subject to any obligations or contractual agreements with a third party that would constrain its inclusion in this thesis. I am the primary author of this paper.				
Signature	<table border="1" style="width: 100%;"> <tr> <td style="width: 80%;"></td> <td style="width: 20%;">Date</td> </tr> <tr> <td></td> <td>17/01/2020</td> </tr> </table>		Date		17/01/2020
	Date				
	17/01/2020				

Co-Author Contributions

By signing the Statement of Authorship, each author certifies that:

- i. the candidate's stated contribution to the publication is accurate (as detailed above);
- ii. permission is granted for the candidate to include the publication in the thesis; and
- iii. the sum of all co-author contributions is equal to 100% less the candidate's stated contribution.

Name of Co-Author	Neil Smith				
Contribution to the Paper	Concept development Assistance with analysis and interpretation of data Drafting of paper				
Signature	<table border="1" style="width: 100%;"> <tr> <td style="width: 80%;"></td> <td style="width: 20%;">Date</td> </tr> <tr> <td></td> <td>29/1/2020</td> </tr> </table>		Date		29/1/2020
	Date				
	29/1/2020				

Chapter 6 – A kinetic model for the hydrothermal liquefaction of microalgae, sewage sludge and pinewood with product characterisation of renewable crude

Name of Co-Author	David Lewis		
Contribution to the Paper	Concept development Assistance with analysis and interpretation of data Drafting of paper		
Signature		Date	22-Feb-2020

Name of Co-Author	Tony Hall		
Contribution to the Paper	Method design and analysis using Source Rock Analyser and GC-MS Drafting of paper		
Signature		Date	23/1/20

Name of Co-Author	Philip van Eyk		
Contribution to the Paper	HTL reactor design and methods Concept development Assistance with analysis and interpretation of data Drafting of paper		
Signature		Date	25/1/2020

✓

A kinetic model for the hydrothermal liquefaction of microalgae, sewage sludge and pine wood with product characterisation of renewable crude

Reem Obeid^a, Neil Smith^a, David M. Lewis^a, Tony Hall^b and Philip van Eyk^{a*}

^a School of Chemical Engineering and Advanced Materials, The University of Adelaide, Adelaide, South Australia 5005, Australia

^b Faculty of Sciences, The University of Adelaide, Adelaide, South Australia 5005, Australia

*E-mail: philip.vaneyk@adelaide.edu.au.

Keywords: hydrothermal liquefaction, kinetics, model, algae, sludge, pine

Abstract

Hydrothermal liquefaction (HTL) of biomass is an emerging technology that is being developed to produce renewable crude oil in water at sub-critical conditions. The development of the process requires an understanding of the reaction products. Different feedstocks and reaction conditions result in different product fractions of the renewable crude and co-products of solid, aqueous and gas phase products. Biomass being considered as feedstocks for HTL include microalgae, sewage sludge and lignocelluloses. Each of these biomass sources contains varying amounts of lipid, carbohydrate, protein and lignin organic fractions as well as some inorganic components. In order to develop a bulk kinetic model to predict the yields of crude, solid, aqueous and gas phase products, HTL

experiments were conducted at reaction temperatures of 250, 300 and 350°C over reaction times of 0 to 60 minutes with *Tetraselmis* sp. microalgae, sewage sludge and Radiata pine. The crude was analysed via gas-chromatography mass-spectrometry to identify variations in the compounds in the crude produced from different types of biomass. The highest crude yield was produced from algae at up to 30%, followed by up to 25% from sludge and up to 10% from pine. A reaction temperature of 300 or 350°C was preferable for maximum crude yield and increasing reaction time over 5 minutes was seen to cause minimum variation in crude yield for most cases. The variation in product distribution is strongly dependent on both the organic and inorganic content of the biomass feedstock. A unified bulk kinetic model for prediction of crude yield from a wide range of biomass was developed. Predictions showed up to 15% variation from measurements illustrating that further experimental data from HTL of a wider range of feedstocks are required to refine the model and build up model rigour.

1. Introduction

The need for renewable energy sources increases with the depleting supply of fossil fuels across the globe. Renewable sources of energy and their technologies require further development to meet global energy demands. Hydrothermal liquefaction (HTL) is an emerging technology that can be used to convert biomass into a renewable crude oil. The HTL process uses water at sub-critical conditions to convert the organic fractions of biomass to a renewable energy source, hence the process is favourable for converting biomass with high water content. The sub-critical water acts as a catalyst that modifies the activation energy for certain

reactions and opens up new reaction pathways for the biomass reactant that vary compared to water at ambient conditions [1]. Co-products of the process include solid, gas and aqueous phase products.

Previous investigations in literature have indicated that crude yield is strongly dependent on the composition of the feed in HTL [2]. Biomass used as a feedstock for the HTL process can have varying composition depending on its source, with various fractions of carbohydrate, lipid, protein, lignin and ash contents. Microalgae has been extensively studied as a feedstock for HTL [3-7]. The organic content of microalgae includes lipids, carbohydrates and proteins. Different species of microalgae and microalgae obtained under varying growth conditions contain different fractions of organic and inorganic components [8, 9]. Maximum crude yield and the conditions for optimum crude yield have been found to vary for different species of microalgae. Optimum crude yields from the HTL of microalgae have been reported to be 20-78% on a dry ash free basis [7]. Sewage sludge is another feed of interest for HTL as a waste management process where a fuel is produced. Sewage sludge is a by-product of the waste water industry and composed of lipid, carbohydrate, protein and lignin organic fractions as well as ash [10, 11]. Lignocellulosic biomass can also be investigated for HTL. Lignocellulosic biomass is rich in carbohydrate (cellulose and hemicellulose) and lignin. As these biomass sources each contain variable amounts of carbohydrate, lipid, protein, lignin and ash, they are likely to produce a range of product compositions and yields. In order to identify the yields of solid, aqueous, crude

and gas phase products from the process, HTL experiments with each feedstock are required.

In addition to feed composition, the yields are determined by reaction conditions, including time and temperature [12]. The yields of solid, aqueous, crude and gas phase products in HTL need to be identified in order to determine the value of the process. A multivariate data analysis which used data from 34 peer reviewed studies has indicated that the most significant factor affecting product distribution in HTL was the composition of the feed. Reaction time was also found to have a significant effect on the distribution of products between the crude and water soluble organic fractions [13]. Other factors affecting yield include the heating rate of the reactor [14]. The separation methods to quantify the solid, crude, aqueous and gas phases, particularly the use of different organic solvents, also impact product yields [4]. Hence, experiments conducted at the same conditions are essential for comparable results. Once the product distribution for the HTL process is identified at various reaction temperatures and reaction times, optimum feedstock composition and the reaction conditions for maximum crude yield for various feedstocks can be identified.

Some biomass sources have inherent catalysts within their composition.

Phosphorus, chlorine, sodium, magnesium and potassium have been identified via inductively coupled plasma-optical emission spectroscopy (ICP-OES) analysis and were found to each make up greater than 0.5wt% of dry microalgae [15]. In another case, atomic absorption spectroscopy (AAS) was used to identify 55,100ppm of potassium, 34,400ppm of sodium, 12,200 ppm of magnesium and

5,100 ppm of calcium in microalgae [16]. Sewage sludge has also been found to contain a high inorganic content, including heavy metals, which vary depending on the time and location of its collection [17]. Commonly used catalysts for hydrothermal liquefaction include potassium hydroxide, potassium carbonate, sodium carbonate, sodium hydroxide and nickel [18]. Hence, the inorganic fractions in biomass could be catalysing the conversion of biomass to crude oil. Some alkali metals can also inhibit conversion to crude and result in higher yield of the aqueous phase as was found in the case for potassium hydroxide by Anastasakis and Ross [16] despite evidence from other work where it was shown to catalyse reactions [18]. The reason for these different behaviours is not yet known. The minerals present in the biomass feedstocks which contain significant ash content should be identified as they may have a catalytic or inhibitory effect which effects the product distribution in HTL.

The properties of crude from different sources of biomass, reacted under different conditions also requires investigation. The varying composition of biomass results in different chemical reactions which produce different molecular products [12, 19]. The crude produced from lipid has been found to be rich in fatty acids. From carbohydrates cyclic hydrocarbons, ketones, aldehydes, esters, fatty acid chains and furans were identified. The crude from protein contained amides and phenolic compounds. Lignin produced a crude which was made up of mostly phenolic compounds [19, 20]. Hence, the crude produced from different sources of biomass should be analysed to give further insight into which organic fractions are contributing to crude yield.

Modelling of experimental data to predict product yields from hydrothermal liquefaction of biomass and model compounds has been conducted. Both multicomponent additivity models and first order kinetic models have been employed in literature. Multicomponent additivity models involve fitting data at one temperature and one time for biomass with various compositions of carbohydrate, lipid, protein and lignin to predict crude yield [21, 22]. Bulk kinetic models use the biomass composition to determine crude yield for a given temperature at a range of reaction times. The reaction mechanisms are simplified to include the biomass reactant as well as the solid, aqueous, crude and gas products. First order kinetic models have been developed at a range of temperatures to obtain Arrhenius parameters [12, 23-26]. The product fractions are determined by the feed concentration in these models. These models have been developed for biomass model compounds and algae, however a model which accounts for the different types of biomass, including algae, sludge and lignocellulosic biomass requires further development.

The aim of this work is to develop a kinetic model for predicting the products from HTL of different types of biomass. By conducting HTL experiments for microalgae, sludge and lignocellulosic biomass under the same set of reaction conditions, the effect of biomass compositions on product yield and crude composition could be investigated. The aim is to use the experimental data to develop a novel kinetic model to be suitable for different types of biomass, and to take into account the composition of the inorganic fraction of the biomass and its influence on product distribution. This model could be used to predict the

optimum processing conditions for each type of biomass for maximum crude yield.

2. Materials and Methods

2.1 Materials and Feedstock Analysis

All three biomass sources were dried in an oven at 50°C over 48 hours before being analysed and used as a feedstock in HTL experiments. The *Tetraselmis* sp. MUR 233 microalgae obtained for experiments was grown in a recycled culture medium with its growth conditions described by Sing, et al. [28]. Sewage sludge from Melbourne Water which was extracted from the wastewater treatment process after treatment in the aerobic lagoons but prior to ultraviolet light treatment, was ground and sieved at <1mm. Radiata pine wood saw dust was ground and sieved at <1mm.

Lipid analysis was conducted via the Bligh and Dyer method [29]. Carbohydrate determination was conducted using the method by Dubois, et al. [30]. Lignin content was determined via acetyl bromide digestion [31, 32]. Ash content was determined using the method defined by Sluiter, et al. [33]. The protein content of biomass was determined using the nitrogen to protein conversion factor of 6.25 where nitrogen content was determined from elemental analysis. For the microalgae the conversion factor of 4.78 was employed as it has been found to more accurately determine protein content in microalgae compared to the conversion factor of 6.25 [34]. The lipid, carbohydrate, protein, lignin and ash content are reported on a dry basis.

In order to determine nitrogen content, samples were analysed by elemental analysis (EA) using a Perkin Elmer 2400 series II CHNS/O Elemental Analyser in CHNS configuration. The combined combustion/reduction tube was packed using Perkin Elmer EA6000 and Perkin Elmer ‘Hi-Purity’ copper with a reaction temperature of 975°C. Results were calibrated to 2mg of Perkin Elmer Organic Analytical Standard of Cystine (formula: $(SCH_2CH(NH_2)CO_2H)_2$) with known abundances of carbon (29.99%), hydrogen (5.07%), nitrogen (11.67%) and sulphur (26.69%). The accepted error range between standards was $\pm 0.3\%$ for carbon, hydrogen and nitrogen calculated against 12 replicates.

To determine the inorganic content of the feedstocks, total metals by acid digestion was conducted by the CSIRO at the Waite Campus, Urrbrae. Acid digestion was first conducted according to the US EPA method 3052: Microwave Assisted Acid Digestion of Siliceous and Organically Based Matrices [35]. The finely ground sample was digested in a microwave oven using nitric acid. The solution was then analysed for a wide range of elements by inductively coupled plasma-optical emission spectrometry (ICP-OES). Three replicates of each sample were completed and the standard deviation for the result for each inorganic compound was calculated.

Dichloromethane (DCM) was selected as the organic solvent used to recover the crude from the product mixture because it has been found to recover a high volume of crude due to its moderate polarity and this is necessary for the product fractions to be defined [4]. DCM has a low boiling point of 40°C which allows

efficient evaporation of the solvent after crude extraction without evaporating high amounts of crude product.

2.2 Hydrothermal Liquefaction in a Batch Reactor

The reactor and HTL procedure has been described in detail in previous work [12]. A mass loading of 30wt% of the oven dried biomass was loaded into the reactor followed by 70wt% water to make up a total of 5.5g reaction mixture. The reactor volume was 11mL. The reactor was pre-charged with nitrogen to achieve a reaction pressure of 200 bar at each reaction temperature. The reactor was heated to 250, 300 and 350°C for reaction times of 5, 10, 20, 30 and 60 minutes. The reactor was heated in a Techne SBL-2D fluidised bed with the Techne-9D temperature controller at a heating rate of approximately 125°C per minute. Once the reactor reached 98% of the desired reaction temperature the timer was started for the desired reaction time. Some reactions would have occurred during heat-up time. At the completion of the reaction time the reactor was cooled to room temperature within 5 minutes.

The gas was released and the mass of nitrogen added to the reactor prior to reactions was subtracted from total gas released to find the mass of gas produced from HTL. The reactor contents were emptied into a centrifuge tube and the reactor was rinsed with DCM to recover any crude bound to the reactor walls. The HTL product-DCM mixture was then centrifuged. The bottom crude layer was extracted with a pipette and dried in a Techne Sample Concentrator at 40°C over 6 hours with a stream of nitrogen to find the mass of crude extracted with solvent. The solid-aqueous product mixture was filtered to separate the solids which were

dried in an oven overnight at 40°C. Pyrolysis measurements were used to determine the crude bound to solids for each experimental product using a Weatherfords Source Rock Analyser™. This allowed the additional crude, which was not extracted from the solids using solvent alone, to be quantified. The method has been described previously [19, 36]. The porous nature of the solids prevents the total extraction of crude using solvent alone. The Weatherfords Source Rock Analyser™ calculates the free hydrocarbons in the sample, S1. This is the mass of crude extracted by heating the sample to 300°C. S1 was used to determine the crude yield while the remaining fractions of solid product in pyrolysis were used to calculate solid yield. The aqueous phase was determined by subtracting the mass of gas, crude and solid products from the mass of the initial biomass feed added to the reactor.

2.4 Analysis of Products from HTL

2.4.1 Ash Content of HTL Products

The ash content in the solid product from HTL was determined using the method by Sluiter, et al. [33]. This allowed the calculation of the mass of ash present in solid. The remaining ash content, determined from the feedstock analysis, was assumed to be part of the aqueous phase. For this calculation, it was assumed that no ash was present in the crude. Previous investigations have indicated that less than 10% of each of the minerals in the initial microalgae biomass feedstock are transferred to the crude [16].

To calculate ash-free yields, the ash free product fractions were divided by the mass of organic biomass initially fed to the reactor (mass of biomass feed minus

the mass of ash in the biomass feed). The ash free solid yield was determined by subtracting the mass of ash in the solids from the total mass of solids and then dividing that by the organic fraction of biomass. The ash free aqueous phase was determined by subtracting the mass of ash in the aqueous phase from the total mass of aqueous phase and dividing by the organic fraction of biomass. Ash free crude and gas yields were determined by dividing the mass of crude and gas by the mass of organic biomass reactant.

2.4.2 GC-MS of Renewable Crude Products

Hydrocarbon characterisation for the crude products was undertaken using a Perkin Elmer SQ8 Gas Chromatograph-Mass Spectrometer (GC-MS). The method has been described previously [19, 20]. Data interpretation was undertaken using Perkin Elmer TurboMass 6.0 software with comparison of compound spectra to the NIST14 Spectral Library Database. The concentration of each compound in the crude was approximated using dodecane as a reference.

2.5 Kinetic Parameters

The kinetic pathways used for each biomass compound are shown in Figure 1 and were determined from experiments with model compounds in previous work [19]. To obtain the kinetic parameters for the kinetic pathways shown in Figure 1, the MATLAB function *ODE45* was employed as the solver for the ordinary differential equations in Equations 1-8. The parameters were fit to experimental data via a least squares algorithm with the MATLAB function *lsqcurvefit*. The bounds for kinetic parameters were set between 0 and 1. The errors in Arrhenius parameters presented in Table 5 are calculated from the 95% confidence intervals.

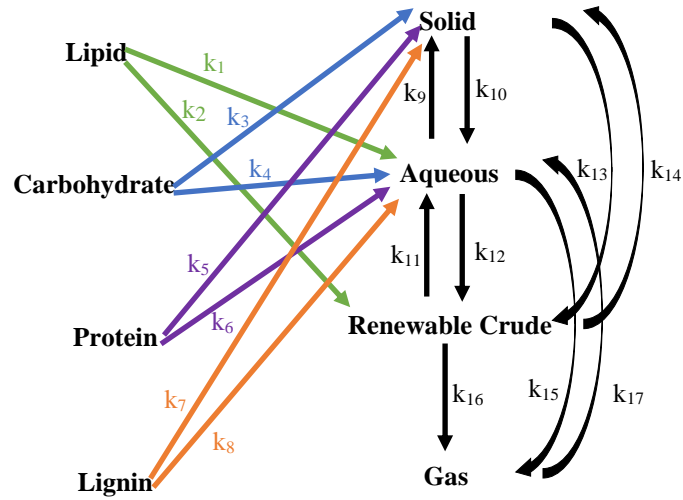


Figure 1. Kinetic pathways for biomass model compounds derived from model compounds taken from [19]

$$\frac{dx_1}{dt} = -(k_1 + k_2)x_1 \quad (1)$$

$$\frac{dx_2}{dt} = -(k_3 + k_4)x_2 \quad (2)$$

$$\frac{dx_3}{dt} = -(k_5 + k_6)x_3 \quad (3)$$

$$\frac{dx_4}{dt} = -(k_7 + k_8)x_4 \quad (4)$$

$$\frac{dx_5}{dt} = -(k_{10} + k_{13})x_5 + k_3x_2 + k_5x_3 + k_7x_4 + k_9x_6 + k_{14}x_7 \quad (5)$$

$$\frac{dx_6}{dt} = -(k_9 + k_{12} + k_{15})x_6 + k_1x_1 + k_4x_2 + k_6x_3 + k_8x_4 + k_{10}x_5 + k_{11}x_7 + k_{17}x_8 \quad (6)$$

$$\frac{dx_7}{dt} = -(k_{11} + k_{14} + k_{16})x_7 + k_2x_1 + k_{12}x_6 + k_{13}x_5 \quad (7)$$

$$\frac{dx_8}{dt} = -k_{17}x_8 + k_{15}x_6 + k_{16}x_7 \quad (8)$$

3. Results and Discussion

3.1 Feedstock composition

The results from elemental and compositional analysis are shown in Table 1. The high ash content of microalgae should be noted and is due to its growth conditions in saltwater. The sludge also had a high ash composition, however the composition of the ash in microalgae is more variable. Previous analysis of the microalgae has shown the inorganic content to be made up mainly of water-soluble alkali salts, where the relative proportions and inorganic elements depend on how it has been cultured and harvested [37]. The ash from the microalgae used in this work is very high is sodium as well as aluminium, magnesium and calcium. The ash in the sludge contains a high concentration of phosphorus, calcium and sulphur as can be seen in Table 1. The pinewood contains much lower concentrations of the inorganic compounds in Table 1.

Table 1: Feedstock Composition

	<i>Microalgae</i>	<i>Sludge</i>	<i>Pine wood</i>
<i>Lipid (%)</i>	4.8±1.2	18.0±2.6	2.8±0.0
<i>Carbohydrate (%)</i>	22.9±1.4	19.4±3.3	66.9±3.5
<i>Protein (%)</i>	12.0±1.4	8.7±1.9	0.5±1.9
<i>Lignin (%)</i>	-	1.3±1.1	19.5±2.5
<i>Ash (%)</i>	62.8±2.7	43.0±3.0	1.4±0.3
<i>Carbon (%)</i>	21.01±0.3	14.61±0.3	44.68±0.3
<i>Hydrogen (%)</i>	3.88±0.3	2.45±0.3	6.15±0.3
<i>Nitrogen (%)</i>	2.52±0.3	1.39±0.3	0.06±0.3
<i>Calcium (ppm)</i>	16,633±262	15,000±0	578±3
<i>Potassium (ppm)</i>	3,923±54	1,733±47	399±5
<i>Magnesium (ppm)</i>	19,433±330	4,833±170	178±2
<i>Sodium (ppm)</i>	150,333±943	2,000±0	61±4
<i>Sulphur (ppm)</i>	9,220±54	14,000±0	45±2
<i>Aluminium (ppm)</i>	43,433±309	8,733±94	19±1
<i>Iron (ppm)</i>	957±17	2,000±0	17±1
<i>Phosphorus (ppm)</i>	3,333±59	20,667±471	26±0

3.2 Product Yields from HTL of Microalgae, Sludge and Pinewood

From the HTL of microalgae, sludge and pinewood at reaction temperatures of 250, 300 and 350°C for residence times of 5 to 60 minutes, the highest crude yield was obtained for microalgae as shown in Figure 2. The yields for sludge are shown alongside the model in Figure 3 and for pinewood in Figure 4. Crude yields were 10 to 30% for microalgae, 10 to 25% for sludge and under 10% for pinewood. Solid yields were highest for pinewood at 25 to 60%, up to 40% for microalgae and up to 30% for sludge. The maximum gas yield of up to 50% was found for microalgae, while pinewood and sludge had gas yields of up to 30%. For each type of biomass, crude yields were mostly lower at 250°C than at 300 or 350°C. Increasing reaction time over 5 minutes was seen to cause minimum variation in crude yield for most cases, which was also seen for quaternary

mixtures of model compounds [19]. Optimum operation conditions to obtain maximum crude yield for HTL of microalgae were 350°C and 60 minutes. For sludge, optimum reaction conditions for maximum crude yield and efficiency were 350°C and 5 minutes. For pinewood the optimum reaction conditions for maximum crude yield were 350°C and 20 minutes.

Experiments with model compounds showed that the highest solid yields were obtained from carbohydrate and lignin organic feedstocks. As pinewood is composed of the highest carbohydrate and lignin content, the HTL product was expected to have the highest solid yield of the three biomass feedstocks and this was seen in this work. The high solid yield correlates with lower crude yield. Previously, the addition of lignin to experiments with biomass model compounds has been seen to result in lower crude yields compared to when the reactions are conducted without lignin. [19, 38]. This is likely due to the stability of the phenolic compounds which result from the decomposition of lignin in HTL and inhibit the formation of crude [39]. The lower crude yields from pinewood are likely due to the presence of around 20% lignin in the feedstock. The absence of lignin in microalgae could contribute to it producing the highest crude yield of the three biomass feedstocks.

Gas yield generally decreased from 30 to 60 minutes residence time by less than 20%. Solid yield was seen to increase from 30 to 60 minutes residence time by less than 10%. This increase is a result of the recombination reactions that occur during HTL. The crude yield from each source of biomass was not seen to vary by more than 15% at different residence times for each temperature. The highest

crude yield was obtained at the highest reaction temperature for each biomass feedstock. At the same reaction conditions the difference in solid yield between sludge and pinewood was up to 34%, with pinewood having a much higher solid yield. Gas yield varied by up to 42% at the same reaction conditions for the three different types of biomass and crude yield varied by up to 21%. Sludge had the highest lipid content of 18% compared to 4.8% in the microalgae, however the microalgae produced up to 18% more crude. At some reaction conditions crude yield was up to 12% higher for sludge. Pinewood had the lowest lipid content of 2.8% and produced the lowest crude yield at almost all the reaction conditions. These differences in yields are likely dependent on the organic fraction of biomass as well as the catalytic or inhibiting effects of the inorganic fraction of the feedstock.

The fraction of ash in the aqueous phase HTL product was between 55 and 83% of the total ash in the microalgae feedstock used in this work. The ash in the aqueous phase for the HTL product of sludge was 2 to 29% of the total ash in the feedstock and the majority of ash remained in the solid phase. The difference is because the inorganic compounds in microalgae have higher solubility in water than those from the sludge. The higher concentration of phosphorus in the sludge of 20,667 ppm compared to 3,333 ppm in microalgae could be causing greater inhibition in crude formation from sludge. The higher concentration of sodium of 150,333 ppm in microalgae compared to 2,000 ppm in sludge is suspected to be having greater catalytic effects on the production of crude from microalgae as has been found previously [40, 41]. The ash distributed in the HTL product from

pinewood was too small to quantify and the concentrations of metals possibly too low to cause catalytic or inhibitory effects on crude formation.

3.3 Comparisons with Model Compounds

From previous work involving reactions with model compounds alone and in mixtures, the biomass with the highest lipid and protein content is expected to result in the highest crude yield. Model compounds of lipid were found to result in the highest crude product followed by protein, carbohydrate and then lignin. As sludge contains the highest lipid as well as the highest combined lipid and protein content, it is expected to result in the highest crude yield at most reaction conditions. This was not the case, instead the microalgae produced a higher crude yield in most cases. This is most likely due to the more concentrated presence of potassium and sodium salts in the microalgae which have been shown to have a catalytic effect on the production of crude and reduction of solids as discussed above [40, 41].

The yields from biomass compared to the yields predicted from model compounds when reacted alone or in mixtures are shown in Figure 5. The yields from biomass are presented beside the mass-averaged yields from individual experiments with monomer compounds, polymer compounds and mixtures of polymer compounds, all calculated from the composition of the given biomass. In experiments where mixtures of model compounds were made to mimic the organic fractions of the biomass feedstocks used in this work, the product fractions from pinewood most closely matched the model compound mixtures. This is likely due to the low ash content of pinewood and confirms that the ash contents in the microalgae and

sludge are significantly influencing HTL reactions. The mass averaged yields from individually reacted monomer and polymer model compounds vary between 2 and 30% compared to real biomass. This variation is likely partially due to the interactions that occur between different fractions of organic biomass and cause variation in product yields. These interactions have been shown to influence product yields in experiments with binary and quaternary mixtures of model compounds [19]. The differences of up to 26% between the mass averaged yields from individual experiments with polymer compounds and those from the mixture experiments with those same polymer compounds is also evidence of interactions. A factor causing this variation is the reduced number of cross-links that occur between model compounds compared to real biomass. A previous investigation with blackcurrant pomace as the HTL feedstock showed that mixtures of model compound polymers represented the biomass feedstock well, however the blackcurrant pomace also contained only 4.5% ash content by dry weight.

In summary, at the reaction temperature of 350°C and time of 5 minutes, the biomass is not perfectly modelled by monomers and polymers reacted alone or polymers reacted in mixtures. This is due to the interactions between organic fractions of biomass which result in varied chemical reactions, the presence of inorganic contents in the biomass and the different chemical structures of biomass compared to model compounds. However, the model compounds provide valuable insights into the reactions that occur during HTL.

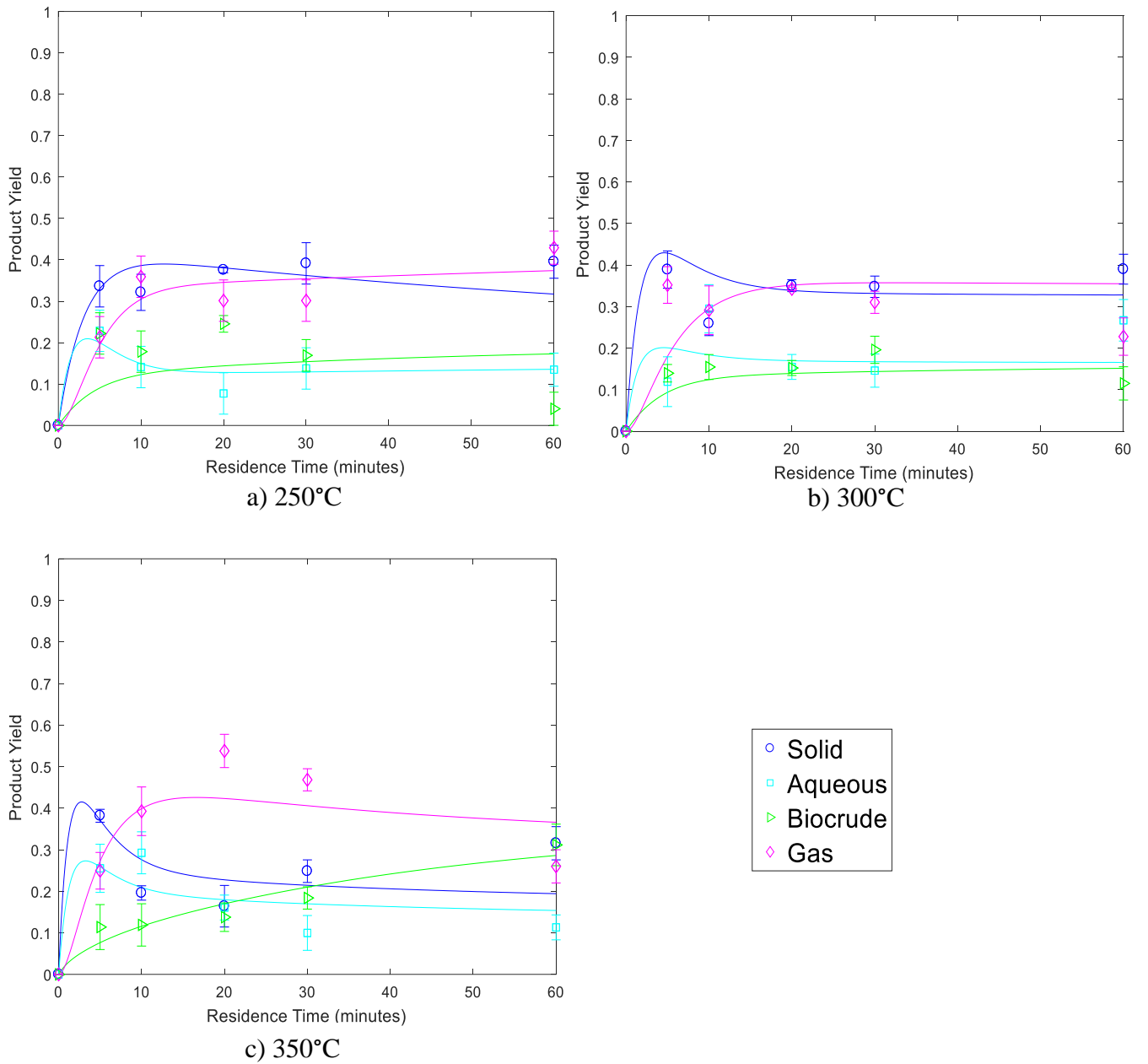


Figure 2. Kinetic model for HTL of *Tetraselmis* sp. microalgae (lines) against experimental data (symbols) with standard deviation given by error bars

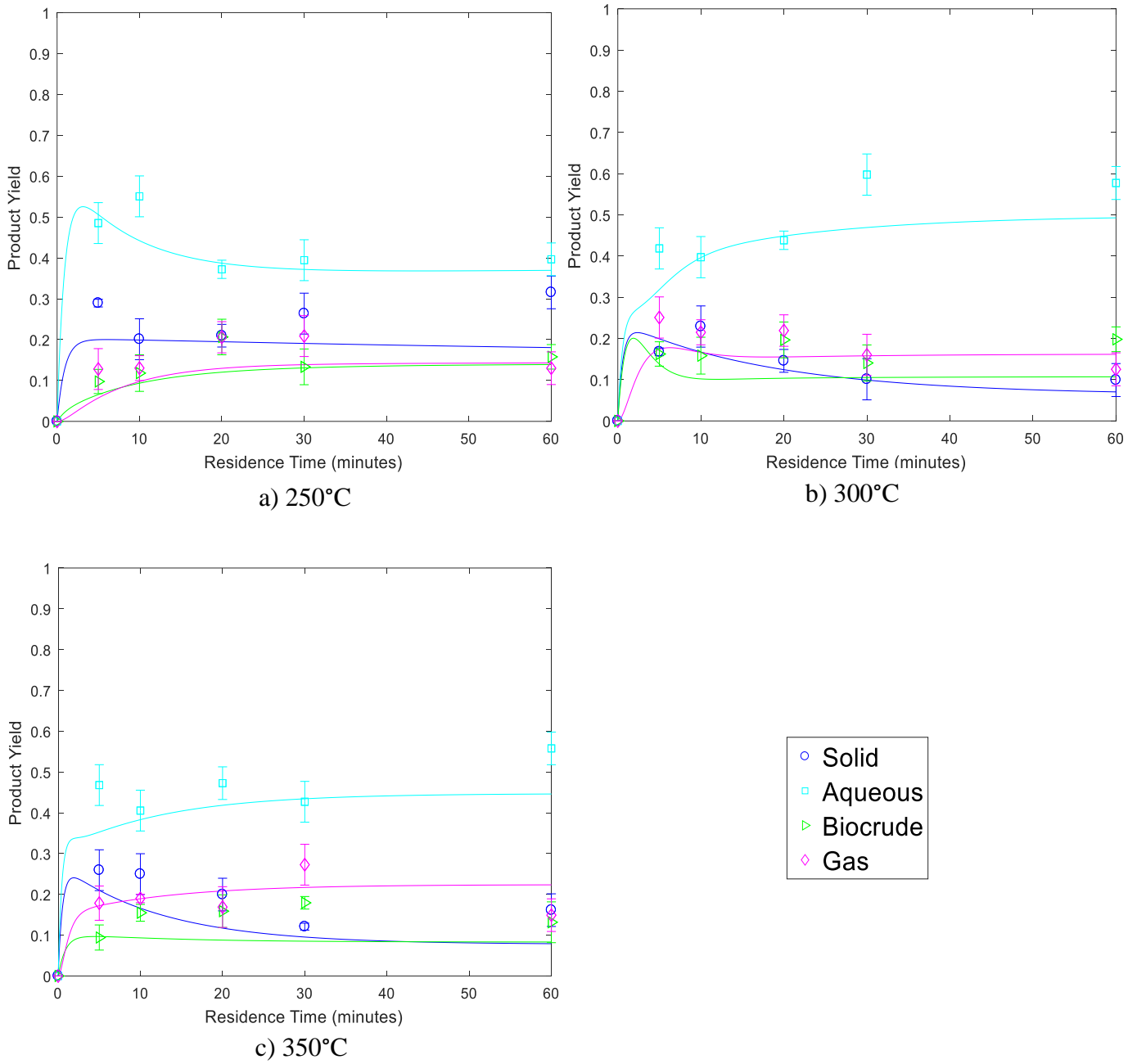


Figure 3. Kinetic model for HTL of sewage sludge (lines) against experimental data (symbols) with standard deviation given by error bars

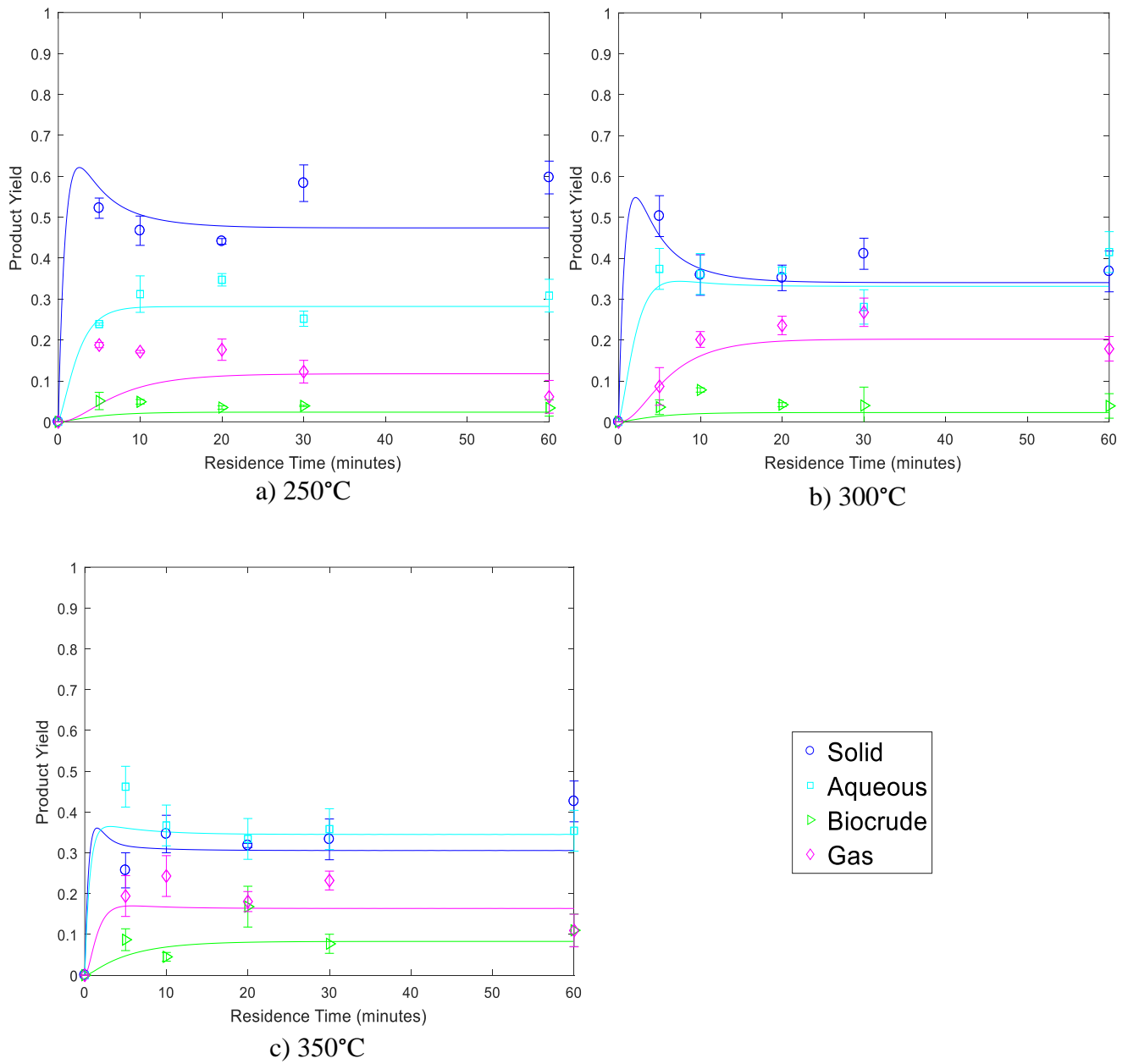
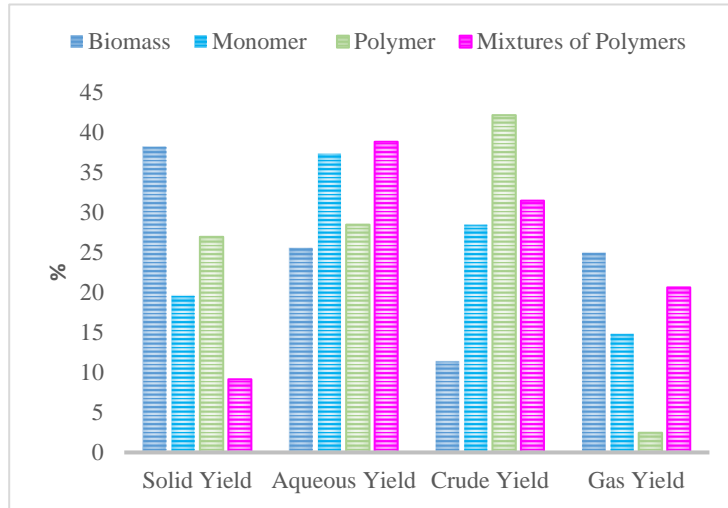
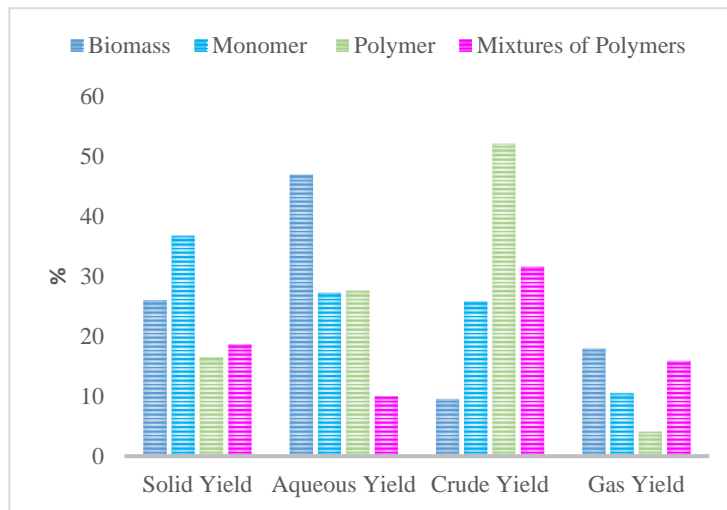


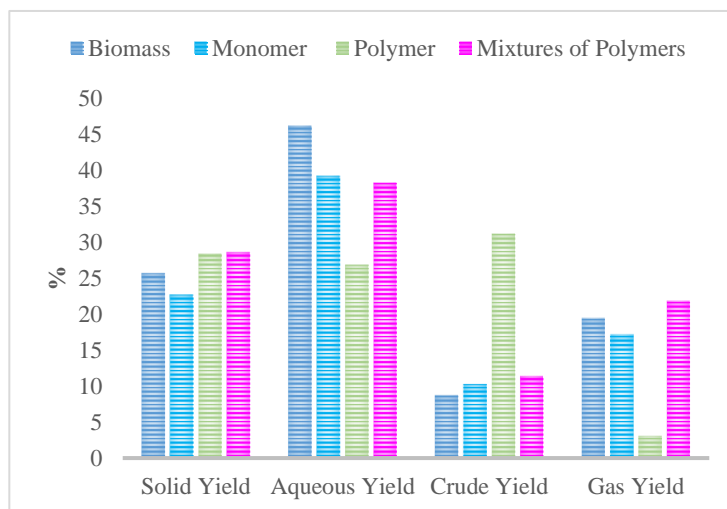
Figure 4. Kinetic model for HTL of Radiate pinewood (lines) against experimental data (symbols) with standard deviation given by error bars



a) Microalgae



b) Sewage Sludge



c) Pinewood

Figure 5: Yields from biomass compared to yield predicted from model compounds when reacted alone or in mixtures at 350°C reaction temperature and 5 minutes reaction time

3.4 Compounds in Crude from HTL of Microalgae, Sludge and Pinewood

GC-MS analysis was conducted on crude produced from the HTL of microalgae, sludge and pinewood. Samples produced at reaction temperatures of 250, 300 and 350°C and a reaction time of 5 minutes were analysed via GC-MS. The compounds identified are listed in the Supporting Information. The percentage of crude identified from GC-MS was 5 to 70% of the total crude extracted with solvent. The compounds identified from GC-MS and their concentrations are presented in the Supporting Information.

From the crude produced from microalgae, phytol compounds, esters, monocyclic aromatic compounds, fatty acids, heterocyclic aromatic compounds and dicarboxylic acids were identified at 250°C. In addition to these, at 300°C sterols, ketones, amides, cyclic dipeptides and ethers were identified. At 350°C even more compounds were identified including pyridine, pyrazine, phenolic compounds, and alkanes. Higher temperatures were found to result in a crude with more varied composition for microalgae. The increase in compounds identified from the crude for microalgae at increasing temperatures indicates conversion of the microalgae is more advanced at higher temperatures at 5 minutes residence time. As expected from experiments with protein model compounds, many nitrogen containing compounds were identified in the crude produced from microalgae due to it having the highest protein content of the three biomass feedstocks [19]. The concentration of esters identified in the crude produced from microalgae increased by approximately four times from the reaction temperature of 250 to 300°C with 5 minutes reaction time. This indicates that these heavier molecular weight

compounds are formed with more severe reaction conditions for HTL of microalgae. The presence of phytol which is a constituent of the untreated microalgae was identified at 250 and 300°C but not at 350°C.

The crude produced from sludge contained phenolic compounds, alkanes, cycloalkenes, ketones, cyclic dipeptides, sterols, furans, fatty acids, esters, pyridines and aromatic heterocyclic compounds. Minimal variation in the compounds identified in the crude produced from sludge at different temperatures was observed. Cholestanol was the highest concentration compound in the crude produced from sludge at 300 and 350°C. This is a cholesterol found in the gut of animals and hence is not unexpected in the crude produced from sludge.

The compounds identified in the crude produced from pinewood included 5-Hydroxymethylfurfural, furans, aldehydes, ketones, phenolic compounds, esters, aldehydes, cycloalkenes, ethers and aromatic compounds. The highest proportion of compounds identified in the pinewood included furans and phenolic compounds. Analysis of the crude from model compounds shows that carbohydrates contribute furans to the crude and lignin contribute many phenolic compounds and this agrees with the results for pinewood which is made up primarily of carbohydrates and lignin. The concentration of 5-Hydroxymethylfurfural was highest at 200 and 300°C but it was not identified at 350°C. Conversion of this compound which results in a higher concentration of other phenolic compounds is evident from the GC-MS results at 350°C and a reaction time of 5 minutes.

The crude produced from each source of biomass contained many different compounds. This is due to the presence of different organic fractions, including lipid, carbohydrate, protein and lignin, in the biomass where each of these fractions contribute specific compounds. Some compounds were identified in the crude from biomass that had not been identified for model compounds. Phytol is obtained by the hydrolysis of chlorophyll, which exist in biomass like microalgae but were not present in model compounds so had not been identified in the crude produced from model compounds. Sterols are another constituent of biomass including plants and animals that were not identified from the model compounds. Sterols are a class of lipids. Cholesterol was also not identified in the crude produced from model compounds because it is an animal by-product that was present in the sludge. Phenolic compounds were the most commonly identified compounds across the three types of feedstocks and identified in all model compound mixtures analysed. The highest concentration of phenolics was present in the pinewood as expected from the high lignin content.

Previous analysis of crude oil via GC-MS has identified mostly nitrogenous compounds from HTL of microalgae and ester, phenolic and nitrogenous compounds from HTL of sludge [2]. Phytol, phenolic and nitrogenous compounds were identified in the crude produced from microalgae by Biller and Ross [42]. Ketones and phenolic compounds were identified in the crude produced from HTL of beech wood by Haarlemmer, et al. [43]. Each of these classes of compounds was also identified in the similar feedstocks used in this work.

The crudes produced from mixtures of model compounds (designed to represent each biomass source) were also analysed via GC-MS. From the microalgae mixture, many fatty acid esters, amides, amines, ketones, phenolic compounds, carboxylic acids, furans and pyrazine were identified. From the sludge mixture, fatty acid esters, alkanes, phenolic compounds and carboxylic acids were identified. The crude produced from the pinewood mixture included phenolic compounds, furans and fatty acid esters.

In the Supporting Information it can be seen that specific compounds identified from biomass and model compound mixtures varied, however most chemical groups were identified in both. The crudes produced from microalgae and the model compound mixture both contained a high quantity of nitrogenous compounds. Fewer compounds were identified in the crude produced from sludge compared to that from the mixture of model compounds. This could be due to the temperature limitations of the GC-MS analysis where high boiling point compounds could not be identified. The crude from pine contained similar compounds to that from the model compound mixture, however fatty acid esters were not identified in the real biomass. The inorganic constituents of biomass and the sources of carbohydrate, lipid, lignin and protein in real biomass can be seen to result in varied compounds identified in the crude, however the chemical groups produced from each organic constituent of biomass are clearly reflected in the data from model compounds.

3.5 Kinetic Models for HTL of Microalgae, Sludge and Pinewood

The results of the kinetic model are shown in Figures 3, 4 and 5. The trends in product yields for product fractions of solid, aqueous, crude and gas are captured by the simplified first order bulk kinetic model. The maximum variation between the model and experimental data was 15%.

Different kinetic rate constants were required to model each type of biomass for the reaction pathways shown in Figure 1 as the interactions between organic and inorganic fractions in the biomass during HTL cause significant variation in product fractions at the same conditions. The parameters from the kinetic model previously developed from mixtures of biomass compounds [19] were also not suitable for modelling the HTL of the microalgae, sludge and pine wood used in experiments. From the experimental results and kinetic modelling, it can be seen that each type of biomass requires its own set of rate constants to model the trends of product yields with varying reaction time and temperature. An example of fitting a model with the same set of rate constants for the three biomass types and varying the initial conditions for each type of biomass at 350°C is shown in Figure 6. The model was developed from the experimental data from the three types of biomass. It does not model the experimental data as accurately as the models generated for each single type of biomass in Figures 3, 4 and 5. The model developed from the combined data for microalgae, sludge and pine deviated by up to 40% from experimental values in Figure 6. This is partly due to the gas yield being up to 40% higher for HTL of microalgae compared to the other two feedstocks. Greater variation in product fractions means different rate constants

are required to model the different feedstocks. As well as this, 8 of the 17 reaction pathways are dependent on feedstock composition, hence dependent on the initial conditions of the model, while the remaining pathways are dependent on interconversion between the different product fractions. Removing the pathways for interconversion between products fractions results in greater error between experimental values and the model as well as the removal of necessary pathways which represent key conversions in HTL.

For some reaction pathways in Table 5 there is a steep increase in the rate constant between two temperatures. This is true for microalgae in the reaction pathways from protein to solid, aqueous to solid and solid to aqueous. For sludge this is seen for lignin to solid and gas to aqueous. In the case of pinewood, this is true for carbohydrate to aqueous, protein to solid, protein to aqueous, lignin to aqueous, aqueous to solid, solid to aqueous and gas to aqueous. For the pathways mentioned here, the rate of conversion from one product to the other is higher at the higher temperature. This indicates that temperature has a significant effect of the reaction pathways between different reactants and products.

Some rate constants are significantly higher than others, indicating that some reaction pathways have a much higher reaction rate relative to others. The pathway with the highest rate constants for microalgae is the aqueous to solid pathway at 300 and 350°C. For sludge, many of the conversion pathways have high rate constants of 60°C/sec at 350°C. This is because there is a significant increase in the reaction rate for these reaction pathways at the highest reaction temperature. For pinewood the highest rate constants are for the pathways from

carbohydrate to solid and lignin to solid at all three temperatures as well as protein to solid at 300 and 350°C. For the solid to aqueous pathway a high reaction rate is present at 350°C. To understand the significance of the relative difference between rate constants, experiments with different feedstocks from the same families of biomass should be conducted. Once these data sets have a model fit to them the rate constants could be compared to see how rate constants vary.

The activation energies for each reaction pathway are seen to vary for each type of biomass in Table 5. Some pathways require much higher activation energies than others particularly in the conversion of microalgae to HTL product where the pathway from renewable crude to aqueous phase is 140kJ/mol higher than that from protein to aqueous phase. Approximating Arrhenius behaviour can be seen to be an oversimplification as shown by some high standard deviations for the Arrhenius parameters in Table 5. The many reactions that occur during HTL which involve depolymerisation of the polymers to monomers, further decomposition via decarboxylation, deamination, dehydration and cleavage, and then recombination of the intermediate products are largely oversimplified by the bulk kinetic model. The lipid, carbohydrate, protein and lignin fractions interact differently in each type of biomass and the different forms of lipid, carbohydrate, protein and lignin result in different reactions, hence different products. This is shown in the variation in Arrhenius parameters for each type of biomass for pathways from lipid, carbohydrate, protein and lignin to solid, aqueous, crude and gas products.

The activation energies for aqueous to solid and solid to aqueous pathways are highest for microalgae compared to pinewood and sludge by up to 126kJ/mol. This is because microalgae produce the lowest quantity of combined solid and aqueous phase product at most reaction conditions. Reaction pathways from solid to crude have higher activation energies than the pathways from crude to solid for microalgae and sludge. This shows the necessity of having a reaction pathway in the model that demonstrates the recombination reactions which convert liquid to solid products. Of the pathways to and from gas phase products, microalgae have the lowest activation energies. This is because microalgae produce the highest yield of gas phase products.

A previous kinetic model for *Tetraselmis* sp. microalgae with a different set of reaction pathways found the highest activation energy for the pathway from aqueous to gas phase and the lowest activation energy for the pathway from protein to aqueous phase [24]. The ash content of the microalgae in their work was found to be 30wt% of the dry weight, which is less than half of the ash content of the microalgae used in this work. From the model derived in this work the path with the highest activation energy was from solid to aqueous phase and the path with the lowest activation energy was from protein to aqueous phase. While the pathway for the lowest activation energy was the same as in this and previous work, the pathway with the highest activation energy was different in this work. This is due to the variation in reaction pathways used in each model. Each of the kinetic models for biomass in literature has varying reaction pathways [23-25]. A recently developed model for the HTL of sewage sludge was presented

by Qian, et al. [44], however their model did not consider lipid, carbohydrate, protein and lignin compositions. The sewage sludge model described here also contained significantly different interconversion pathways. Another reason for variation between models is the variations in the methods used to define product yields in literature.

Table 2 compares some crude yields found in literature to what is predicted by the models produced in this work. Variation is seen to be between 0-33%. Different ash contents is seen to result in different crude yields for different species of microalgae at the same reaction conditions. This suggests that ash contents can affect crude yield. Some of the variation between the modelled and measured results from other works could also be due to the different solvents and separation methods used, different heat-up times and reactor configurations.

Table 2: Crude Yields from Literature Compared to Model

Reference	Feedstock	Ash Content (%)	Temp. (°C)	Time (min)	Literature Yield (%)	Model Prediction (%)	Difference in Yields (%)
Brown, et al. [3]	<i>Nannochloropsis</i> sp.	8	250	60	38	17	21
Brown, et al. [3]	<i>Nannochloropsis</i> sp.	8	300	60	32	15	17
Brown, et al. [3]	<i>Nannochloropsis</i> sp.	8	350	60	43	28	15
Valdez, et al. [4]	<i>Nannochloropsis</i> sp.	6.25	350	60	30	28	2
Biller and Ross [42]	<i>Chlorella vulgaris</i>	7	350	30	38	10	28
Biller and Ross [42]	<i>Spirulina</i>	7.6	350	30	30	20	10
Biller and Ross [42]	<i>Nannochloropsis occulta</i>	26.4	350	30	35	20	15
Biller and Ross [42]	<i>Porphyridium creuntum</i>	24.4	350	30	20	20	0
Vardon, et al. [2]	<i>Spirulina</i> algae	10	300	30	32	11	21
Vardon, et al. [2]	Anaerobic sludge	31	300	30	9.4	10	-0.6
Xu, et al. [45]	Sewage Sludge	36.5	350	10	20	10	10
Anastasakis, et al. [46]	Primary Sewage Sludge	-	350	300	25	<10	15
Feng, et al. [47]	White pine bark	1.07	300	15	35	2	33
Saba, et al. [48]	Loblolly pine	0.4	250	30	9	2	7
Saba, et al. [48]	Loblolly pine	0.4	300	30	10	2	8

Further, the influence of reaction temperature and reaction time on crude yield were analysed in order to determine if the experimental conditions were adequate to evaluate kinetic parameters. This was done using the ANOVA Data Analysis Toolpak in Microsoft Excel. The ANOVA: Two-Factor with Replication function was selected to evaluate the experimental yields for replicates of experiments with

an alpha value of 0.05. Crude yield was used for the statistical analysis because it is the main product of interest for HTL.

The p-value calculated via ANOVA quantifies the variability between the crude yields for one group, temperature, and the variability between the crude yields for the other group, time, relative to how much variability there is within the same group. The p-value calculated via ANOVA is greater than 0.05 for all of the groups except for reaction temperature in the case of pine wood as seen in Table 3. This means that for all of the other groups except for the reaction temperature for pine, the mean crude yields for different temperatures and times were similar. For pinewood, temperature resulted in varied mean values for crude yield. Overall, the variability for crude yield with different reaction temperature and reaction time is adequately captured by the range of experimental conditions selected to build this kinetic model. The ANOVA test also shows that reaction time and reaction temperature are not interacting.

The F-values in Table 4 indicate that reaction temperature has a greater influence on crude yield overall for all of the feedstocks. While the most significant change in the product yields for each feedstock appears in the first 5 minutes for each temperature selected, overall there is greater variation between crude fractions at different reaction temperatures than at different reaction times. This is because the data collected from 10 min up to 60 min at constant temperature follows a steady-state behaviour; the changes in several of the product yields are within the error bars of each experimental point. Future work could include experiments with smaller time steps in the 0-5 minute range to obtain more detailed results.

Table 3: P-values for ANOVA Analysis on Crude Yields

	Microalgae	Sludge	Pine
Reaction Time	0.673	0.909	0.790
Reaction Temperature	0.084	0.627	0.001
Combined Reaction Time and Reaction Temperature	0.958	0.553	0.110

Table 4: F-values for ANOVA Analysis on Crude Yields

	Microalgae	Sludge	Pine
Reaction Time	0.593	0.243	0.423
Reaction Temperature	2.944	0.481	10.664
Combined Reaction Time and Reaction Temperature	0.291	0.882	2.046

An accurate unified kinetic model awaits further development. To further develop the model, reactions with a broader range of feedstocks including different species of microalgae and wood should be used in experiments at the same reaction conditions and their data can be used to vary the kinetic parameters. Sludge collected from various points in the wastewater treatment process from different locations and at different times should also be used in experiments. The effect of inorganics could also be explored by conducting HTL experiments with biomass including different compositions of organic and inorganic content.

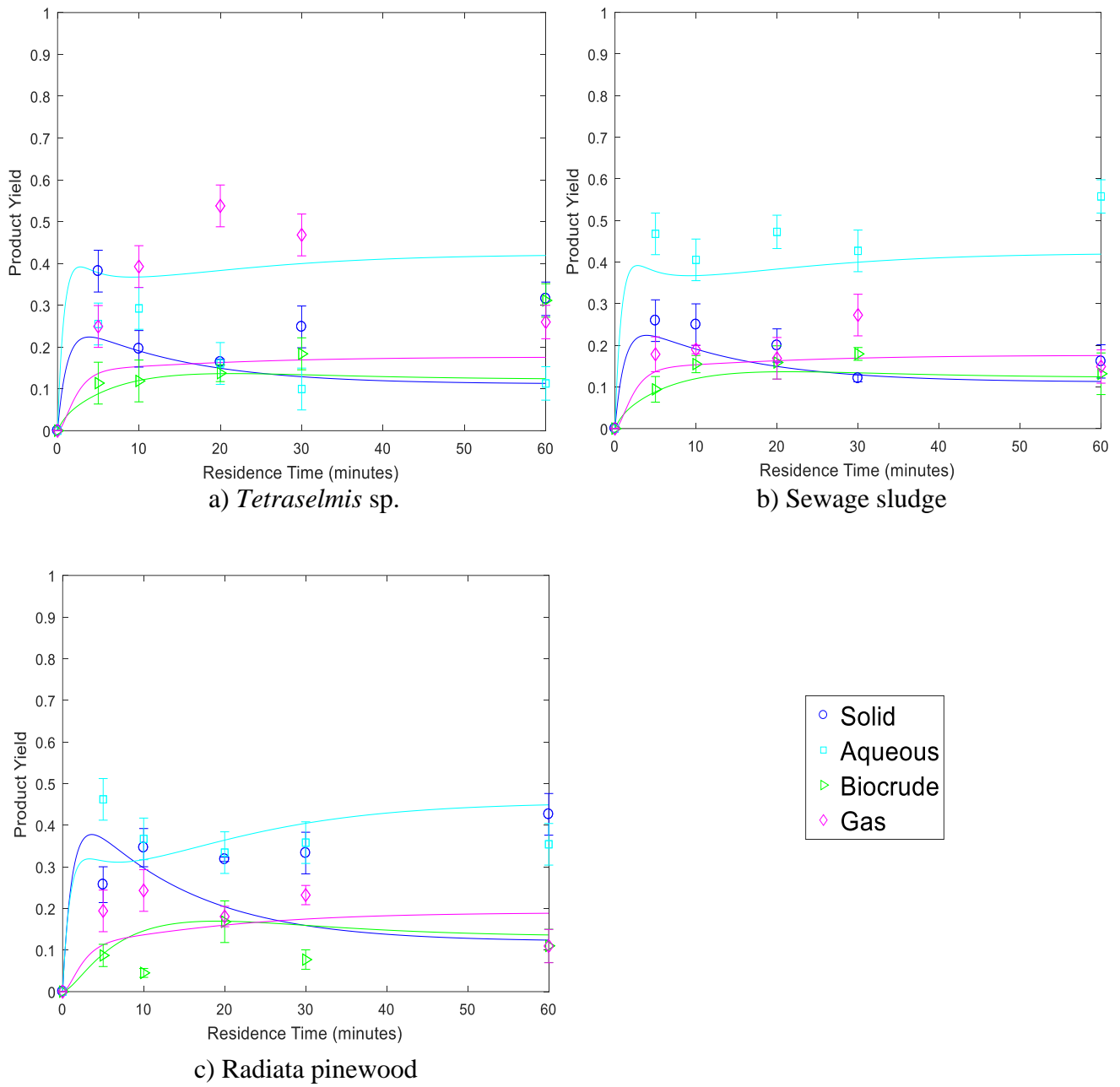


Figure 6. Kinetic model with same parameters, varying initial conditions for HTL at 350°C (lines) against experimental data (symbols) with standard deviation given by error bars

Table 5: Kinetic parameters for monomer model compounds

Compound	Path	Reaction	k[°C](sec ⁻¹)			lnA	E _A (kJ/mol)
			Temperature (°C)				
			250	300	350		
Algae	1	Lipid to Aqueous	0.30	0.30	43.82	28.05±30.9	130.76±25.0
	2	Lipid to renewable crude	14.40	15.0	16.69	3.56±0.5	3.94±0.4
	3	Carbohydrate to solid	13.84	32.85	36.13	8.84±3.9	26.54±3.2
	4	Carbohydrate to aqueous	6.00	6.00	6.55	2.31±0.5	2.31±0.4
	5	Protein to solid	0.30	0.30	28.55	25.53±28.2	119.51±22.9
	6	Protein to aqueous	24.00	24.00	24.26	3.24±0.1	0.28±0.1
	7	Lignin to solid	5.88	5.94	6.00	1.90±0	0.55±0
	8	Lignin to aqueous	5.88	5.94	6.00	1.90±0	0.55±0
	9	Aqueous to solid	0.82	59.39	59.83	27.85±22.3	119.41±18.0
	10	Solid to aqueous	0.30	29.85	47.66	31.60±21.0	140.19±17.0
	11	Renewable crude to aqueous	0.18	0.24	0.30	1.47±0.0	13.85±0.0
	12	Aqueous to renewable crude	0.30	0.30	2.01	9.96±0.1	49.90±0.1
	13	Solid to renewable crude	0.18	0.24	0.30	1.47±0.0	13.85±0.0
	14	Renewable crude to solid	0.30	0.30	0.31	-0.97±0.1	1.03±0.1
	15	Aqueous to gas	16.80	17.70	19.18	3.63±0.23	3.56±0.19
	16	Renewable crude to gas	0.30	0.30	0.31	-0.97±0.1	1.03±0.1
	17	Gas to aqueous	6.14	8.40	8.45	3.90±1.6	8.87±1.29
Sludge	1	Lipid to Aqueous	58.73	59.89	60.00	4.21±0.1	0.59±0.1
	2	Lipid to renewable crude	6.00	7.67	21.00	9.31±5.0	33.25±3.6
	3	Carbohydrate to solid	58.80	59.40	60.00	4.20±5.3	0.55±3.8
	4	Carbohydrate to aqueous	43.55	53.99	60.00	5.80±16.5	8.75±9.9
	5	Protein to solid	30.00	37.45	60.00	7.62±1.8	18.53±1.4
	6	Protein to aqueous	33.30	42.00	45.00	5.4±0.8	8.26±0.6
	7	Lignin to solid	24.00	26.00	60.00	8.61±4.8	24.2±3.9
	8	Lignin to aqueous	42.51	54.00	57.00	5.63±0.9	8.07±0.7
	9	Aqueous to solid	0.18	0.24	0.30	1.47±0.0	13.85±0.0
	10	Solid to aqueous	0.30	0.60	0.96	6.08±0.7	31.60±0.6
	11	Renewable crude to aqueous	3.11	7.24	16.55	11.50±0.7	45.2±0.6
	12	Aqueous to renewable crude	1.18	2.96	3.00	6.27±4.7	26.02±3.8
	13	Solid to renewable crude	0.30	2.56	3.98	15.40±8.4	71.22±6.8
	14	Renewable crude to solid	0.18	0.24	0.30	1.47±0.0	13.85±0.0

Chapter 6 – A kinetic model for the hydrothermal liquefaction of microalgae, sewage sludge and pinewood with product characterisation of renewable crude

	15	Aqueous to gas	1.80	21.70	30.00	18.75±10.9	77.72±8.9
	16	Renewable crude to gas	0.18	0.24	0.30	1.47±0.0	13.85±0.0
	17	Gas to aqueous	4.80	59.40	60.00	18.06±13.0	70.22±10.5
Pinewood	1	Lipid to Aqueous	10.63	30.00	30.60	9.26±5.10	29.38±5.0
	2	Lipid to renewable crude	1.80	2.10	2.20	1.86±0.5	5.46±0.4
	3	Carbohydrate to solid	58.80	59.40	60.00	4.20±0.0	0.55±0.0
	4	Carbohydrate to aqueous	3.00	3.00	43.27	16.76±16.5	70.02±13.4
	5	Protein to solid	2.07	60.00	60.00	22.72±17.5	93.62±14.2
	6	Protein to aqueous	3.00	3.00	58.70	18.55±18.4	78.02±14.9
	7	Lignin to solid	59.83	60.00	60.00	4.12±0.0	0.08±0.0
	8	Lignin to aqueous	3.00	3.00	32.56	15.1±14.8	62.56±12.0
	9	Aqueous to solid	16.80	17.42	51.08	9.37±6.48	29.2±5.2
	10	Solid to aqueous	10.14	17.26	59.95	13.1±4.9	47.45±4.0
	11	Renewable crude to aqueous	0.30	0.30	0.37	-0.04±1.2	5.22±1.0
	12	Aqueous to renewable crude	0.30	0.35	2.18	10.53±10.6	52.54±8.6
	13	Solid to renewable crude	0.18	0.24	0.30	1.47±0.0	13.85±0.0
	14	Renewable crude to solid	9.00	9.00	9.52	2.52±0.3	1.46±0.3
	15	Aqueous to gas	4.48	6.80	28.37	12.61±6.7	49.11±5.41
	16	Renewable crude to gas	0.18	0.24	0.30	1.47±0.0	13.85±0.0
	17	Gas to aqueous	10.80	11.16	59.99	12.46±10.2	45.03±8.3

3 Conclusions

Each of the *Tetraselmis* sp. microalgae, sewage sludge and Radiata pinewood feedstocks contains variable organic and inorganic fractions that result in different product yields where crude yields were 10 to 30% for microalgae, 10 to 25% for sludge and under 10% for pinewood. Analysis of the crude indicated that each biomass feedstock produced a crude which contained different types of compounds. The microalgae produced a crude which was high in nitrogenous compounds, while esters, aromatic compounds and phenolic compounds were identified in the crude produced from all three types of biomass. The product yields from microalgae and sludge biomass varied by up to 42% compared to what was expected from model compounds and the inorganic content in the biomass is suspected to be a major cause for this. The inorganic fractions of biomass have been seen to catalyse and inhibit the production of crude depending on its composition. The inorganics in the sludge are seen to inhibit crude formation while the inorganics in the microalgae appear to be catalysing the formation of crude for the feedstocks used in this work. A kinetic model was further developed to describe the reaction products of the three types of biomass. Each type of biomass required different reaction parameters for the set of reaction pathways due to the high variability in product fractions, depending on both the organic and inorganic content of the biomass feedstock. The kinetic model shows the trends of product fractions for each type of biomass with time and temperature and is able to predict product fractions from experiments with less than 15% error.

To further develop the model for other biomass types and reaction variables, reactions with these other biomass feedstocks should be conducted.

Acknowledgements

The authors acknowledge the financial support of the Australian Research Council's Linkage Project grant (LP150101241) and our industry partner Southern Oil Refining Pty Ltd.

References

- [1] A. Kruse, E. Dinjus, Hot compressed water as reaction medium and reactant: 2. Degradation reactions, *The Journal of Supercritical Fluids* 41 (2007) 361-379.
- [2] D.R. Vardon, B.K. Sharma, J. Scott, G. Yu, Z. Wang, L. Schideman, Y. Zhang, T.J. Strathmann, Chemical properties of biocrude oil from the hydrothermal liquefaction of *Spirulina* algae, swine manure, and digested anaerobic sludge, *Bioresource Technology* 102 (2011) 8295-8303.
- [3] T.M. Brown, P. Duan, P.E. Savage, Hydrothermal Liquefaction and Gasification of *Nannochloropsis* sp, *Energy & Fuels* 24 (2010) 3639-3646.
- [4] P.J. Valdez, J.G. Dickinson, P.E. Savage, Characterization of Product Fractions from Hydrothermal Liquefaction of *Nannochloropsis* sp. and the Influence of Solvents, *Energy & Fuels* 25 (2011) 3235-3243.
- [5] J.L. Faeth, P.J. Valdez, P.E. Savage, Fast Hydrothermal Liquefaction of *Nannochloropsis* sp. To Produce Biocrude, *Energy & Fuels* 27 (2013) 1391-1398.
- [6] P.J. Valdez, M.C. Nelson, H.Y. Wang, X.N. Lin, P.E. Savage, Hydrothermal liquefaction of *Nannochloropsis* sp.: Systematic study of process variables and analysis of the product fractions, *Biomass and Bioenergy* 46 (2012) 317-331.
- [7] C. Tian, B. Li, Z. Liu, Y. Zhang, H. Lu, Hydrothermal liquefaction for algal biorefinery: A critical review, *Renewable and Sustainable Energy Reviews* 38 (2014) 933-950.
- [8] I. Morris, H.E. Glover, C.S. Yentsch, Products of photosynthesis by marine phytoplankton: the effect of environmental factors on the relative rates of protein synthesis, *Marine Biology* 27 (1974) 1-9.
- [9] J. Fábregas, A. Maseda, A. Domínguez, A. Otero, The cell composition of *Nannochloropsis* sp. changes under different irradiances in semicontinuous culture, *World Journal of Microbiology and Biotechnology* 20 (2004) 31-35.
- [10] H.-j. Huang, X.-z. Yuan, H.-n. Zhu, H. Li, Y. Liu, X.-l. Wang, G.-m. Zeng, Comparative studies of thermochemical liquefaction characteristics of microalgae, lignocellulosic biomass and sewage sludge, *Energy* 56 (2013) 52-60.
- [11] G. Li, F. Zhang, Y. Sun, J.W.C. Wong, M. Fang, Chemical Evaluation of Sewage Sludge Composting as a Mature Indicator for Composting Process, *Water, Air, and Soil Pollution* 132 (2001) 333-345.

- [12] R. Obeid, D. Lewis, N. Smith, P. van Eyk, The elucidation of reaction kinetics for hydrothermal liquefaction of model macromolecules, *Chemical Engineering Journal* 370 (2019) 637-645.
- [13] K.R. Arturi, S. Kucheryavskiy, E.G. Søgaaard, Performance of hydrothermal liquefaction (HTL) of biomass by multivariate data analysis, *Fuel Processing Technology* 150 (2016) 94-103.
- [14] Zhang, M. von Keitz, K. Valentas, Thermal Effects on Hydrothermal Biomass Liquefaction, in: W.S. Adney, J.D. McMillan, J. Mielenz, K.T. Klasson (Eds.) *Biotechnology for Fuels and Chemicals*, Humana Press, Totowa, NJ, 2008, pp. 511-518.
- [15] P.S. Christensen, G. Peng, F. Vogel, B.B. Iversen, Hydrothermal Liquefaction of the Microalgae *Phaeodactylum tricorutum*: Impact of Reaction Conditions on Product and Elemental Distribution, *Energy & Fuels* 28 (2014) 5792-5803.
- [16] K. Anastasakis, A.B. Ross, Hydrothermal liquefaction of the brown macro-alga *Laminaria Saccharina*: Effect of reaction conditions on product distribution and composition, *Bioresource Technology* 102 (2011) 4876-4883.
- [17] L.E. Sommers, D.W. Nelson, K.J. Yost, Variable Nature of Chemical Composition of Sewage Sludges¹, *Journal of Environmental Quality* 5 (1976) 303-306.
- [18] S.S. Toor, L. Rosendahl, A. Rudolf, Hydrothermal liquefaction of biomass: A review of subcritical water technologies, *Energy* 36 (2011) 2328-2342.
- [19] R. Obeid, D.M. Lewis, N. Smith, T. Hall, P. van Eyk, Reaction Kinetics and Characterization of Species in Renewable Crude from Hydrothermal Liquefaction of Mixtures of Polymer Compounds To Represent Organic Fractions of Biomass Feedstocks, *Energy & Fuels* 34 (2020) 419-429.
- [20] R. Obeid, D.M. Lewis, N. Smith, T. Hall, P. van Eyk, Reaction kinetics and characterisation of species in renewable crude from hydrothermal liquefaction of monomers to represent organic fractions of biomass feedstocks, *Chemical Engineering Journal* (2020) 1385-8947.
- [21] L. Sheng, X. Wang, X. Yang, Prediction model of biocrude yield and nitrogen heterocyclic compounds analysis by hydrothermal liquefaction of microalgae with model compounds, *Bioresource Technology* 247 (2018) 14-20.
- [22] J. Yang, Q. He, K. Corscadden, H. Niu, J. Lin, T. Astatkie, Advanced models for the prediction of product yield in hydrothermal liquefaction via a mixture design of biomass model components coupled with process variables, *Applied Energy* 233-234 (2019) 906-915.
- [23] D.C. Hietala, J.L. Faeth, P.E. Savage, A quantitative kinetic model for the fast and isothermal hydrothermal liquefaction of *Nannochloropsis* sp, *Bioresource Technology* 214 (2016) 102-111.
- [24] T.K. Vo, S.-S. Kim, H.V. Ly, E.Y. Lee, C.-G. Lee, J. Kim, A general reaction network and kinetic model of the hydrothermal liquefaction of microalgae *Tetraselmis* sp, *Bioresource Technology* 241 (2017) 610-619.
- [25] Sheehan, Savage, Modeling the effects of microalga biochemical content on the kinetics and biocrude yields from hydrothermal liquefaction, *Bioresource Technology* 239 (2017) 144-150.

- [26] P.J. Valdez, V.J. Tocco, P.E. Savage, A general kinetic model for the hydrothermal liquefaction of microalgae, *Bioresource Technology* 163 (2014) 123-127.
- [27] S. Fon Sing, A. Isdepsky, M.A. Borowitzka, D.M. Lewis, Pilot-scale continuous recycling of growth medium for the mass culture of a halotolerant *Tetraselmis* sp. in raceway ponds under increasing salinity: A novel protocol for commercial microalgal biomass production, *Bioresource Technology* 161 (2014) 47-54.
- [28] S.F. Sing, A. Isdepsky, M. Borowitzka, D. Lewis, Pilot-scale continuous recycling of growth medium for the mass culture of a halotolerant *Tetraselmis* sp. in raceway ponds under increasing salinity: a novel protocol for commercial microalgal biomass production, *Bioresource technology* 161 (2014) 47-54.
- [29] E.G. Bligh, W.J. Dyer, A rapid method of total lipid extraction and purification, *Canadian Journal of Biochemistry and Physiology* 37 (1959) 911-917.
- [30] M. Dubois, K.A. Gilles, J.K. Hamilton, P.t. Rebers, F. Smith, Colorimetric method for determination of sugars and related substances, *Analytical chemistry* 28 (1956) 350-356.
- [31] W.J. Barnes, C.T. Anderson, Acetyl Bromide Soluble Lignin (ABSL) Assay for Total Lignin Quantification from Plant Biomass, *Bio-protocol* 7 (2017) e2149.
- [32] B.G. Keiller, R. Muhlack, R.A. Burton, P.J. van Eyk, Biochemical Compositional Analysis and Kinetic Modeling of Hydrothermal Carbonization of Australian Saltbush, *Energy & Fuels* 33 (2019) 12469-12479.
- [33] A. Sluiter, B. Hames, R. Ruiz, C. Scarlata, J. Sluiter, D. Templeton, Determination of ash in biomass, *National Renewable Energy Laboratory* (2008).
- [34] S.O. Lourenço, E. Barbarino, P.L. Lavín, U.M. Lanfer Marquez, E. Aidar, Distribution of intracellular nitrogen in marine microalgae: Calculation of new nitrogen-to-protein conversion factors, *European Journal of Phycology* 39 (2004) 17-32.
- [35] U.E.P.A. US Environmental Protection Agency, SW-846 Test Method 3052: Microwave Assisted Acid Digestion of Siliceous and Organically Based Matrices, Washington, DC, 1996.
- [36] R. Obeid, D.M. Lewis, N. Smith, T. Hall, P. van Eyk, Reaction kinetics and characterisation of species in renewable crude from hydrothermal liquefaction of monomers to represent organic fractions of biomass feedstocks, *Chemical Engineering Journal* 389 (2020) 124397.
- [37] D.J. Lane, M. Zevenhoven, P.J. Ashman, P.J. van Eyk, M. Hupa, R. de Nys, D.M. Lewis, Algal Biomass: Occurrence of the Main Inorganic Elements and Simulation of Ash Interactions with Bed Material, *Energy & Fuels* 28 (2014) 4622-4632.
- [38] M. Déniel, G. Haarlemmer, A. Roubaud, E. Weiss-Hortala, J. Fages, Modelling and Predictive Study of Hydrothermal Liquefaction: Application to Food Processing Residues, *Waste and Biomass Valorization* 8 (2017) 2087-2107.
- [39] F. Jin, J. Cao, H. Kishida, T. Moriya, H. Enomoto, Impact of phenolic compounds on hydrothermal oxidation of cellulose, *Carbohydrate research* 342 (2007) 1129-1132.

- [40] S. Karagöz, T. Bhaskar, A. Muto, Y. Sakata, T. Oshiki, T. Kishimoto, Low-temperature catalytic hydrothermal treatment of wood biomass: analysis of liquid products, *Chemical Engineering Journal* 108 (2005) 127-137.
- [41] A. Hammerschmidt, N. Boukis, E. Hauer, U. Galla, E. Dinjus, B. Hitzmann, T. Larsen, S.D. Nygaard, Catalytic conversion of waste biomass by hydrothermal treatment, *Fuel* 90 (2011) 555-562.
- [42] P. Biller, A.B. Ross, Potential yields and properties of oil from the hydrothermal liquefaction of microalgae with different biochemical content, *Bioresource Technology* 102 (2011) 215-225.
- [43] G. Haarlemmer, C. Guizani, S. Anouti, M. Déniel, A. Roubaud, S. Valin, Analysis and comparison of bio-oils obtained by hydrothermal liquefaction and fast pyrolysis of beech wood, *Fuel* 174 (2016) 180-188.
- [44] L. Qian, S. Wang, P.E. Savage, Fast and isothermal hydrothermal liquefaction of sludge at different severities: Reaction products, pathways, and kinetics, *Applied Energy* 260 (2020) 114312.
- [45] D. Xu, G. Lin, L. Liu, Y. Wang, Z. Jing, S. Wang, Comprehensive evaluation on product characteristics of fast hydrothermal liquefaction of sewage sludge at different temperatures, *Energy* 159 (2018) 686-695.
- [46] K. Anastasakis, P. Biller, R.B. Madsen, M. Glasius, I.J.E. Johannsen, Continuous hydrothermal liquefaction of biomass in a novel pilot plant with heat recovery and hydraulic oscillation, *11* (2018) 2695.
- [47] S. Feng, Z. Yuan, M. Leitch, C.C. Xu, Hydrothermal liquefaction of barks into bio-crude – Effects of species and ash content/composition, *Fuel* 116 (2014) 214-220.
- [48] A. Saba, B. Lopez, J.G. Lynam, M.T.J.A.o. Reza, Hydrothermal liquefaction of loblolly pine: effects of various wastes on produced biocrude, *3* (2018) 3051-3059.

Supporting Information

Reaction kinetics and product characterisation of renewable crude from hydrothermal liquefaction microalgae, sewage sludge and pinewood

Reem Obeid^a, Neil Smith^a, David Lewis^a, Tony Hall^b and Philip van Eyk^{a*}

^a School of Chemical Engineering, The University of Adelaide, Adelaide, South Australia 5005, Australia

^b Faculty of Sciences, The University of Adelaide, Adelaide, South Australia 5005, Australia

*E-mail: philip.vaneyk@adelaide.edu.au.

Microalgae 250°C, 5 minutes

Retention Time (minutes)	AREA	ug/mL (ppm)	Compound
3.00	11728380	9.96	Propanoic acid, 2,2-dimethyl-, 2-ethylhexyl ester
16.33	9024687	7.66	Neophytadiene
18.98	4141930	3.52	Phytol
17.43	2552883	2.17	Isophytol
16.26	2089182	1.77	Cyclopropane, 1-(2-methylbutyl)-1-(1-methylpropyl)-
2.72	2000277	1.70	1-Benzylcyclopentanol-1
16.58	1852113	1.57	Neophytadiene
21.99	1230871	1.04	Butyl 9-tetradecenoate
17.22	1144683	0.97	Docosanoic acid, methyl ester
20.27	785305	0.67	Methyl 2-hydroxy-eicosanoate
18.33	736829	0.63	Methyl 7,10,13,16-docosatetraenoate
14.60	553001	0.47	3,7,11-Trimethyl-2,4-dodecadiene
19.08	482801	0.41	4-Methyl-2-(3,7,11-trimethyldodecyl)thiophene
20.00	425770	0.36	Cyclobarbital
19.61	386036	0.33	Succinic acid, cyclohexylmethyl 2-ethoxyethyl ester
18.87	376547	0.32	Cyclobarbital
15.80	334074	0.28	Docosanoic acid, docosyl ester

Microalgae 300°C, 5 minutes

Retention Time (minutes)	AREA	ug/mL (ppm)	Compound
27.25	44857852	38.08	Ergost-5-en-3-ol, (3.Beta)-
16.39	40018636	33.97	Chloracetic acid, tetradecyl ester
17.49	22586302	19.17	L-Pyroline, N-valeryl-, butyl ester
16.27	16491196	14.00	Cyclobutanone, 2,3,3,4-tetramethyl-
17.53	15384389	13.06	Pyrrolo[1,2-A]pyrazine-1,4-dione, hexahydro-3-(2-methylpropyl)-
17.38	15258057	12.95	L-Pyroline, N-valeryl-, butyl ester
16.53	14923613	12.67	Octahydro-2H-pyrido(1,2-A)pyrimidin-2-one
17.43	14260148	12.11	Docosyl octyl ether
20.92	13602860	11.55	Cyclo-(L-leucyl-L-phenylalanyl)
19.62	13256112	11.25	Hexadecanamide
17.33	12824016	10.89	2,5-Piperazinedeione, 3-6-bis(2-methylpropyl)-
16.77	11226488	9.53	Phytol tetradecanoate
21.05	9448302	8.02	Pyrrolo[1,2-A]pyrazine-1,4-dione, hexahydro-3-(phenylmethyl)-
17.22	7474845	6.35	Tetradecanoic acid, 10,13-dimethyl-,methyl ester

18.99	7379805	6.26	Phytol
20.41	6675431	5.67	2,5-Piperazinedione, 3-benzyl-6-isopropyl-
20.12	6431109	5.46	2,5-Piperazinedione, 3-benzyl-6-isopropyl-
20.56	4785197	4.06	Glycidyl palimate

Microalgae 350°C, 5 minutes

Retention Time (minutes)	AREA	ug/mL (ppm)	Compound
19.91	67256600	57.09	Myristamide, N-methyl-
16.39	52565192	44.62	Chloracetic acid, tetradecyl ester
16.27	43826228	37.20	Chloracetic acid, tetradecyl ester
2.52	42666528	36.22	Pyridine
22.22	38003216	32.26	Octadecanoic acid, morpholide
19.62	35357072	30.01	Hexadecanamide
21.39	29349080	24.91	Octadecanamide, N-butyl-
21.43	26511982	22.51	Myristamide, N-methyl-
25.43	21817572	18.52	Cholest-4-ene
20.25	20706726	17.58	Dodecanamide, N-ethyl-
25.51	18073746	15.34	Lithocholic acid, methyl ester, methyl ether
21.74	17955822	15.24	9-Octadecanamide, N,N-dimethyl-
21.18	16775347	14.24	9-Octadecanamide
22.83	16720172	14.19	13-Cyclopentyl tridecanoic acid, pyrrolidide
23.58	13766171	11.69	Oleic diethanolamide
8.54	13145500	11.16	2H-Pyran-2-one, tetrahydro-6-octyl-
7.00	13056215	11.08	P-Creosol
5.58	12500968	10.61	Phenol
16.15	12224437	10.38	Chloracetic acid, tetradecyl ester
17.85	11687582	9.92	9H-Pyridio[3,4-B]indole, 1-methyl-
8.34	11648019	9.89	Phenol, 4-ethyl-
7.20	11363383	9.65	2-Cyclopenten-1-one, 2-hydroxy-3,4-dimethyl-
16.03	11314815	9.60	Hentriacontane
16.99	10869006	9.23	Eiconsen-1-ol, cis-9-
3.01	10710112	9.09	Propanoic acid, 2,2-dimethyl-, 2-ethylhexyl ester
25.35	10597009	9.00	Phthalic acid, methyl 3-phenylethyl ester
25.83	9829909	8.34	Sigmast-5-en-3-ol, oleate
20.22	9673116	8.21	Dodecanamide, N-ethyl-
12.83	9249809	7.85	Benzenebutanal
11.40	9105433	7.73	Indolizine, 3-methyl

16.62	8595394	7.30	Cyclohexanecarboxylic acid, 4-butyl-, 4-cyanophenyl ester, tra
6.36	8250767	7.00	2-Cyclopenten-1-one, 2,3-dimethyl-
15.80	7968169	6.76	3-Methyl-2-(2-oxopropyl)furan
11.18	7178168	6.09	N-[2-hydroxyethyl]succinimide
7.41	7038140	5.97	Piperazine, 2,5-dimethyl-
21.59	6728754	5.71	Myristamide, N-methyl-
5.84	6308296	5.35	Pyrazine, 2-ethyl-5-methyl-
12.57	5898558	5.01	2,4,6-Trimethylbenzotirile
16.19	5755222	4.89	Chloracetic acid, tetradecyl ester
7.81	5665348	4.81	Neopentyl glycol
17.22	5223148	4.43	Tetradecanoic acid, 10,13-dimethyl-, methyl ester
10.17	5114670	4.34	Indole
21.14	5007846	4.25	9-Octadecenamide
9.65	4897026	4.16	N-(but-1-enyl)-pyrrolidin-2-one
4.52	4580131	3.89	1,3-Phenylenediamine
8.89	4518722	3.84	2-Acetyl-5-methylthiophene
5.78	4501289	3.82	1H-Purine-6-methanol, 6,7-dihydro-
21.01	4429919	3.76	Myristamide, N-propyl-
23.52	4389176	3.73	Cyclohexane, 1-(4-morpholoyl)-4-pentyl-
3.36	4320622	3.67	Pyrazine, methyl-
16.33	4193115	3.56	Neophytadiene
15.20	4119794	3.50	Cyclopropane, 1-(1-methylethyl)-2-nonyl-

Sludge 250°C, 5 minutes

Retention Time (minutes)	AREA	ug/mL (ppm)	Compound
7.15	6328869	5.37	Phenol, 2-methoxy-
3.00	4481290	3.80	Nonane, 4-5-dimethyl-
8.66	2251109	1.91	Creosol
9.84	1148251	0.97	Phenyl, 4-ethyl-2-methoxy-
4.45	1050513	0.89	Cyclopentene, 1,2,3-trimethyl-
6.39	600529	0.51	2-Cyclopenten-1-one, 2-3-dimethyl-
11.03	580944	0.49	3-Methoxytyrosine

Sludge 300°C, 5 minutes

Retention Time (minutes)	AREA	ug/mL (ppm)	Compound
26.38	350909248	297.88	Cholestanol
26.90	178417488	151.46	Cholestanol
17.41	149296304	126.73	2,5-Piperazinedione, 3,6-bis(2-methylpropyl)-
24.84	89516040	75.99	Cholest-2-ene, (5alpha)-
20.97	84624888	71.84	Cyclo-(L-leucyl-L-phenylalanyl)
27.81	81465248	69.15	Stigmasterol
16.58	79239112	67.26	Pyrrolidine, 1-(1-oxobutyl)-
27.67	76621744	65.04	3-Methyl-2-(2-oxopropyl)furan
27.57	74098120	62.90	Stigmastanol
26.67	70228984	59.62	Cholestanol
27.94	69457528	58.96	Lanosterol
16.40	60131228	51.04	Pyrrolidine, 1-(1-oxopentadecyl)-
25.13	59997224	50.93	Sigmasterol
7.14	57852224	49.11	Phenol, 2-methoxy-
15.47	56867500	48.27	2,5-Piperazinedione, 3-methyl-6-(1-methylethyl)-
15.66	56085836	47.61	Benzenepropanoic acid, 2-propenyl ester
27.54	51194920	43.46	Obtusifoliol
11.01	50998044	43.29	Phenol, 2-methoxy-4-propyl-
26.08	47411140	40.25	1-Hexyl-2-nitrocyclohexane
15.57	46424384	39.41	Phenol, 4-(1,1-dimethylpropyl)-
15.37	46347024	39.34	Benzestrol
10.81	43555648	36.97	Phenol, 2,6-dimethoxy-
21.15	43404300	36.85	Cyclo-(L-leucyl-L-phenylalanyl)
9.83	40666044	34.52	Phenol, 4-ethyl-2-methoxy-

Sludge 350°C, 5 minutes

Retention Time (minutes)	AREA	ug/mL (ppm)	Compound
24.80	116574496	98.96	Cholest-2-ene, (5 α)-
26.37	88131656	74.81	Cholestanol
26.89	75859320	64.40	Cholestan-3-one
24.43	60417464	51.29	Cholest-4-ene
24.72	37138188	31.53	Cholest-4-ene
17.31	31442932	26.69	2,5-Piperazinedione, 3,6-bis(2-methylpropyl)-
26.66	25719630	21.83	Cholestan-3-ol
25.72	25451202	21.61	Lithocholic acid, methyl ester, methyl ether
16.35	25298884	21.48	3-Diisopropylpiperazin-2,5-dione
15.65	20432886	17.35	Phthalic acid, ethyl 2-phenylethyl ester
16.54	18100672	15.37	Pyrrolidine, 1-(1-oxobutyl)-
17.38	12859237	10.92	L-Proline, N-valeryl-, heptadecyl ester
11.01	10015643	8.50	Phenol, 2-methoxy-4-propyl-
6.99	8537952	7.25	P-Cresol
10.81	6407149	5.44	Phenol, 2,6-dimethoxy-
7.14	6375262	5.41	Phenol, 2-methoxy-
10.17	5856541	4.97	Indole
9.83	5348149	4.54	Phenol, 4-ethyl-2-methoxy-
6.22	5298466	4.50	2-Tert-butyl-3,4,5,6-tetrahydropyridine
8.33	5021791	4.26	Phenol, 2-ethyl-
7.17	4653258	3.95	2,5-Pyrrolidinedione, 1-methyl-

Pinewood 250°C, 5 minutes

Retention Time (minutes)	AREA	ug/mL (ppm)	Compound
9.25	353920704	300.44	5-Hydroxymethylfurfural
15.42	152522032	129.47	Coniferyl aldehyde
3.46	136522976	115.89	Furyl hydroxymethyl ketone
11.49	129775840	110.16	Vanillin
14.44	61367088	52.09	Benzenepropanol, 4-hydroxy-3-methoxy
12.20	47845692	40.62	Phenol, 2-methoxy-4-propyl-
25.24	31123742	26.42	Carinol
19.67	29760908	25.26	3-Keto-isosteviol
13.04	28377272	24.09	2-Propanone, 1-(4-hydroxy-3-methoxyphenyl)-
5.25	26451822	22.45	2-Furancarboxaldehyde, 5-methyl-
13.73	23782868	20.19	Butyrovanillone
19.61	21713750	18.43	2-Heptenoic acid, hex-4-yn-3-yl ester
7.14	20638726	17.52	Phenol, 2-methoxy-
6.19	18181704	15.43	2-Ethyl-5-propylcyclopentanone
10.23	17784850	15.10	5-Acetoxyethyl-2-furaldehyde
12.11	16477545	13.99	Phenol, 2-methoxy-4-(1-propenyl)-
15.29	15765030	13.38	2-Propanone, 1-(4-hydroxy-3-methoxyphenyl)-
10.35	13927410	11.82	2-Methoxy-4-vinylphenol
21.04	12999122	11.03	Methyl dehydroabietate
18.16	12290942	10.43	Phthalic acid, pentyl 1-phenylpropyl ester
12.79	10170997	8.63	5-Butyl-5-ethylheptadecane
10.88	7460640	6.33	Phenol, 2-methoxy-3-(2-propenyl)-
9.42	7456056	6.33	Benzene, 1,3-bis(1,1-dimethylethyl)-
4.50	6701655	5.69	4(1H)-Pyridone
6.34	6530158	5.54	2-Acetyl-5-methylfuran
4.71	5872043	4.98	4-Butyl-1,3-thiazole
12.56	5358935	4.55	Apocynin
11.55	4760908	4.04	Phenol, 2-methoxy-4-(1-propenyl)-
7.09	4755504	4.04	2-Furoic acid, tridec-2-ynyl ester
11.90	4340984	3.68	3H-Indazol-3-one, 1-ethyl-1,2-dihydro-
7.02	4318332	3.67	Orcinol
6.78	3904067	3.31	Cyclohexene, 1-methyl-3-(1-methylethyl)-

Pinewood 300°C, 5 minutes

Retention Time (minutes)	AREA	ug/mL (ppm)	Compound
9.29	579723584	492.12	5-Hydroxymethylfurfural
11.50	194371488	165.00	Vanillin
3.45	177898304	151.01	Furfural
15.42	152226992	129.22	Coniferyl aldehyde
14.45	125121344	106.21	Benzenepropanol, 4-hydroxy-3-methoxy-
12.20	67900976	57.64	Phenol, 2-methoxy-4-propyl-
5.24	62057096	52.68	2-Furancarboxaldehyde, 5-methyl-
13.05	60475304	51.34	2-Propanone, 1-(4-hydroxy-3-methoxyphenyl)-
7.14	59788528	50.75	Phenol, 2-methoxy-
6.19	49245764	41.80	2-Ethyl-5-propylcyclopentanone
13.74	36933964	31.35	Butyrovannillone
12.79	34286344	29.11	2,4-Di-tert-butylphenol
15.72	25460044	21.61	2-Propanone, 1-hydroxy-3-(4-hydroxy-3-methoxyphenyl)-
18.16	19683860	16.71	Benzene, 2-methoxy-1-methyl-4-(1-methylethyl)-
12.11	19469406	16.53	Phenol, 2-methoxy-4-(1-propenyl)-
6.32	18792056	15.95	2-Acetyl-5-methylfuran
19.67	18470668	15.68	Methyl 4-oxadamantane-1-carboxylate
12.56	17470672	14.83	Apocynin
15.29	15683227	13.31	2-Propanone, 1-hydroxy-3-(4-hydroxy-3-methoxyphenyl)-
4.69	15251750	12.95	4-Butyl-1,3-thiazole
9.42	13756940	11.68	Benzene, 1,3-bis(1,1-dimethylethyl)-
17.93	13449046	11.42	2-Decylfuran
21.04	13398281	11.37	Methyl dehydroabietate
10.35	11631787	9.87	2-Methoxy-4-vinylphenol
4.49	11624374	9.87	Ethanone, 1-(2-furanyl)-
10.88	11113179	9.43	Eugenol
10.23	11086982	9.41	5-Acetoxymethyl-2-furaldehyde
10.98	10954033	9.30	Hexadecanoic acid, oct-3-en-2-yl ester
7.00	9805084	8.32	Orcinol
6.66	8973223	7.62	Nonyl octacosyl ether
21.37	8847251	7.51	N-[2-(4-Methylphenylthio)ethyl]propionamide
11.90	8711511	7.40	4-(T-Butyl)benzaldehyde
13.59	7933662	6.73	4-(1-Hydroxyallyl)-2-methoxyphenol
3.00	7782895	6.61	Propanoic acid, 2,2-dimethyl-, 2-ethylhexyl ester
9.87	7203481	6.11	Resorcinol, 2-acetyl-
10.41	6902636	5.86	Salicyl hydrazide
5.57	6637704	5.63	Phenol

9.83	6175244	5.24	Phenol, 4-ethyl-2-methoxy-
8.09	6056860	5.14	7-Hydroxyisotrichodermol
6.14	6024612	5.11	Hexanamide, N-allyl-

Pinewood 350°C, 5 minutes

Retention Time (minutes)	AREA	ug/mL (ppm)	Compound
7.15	313048992	265.74	Phenol, 2-methoxy
8.65	147138800	124.90	Creosol
13.05	120718328	102.48	2-Propanone, 1-(4-hydroxy-3-methoxyphenyl)-
9.83	101529264	86.19	Phenol, 4-ethyl-2-methoxy-
20.97	93982752	79.78	2-Propanone, 1-hydroxy-3-(4-hydroxy-3-methoxyphenyl)-
11.49	89102096	75.64	Vanillin
25.24	77489552	65.78	Carinol
14.45	76270408	64.74	Benzenepropanol, 4-hydroxy-3-methoxy-
4.68	52414864	44.49	4-Butyl-1,3-thiazole
5.27	51304436	43.55	2-Cyclopenten-1-one, 3-methyl-
11.01	42483564	36.06	Phenol, 2-methoxy-4-propyl-
10.40	41970496	35.63	Carvenone
12.56	37935920	32.20	Apocynin
12.78	35639976	30.25	Benzaldehyde, 2,3,4,5-tetramethyl-
4.40	33758808	28.66	2-Cyclopenten-1-one, 2-methyl-
5.56	33721272	28.63	Phenol
6.35	33410974	28.36	2-Cyclopenten-1-one, 2,3-dimethyl-
3.45	30406738	25.81	2-Cyclopenten-1-one
21.13	29536632	25.07	Ethyl homovanillate
10.97	27425172	23.28	Thiazole, 4-propyl
14.70	25391684	21.55	1,2-Naphthoquinone, 5-methoxy-7-methyl-
6.99	25009854	21.23	Phenol, 3-methyl-
6.19	24544618	20.84	2-Ethyl-5-propylcyclopentanone
6.13	23683182	20.10	3-Methyl-2-(2-oxopropyl)furan
3.00	17603444	14.94	Pentanoic acid, 2-ethylhexyl ester
18.30	16587212	14.08	8,9-Dehydrothymol methyl ether
15.42	16296468	13.83	Methyleugenol
11.64	15631146	13.27	Dihydrjasmone
8.05	14348893	12.18	Phenol, 2,4-dimethyl
4.48	14337085	12.17	Ethanone, 1-(2-furanyl)-
20.08	14025775	11.91	Retene
11.79	13855154	11.76	Benzaldehyde, 2,4,5-trimethyl-

8.90	13072867	11.10	2-Propyn-1-ol, 3-(4-methylphenyl)-
9.38	12776581	10.85	2-Cyclohexen-1-one, 4-(1-methylethyl)-
14.40	12630774	10.72	2-Butanone, 4-(4-hydroxy-3-methoxyphenyl)-
21.04	12424167	10.55	Methyl dehydroabietate
12.36	12232245	10.38	Phenol, 3,5-diethyl-
17.71	12049757	10.23	2-Propanone, 1-hydroxy-3-(4-hydroxy-3-methoxyphenyl)-
10.88	11309183	9.60	Phenol, 2,6-dimethoxy-
8.99	11208122	9.51	Benzofuran, 4,7-dimethyl-
7.73	11134020	9.45	2-Cyclopenten-1-one, 3,4,5-trimethyl-
13.25	11019586	9.35	Benzene, 4-butyl-1,2-dimethoxy-
6.66	10653685	9.04	Phenol, 2-methyl-
7.47	10425327	8.85	Benzofuran, 2-methyl-
8.58	10142787	8.61	Creosol

Microalgae Mixture with Polymers 350°C, 5 minutes

Retention Time (minutes)	AREA	ug/mL (ppm)	Compound
21.34	525821056	3.20	9-Octadecanamide
21.39	467506624	2.85	9-Octadecanamide
23.72	273044768	1.66	Glycidyl oleate
21.29	222854784	1.36	9,12-Hexadecadienoic acid
21.62	141663760	0.86	1-Nonylcycloheptane
21.57	140271248	0.85	Propanamide, 3-cyclopentyl-N-methyl-
26.78	127616288	0.78	Succinic acid, heptadecyl 2-methylbenzyl ester
19.86	121599216	0.74	Hexadecanamide
21.53	116869568	0.71	Octadecanamide
21.88	102427328	0.62	Propanamide, 3-cyclopentyl-N-ethyl-
21.93	96418184	0.59	Propanamide, 3-cyclopentyl-N-ethyl-
7.12	94868512	0.58	P-Cresol
22.04	75970984	0.46	9,12-Octadecadienoic acid
22.93	70460040	0.43	1-Nonylcycloheptane
22.28	67481232	0.41	9,12-Octadecadienoic acid
17.76	64933648	0.40	L-Propylglycine, N-butoxycarbonyl-, methyl ester
17.70	58726140	0.36	2,5-Piperazinedione, 3,6-bis(2-methylpropyl)-
4.44	55417612	0.34	2-Cyclopenten-1-one, 2-methyl-
24.35	55389712	0.34	Pyrrolidine, 1-(1-oxo-14-methyl-8-hexadecenyl)-
2.44	54667708	0.33	Pyrazine
5.64	52925528	0.32	Phenol
11.24	52635988	0.32	Pyrrolidine, 1-(1-oxo-7-methyl-8-hexadecenyl)-

3.37	50135232	0.31	Pyrazine, methyl-
24.44	48526460	0.30	9-Octadecanamide
22.98	45259160	0.28	Decane, 2-cyclohexyl-
22.58	43676708	0.27	Succinic acid, di(dec-9-en-1-yl)ester
20.92	43365032	0.26	N-Propyl 11-octadecenoate
24.39	43026680	0.26	Pyrrolidine, 1-(1-oxo-7-methyl-8-hexadecenyl)-
8.40	42906232	0.26	1,2-Benzenediamine, N-methyl-
16.77	42519632	0.26	3,6-Diisopropylpiperazin-2,5-dione
20.43	40374920	0.25	Fumaric acid, 4-octyl dodec-2-en-1-yl ester
7.00	39944264	0.24	2,4-Hexadiene, 3,4-dimethyl-
7.85	39874212	0.24	2,5-Pyrrolidinedione, 1-ethyl-
20.07	39657168	0.24	3-Methyl-2-(2-oxopropyl)furan
7.22	35188532	0.21	2,5-Pyrrolidinedione, 1-methyl-
23.01	34828472	0.21	Pyrrolidine, 1-(1-oxo-12-octadecynyl)-
9.75	34619228	0.21	Caprolactam
7.08	34332000	0.21	Succinic acid, di(2-methylpent-3-yl)ester
22.40	33896572	0.21	Eicosen-1-ol, cis-9-
5.32	33027980	0.20	2-Cyclopenten-1-one, 3-methyl-
8.55	32474514	0.20	Octanoic acid
7.43	32172472	0.20	1-Ethyl-2-pyrrolidinone
23.46	31369442	0.19	Isopropyl linoleate
20.67	30776602	0.19	11,14-Eicosadienoic acid, methyl ester
20.40	26327740	0.16	Cyclobutanecarboxylic acid, oct-3-en-2-yl ester
15.62	26107644	0.16	Cyclopentane, 1,2-dimethyl-3-(1-methylethenyl)-
11.99	25959230	0.16	2-Cyclohexen-1-one, 3,5,5-trimethyl-4-(3-oxobutyl)-
21.83	24837574	0.15	17-Octadecynoic acid, methyl ester
7.63	24372206	0.15	2-Ethoxy-2-cyclohexylethylphthamide
22.89	24317144	0.15	Isopropyl linoleate

Sludge Mixture with Polymers 350°C, 5 minutes

Retention Time (minutes)	AREA	ug/mL (ppm)	Compound
24.40	321630272	1.96	1-Nonylcycloheptane
17.81	127729544	0.78	N-Hexadecanoic acid
23.80	121655456	0.74	Isopropyl linoleate
18.99	117990928	0.72	13-Octadecenoic acid, methyl ester
7.10	116738520	0.71	Phenol, 2-methoxy-
18.94	110968264	0.68	13-Octadecenoic acid, methyl ester
25.42	98670848	0.60	Carinol

13.06	96528424	0.59	2-Propanone, 1-(4-hydroxy-3-methoxyphenyl)-
20.88	95809848	0.58	Palmitoleic acid
22.11	89877608	0.55	Eicosen-1-ol, cis-9-
6.97	85800184	0.52	2-Methylphenyl-N-methylcarbamate
12.81	81632264	0.50	2,4-Di-tert-butylphenol
22.08	76367416	0.47	N-Propyl 9,12-hexadecadienoate
21.09	55955600	0.34	Fumaric acid, dec-4-enyl hexadecyl ester
21.28	55531548	0.34	3-Methyl-2-(2-oxopropyl)furan
7.26	51460444	0.31	Butanoic acid, 2-methyl-, 2-methyl-2-propenyl ester
29.27	51129304	0.31	Phenol, 3,5-bis(1,1-dimethylethyl)-
9.81	43721384	0.27	Phenol, 4-ethyl-2-methoxy-
17.78	41931336	0.26	N-Hexadecanoic acid
3.02	41715884	0.25	Propanoic acid, 2,2-dimethyl-, 2-ethylhexyl ester
10.40	40790696	0.25	Carvenone
8.48	38620764	0.24	Octanoic acid
14.48	38252288	0.23	Benzenepropanol, 4-hydroxy-3-methoxy-
5.55	34365580	0.21	Phenol
17.27	32864352	0.20	Tetradecanoic acid, 10,13-dimethyl-, methyl ester
8.62	32575112	0.20	Creosol
18.88	32434890	0.20	N-Propyl 9,12-hexadecadienoate
10.81	32426838	0.20	Phenol, 2,6-dimethoxy-
19.16	31927678	0.19	Heptacosanoic acid, 25-methyl-, methyl ester
12.57	31483544	0.19	Apocynin
21.16	30547574	0.19	Eicosen-1-ol, cis-9-
11.49	30246210	0.18	Vanillin
8.42	25030198	0.15	Octanoic acid
20.67	24952198	0.15	Eicosen-1-ol, cis-9-
19.87	18343686	0.11	Eicosen-1-ol, cis-9-

Pinewood Mixture with Polymers 350°C, 5 minutes

Retention Time (minutes)	AREA	ug/mL (ppm)	Compound
35.882	1371721600.000	8.355522601	Butyl 9, 12-octadecadienoate
23.867	1128045312.000	6.871225254	Isopropyl linoleate
21.346	398034016.000	2.424531491	Ethyl 9,12-hexadecadienoate
23.682	341755104.000	2.081721608	Apidic acid, butyl dec-4-enyl ester
21.301	312500288.000	1.903522711	11,14-Octadecadienoic acid, methyl ester
33.636	218898864.000	1.33337144	Butyl 9, 12-octadecadienoate
22.131	161241696.000	0.982166232	Ethyl 9,12-hexadecadienoate
26.748	108830920.000	0.662918198	Vitamin E
21.526	105140384.000	0.640438158	Methyl 12,13-octadecadienoate
21.566	94700664.000	0.576847035	3-Methyl-2-(2-oxopropyl)furan
23.447	92318360.000	0.562335786	Succinic acid, 2,2-dichloroethyl dec-4-en-1-yl ester
17.875	78297720.000	0.476932323	Diethyl glutaconate
8.496	74769096.000	0.455438532	Octanoic acid
19.920	74551248.000	0.454111561	Eicosen-1-ol, cis-9-
24.432	72957064.000	0.444400961	1-Nonylcycloheptane
21.406	67136288.000	0.40894506	9-Octadecanamide
22.161	63356648.000	0.385922263	Isopropyl linoleate
29.749	62730612.000	0.382108911	12,15-Octadecadienoic acid, methyl ester
21.876	61177140.000	0.372646298	17-Octadecynoic acid, methyl ester
24.342	54350396.000	0.331062777	Pyrrolidine, 1-(1-oxo-7-methyl-8-hexadecenyl)-
28.024	53791916.000	0.327660926	1-Heptatriacotanol
21.831	52526436.000	0.31995255	9,12-Octadecadienoic acid
24.312	45042572.000	0.274366335	Pyrrolidine, 1-(1-oxo-12-octadecynyl)-
20.686	39508600.000	0.240657434	Eicosen-1-ol, cis-9-
17.955	35783236.000	0.217965247	2,5-Piperazinedione, 3,6-bis(2-methylpropyl)-
7.050	33088074.000	0.201548295	P-Creosol
25.573	30348870.000	0.184863072	1,7-Hexadecadiene
7.190	25982324.000	0.158265274	Phenol, 2-methoxy-
22.922	25157472.000	0.153240881	12,15-Octadecadienoic acid, methyl ester
12.873	24742112.000	0.150710812	Succinic acid, di(3-methylphenyl)ester
2.453	23882866.000	0.145476915	1H-Pyrrole, 3-ethyl-
4.449	21727734.000	0.13234943	2-Cyclopenten-1-one, 2-methyl-
9.476	20317606.000	0.123759964	Benzene, 1,2-bis(1,1-dimethylethyl)-
5.615	20002442.000	0.121840216	Phenol
11.247	19001352.000	0.11574231	Pyrrolidine, 1-(1-oxo-7-methyl-8-hexadecenyl)-

Chapter 7



Conclusions

7.1 Conclusions

This thesis advances our understanding on the effect of reaction time, temperature and biomass composition on product distribution and crude composition in HTL. The first major contribution is the development of a set of reaction pathways which can be used to predict the conversion of various types of biomass to solid, aqueous, crude and gas phase products depending on the organic composition of the biomass. The trend of product distribution for reaction temperatures of 250, 300 and 350°C over reaction times 0 to 60 minutes are clearly visible from the model, though fitting the HTL reactions to first order equations is an approximation that simplifies the hundreds of complex reactions occurring in HTL. Nevertheless, the model allows optimum reaction conditions for producing renewable crude from feedstocks of interest to be identified. The second major contribution is the characterisation of crude composition from various model compounds and types of biomass. The specific conclusions from each part of the study are given below.

7.1.1 The elucidation of reaction kinetics for hydrothermal liquefaction of model macromolecules

This study involved HTL experiments using individual polymer model compounds to represent the organic fractions of biomass. The effect of reaction time and temperature on the boiling point distribution of the crude oil was analysed. A kinetic model was developed to describe the conversion of each of the carbohydrate, lipid, lignin and protein compounds to solid, aqueous, crude and gas phase products. The following conclusions were drawn:

1. HTL of the lipid polymer resulted in a higher product distribution of aqueous and gas phase products, hence reducing the yield of renewable crude (obtained by solvent extraction) compared to that obtained from HTL of the original feedstock by up to 90%. However, HTL treatment resulted in an increase in the fraction of crude with a lower boiling point in the range of diesel.
2. For maximum crude yield from cellulose at around 20%, short residence times and higher temperatures were favourable. Most of the crude

produced from the HTL of the carbohydrate was in the higher boiling point range. The crude was found to bind to the solids and could not be efficiently extracted with solvent alone.

3. For HTL treatment of the protein, temperatures of 300 and 350°C and a residence time of around 30 minutes resulted in optimum renewable crude yield of around 30%, which was made up of a greater proportion of the more favourable lighter distillate fraction compared to the initial feed.
4. Less than 7% crude yield was obtained from using lignin as a feedstock for HTL. The crude that was formed was mostly heavy oil and HTL treatment of lignin resulted in mostly aqueous phase products.
5. The dominant reaction pathways for each of the model compounds were identified and a bulk first order kinetic model developed for each individual model compound at reaction temperatures of 250, 300 and 350°C, over 0 to 60 minutes.

7.1.2 Reaction kinetics and characterisation of species in renewable crude from hydrothermal liquefaction of monomers to represent organic fractions of biomass feedstocks

In this section of work, monomer model compounds were used to represent the organic fractions of biomass feedstocks. While monomers do not represent biomass as well as polymers, the conversion pathways between intermediate products formed through HTL could be identified. The monomers were reacted under HTL conditions at various reaction times and temperatures. Analysis of the crude was conducted via GC-MS and a kinetic model was developed for each of the organic fractions of biomass. This resulted in the following conclusions:

1. HTL of carbohydrate, lipid, protein and lignin monomers generally resulted in higher aqueous phase product yields and lower renewable crude yields than the polymer compounds from the same families, except in the case of guaiacol where up to 62% higher crude yields were produced for the lignin monomer model compound. While lignin may not produce a high crude yield, its decomposition products can result in the constituents of crude oil. At the same temperatures, longer residence times resulted in

decreasing crude yield for all four monomer model compounds. Crude yield was decreased by up to 44% with increasing residence time. Increased residence time results in further decomposition of the monomer model compounds to low molecular weight aqueous and gas phase products.

2. For each of the four model compounds, the same 15 compounds could be identified in the renewable crude produced at temperatures of 250, 300 and 350°C at 5 and 30 minutes. While the amount of each compound in the crude may vary, reaction time and temperature did not affect the types of compounds produced by each monomer as identified by GC-MS. The crude produced from the lipid was composed of fatty acids. HTL of carbohydrates produced crude consisting mainly of phenol, furans, aldehydes, aromatics and ketones. HTL of the protein monomer resulted in a crude composed of amides, aromatics, amines, carboxylic acids and short hydrocarbon chains. From lignin, phenolic compounds made up the majority of the crude.
3. A kinetic model was produced for HTL of model monomer compounds which could be compared to that for polymer model compounds. Optimum reaction conditions to produce maximum crude yield varied significantly for feedstocks from the same families of carbohydrate, lipid, protein and lignin.

7.1.3 Reaction kinetics and characterisation of species in renewable crude from hydrothermal liquefaction of mixtures of polymer compounds to represent organic fractions of biomass feedstocks

This study required HTL experiments with mixtures of polymer model compounds at the same reaction times and temperatures as had been completed for individual polymer and monomer model compounds. This allowed a kinetic model for mixtures of model compounds to be developed. The crude was analysed via GC-MS so that the variation in crude composition from monomers and polymers reacted alone and in mixtures could be identified. The following conclusions were made:

1. Solid, aqueous, crude and gas phase yields from binary and quaternary mixtures of model compounds resulted in different yields compared to the mass averaged yields from experiments with individual model compounds. Product yields from mixtures were neither consistently higher nor lower than yields from individual compounds. Product yields varied with time and temperature. This variation in yields between mixtures and individual compounds was 0 to 35%.
2. The addition of lignin to binary mixtures mostly resulted in lower crude yields from experiments with mixtures compared to individual model compounds. Hence, the presence of lignin in biomass is suspected to inhibit the production of crude in HTL.
3. GC-MS results of the crude identified that the lipid contributes phenolic compounds and fatty acids chains. Carbohydrate contributes cyclic hydrocarbons, ketones, aldehydes, esters, fatty acid chains and furans. Protein contributes amides, phenolic and low molecular weight compounds. Lignin contributes phenolic compounds as well as other organic cyclic compounds.
4. GC-MS results indicated that the compounds in the crude produced from individual model compounds mostly also exist in the crude produced from mixtures with those model compounds.
5. A first order kinetic model was developed using experimental data from quaternary mixtures of model compounds which predicted the experimental yields with an error of less than 10%. Further experiments could be conducted to establish suitable kinetic parameters for HTL of biomass with varying organic content, so that the model can be applied more widely.

7.1.4 A kinetic model for the hydrothermal liquefaction of microalgae, sewage sludge and pinewood with product characterisation of renewable crude
In this study biomass feedstocks including microalgae, sludge and pinewood were used in HTL experiments at a range of reaction times and temperatures. This allowed the model for mixtures of polymer compounds to be further developed for

biomass. The effects of the inorganic contents of biomass on product distribution could also be identified. GC-MS was utilised to identify the variation in crude produced from different sources of biomass. The following conclusions were drawn:

1. The *Tetraselmis* sp. microalgae, sewage sludge and Radiata pinewood feedstocks contained variable organic and inorganic fractions that resulted in different product yields. Crude yields were 10 to 30% for microalgae, 10 to 25% for sludge and under 10% for pinewood.
2. The microalgae produced a crude which was high in nitrogen containing compounds, while esters, aromatic compounds and phenolic compounds were identified in the crude produced from all three types of biomass.
3. Product yields from real biomass varied compared to what was expected from model compounds. The inorganic content in the biomass is suspected to be a major cause for this variation. The inorganic fractions of biomass are known to catalyse and inhibit the production of crude depending on its composition.
4. A kinetic model was developed to describe the reaction products of the three types of biomass. Each type of biomass required different reaction parameters for the set of reaction pathways due to the high variability in product fractions. The kinetic model predicts the trends of product fractions for each type of biomass with time and temperature and was able to predict product fractions from experiments with less than 15% error.

7.2 Recommendations for Future Work

This thesis has resulted in an advancement in the understanding of products from the HTL of biomass and the effects of reaction time, temperature and biomass composition on product distribution and crude composition. However, further studies are required to increase our knowledge of the products from HTL of biomass:

1. The experimental results are limited by reactor configuration. An 11 mL volume batch reactor was used for all experiments in this work and the

variation between continuous and batch processes in HTL is yet to be clearly identified in literature. Hence, experiments which determine product distributions from the same feedstocks as well as consistent reaction temperatures and times are required on continuous systems for comparison. Continuous systems may be more representative of industrial applications

2. Reactions were also limited to one heating rate and mass loading of feedstock. These variables have been shown to result in some variation in product distribution. Further experiments with various heating rates and mass loadings could be conducted to develop a model which accommodates these reaction variables.
3. The separation methods for the HTL product mixture greatly affect product distribution. The separation methods to be used at industrial scale for HTL are yet to be determined, but once they are, they should be employed to develop a model which can predict the product distribution for a given processing method.
4. The detailed mechanisms of lignin decomposition and how the stability of phenolic compounds could result in reduced crude yield from biomass should be further investigated. Hence, detailed studies on the reaction chemistry of lignin during HTL are required.
5. The effect of the presence of inorganic compounds which are inherent in different biomass feedstocks should be further investigated. Experiments with model compounds where these inorganics are added to the reaction mixture could help identify their catalytic or inhibitory effect.
6. Further experiments with a greater number of biomass types will allow more reaction parameters to be developed to describe other biomass types.
7. Finally, a study of the detailed reaction pathways to produce specific compounds could be developed. This would be extremely complex and would require hundreds of specific reactions to be identified for each type of biomass but could be useful if particular compounds are being targeted as HTL products.

References

The following references are cited in Chapters 1, 2 and 7. References for Chapters 3-6 are included within each of these chapters.

References

- Abdel Kader, E, Hussein, H.S., Hussien, N.H., El Diwani, G. & Hawash, S.I. 2015, 'Effect of Extractive Solvents on Bio – Oil Production From Microalgae via Hydrothermal Liquefaction', *Chemical Engineering and Process Engineering Research*, vol. 38.
- Anastasakis, K, Biller, P, Madsen, RB, Glasius, M & Johannsen, IJE 2018, 'Continuous hydrothermal liquefaction of biomass in a novel pilot plant with heat recovery and hydraulic oscillation', vol. 11, no. 10, p. 2695.
- Anastasakis, K & Ross, AB 2011, 'Hydrothermal liquefaction of the brown macro-alga *Laminaria Saccharina*: Effect of reaction conditions on product distribution and composition', *Bioresource Technology*, vol. 102, no. 7, 4//, pp. 4876-4883.
- Ando, H, Sakaki, T, Kokusho, T, Shibata, M, Uemura, Y & Hatate, Y 2000, 'Decomposition Behavior of Plant Biomass in Hot-Compressed Water', *Industrial & Engineering Chemistry Research*, vol. 39, no. 10, 2000/10/01, pp. 3688-3693
- Anthony, JR 2015, 'Hydrothermal liquefaction of municipal sludge and biosolids', Mechanical Engineering Master of Science in Engineering thesis, The University of Texas, Austin.
- Arturi, KR, Kucheryavskiy, S & Søggaard, EG 2016, 'Performance of hydrothermal liquefaction (HTL) of biomass by multivariate data analysis', *Fuel Processing Technology*, vol. 150, 2016/09/01/, pp. 94-103.
- Biller, P, Johannsen, I, dos Passos, JS & Ottosen, LDM 2018, 'Primary sewage sludge filtration using biomass filter aids and subsequent hydrothermal co-liquefaction', *Water Research*, vol. 130, 2018/03/01/, pp. 58-68.
- Biller, P, Riley, R & Ross, AB 2011, 'Catalytic hydrothermal processing of microalgae: Decomposition and upgrading of lipids', *Bioresource Technology*, vol. 102, no. 7, 2011/04/01/, pp. 4841-4848.
- Biller, P & Ross, AB 2011, 'Potential yields and properties of oil from the hydrothermal liquefaction of microalgae with different biochemical content', *Bioresource Technology*, vol. 102, no. 1, pp. 215-225.
- Biller, P, Sharma, BK, Kunwar, B & Ross, AB 2015, 'Hydroprocessing of bio-crude from continuous hydrothermal liquefaction of microalgae', *Fuel*, vol. 159, pp. 197-205.
- Brown, TM, Duan, P & Savage, PE 2010, 'Hydrothermal Liquefaction and Gasification of *Nannochloropsis* sp', *Energy & Fuels*, vol. 24, no. 6, 2010/06/17, pp. 3639-3646.
- Castello, D, Pedersen, T & Rosendahl, L 2018, 'Continuous Hydrothermal Liquefaction of Biomass: A Critical Review', *Energies*, vol. 11, 11/15, p. 3165.
- Chan, YH, Yusup, S, Quitain, AT, Tan, RR, Sasaki, M, Lam, HL & Uemura, Y 2015, 'Effect of process parameters on hydrothermal liquefaction of oil palm

References

- biomass for bio-oil production and its life cycle assessment', *Energy Conversion and Management*, vol. 104, 2015/11/01/, pp. 180-188.
- Croce, A, Battistel, E, Chiaberge, S, Spera, S, De Angelis, F & Reale, S 2017, 'A Model Study to Unravel the Complexity of Bio-Oil from Organic Wastes', *ChemSusChem*, vol. 10, no. 1, pp. 171-181.
- Déniel, M, Haarlemmer, G, Roubaud, A, Weiss-Hortala, E & Fages, J 2017a, 'Hydrothermal liquefaction of blackcurrant pomace and model molecules: understanding of reaction mechanisms', *Sustainable Energy & Fuels*, vol. 1, no. 3, pp. 555-582.
- Déniel, M, Haarlemmer, G, Roubaud, A, Weiss-Hortala, E & Fages, J 2017b, 'Modelling and Predictive Study of Hydrothermal Liquefaction: Application to Food Processing Residues', *Waste and Biomass Valorization*, vol. 8, no. 6, September 01, pp. 2087-2107.
- Dote, Y, Hayashi, T, Suzuki, A & Ogi, T 1992, 'Analysis of oil derived from liquefaction of sewage sludge', *Fuel*, vol. 71, no. 9, pp. 1071-1073.
- Duan, P & Savage, PE 2011, 'Hydrothermal Liquefaction of a Microalga with Heterogeneous Catalysts', *Industrial & Engineering Chemistry Research*, vol. 50, no. 1, 2011/01/05, pp. 52-61.
- Fábregas, J, Maseda, A, Domínguez, A & Otero, A 2004, 'The cell composition of *Nannochloropsis* sp. changes under different irradiances in semicontinuous culture', *World Journal of Microbiology and Biotechnology*, vol. 20, no. 1, 2004/02/01, pp. 31-35.
- Faeth, JL, Valdez, PJ & Savage, PE 2013, 'Fast Hydrothermal Liquefaction of *Nannochloropsis* sp. To Produce Biocrude', *Energy & Fuels*, vol. 27, no. 3, 2013/03/21, pp. 1391-1398.
- Fan, Y, Hornung, U, Dahmen, N & Kruse, A 2018, 'Hydrothermal liquefaction of protein-containing biomass: study of model compounds for Maillard reactions', *Biomass Conversion and Biorefinery*, vol. 8, no. 4, December 01, pp. 909-923.
- Feng, S, Yuan, Z, Leitch, M & Xu, CC 2014, 'Hydrothermal liquefaction of barks into bio-crude – Effects of species and ash content/composition', *Fuel*, vol. 116, 2014/01/15/, pp. 214-220.
- Gai, C, Zhang, Y, Chen, W-T, Zhang, P & Dong, Y 2015, 'An investigation of reaction pathways of hydrothermal liquefaction using *Chlorella pyrenoidosa* and *Spirulina platensis*', *Energy Conversion and Management*, vol. 96, 2015/05/15/, pp. 330-339.
- Gao, Y, Chen, H-p, Wang, J, Shi, T, Yang, H-P & Wang, X-H 2011, 'Characterization of products from hydrothermal liquefaction and carbonation of biomass model compounds and real biomass', *Journal of Fuel Chemistry and Technology*, vol. 39, no. 12, 2011/12/01/, pp. 893-900.

References

- Gao, Y, Wang, X-H, Yang, H-P & Chen, H-P 2012, 'Characterization of products from hydrothermal treatments of cellulose', *Energy*, vol. 42, no. 1, 2012/06/01/, pp. 457-465.
- Guo, Y, Yeh, T, Song, W, Xu, D & Wang, S 2015, 'A review of bio-oil production from hydrothermal liquefaction of algae', *Renewable and Sustainable Energy Reviews*, vol. 48, 2015/08/01/, pp. 776-790.
- Hardi, F, Mäkelä, M & Yoshikawa, K 2017, 'Non-catalytic hydrothermal liquefaction of pine sawdust using experimental design: Material balances and products analysis', *Applied Energy*, vol. 204, 2017/10/15/, pp. 1026-1034.
- He, C, Chen, C-L, Giannis, A, Yang, Y & Wang, J-Y 2014, 'Hydrothermal gasification of sewage sludge and model compounds for renewable hydrogen production: a review', *Renewable and Sustainable Energy Reviews*, vol. 39, pp. 1127-1142.
- Hietala, DC, Faeth, JL & Savage, PE 2016, 'A quantitative kinetic model for the fast and isothermal hydrothermal liquefaction of *Nannochloropsis* sp', *Bioresource Technology*, vol. 214, 2016/08/01/, pp. 102-111.
- Huang, H-j, Yuan, X-z, Zhu, H-n, Li, H, Liu, Y, Wang, X-l & Zeng, G-m 2013, 'Comparative studies of thermochemical liquefaction characteristics of microalgae, lignocellulosic biomass and sewage sludge', *Energy*, vol. 56, 2013/07/01/, pp. 52-60.
- Jazrawi, C, Biller, P, Ross, AB, Montoya, A, Maschmeyer, T & Haynes, BS 2013, 'Pilot plant testing of continuous hydrothermal liquefaction of microalgae', *Algal Research*, vol. 2, no. 3, pp. 268-277.
- Jindal, MK & Jha, MK 2016, 'Effect of process parameters on hydrothermal liquefaction of waste furniture sawdust for bio-oil production', *RSC Advances*, vol. 6, no. 48, pp. 41772-41780.
- Kamio, E, Takahashi, S, Noda, H, Fukuhara, C & Okamura, T 2008, 'Effect of heating rate on liquefaction of cellulose by hot compressed water', *Chemical Engineering Journal*, vol. 137, no. 2, pp. 328-338.
- Kanetake, T, Sasaki, M & Goto, M 2007, 'Decomposition of a lignin model compound under hydrothermal conditions', *Chemical Engineering & Technology*, vol. 30, no. 8, pp. 1113-1122.
- Klingler, D, Berg, J & Vogel, H 2007, 'Hydrothermal reactions of alanine and glycine in sub- and supercritical water', *The Journal of Supercritical Fluids*, vol. 43, no. 1, 11//, pp. 112-119.
- Knežević, D, van Swaaij, W & Kersten, S 2010, 'Hydrothermal Conversion Of Biomass. II. Conversion Of Wood, Pyrolysis Oil, And Glucose In Hot Compressed Water', *Industrial & Engineering Chemistry Research*, vol. 49, no. 1, pp. 104-112.

References

- Knežević, D, van Swaaij, WPM & Kersten, SRA 2009, 'Hydrothermal Conversion of Biomass: I, Glucose Conversion in Hot Compressed Water', *Industrial & Engineering Chemistry Research*, vol. 48, no. 10, pp. 4731-4743.
- Kruse, A, Maniam, P & Spieler, F 2007, 'Influence of Proteins on the Hydrothermal Gasification and Liquefaction of Biomass. 2. Model Compounds', *Industrial & Engineering Chemistry Research*, vol. 46, no. 1, pp. 87-96.
- Li, G, Zhang, F, Sun, Y, Wong, JWC & Fang, M 2001, 'Chemical Evaluation of Sewage Sludge Composting as a Mature Indicator for Composting Process', *Water, Air, and Soil Pollution*, vol. 132, no. 3, December 01, pp. 333-345.
- Li, Y, Leow, S, Fedders, AC, Sharma, BK, Guest, JS & Strathmann, TJ 2017, 'Quantitative multiphase model for hydrothermal liquefaction of algal biomass', *Green Chemistry*, vol. 19, no. 4, pp. 1163-1174.
- Lu, J, Liu, Z, Zhang, Y & Savage, PE 2018, 'Synergistic and Antagonistic Interactions during Hydrothermal Liquefaction of Soybean Oil, Soy Protein, Cellulose, Xylose, and Lignin', *ACS Sustainable Chemistry & Engineering*, vol. 6, no. 11, 2018/11/05, pp. 14501-14509.
- Luo, L, Sheehan, JD, Dai, L & Savage, PE 2016, 'Products and Kinetics for Isothermal Hydrothermal Liquefaction of Soy Protein Concentrate', *ACS Sustainable Chemistry & Engineering*, vol. 4, no. 5, pp. 2725-2733.
- Minowa, T, Inoue, S, Hanaoka, T & Matsumura, Y 2004, 'Hydrothermal reaction of glucose and glycine as model compounds of biomass', *Journal of the Japan Institute of Energy*, vol. 83, no. 10, pp. 794-798.
- Möller, M, Nilges, P, Harnisch, F & Schröder, U 2011, 'Subcritical water as reaction environment: fundamentals of hydrothermal biomass transformation', *ChemSusChem*, vol. 4, no. 5, pp. 566-579.
- Morris, I, Glover, HE & Yentsch, CS 1974, 'Products of photosynthesis by marine phytoplankton: the effect of environmental factors on the relative rates of protein synthesis', *Marine Biology*, vol. 27, no. 1, 1974/10/01, pp. 1-9.
- Peters, K 1986, 'Guidelines for evaluating petroleum source rock using programmed pyrolysis', *AAPG bulletin*, vol. 70, no. 3, pp. 318-329.
- Peterson, AA, Lachance, RP & Tester, JW 2010, 'Kinetic Evidence of the Maillard Reaction in Hydrothermal Biomass Processing: Glucose–Glycine Interactions in High-Temperature, High-Pressure Water', *Industrial & Engineering Chemistry Research*, vol. 49, no. 5, 2010/03/03, pp. 2107-2117.
- Prestigiacomio, C, Costa, P, Pinto, F, Schiavo, B, Siragusa, A, Scialdone, O & Galia, A 2019, 'Sewage sludge as cheap alternative to microalgae as feedstock of catalytic hydrothermal liquefaction processes', *The Journal of Supercritical Fluids*, vol. 143, 2019/01/01/, pp. 251-258.

References

- Promdej, C & Matsumura, Y 2011, 'Temperature Effect on Hydrothermal Decomposition of Glucose in Sub- And Supercritical Water', *Industrial & Engineering Chemistry Research*, vol. 50, no. 14, pp. 8492-8497.
- Qian, L, Wang, S & Savage, PE 2017, 'Hydrothermal liquefaction of sewage sludge under isothermal and fast conditions', *Bioresource Technology*, vol. 232, 2017/05/01/, pp. 27-34.
- Qian, L, Wang, S & Savage, PE 2020, 'Fast and isothermal hydrothermal liquefaction of sludge at different severities: Reaction products, pathways, and kinetics', *Applied Energy*, vol. 260, 2020/02/15/, p. 114312.
- Saba, A, Lopez, B, Lynam, JG & Reza, MT 2018, 'Hydrothermal Liquefaction of Loblolly Pine: Effects of Various Wastes on Produced Biocrude', *ACS Omega*, vol. 3, no. 3, 2018/03/31, pp. 3051-3059.
- Sasaki, M, Adschiri, T & Arai, K 2004, 'Kinetics of cellulose conversion at 25 MPa in sub-and supercritical water', *AIChE Journal*, vol. 50, no. 1, pp. 192-202.
- Shanableh, A & Jones, S 2001, 'Production and transformation of volatile fatty acids from sludge subjected to hydrothermal treatment', *Water Science and Technology*, vol. 44, no. 10, pp. 129-135.
- Sheehan, JD & Savage, PE 2017a, 'Modeling the effects of microalga biochemical content on the kinetics and biocrude yields from hydrothermal liquefaction', *Bioresource Technology*, vol. 239, 2017/09/01/, pp. 144-150.
- Sheehan, JD & Savage, PE 2017b, 'Molecular and Lumped Products from Hydrothermal Liquefaction of Bovine Serum Albumin', *ACS Sustainable Chemistry & Engineering*, vol. 5, no. 11, pp. 10967-10975.
- Sheng, L, Wang, X & Yang, X 2018, 'Prediction model of biocrude yield and nitrogen heterocyclic compounds analysis by hydrothermal liquefaction of microalgae with model compounds', *Bioresource Technology*, vol. 247, 2018/01/01/, pp. 14-20.
- Shuping, Z, Yulong, W, Mingde, Y, Kaleem, I, Chun, L & Tong, J 2010, 'Production and characterization of bio-oil from hydrothermal liquefaction of microalgae *Dunaliella tertiolecta* cake', *Energy*, vol. 35, no. 12, 2010/12/01/, pp. 5406-5411.
- Singh, R, Prakash, A, Balagurumurthy, B, Singh, R, Saran, S & Bhaskar, T 2015, 'Hydrothermal liquefaction of agricultural and forest biomass residue: comparative study', *Journal of Material Cycles and Waste Management*, vol. 17, no. 3, July 01, pp. 442-452.
- Sommers, LE, Nelson, DW & Yost, KJ 1976, 'Variable Nature of Chemical Composition of Sewage Sludges1', *Journal of Environmental Quality*, vol. 5, no. 3, pp. 303-306.

References

- Teri, G, Luo, L & Savage, PE 2014, 'Hydrothermal Treatment of Protein, Polysaccharide, and Lipids Alone and in Mixtures', *Energy & Fuels*, vol. 28, no. 12, pp. 7501-7509.
- Tian, C, Li, B, Liu, Z, Zhang, Y & Lu, H 2014, 'Hydrothermal liquefaction for algal biorefinery: A critical review', *Renewable and Sustainable Energy Reviews*, vol. 38, 2014/10/01/, pp. 933-950.
- Toor, SS, Rosendahl, L & Rudolf, A 2011, 'Hydrothermal liquefaction of biomass: A review of subcritical water technologies', *Energy*, vol. 36, no. 5, pp. 2328-2342.
- Tungal, R & Shende, RV 2014, 'Hydrothermal liquefaction of pinewood (*Pinus ponderosa*) for H₂, biocrude and bio-oil generation', *Applied Energy*, vol. 134, 2014/12/01/, pp. 401-412.
- Valdez, PJ, Dickinson, JG & Savage, PE 2011, 'Characterization of Product Fractions from Hydrothermal Liquefaction of *Nannochloropsis* sp. and the Influence of Solvents', *Energy & Fuels*, vol. 25, no. 7, pp. 3235-3243.
- Valdez, PJ, Nelson, MC, Wang, HY, Lin, XN & Savage, PE 2012, 'Hydrothermal liquefaction of *Nannochloropsis* sp.: Systematic study of process variables and analysis of the product fractions', *biomass and bioenergy*, vol. 46, 2012/11/01/, pp. 317-331.
- Valdez, PJ, Tocco, VJ & Savage, PE 2014, 'A general kinetic model for the hydrothermal liquefaction of microalgae', *Bioresource Technology*, vol. 163, pp. 123-127.
- Vardon, DR, Sharma, BK, Scott, J, Yu, G, Wang, Z, Schideman, L, Zhang, Y & Strathmann, TJ 2011, 'Chemical properties of biocrude oil from the hydrothermal liquefaction of *Spirulina* algae, swine manure, and digested anaerobic sludge', *Bioresource Technology*, vol. 102, no. 17, pp. 8295-8303.
- Wahyudiono, Sasaki, M & Goto, M 2008, 'Recovery of phenolic compounds through the decomposition of lignin in near and supercritical water', *Chemical Engineering and Processing: Process Intensification*, vol. 47, no. 9, 2008/09/01/, pp. 1609-1619.
- Xu, D, Lin, G, Liu, L, Wang, Y, Jing, Z & Wang, S 2018, 'Comprehensive evaluation on product characteristics of fast hydrothermal liquefaction of sewage sludge at different temperatures', *Energy*, vol. 159, 2018/09/15/, pp. 686-695.
- Yang, J, He, Q, Corcadden, K & Niu, H 2018, 'The impact of downstream processing methods on the yield and physiochemical properties of hydrothermal liquefaction bio-oil', *Fuel Processing Technology*, vol. 178, 2018/09/01/, pp. 353-361.
- Yang, J, He, Q, Corcadden, K, Niu, H, Lin, J & Astatkie, T 2019, 'Advanced models for the prediction of product yield in hydrothermal liquefaction via a mixture design of biomass model components coupled with process variables', *Applied Energy*, vol. 233-234, 2019/01/01/, pp. 906-915.

References

- Yang, J, He, Q, Niu, H, Corscadden, K & Astatkie, T 2018, 'Hydrothermal liquefaction of biomass model components for product yield prediction and reaction pathways exploration', *Applied Energy*, vol. 228, 2018/10/15/, pp. 1618-1628.
- Ye, Y, Fan, J & Chang, J 2012, 'Effect of reaction conditions on hydrothermal degradation of cornstalk lignin', *Journal of Analytical and Applied Pyrolysis*, vol. 94, 2012/03/01/, pp. 190-195.
- Yin, F, Chen, H, Xu, G, Wang, G & Xu, Y 2015, 'A detailed kinetic model for the hydrothermal decomposition process of sewage sludge', *Bioresource Technology*, vol. 198, pp. 351-357.
- Yin, S & Tan, Z 2012, 'Hydrothermal liquefaction of cellulose to bio-oil under acidic, neutral and alkaline conditions', *Applied Energy*, vol. 92, pp. 234-239.
- Yong, TL-K & Matsumura, Y 2013, 'Kinetic Analysis of Lignin Hydrothermal Conversion in Sub- and Supercritical Water', *Industrial & Engineering Chemistry Research*, vol. 52, no. 16, pp. 5626-5639.
- Yu, G, Zhang, Y, Schideman, L, Funk, TL & Wang, Z 2011, 'Hydrothermal liquefaction of low lipid content microalgae into bio-crude oil', *Transactions of the ASABE*, vol. 54, no. 1, pp. 239-246.
- Zhang, B, von Keitz, M & Valentas, K 2008, 'Thermal Effects on Hydrothermal Biomass Liquefaction', *Applied Biochemistry and Biotechnology*, vol. 147, no. 1, pp. 143-150.
- Zhang, B, von Keitz, M & Valentas, K 2009, 'Thermochemical liquefaction of high-diversity grassland perennials', *Journal of Analytical and Applied Pyrolysis*, vol. 84, no. 1, pp. 18-24.
- Zhang, C, Tang, X, Sheng, L & Yang, X 2016, 'Enhancing the performance of Co-hydrothermal liquefaction for mixed algae strains by the Maillard reaction', *Green Chemistry*, vol. 18, no. 8, pp. 2542-2553.
- Zhou, X-F 2014, 'Conversion of kraft lignin under hydrothermal conditions', *Bioresource Technology*, vol. 170, 10//, pp. 583-586.